CONTROL OF ION CHANNEL EXPRESSION

by

David McKinnon

A Thesis Submitted to the Australian National University
for the Degree of Doctor of Philosophy.

April, 1987

Statement.

Unless otherwise stated in the acknowledgements, all experiments were designed and performed by the candidate.

David McKinnon

David McKinnon

Acknowledgements.

The work reported in this thesis was carried out during the tenure of a Commonwealth Postgraduate Scholarship, in the Department of Physiology, at the John Curtin School of Medical Research (JCSMR).

The two colour, flowmicrofluorometric graph presented in Chapter 2 (Fig. 7) was provided by Dr R. Ceredig of the Department of Experimental Pathology, JCSMR. Experiments reported in Chapter 4 of this thesis were done in collaboration with Mary Martinson of the Medical Molecular Biology Unit, JCSMR and the electronmicrography presented in Chapter 5 was performed with Lesley Maxwell of the Electron Microscopy and Histology Unit, JCSMR. The experiments reported in the Appendix were done in collaboration with Dr P. Hodgkin.

I would like to thank my supervisor, Professor Peter Gage for his guidance and advice, during the course of my PhD. Thanks are also extended to Dr Rod Ceredig for his introduction to thymology and the FACS, and to Dr Ian Young for his helpful discussions on molecular biology.

Thanks to all members of Physiology, Pharmacology, Experimental Pathology and Photography, for their support and advice during my stay at JCSMR. In particular, I am grateful to Jane, Pankaj, Anne and Bruce for their excellent proof reading.

Abstract

Modulation of ion channel expression is thought to be a source of neuronal plasticity and, as such, may be one molecular mechanism underlying behavioral plasticity. Understanding such modulation, however, has been hampered by the lack of suitable in vitro cell systems which can be used to study the regulation of channel protein expression. With this in view, an attempt has been made to develop and describe cell systems in which ion channel expression is modulated in a defined manner. These include; the isolation of thymocytes during various stages of T lymphocyte development; denervation of adult skeletal muscle; the *Xenopus* oocyte system for expressing mRNAs; and tumorigenic versus non-tumorigenic cells lines.

The developmental regulation of a number of cell surface markers of thymocytes is well understood and, because thymus-derived lymphocytes are known to express delayed-rectifier K^+ channels, subsets of thymocytes were examined for K^+ channel expression. Using the whole-cell recording technique, and flowmicrofluorometry to isolate phenotypically defined cells, it was found that J11d$^-$/Lyt-2$^-$ / L3T4$^-$ cells express none or very few delayed-rectifier K^+ channels. Most other Lyt-2$^-$ /L3T4$^-$ cells, as well as typical cortical thymocytes (Lyt-2$^+$/ L3T4$^+$), did express K^+ channels. Mature (Lyt-2$^+$/L3T4$^-$ or Lyt-2$^-$ /L3T4$^+$) thymocytes, which are heterogenous for J11d expression, were found to be heterogenous for K^+ channel expression. Consistent with this finding was the observation that the cortisone-resistant subpopulation of thymocytes, which express low levels of J11d, were enriched for cells expressing low levels of K^+ channels. Mature peripheral T lymphocytes expressed very low levels of K^+ channels, but upon in vitro activation with concanavalin A were found to express high levels of this channel. These results suggest that K^+ channel expression is developmentally regulated, and increased expression of the channel is induced in response to mitogenic signals throughout the T lymphocyte lineage.

In skeletal muscle of adult rats, modulation of the acetylcholine receptor (AChR) channel can be achieved by cutting the innervating nerve. Using the patch-clamp technique, it was found that the AChRs from the extrajunctional region of denervated muscle were heterogenous, consisting of channels which are electrophysiologically similar to the junctional AChRs normally found at the end-plate, and channels which resemble the extrajunctional AChR of embryonic muscle. Control of the expression of AChRs in the extrajunctional region of denervated muscle was similar to that seen in embryonic muscle.

Xenopus oocytes were used as an expression system to detect neuronal mRNAs coding for a variety of pharmacological receptors. Following injection of 14-16 day rat brain mRNA, oocytes became responsive to micromolar concentrations of serotonin, glutamate and histamine. Both an inward and outward current response could be

elicited with histamine, the latter being mediated by a H_2 receptor and carried by K^+ ions.

Because of reports indicating the alteration of ion channel expression during tumorigenesis, a study of the passive electrical properties of two closely related tumorigenic and non-tumorigenic hybrid cell lines was performed. The membrane properties of these two cell lines, however, were similar and apparent differences were associated with differences in the average cell sizes of the two lines. The membrane potential could be well controlled during voltage clamp experiments on colonies up to thirty-two cells in size, using the whole-cell voltage clamp technique. There was a linear relationship between the number of cells in a colony and the total membrane capacitance and conductance of a colony. The membrane properties of single isolated cells were the same as cells from small colonies and had relatively high input resistances.

In conclusion, a number of different biological systems were studied for modulation of ion channel expression. In particular, the T lymphocyte system proved to be very amenable to study, using a range of cell biological techniques. This system will undoubtedly prove to be useful in further studies on the regulation of voltage-gated ion channel expression, particularly when molecular genetic techniques become available for the study of potassium channels.

CONTENTS

CHAPTER ONE

Control of Ion Channel Expression

1.1 INTRODUCTION

Many and various have been the attempts to understand the biochemical and genetic mechanisms which control ion channel expression. On one level these attempts have all been part of a much larger and more general problem, the control of protein expression. As an intellectual problem, however, studying the mechanisms which control the expression of ion channels has offered one significant attraction. It is very probable that modulation of ion channel expression is one important source of neuronal plasticity and, as such, control of ion channel expression is a candidate for an important role in the processes of learning and memory.

1.2 OUTLINE OF THESIS

I first became interested in the control of ion channel expression during work on the acetylcholine receptors in denervated rat muscle, and some of this initial work is reported in Chapter 3 of this thesis. I then began to look for a suitable in vitro system for studying channel expression, and the comparison of tumorigenic and non-tumorigenic human hybrid cell lines is a first attempt to find such a system (Chapter 5). I was also involved in a project to model the cell interactions which trigger lymphokine release from activated T lymphocytes (Appendix 1). Through this study I became aware of the great advantages of T cells for cell biology studies and the study on potassium channel expression during T cell development, reported in Chapter 2, is the outcome of this realization. Finally, I attempted to use the *Xenopus* oocyte expression system as an assay system for cloning the T cell potassium channel, using a strategy similar to that which was used successfully to clone interleukin-3 (Fung et al, 1985). This system proved too slow and cumbersome to be suitable for screening a large library of cDNAs, particularly when the messenger RNA in question was undoubtedly rare. The work described in Chapter 4 on the expression of histamine receptors in the oocyte is the outcome of preliminary experiments using this expression system.

The rest of this chapter is a survey of the literature on the control of ion channel expression.

1.3 THE NICOTINIC ACETYLCHOLINE RECEPTOR OF SKELETAL MUSCLE

The nicotinic acetylcholine receptor (AChR) of skeletal muscle is, by far, the best studied ion channel with respect to structure, function and control of expression. I begin, therefore, with a review of the literature on the AChR, since it is the paradigm within which much of the thinking about ion channel expression has been conducted.

1.3.1 Structure

Analysis of amino acid composition and amino-terminal sequence data obtained from the AChR of both *Torpedo californica* and fetal calf skeletal muscle has shown that the AChR is a pentameric complex with four homologous subunits in the stoichiometric ratio $\alpha_2 \beta \gamma \delta$ (Raftery et al, 1980; Conti-Tronconi et al, 1982). Considerable further progress in

elucidating the structure of the AChR has been made using recombinant DNA technology. From the protein sequence data, synthetic oligonucleotide probes have been constructed, and by isolation and sequencing of DNA complementary to the mRNAs coding for the AChR in *Torpedo*, the complete primary structure of the four subunits has been determined (Noda et al, 1982; Noda et al, 1983b; Claudio et al, 1983; Noda et al, 1983c). Subsequently, complete complementary DNA (cDNA) sequences for the four subunits of the calf AChR have been obtained (Noda et al, 1983a; Takai et al, 1984; Tanabe et al, 1984; Kubo et al, 1985). In addition, the structure of a fifth homologous ε subunit has been reported (Takai et al, 1985). This subunit was isolated following cross-hybridization with the calf γ subunit with which it has approximately 53% homology. Clones coding for the mouse skeletal muscle α and δ subunits have also been isolated and sequenced (LaPolla et al, 1984; Boulter et al, 1985).

Genomic sequences coding for the δ and γ subunits of chicken have been described (Nef et al, 1984). These two genes were found to be contiguous in the genomic DNA fragment isolated, a result which is consistent with the hypothesis that the two genes arose by gene duplication. The human genomic sequences for the α and γ subunits have also been isolated and sequenced (Noda et al, 1983a; Shibahara et al, 1985).

A number of structural features are common to all the subunits sequenced so far. Each subunit has four strongly hydrophobic regions which probably form α-helices spanning the lipid membrane. In addition, a fifth amphipathic α-helix membrane spanning region has been proposed (Guy, 1984; Finer-Moore and Stroud, 1984), and corresponding amphipathic regions have been found in all sequenced subunits. This amphipathic region may form part of the channel wall. Three cysteine residues and one potential N-glycosylation site are also conserved in all the known sequences.

Sequence homology between the various species is considerable. For the α subunit, homology between the mammals (mouse, human, calf) and *Torpedo* is approximately 80%. Homology between the three mammal sequences is of the order of 95%, and is even higher in selected regions. The first three hydrophobic membrane spanning regions of the α subunit show close to 100% conservation between several species (Boulter et al, 1985; Shibahara et al, 1985). Similary, the region including the acetylcholine (ACh) binding site is very highly conserved. Cross-species homology for the other three subunits is less than that for the α subunit, being in the range 54-59% for mammal versus *Torpedo*, and in the range 87-92% between mammals. Not surprisingly, chick sequence homology is intermediate between mammals and fish.

The quaternary structure of the AChR is thought to resemble a barrel, with each of the five subunits acting like a barrel stave surrounding the central cation channel, resulting in a structure with approximately pentagonal symmetry (Stroud and Finer-Moore, 1985; Brisson and Unwin, 1985). When viewing the extracellular face, the subunits may be arranged in the clockwise order α, γ, α, δ, β (Changeux et al, 1984). Each subunit has an extracellular domain that extends 55-70 Å above the membrane, a transmembrane domain that contains

α-helices oriented perpendicularly to the membrane surface, and a cytoplasmic domain that extends 20-45 Å below the membrane surface (Kistler et al, 1982; Brisson and Unwin, 1985). The overall diameter of the receptor is approximately 80-90 Å.

1.3.2 Function

Using cDNA directed synthesis of mRNAs coding for the four subunit precursors of the*Torpedo* AChR, it has been possible to induce expression of functional AChRs in *Xenopus* oocytes (Mishina et al, 1984). The results showed clearly that the coordinate expression of the α, β, γ and δ subunits was both a necessary and sufficient condition for full expression of AChR function.

The approach used in two further studies was to mix AChR subunits from different species and examine the properties of AChRs composed of different combinations of receptor subunits. Using *Torpedo* and calf subunits, Sakmann et al (1985) found that the average open time of the calf AChR single channel currents was approximately 10 times greater than that of *Torpedo*, and that the channel open time of the *Torpedo* AChR was independent of membrane potential whereas the calf channel open time was strongly dependent upon membrane voltage. The single channel conductance of the two channels was not significantly different. Thus, it was theoretically possible to determine which subunit substitution had the greatest effect upon channel lifetime and/or voltage dependence. It was found that both the calf α or δ subunits could substitute for the equivalent *Torpedo* subunits i.e. AChRs containing either $\alpha_C \beta_T \gamma_T \delta_T$ or $\alpha_T \beta_T \gamma_T \delta_C$ combinations of subunits were functional receptors. Substitution of the calf β or γ subunits, however, resulted in a considerably impaired ability of the receptor to assemble correctly in the membrane (Sakmann et al, 1985). The results obtained with the two functional substitutions suggested that the average open time of single channel currents was more strongly dependent upon the δ subunit than the α subunit, the subunit containing most of the ACh binding site. This result supports the idea that channel lifetime is dependent upon the rate of receptor conformational change rather than upon the rate of agonist dissociation. The voltage dependence of channel lifetime appeared to be solely a property of the δ subunit. Single channel conductance was not greatly affected by either subunit substitution. White et al (1985) found that the mouse δ subunit could also substitute for the *Torpedo* δ subunit to give functional receptors. They found that oocytes injected with only the α, β and δ subunits exhibited a small response to ACh.

1.3.3 Control of Expression

In normally innervated mammalian skeletal muscle the distribution of AChRs is restricted to a small synaptic region of the muscle. The number of AChRs in this synaptic region can be measured using autoradiography following binding of ^{125}I-labelled α-bungarotoxin. For rat skeletal muscle, the number of binding sites is of the order of 2-4 x 10^7 per neuromuscular junction (Fambrough and Hartzell, 1972). This number must be divided by two to give the actual number of AChRs, since there are two α-bungarotoxin binding sites per molecule. Using electrophysiological techniques a considerably lower

estimate, approximately 2 x 10^6 AChR channels per end-plate, was obtained for rat skeletal muscle (Sterz et al, 1983). Possible errors in the electrophysiological study which could lead to an underestimate of receptor numbers include receptor desensitization and an overestimation of ACh efficacy. Possible errors in the binding studies include non-specific binding, binding to non-functional receptors and binding to the presynaptic membrane, all of which will lead to an overestimate of receptor numbers at the end-plate (Fambrough, 1979). These potential sources of error suggest that binding studies and electrophysiological studies will give upper and lower limits for actual receptor numbers respectively. In general, however, there is good agreement between these two techniques when relative changes are measured although the absolute values are often at variance.

AChRs are not uniformly distributed at the end-plate but are localized to the juxtaneural portions of the folded postsynaptic surface where they occur at very high packing densities, of the order of 30,000 α-bungarotoxin binding sites per square micron (Fertuck and Salpeter, 1974). Regions of the muscle membrane away from the point of innervation have much lower concentrations of receptors, of the order of 10 binding sites per square micron (Fambrough, 1974 , 1979). Electrophysiological techniques can detect no response at all to ACh in the extrajunctional regions of fast twitch muscles, although a weak extrajunctional response can be obtained from slow twitch muscles (Miledi and Zelena, 1966).

If the nerve innervating a skeletal muscle is cut, a large increase in the extrajunctional receptivity for ACh occurs over a period of a few days (Axelsson and Thesleff, 1959; Miledi, 1960). A corresponding increase in the number of α-bungarotoxin binding sites is also observed, with 14 day denervated rat diaphragm muscle having approximately 640 binding sites per square micron (Fambrough, 1974). Distribution of receptors is non-uniform, with regions or localized patches of higher receptor density (Fambrough, 1979). It has been shown that prior to innervation, fetal muscle also has considerable numbers of AChRs spread over the entire surface of the muscle (Fambrough, 1979).

The increase in AChR numbers following denervation involves activation of the relevant genes. If RNA synthesis is blocked with 1μg/ml actinomycin D, a concentration capable of blocking 80% of RNA synthesis in muscle, then the rise in extrajunctional ACh sensitivity is completely blocked (Fambrough, 1970). Similarly, if protein synthesis is blocked with cycloheximide (10 μg/ml), development of extrajunctional ACh sensitivity is also blocked (Fambrough, 1970).

It has been known for some time that there are a number of differences between the junctional AChR of adult skeletal muscle and the extrajunctional AChR of denervated and fetal muscle. Brockes and Hall (1975) have shown that the isoelectric point of the two forms of the receptor is different. It has been shown for rat muscle that the single channel conductance of the junctional channel is approximately 50% greater than that of the extrajunctional channel, and that the average channel open time of the junctional receptor is approximately four times shorter than that of the extrajunctional receptor (Sakmann, 1975).

The turnover rate of extrajunctional receptors is also much greater than that of junctional receptors. Junctional receptors have a mean half-life in the membrane of at least 7 days, compared with a half-life of less than 24 hours for the extrajunctional receptor (Edwards, 1979; Fambrough, 1979). More recent studies, using single channel recording techniques, have shown that AChRs in the non-synaptic region of fetal and denervated muscle are not solely of the extrajunctional form. The high conductance, brief lifetime junctional channel has been observed in both fetal muscle (Sakmann et al, 1983) and in non-junctional regions of denervated muscle (Chapter 3). However, in both these tissues the predominant form of the receptor is the extrajunctional one.

A recent paper by Mishina et al (1986) has thrown new light upon the relationship between the extrajunctional and junctional forms of the AChR. Their results suggest that the difference between the two forms of the AChR is due to a change in one of the AChR subunits. Substitution of the γ subunit with the ε subunit appears to be responsible for the change from the extrajunctional to the junctional form. When *Xenopus* oocytes were injected with mRNAs specific for the α, β, δ and γ subunits, a low conductance ($\approx$ 40 pS), long lifetime ($\approx$ 10 ms) form of the AChR was produced. In contrast, when oocytes were injected with mRNA coding for the α, β, δ and ε subunits, a higher conductance ($\approx$ 60 pS) and shorter lifetime ($\approx$ 5 ms) channel was observed. The kinetic and ion permeation properties of these two channels was very similar to those of the extrajunctional and junctional AChRs found in fetal and adult bovine muscle respectively, suggesting that the extrajunctional AChR has a subunit structure of $\alpha_2 \beta \gamma \delta$, whereas the junctional AChR has the structure $\alpha_2 \beta \varepsilon \delta$.

Data obtained from blotting experiments is consistent with the electrophysiological evidence (Mishina et al, 1986). In these experiments, Northern blot hybridization analysis of total RNA from diaphragms of calves at different stages of fetal and postnatal development was conducted using cDNAs coding for each of the five sequenced calf AChR subunits. The amounts of mRNA coding for the γ and ε subunits showed reciprocal changes during development. The γ subunit was abundant at early stages of fetal development, but was barely detectable after birth. Conversely, the ε subunit mRNA was not detectable until late fetal and postnatal stages. The change from the extrajunctional form of the AChR found in fetal muscle to the junctional form found in adult muscle appears, therefore, to be due to a gradual switch from production of the γ subunit to production of the ε subunit. The greater number of acidic residues and fewer basic residues of the ε subunit, compared with the γ subunit, probably accounts for the difference in isolelectric point observed between the junctional and extrajunctional AChRs (Brockes and Hall, 1975). The exact nature of the genetic mechanism controlling the switch in production from the γ subunit to the ε subunit during development remains uncertain.

Understanding of the mechanisms which control the overall expression of functional AChRs also remains confused. The evidence to date suggests that there is both transcriptional and post-translational control of AChR expression. Following denervation of

mouse lower hind limb muscles there is a 100-fold increase in the amount of mRNA coding for the α subunit of the AChR (Merlie et al, 1984). However only a 7-fold increase in α subunit mRNA was observed after denervation of rat diaphragm (Goldman et al, 1985). It is probable that the increase in α subunit mRNA production observed in the rat diaphragm is too small to account for both the increase in total receptor number and the increased rate of AChR degradation seen following denervation (Edwards, 1979). The 100-fold increase in α subunit mRNA observed in mouse however (Merlie et al, 1984) appears to be sufficent to account for both processes.

In cultured chick myotubes, there is a decrease in AChR numbers after the onset of spontaneous contractile activity. If spontaneous contraction is then blocked with tetrodotoxin (TTX), there is a subsequent increase in AChR expression. Klarsfeld and Changeux (1985) found an approximately two-fold increase in AChR expression following TTX treatment of spontaneously contracting chick myotubes but found a 13-fold increase in α subunit mRNA. The discrepancy between increases in α subunit mRNA and AChR expression suggested to the authors that mechanisms other than transcriptional control were important in regulating AChR expression.

It is possible that transcription of mRNA for a subunit other than the α subunit is the limiting factor in controlling expression of functional AChRs, but at present, there are no studies in which changes in both the level of transcription of all five AChR mRNA species and the amount of AChR expressed have been measured. Mishina et al (1986) found that mRNAs coding for the α and β subunits were present at much higher levels in innervated muscle than was the δ subunit mRNA. If the efficiency of translation of these three mRNAs is equal, then the rate of production of the δ subunit rather than the α or β subunits would control the overall rate of AChR assembly. Similarly, both the γ and ε subunits could well be more important than the α and β subunits in controlling AChR expression.

To understand the potential sites of post-transcriptional control of AChR expression it is first necessary to have a model of the steps involved in production of the functional AChR. To date, four distinct stages in AChR synthesis have been identified (Anderson and Blobel, 1983; Merlie et al, 1983; Merlie and Smith, 1986). 1) Protein synthesis of the AChR subunits occurs in the rough endoplasmic reticulum (RER), and insertion of each subunit into the RER membrane occurs concomitantly with elongation of the nascent polypeptide. Core N-glycosylation also occurs during translation as does cleavage of the signal peptide. 2) Maturation of the α subunit in the endoplasmic reticulum appears to be necessary to gain α-bungarotoxin binding activity (Merlie and Lindstrom, 1983). Newly synthesized α subunits do not have detectable binding activity until 15 to 30 minutes after completion of primary translation. The changes occuring during this maturation process may depend upon covalent modifications such as disulfide bond formation (Merlie and Lindstrom, 1983). In the muscle cell line BC_3H-1, this step appears to be very inefficient, with only approximately 30% of synthesized α subunits being converted to the toxin-binding form. The other 70% of α subunits are rapidly degraded (Merlie et al, 1983). 3) Assembly of the α subunit into a

functional multisubunit AChR occurs between 60 and 90 minutes after initial synthesis. 4) Transport of the AChR to the cell surface in coated vesicles is the final step leading to AChR expression (Bursztajn and Fischbach, 1984).

There is some evidence that post-translational control is important in determining the number of functional AChRs present in the surface membrane of BC_3H-1 cells (Olsen et al, 1984). During log growth phase BC_3H-1 cells do not express significant numbers of the AChR, but produce considerable quantities of the α subunit mRNA. After growth arrest, cell surface AChR numbers increase greater than 100-fold, whereas the amount of α subunit mRNA increase is only 4-fold. A significant rate of synthesis of the α subunit is maintained throughout the log growth phase, but the efficiency of assembly of α subunits into mature AChRs is only one-half to one-third that observed in quiescent cells (Olsen et al, 1983). In addition, the receptors that are assembled are not transported to the cell surface. In light of these findings, it was suggested that post-translational control of AChR expression could occur at the level of subunit assembly and/or transport to the surface membrane. The possibility that translational control of a receptor subunit, other than the α subunit, is responsible for the apparent post-translational control of AChR expression seen in BC_3H-1 cells cannot be conclusively eliminated at present.

The two physiological signals which regulate AChR expression in skeletal muscle are muscle activity and neurotrophic factors. The expression of extrajunctional AChRs following denervation is very dependent upon changes in the pattern of muscle activity (Lomo and Westgaard, 1976). If denervated muscles are stimulated with direct electrical current pulses, either in vivo or in vitro, extrajunctional ACh sensitivity can be markedly reduced (Lomo and Rosenthal, 1972; Drachman and Witzke, 1972; Cohen and Fischbach, 1973; Purves and Sakmann, 1974). The rate at which ACh sensitivity falls is dependent upon the amount and pattern of electrical activation. Brief, high-frequency bursts of stimulation are much more effective than low frequency stimulation rates, even if the total amount of stimulation is kept constant (Lomo and Westgaard, 1975). Increasing the total amount of stimulation increases both the rate and effectiveness of suppression of extrajunctional ACh sensitivity (Lomo and Westgaard, 1975). Whether muscle activity by itself can completely account for the suppression of extrajunctional AChRs following muscle innervation is difficult to establish (Fambrough, 1979). Using both electrophysiological and α-bungarotoxin binding techniques, it has been shown that direct stimulation of denervated soleus muscles can reduce the number of extrajunctional AChRs back to, or even below, control innervated muscle levels (Lomo and Westgaard, 1976; Frank et al, 1975). These results suggest that, under some experimental conditions at least, muscle activity per se is sufficient to account for the loss of extrajunctional AChRs following innervation. The fall in extrajunctional AChR numbers during direct electrical stimulation occurs as a result of a decreased rate of AChR synthesis (Reiness and Hall, 1977; Linden and Fambrough, 1979).

The mechanism by which direct electrical stimulation of muscle suppresses denervation supersensitivity remains uncertain. It has been suggested that the increase in

intracellular calcium concentration during muscle activity may be one important biochemical signal (Lomo and Westgaard, 1976; Edwards, 1979). Forrest et al (1981) have shown that, following organ culture of denervated rat diaphragm muscles for 48 hrs in the presence of 1 μM A23187, a divalent cation ionophore, the number of extrajunctional AChRs falls to 39% of the level found in control denervated muscles. Suppression of extrajunctional ACh sensitivity by A23187 was dependent upon extracellular calcium. The ionophore did not affect the degradation rate of the AChR, implying that it was suppression of AChR synthesis which caused the fall in AChR numbers.

Similar results have been found using cultured embryonic rat muscle fibres in which spontaneous contraction was blocked with TTX (Rubin, 1985). In this case treatment with 1 μM A23187 for 48 hr produced a 4-5 fold decrease in AChR numbers compared with controls. Calcium ionophore when added to chick cultures treated with TTX produced a greater than two-fold decrease in AChR numbers in 20 hrs (McManaman et al, 1982). This incubation time was probably too short to see the full effect of treatment because assembly of functional AChRs and insertion into the plasma membrane can continue for some time after suppression of AChR mRNA synthesis (Olsen et al, 1983).

One group have described apparently contradictory results. They found that A23187 produced a 40% increase in AChR numbers in cultured chick myoblasts after 48 hrs (Birnbaum et al, 1980). This study did not control for the effects of the ionophore on spontaneous contraction. If, as has been shown using rat skeletal muscle (Forrest et al, 1981), the ionophore produced a significant hyperpolarization of the cultured chick muscle cells, then spontaneous contraction could have been markedly inhibited. Birnbaum et al (1980) confirmed in their study that inhibition of spontaneous contraction could result in a significant increase in AChR production.

In the case of synaptogenesis, the mechanisms controlling AChR expression are more complex than those controlling denervation supersensitivity, and both trophic factors and muscle activity appear to be important. Initiation of synaptogenesis requires contact between the muscle and the innervating nerve. It is not known whether the contact required is direct cell-cell interaction between the nerve and muscle or whether the release of trophic factors from the nerve terminal is sufficient to initiate the local differentiation process. One trophic factor from nerve extracts has been identified and isolated (Jessell et al, 1979; Usdin and Fischbach, 1986). It is a large (42 kD) protein whose activities include increasing the rate of receptor incorporation into myotube membranes and promotion of the formation of receptor clusters (Usdin and Fischbach, 1986). It is uncertain whether this factor acts by increasing the rate of AChR subunit synthesis or whether it increases the efficiency of receptor assembly. The apperent function of this factor is to stimulate the rapid accumulation of AChRs into a high density cluster at the site of nerve-muscle contact. The AChRs which accumulate at the developing synapse are both newly synthesized receptors and receptors which previously were distributed diffusely across the muscle surface (Ziskind-Conhaim et al, 1984; Role et al, 1985).

Muscle activity appears to be important for completion of the later stages of synaptogenesis. One strategy for studying the role of electrical activity in synaptogenesis is to examine the formation of ectopic synapses in adult muscle by a foreign nerve after sectioning of the original nerve. The foreign nerve can then be cut at different times after initiation of ectopic synapse formation and the contribution of electrical activity to the continued development of the ectopic synapse can be seen (Lomo and Slater, 1980). It has been shown that, during the formation of both normal and ectopic rat muscle synapses, the average channel lifetime of the AChR changes from about 4 ms to 1 ms and that there is a transition period during which there are significant numbers of both long and short lifetime AChRs (Sakmann and Brenner, 1978; Fischbach and Schuetze, 1980; Brenner and Sakmann, 1983). This change in channel lifetime may be due to a change in the subunit structure of the AChR from $\alpha_2 \beta \delta \gamma$ to $\alpha_2 \beta \delta \varepsilon$ (Mishina et al, 1986). The change in channel kinetics at ectopic synapses is not complete until about 18 days after cutting of the original nerve (Brenner and Sakmann, 1983). If the ectopic nerve is cut 3-7 days post denervation, before any change in channel kinetics occurs, and muscle activity is maintained by direct electrical stimulation, then the change from slow to fast channel kinetics can continue in the absence of any further neural presence (Brenner et al, 1983). This result suggests that a relatively brief period of contact between the nerve and muscle can trigger a sequence of differentiation events which are then independent of further input from the nerve itself. It has been shown that the development of acetylcholinesterase activity at ectopic synapses can also continue after only a brief contact from the nerve if muscle activity is maintained by direct electrical stimulation (Lomo and Slater, 1980).

How neural contact can induce an apparently permanent change in gene expression at a discrete site in the muscle membrane remains largely undetermined. It is interesting to note that nuclei directly adjacent to the synapse produce mRNA coding for the α and δ subunits of the AChR at a much greater rate than do nuclei in extrasynaptic regions of the muscle suggesting that innervation has selective effects on synaptic nuclei compared with extrasynaptic nuclei (Merlie and Sanes, 1985).

1.4 THE NEURONAL NICOTONIC ACETYLCHOLINE RECPTOR

It has been known for some time that there is a class of neuronal nicotinic acetylcholine receptors which can be differentiated pharmacologically from the nicotinic receptor of the neuromuscular junction. Nicotinic receptors in autonomic ganglia are blocked by hexamethonium but not by decamethonium, a compound which blocks neuromuscular transmission (Paton and Zaimis, 1951). Neuronal AChRs found on Renshaw cells and the rat phaeochromocytoma cell line PC12 can be activated by nicotinic agonists, but are not blocked by α-bungarotoxin (Duggan et al, 1976; Patrick and Stallcup, 1977a). The neuronal AChRs found on PC12 cells are, however, structurally related to the muscle AChRs because antibodies directed against the muscle AChR can cross-react with neuronal AChRs (Patrick and Stallcup, 1977b). In addition to the neuronal AChR there is an α-bungarotoxin binding

protein on some neurons and on PC12 cells (Salvalterra and Moore, 1973; Patrick and Stallcup, 1977b). The function of this protein is not clear since it does not appear to act as an ion channel (Patrick and Stallcup, 1977a), and the profile of toxin binding in brain sections is quite different to the binding profile of acetylcholine (Clarke et al, 1985).

The neuronal AChR has electrophysiological properties similar to those of the muscle AChR. AChRs in bovine chromaffin cells have a single channel conductance of approximately 44 pS, an average lifetime of 27 ms and a desensitization time constant of several seconds (Fenwick et al, 1982). Channels in chick ciliary ganglion neurons have a conductance of 40 pS, a much shorter lifetime of 1 ms, and desensitization half time of 3s (Ogden et al, 1984).

Three different neuronal α subunits have been cloned by means of low stringency hybridization between cDNA clones of the α subunits from muscle AChRs, and cDNA libraries prepared from the PC12 cell line or from rat or chick brain (Mauron et al, 1985; Boulter et al, 1986; Goldman et al, in press). These neuronal α subunits have been designated as α-2, α-3 and α-4 to distinguish them from the muscle α subunit which is known as α-1. The rat α-3 neuronal subunit has 47% amino acid homology with the mouse muscle α-1 subunit and a number of key structural features of the muscle AChR have been well conserved (Boulter et al, 1986). In particular, there is strong homology between the two receptors in the four hydrophobic membrane spanning regions and retention of an amphipathic helix sequence with a similar distribution of charged and uncharged residues. In addition, the four cysteine residues thought to form disulfide bonds essential for secondary structure are conserved, and the potential glycosylation site at Asparagine 141 is retained (Boulter et al, 1986). The protein encoded by the rat α-4 gene exhibits 42% amino acid sequence homology with the protein encoded by the α-3 gene and 35% homology with the muscle α-1 subunit. This α-4 subunit also retains all the key structural features which are common to the other α subunits (Goldman et al, in press).

The picture of the AChR gene family that is gradually emerging suggests that a single primordial AChR gene has undergone gene duplication and subsequent differentiation to give the five different genes known to contribute to formation of muscle AChRs, as well as the still undetermined number of genes involved in formation of the different neuronal AChRs. At what stage during evolution the duplication of this primordial gene occurred is uncertain, although recent results on the insect neuronal AChR suggest the possibility that gene duplication may have ocurred subsequent to the divergence of insects.

One neuronal insect AChR has been identified and isolated in locusts by means of its ability to bind α-bungarotoxin (Breer et al, 1985). A surprisingly high degree of conservation of amino acid sequence between the insect and vertebrate AChRs is suggested by the fact that both α-bungarotoxin and a number of antibodies directed against the torpedo AChR can bind to this insect neuronal AChR (Breer et al, 1985). That this α-bungarotoxin binding protein can indeed form a functional AChR has been shown by reconstitution of the protein into lipid bilayers, where it forms an ACh-activated cation-selective ion channel with

a conductance of ≈75 pS (Hanke and Breer, 1986). This insect AChR appears to be composed of identical or very similar subunits ($M_r \approx 65,000$) which combine to form a tetramer with a molecular size of 250,000 to 300,000 (Breer et al, 1985). To determine whether this insect AChR is in fact composed of identical subunits coded for by a single gene will require the application of recombinant DNA technology. Assuming that the insect AChR is formed from identical subunits, the gene coding for those subunits would presumably be related directly to the putative primordial AChR gene. The ability of this gene product to bind α-bungarotoxin suggests that the muscle α subunit gene may be the AChR gene in vertebrates which is most closely related to the ancestral AChR gene, a hypothesis which is supported by the fact that the α-1 subunit gene is the most slowly evolving of all of the AChR genes for which data is available.

Relatively little is known about the control of neuronal AChR expression, although one recent finding is of interest. There are two classes of neurons in sympathetic ganglia of the frog, known as B and C cells, which are innervated by two different classes of cholinergic preganglionic axons, called B and C fibres, respectively (Marshall, 1985, 1986). The mean channel open time for AChRs in B and C cells is ≈5 ms and ≈10 ms, respectively (Marshall, 1986). If B cells are denervated and allowed to become innervated with C fibres, the B cells acquire the long open time ACh channels normally seen in C cells (Marshall, 1985). These results suggest that the kinetic properties of synaptic channels can be influenced by the type of innervating fibre. Whether this effect is due to neurotrophic factors or to differences in the discharge pattern of the preganglionic fibres remains to be determined. It would be of interest to know whether the change in channel kinetics involves a subunit substitution, such as is seen at the developing end-plate.

1.5 BIOCHEMICAL AND GENETIC STUDIES ON THE CONTROL OF VOLTAGE-ACTIVATED ION CHANNEL EXPRESSION

As noted previously, current understanding of all facets of the nicotinic AChR is far greater than for any other ion channel. There is, however, a considerable body of work relating to other channels which is reviewed here with respect to control of ion channel expression.

1.5.1 Sodium Channels

DNA complementary to the mRNA coding for the voltage-activated sodium channel of the electric eel has been cloned and sequenced using a strategy essentially identical to that used to clone the AChR (Noda et al, 1984). The sodium channel protein was isolated and partial amino acid sequences were determined. Oligonucleotide probes containing all possible cDNA sequences predicted by one of the partial amino acid sequences were then used to screen a cDNA library to identify positive clones. From a complete cDNA sequence it was concluded that the sodium channel was composed of 1,820 amino acid residues with a molecular weight of 208,321 (Noda et al, 1984).

Using the sodium channel cDNA from electric eel as a probe, cDNA clones for two

distinct rat brain sodium channels have also been isolated (Noda et al, 1986a). From the cDNA sequences it was calculated that the two sodium channels from rat brain are composed of 2,009 and 2,005 amino acid residues with calculated molecular weights of 228,758 and 227,840 respectively. Amino acid sequence homology between the two rat brain sodium channels is 87%. Between the rat brain channels and the electric eel, homology is 62%. From partial sequence data and hybridization experiments it was concluded that there may be a number of other distinct forms of the sodium channel gene yet to be isolated (Noda et al, 1986a).

It has been suggested that the channel protein contains four repeated homology units which are orientated across the membrane in a pseudosymmetric fashion, similar to that proposed for the five subunits of the AChR (Noda et al, 1984; Noda et al, 1986a). Within each of the four homologous regions, there are thought to be six membrane spanning regions which presumably contribute to the formation of the ion channel (Noda et al, 1986a). One of the membrane spanning regions is rich in positively charged arginine and lysine residues, and this region may act as a voltage sensor, and would therefore be important in gating of the ion channel (Noda et al, 1986a). One unusual feature of the sodium channel amino acid sequence is the absence of an amino terminal signal peptide sequence, which is found in most membrane spanning proteins, including the AChR. This suggests that both the N-terminal and C-terminal end of the sodium channel polypeptide are on the cytoplasmic side of the membrane (Noda et al, 1984; Noda et al, 1986a).

It has been shown that the rat brain sodium channel cDNA clones can act as templates for the synthesis of mRNA which, when injected into *Xenopus* oocytes, can direct the synthesis of functional sodium channels (Noda et al, 1986b). This result has suggested that formation of functional rat brain sodium channels requires only a single polypeptide chain, and is not dependent upon auxillary polypeptides as suggested from biochemical studies (Messner and Catterall, 1986).

Biosynthesis of the sodium channel protein involves a number of post-translational processing steps which are broadly similar to those described for the biosynthesis of the AChR (Schmidt and Catterall, 1986). Biosynthesis is dependent upon glycosylation (Bar-Sagi and Prives, 1983; Waechter et al, 1983), and the glycosylation process is relatively complex and slow, involving a number of intermediate steps (Schmidt and Catterall, 1986). The degradation rate of the sodium channel is slow. The half-life of the channel in the cell membrane of neurons in primary culture is approximately 50 hrs (Schmidt and Catterall, 1986).

Little is known about the physiological signals which regulate sodium channel expression. Control of expression has been studied in developing and denervated skeletal muscle and in cultured muscle cells. There are a number of similarities between sodium channel regulation in these tissues and regulation of the AChR. Fetal rat muscle initially expresses a sodium channel which is relatively resistant to TTX (Harris and Marshall, 1973). The level of expression of this channel falls during synaptogenesis, and there is a

concomitant increase in the numbers of the adult TTX-sensitive channel (Harris and Marshall, 1973; Sherman and Catterall, 1982). Upon denervation of adult skeletal muscle the TTX-resistant channel reappears, and there is a fall in the level of expression of the TTX-sensitive channel (Redfern et al, 1970; Pappone, 1980; Sherman and Catterall, 1982).

Fetal rat muscle cells in primary culture express both the TTX-sensitive and TTX-resistant sodium channels, and these cells have been used to study regulation of sodium channel expression (Sherman et al, 1983). As with the extrajunctional AChR, electrical activity of the muscle appears to be important in regulating sodium channel expression, and the biochemical mediator of the effect of electrical activity is possibly calcium ions (Sherman and Catterall, 1984). Blockade of spontaneous contraction with the local anesthetic bupivacaine, TTX or high potassium results in a significant increase in the number of TTX-sensitive sodium channels (Sherman and Catterall, 1984). On the other hand, treatment with the ionophore A23187 causes a decrease in TTX-sensitive sodium channel expression (Sherman and Catterall, 1984). On the basis of these results it has been suggested that calcium influx and release during action potentials could act to reduce the numbers of sodium channels and therefore the electrical excitability of the cell (Sherman and Catterall, 1984).

Regulation of the expression of sodium channels in unmyelinated axons is an interesting but poorly understood problem. If there are too few sodium channels in the axon membrane, action potentials will not be propagated. However, if there are too many channels, the action potential conduction velocity may actually be reduced (Hodgkin, 1975; Adrian, 1975). Thus, overproduction of sodium channels is inefficient because of a reduced rate of electrical conduction and unnecessary protein synthesis. It has been suggested that an increased level of excitability of the nerve cell body, due to overproduction of sodium channels, could increase the basal calcium level in the cell, which could in turn act to decrease sodium channel synthesis (Sherman and Catterall, 1984). However, cells with both high and low rates of excitatory synaptic input and, therefore, high and low rates of activation and calcium influx, would require the same rate of synthesis of sodium channels to maximize conduction velocity in the axon. Intracellular calcium levels do not, therefore, seem to be a good feed-back indicator for regulation of sodium channel production.

There is, however, no other obvious biochemical signal which could give information to the cell on the numbers of sodium channels in the axonal plasma membrane and thereby act in a feed-back system controlling gene expression. One possibility is that regulation of sodium channel gene transcription is not the rate limiting step controlling the number of channels inserted into the cell membrane. It is possible that a cytoskeletal channel-anchoring protein may regulate the number of functional channels found in the membrane (Salkoff and Tanouye, 1986). For example, the cytoskeletal protein, fodrin, appears to play such a role in the regulation of glutamate receptor numbers in hippocampal neurons (Siman et al, 1985).

In nerve cells with myelinated axons, control of sodium channel expression is even more complex. An important property of these cells is the ability to discretely compartmentalize sodium channels to the membrane of the initial segment of the axon and the

nodes of Ranvier, with very few sodium channels in the dendrites and internode membranes, and relatively few on the cell body (Catterall, 1984; Waxman and Ritchie, 1985). The compartmentalization of ion channels to different regions of the nerve cell membrane, as exemplified by the sodium channel, is critical in determining the electrophysiological properties and function of neurons, but the biochemical mechanisms by which nerve cells sort and localise ion channels remain poorly understood, although the cytoskeleton almost certainly plays an important role (Almers and Stirling, 1984).

1.5.2 Potassium Channels

Molecular details on any of the voltage-activated potassium channels are scarce. This omission is due, in part, to the fact that potassium channels make up a tiny fraction of the total cellular protein, making biochemical studies very difficult. Also, the lack of a suitable biochemical probe, such as tetrodotoxin or α-bungarotoxin, which could be used to label the protein has greatly limited progress in this area. Recently, however, two toxins, β-bungarotoxin and dendrotoxin, and the psychotomimetic, phencyclidine, have been shown to block potassium channel function and to bind with high affinity (Peterson et al, 1986; Penner et al, 1986; Sorensen and Blaustein, 1986). It is possible that one of these compounds may ultimately prove to be a useful biochemical probe.

Genetic studies on potassium channel expression using *Drosophila* mutants have given some information. The best studied mutants involving potassium channels are those at the gene locus *Shaker* (Salkoff and Tanouye, 1986; Tanouye et al, 1986). *Shaker* mutants get their name from the fact that mutant flies shake their legs vigorously under ether anesthesia (Salkoff and Tanouye, 1986). The primary lesion of this mutation appears to affect the I_A potassium conductance, which is a rapidly activating and inactivating potassium conductance (Hagiwara et al, 1961; Connor and Stevens, 1971; Neher, 1971).

In *Drosophila* axons, the I_A current is responsible for the rapid repolarization of the membrane potential during action potentials. *Shaker* mutants have an abnormally prolonged action potential, which causes a significant increase in the amount of neurotransmitter released at the neuromuscular junction (Jan et al, 1977; Tanouye et al, 1981). Using voltage-clamp analysis, mutants which have lesions of differing severity have been identified. Some mutants completely eliminate the I_A channel (Salkoff and Wyman, 1981). Complete loss of function of an ion channel normally appears to result in a fatal mutation in *Drosophila*, but I_A channels are partly redundant because of the presence of a second, calcium-dependent, rapidly inactivating potassium conductance which appears at a later developmental stage and acts to reduce the phenotypic severity of the I_A lesion (Salkoff, 1983). One *Shaker* mutant changes the kinetics of the I_A channel without affecting the number of channels present in the membrane (Salkoff and Wyman, 1981), and this mutant provides the best evidence for the suggestion that the *Shaker* locus contains the structural gene of the I_A channel (Salkoff, 1983).

Gene dosage experiments have been performed in which the *Shaker* locus on the X chromosome has been either eliminated or duplicated (Salkoff, 1983). Elimination of the

locus resulted in a complete failure to express the I_A channel as expected, but duplication of the locus did not result in any increase in I_A channel numbers above the levels found in wild type animals (Salkoff, 1983). This result suggests that there is an upper limit to the number of I_A channels that the membrane can accommodate, which is possibly constrained by a cytoskeletal channel-anchoring component (Salkoff and Tanouye, 1986). Thus, regulation of the number of functional I_A channels in the membrane is not exclusively dependent upon regulation of gene transcription, a conclusion which is concordant with the studies on AChR regulation.

There is some evidence that only a single gene product from the *Shaker* locus is necessary for formation of the I_A channel. Flies which are the first generation progeny of a cross between wild type and homozygous I_A channel negative *Shaker* mutants have 50% of the wild type number of channels (Salkoff and Wyman, 1981). If more than one copy of the *Shaker* gene product was necessary to make a functional channel, the number of channels expressed by the heterozygous progeny would be considerably less than 50% (Salkoff and Tanouye, 1986). However, it has not been proven formally that a single gene product is sufficient for the formation of the I_A channel. Of relevance to this question is the finding that a single fraction of size-fractionated mRNA from chick brain has the ability to direct the synthesis of the I_A channel in *Xenopus* oocytes (Sumikawa et al, 1984). However, this result is consistent with either a single gene product or with two or more similar sized products being necessary for channel formation. The mRNA coding for the potassium channel is smaller than that coding for the sodium channel, which suggests that the I_A channel may also be a smaller protein (Sumikawa et al, 1984).

1.5.3 Calcium Channels

The unicellular *Paramecium* have proven to be fertile material for the identification and study of mutations which affect calcium channels. Mutant *Paramecium*, with reduced calcium channel numbers in their cell membrane, have been identified using behavioral criteria and are known as *Pawn* mutants because they can only swim in a forward direction (Kung, 1979). Mutations which can reduce calcium channel numbers affect at least three separate genes (Schein et al, 1976; Kung, 1979). There is no definitive evidence that the primary defect in any of the *Pawn* mutants is in a structural gene of the calcium channel. However, a multi subunit structure for the calcium channel would be consistent with the complex control that many cells can exert over calcium channel function via intracellular messengers. Modification of channel function by allosteric modification of channel structure would most easily be achieved in a multisubunit protein (Changeux et al, 1984). A three subunit structure for the calcium channel is consistent with biochemical studies on the dihydropyridine receptor of skeletal muscle (Curtis and Catterall, 1986).

A second class of *Paramecium* mutant, known as the *cnrC* mutant, also has altered calcium channel function, but in this case the mutation is thought to be due to modification of a small, soluble, cytoplasmic protein which is not a structural component of the calcium channel (Haga et al, 1984). This protein appears to be important in regulating the number of

functional calcium channels in the cell membrane, and injection of the wild-type soluble protein into *cnrC* mutants can rescue the function of apparently defective calcium channels (Haga et al, 1984).

Only one calcium channel mutant has been identified in a multicellular organism. Muscular dysgenic mice have a mutation which causes the failure of excitation-contraction (E-C) coupling in skeletal muscle and associated with this loss of function, is the elimination of the slow calcium current in skeletal muscle, but not in heart muscle or sensory neurons (Beam et al, 1986). It is not known which gene is affected by this mutation. One suggestion is that the slow calcium channel may act as the 'voltage sensor' of E-C coupling, and that failure of calcium channel expression is directly responsible for E-C coupling failure (Rios et al, 1986). This hypothesis remains to be proven. It is possible that the primary defect is due to incorrect morphological association between the t-tubules and the sarcoplasmic reticulum, and that it is this defect which is directly responsible for the loss of both channel function and E-C coupling (Beam et al, 1986).

1.6 DEVELOPMENTAL CONTROL OF VOLTAGE-ACTIVATED ION CHANNEL EXPRESSION

Developmental control of voltage-activated ion channel expresssion has been studied in a number of different biological systems. The Rohon-Beard cells of *Xenopus* embryos have been used to advantage by Spitzer and his colleagues (Spitzer and Baccaglini, 1976; Baccaglini and Spitzer, 1977; Spitzer, 1979, 1985). These sensory neurons are present in the spinal cords of *Xenopus* larvae until metamorphosis, during which time they undergo a programmed cell death. The Rohon-Beard cells are initially electrically inexcitable. During development they gain electrical excitability, first by a calcium-dependent action potential lasting more than 200ms. The action potential then matures over a period of a few days, becomes shorter in duration and more dependent upon sodium ions, until finally the action potential is of brief duration (1-2 ms) and is dependent primarily upon sodium ions. This pattern of development of electrical excitability seems to be quite general for a number of different neuronal and muscle cell types, although it is not universal (Spitzer, 1979, 1985).

The in vivo pattern of development of electrical excitability observed in Rohon-Beard cells can be reproduced in vitro using cultured *Xenopus* spinal cord neurons (Spitzer and Lamborghini, 1976). This system has allowed experimental manipulation of the developmental process using inhibitors of RNA and protein synthesis (O'Dowd, 1983; Blair, 1983). Actinomycin D, a RNA synthesis inhibitor, when added to *Xenopus* spinal cord neuron cultures between 1.5 and 4 hrs after plating, blocks the normal transition from a long calcium-dependent spike to the fast, primarily sodium dependent spike (O'Dowd, 1983). Complete development of the fast sodium dependent action potential appeared to require continued RNA synthesis over an extended period 1.5 to 17 hrs after plating (O'Dowd, 1983). Similar results were obtained when cycloheximide, a protein synthesis inhibitor, was added to the culture media of cells which had been in culture for 5 hrs (Blair, 1983).

There is some evidence to suggest that the shift in ionic sensitivity of electrical excitability observed in the cell body is preceded by a similar change in the membranes of neurites (Willard, 1980). When neurites of cultured embryonic *Xenopus* spinal cord neurons were stimulated with extracellular electrodes the appearance of sodium dependent action potentials in neurites preceded the appearance of similar responses in the cell body by 3 to 5 hours (Willard, 1980). The neurites also rapidly lost the ability to generate calcium or barium dependent action potentials whereas the cell bodies never completely lost this property. These results suggest that during development there are differential rates of insertion and loss of sodium and calcium channels in the membranes of neurites compared with the cell body, which is consistent with the gradients of these channels found in the membranes of adult neurons.

Differential rates of acquisition of channels by cell bodies compared with nerve processes has also been described in developing rat Purkinje cells (Llinas and Sugimori, 1979). At birth these cells do not have a developed dendritic tree, although they do have a distinct axon, and action potential generation is dependent upon sodium ions. Four days after birth, when the cells begin to form dendrites, TTX-insensitive calcium-dependent action potentials can be recorded. This result has been interpreted to mean that calcium channels are inserted primarily into the membrane of developing dendrites, a hypothesis which is consistent with the high density of voltage-activated calcium channels in the adult dendritic tree (Llinas and Sugimori, 1979).

The electrophysiological studies described above primarily used current-clamp recording techniques, and very little information of a quantitative nature was obtained about changes in ion channel numbers or possible developmental changes in the kinetics of the active conductances. In an excellent study, Barish (1985, 1986) has given a quantitative account of the changes that occur both in the number and function of ion channels in neurons from the axolotl *Ambystoma mexicanum*, during development in vitro. Dissociated *Ambystoma* neural plate cells, when first placed in culture, are non-excitable. After 2-3 days in culture the cells extend neurites and become electrically excitable, with action potentials of approximately 100 ms duration. The duration of the action potential gradually shortens to about 1 ms during subsequent maturation over a period of several days (Barish, 1986). Voltage-clamp recordings revealed the presence of voltage-activated sodium, calcium and delayed rectifier potassium conductances in 2 day old neurons. The net inward current measured during depolarizing voltage steps was seen to increase in magnitude during development. Most of this increase was due to an increase in the sodium conductance rather than the calcium conductance, which changed only marginally during maturation. The increase in potassium currents was relatively much greater than the change in inward currents, and the rate of activation of the potassium conductance following depolarizing voltage steps became markedly faster during development (Barish, 1986).

A mathematical model of the conductances in *Ambystoma* neurons showed that it was the increase in potassium channel numbers and increased rate of potassium channel activation

which primarily determined the decrease in duration of the action potential and the apparent shift in ionic dependency of the action potential from calcium to sodium during development (Barish, 1985, 1986). In immature neurons a calcium dependent spike was possible because of the small size and slow rate of activation of the potassium conductance, whereas in mature neurons the rapid activation of the potassium conductance meant that only the rapidly activating sodium conductance could support a regenerative action potential. A calcium-independent action potential was not supported in immature neurons because of the relatively small size of the sodium conductance at this stage (Barish, 1986).

In addition to the changes which the delayed rectifier potassium conductance undergoes during development, a maturation-dependent increase in the number of calcium-activated potassium channels has been reported. This increase will also tend to reduce the duration of calcium dependent action potentials in developing neurons (Blair and Dionne, 1985).

In a voltage-clamp study on developing neurons from the quail neural crest, it was shown that potassium currents are the first active conductances to appear during development (Bader et al, 1983; Bader et al, 1985a). By kinetic and pharmacological criteria, at least two different potassium conductances could be identified in these neurons (Bader et al, 1985a). These two conductances were identified by Bader and colleagues (1985a) as the I_A and the delayed rectifier potassium conductances. Both potassium conductances were present in neurons cultured in vitro for 24 hours but their rate of development was different, and after 4 days in culture the slowly inactivating conductance had increased more than 2-fold, whereas there was no increase in the magnitude of the I_A conductance (Bader et al, 1985a). A further developmental change was observed when neurons were co-cultured with striated muscle cells (Bader et al, 1985b). Under these conditions the rate of inactivation of I_A appeared to be much faster, but it was not certain whether this change was due to selective survival of a subpopulation of neurons with a fast I_A or whether it was due to a developmental change in the type of I_A channel expressed. It was noted that in developing quail neurons, in contrast to the amphibian neurons, the voltage-activated sodium channel appeared before the calcium channel during development in vitro (Bader et al, 1983).

A temporal sequence of expression of ion channels similar to that observed in quail neurons has been seen in developing grasshopper neurons (Goodman and Spitzer, 1981). The complete development of electrical excitability occurs between days 10 and 16 of embryogenesis. On day 10, neurons are electrically inexcitable, but by day 11 a delayed rectifier conductance can be seen in the cell soma. Sodium channels appear first on day 11 in the axon and later at day 11.5 or day 12 in the soma. Calcium channels appear in the cell body on days 12 and 13 and, between days 13 and 16, a calcium-activated potassium conductance becomes apparent (Goodman and Spitzer, 1981).

In the dorsal longitudinal flight muscles of *Drosophila*, ion channel expression can be examined relatively easily using voltage clamp techniques, and the temporal sequence of expression of five different types of voltage activated ion channels has been described

(Salkoff and Wyman, 1983; Salkoff, 1985). In order of appearance these are: the I_A channel, the delayed rectifier channel, an inactivating calcium conductance, a calcium-activated rapidly inactivating potassium conductance and a persistent inward current dependent upon both calcium and sodium ions. The genetic defect at the *Shaker* locus has greatly aided in dissecting out the contributions of the different potassium channels found in this tissue.

In summary, the acquisition of electrical excitability has been studied in a number of biological systems. Few, if any, general rules have emerged and the temporal sequence of channel acquisition has yet to be shown to be of any fundamental importance to the developing organism. The final result, a full complement of channels correctly distributed in the cell membrane, is, of course, critical to the normal function of all higher organisms. For this reason, it is of interest to understand how the final numbers and location of voltage-gated channels is determined. Presumably, for a given neuron, there is a fixed programme of expression of the channel genes, which may depend, in part, on appropriate cellular interactions for complete expression. In addition to this predetermined pattern of gene expression, developing and mature neurons may exhibit a certain amount of plasticity in the level of expresion of different ion channels. Plasticity at the cellular and molecular level must ultimately be the basis of the behavioral plasticity observed in the whole animal and, for this reason, the role of ion channel expression in learning and memory is considered in the next section.

1.7 CONTROL OF ION CHANNEL EXPRESSION IN LEARNING AND MEMORY

Learning can be broadly defined as, 'that change in an organism's behavior in response to a given stimulus which occurs as a result of experience', and memory can be defined as, 'the ability to retain or store that behavioral modification' (Kandel, 1976; Bower and Hilgard, 1981). A large number of psychological and physiological experiments have been performed in an attempt to understand the processes involved in learning and memory. The acquisition of memory appears to be a time-dependent process and the complete establishment of a particular memory involves a period of consolidation, which in humans may last up to two years (Squire et al, 1975). The early phases of memory consolidation are subject to disruption by a number of experimental interventions such as electroconvulsive shock treatment (McGaugh, 1966). Protein synthesis during learning appears to be necessary for the development of permanent memory since protein synthesis inhibitors given during training of experimental animals can block memory consolidation without interfering with initial learning (Davis and Squire, 1984). In some human subjects, following discretely localised brain damage, the ability to establish new permanent memories is lost, while recall of memories established before brain injury remains intact as does the subject's general intellectual abilities and short-term memory (Squire, 1986). Psychological experiments on the recall of nonsense syllables suggest that there is a temporary memory store from which

information is rapidly lost if rehearsal is prevented (Peterson and Peterson, 1959).

On the basis of these and other results, a number of operational models of memory have been proposed, the simplest of which divides memory into short and long term processes. Short-term memory is, by definition, labile, whereas long-term memory is more permanent, lasting weeks or years. The relationship between short- and long-term memories remains undefined and there are at least three logical possibilities: i) memory is a single process and short- and long-term memory are simply two different aspects of this unitary process that can be observed experimentally, ii) memory is a multi-process event, with the formation of long-term memories being dependent upon the prior formation of short-term memories, iii) memory formation involves two or more parallel independent processes with different time courses of formation and decay (Hebb, 1949 pp. 61; McGaugh, 1969; Craik and Lockhart, 1972; Goelet et al, 1986). It is unlikely that the experimental evidence necessary to decide between these competing theories of memory will become available without a detailed understanding of the cellular and molecular bases of learning and memory.

Specific cellular and molecular models of learning have been proposed, and in two theories, modulation of ion channel function is thought to be a fundamental step in the formation of memory. The following is a brief account of these models.

A model of a very simple form of non-associative learning, known as sensitization, has been proposed which depends upon the covalent modification of a potassium channel (Kandel et al, 1986). Sensitization occurs when the presentation of a strong or noxious stimulus causes enhancement of a response to a different stimulus which is normally ineffective or only weakly effective. During sensitization, the enhancement of the reflex response to the weak stimulus by presentation of the strong stimulus is not dependent upon any temporal association between the two stimuli (Kandel, 1976).

In *Aplysia*, stimulation of the siphon elicits a weak gill-withdrawal reflex. This reflex can be sensitized by strong stimulation of the tail. Sensitization of the reflex involves the enhancement of synaptic transmission between the sensory neurons of the siphon and the motor neurons responsible for gill withdrawal. Neurons which are excited by the strong stimulus to the tail are thought to form axo-axonic synapses on the terminals of the siphon sensory neurons and, when stimulated, release serotonin, two small peptides and other unidentified neurotransmitters. It is further suggested that stimulation of putative serotonin receptors on the sensory nerve terminals causes an increase in cAMP levels, which ultimately results in the phosphorylation of a potassium channel in the presynaptic terminal, causing the channel to become inactivated. Inactivation of the potassium channel results in a prolongation of the action potential in the nerve terminal and an increase in the amount of neurotransmitter released. By means of this mechanism synaptic efficiency is thought to be enhanced (Kandel et al, 1986).

Criticisms of this model include: i) anatomical interconnections between neurons which mediate sensitization of the gill-withdrawal reflex are poorly defined; ii) there is no evidence that axo-axonal synapses are solely responsible for sensitization; iii) the

neurotransmitters involved have not been definitely identified; and iv) the model has limited generality since no other example of a similar serotonin sensitive potassium channel has been found in any other organism (Farley and Alkon, 1985). In addition, the inability to record from the presynaptic terminal of the sensory nerve means that the assumption that ion channels in the nerve terminal are modulated by serotonin in the same way as those in the soma has remained untested. In an attempt to answer some of these criticisms, a culture system which attempts to reconstruct the neuronal circuit of the gill-withdrawal reflex in vitro has been developed (Rayport and Schacher, 1986; Belardetti et al, 1986). Whether this system offers any real advantage over the in vivo preparation is debatable, since the entire rationale for using invertebrate preparations for the study of learning is their in vivo simplicity. Cell networks can be constructed in vitro using mammalian cells, and these networks will presumably have an equal probability of reflecting the in vivo situation as does the *Aplysia* culture system.

In the sea mollusc, *Hermissenda*, a form of associative learning, known as classical conditioning, is correlated with a change in the number of active potassium channels in a subset of photoreceptor cells (Crow and Alkon, 1980; Alkon et al, 1982, 1985). Following conditioning experiments in which a light stimulus is paired with rotation of the animal, changes in the photactic behavior of *Hermissenda* can last up to 4 days. Conditioning increased the time taken by an animal to progress towards the light. Associated with this behavioral change was a decrease in the size of two potassium currents, an I_A current and a calcium-activated potassium current (Alkon et al, 1985). The change in active potassium channel numbers is thought to contribute to conditioning by increasing the depolarizing response of the photoreceptor to a light stimulus. This increased excitability of the photoreceptor acts to inhibit a neuronal circuit which mediates the unconditioned response to light, which is an increase in muscle activity resulting in progression towards the light. The biochemical mechanism by which training decreases the potassium conductances is believed to require an increase in intracellular calcium, which may result in the calcium dependent phosphorylation of a number of membrane proteins including the potassium channels (Alkon, 1984; Neary, 1984).

Crow (1985a,b) has suggested that there is a possible paradox in the model proposed by Alkon and colleagues to explain conditioning of the phototactic response. Since *Hermissenda* is positively phototactic and conditioning causes a decrease in phototaxis, how does an enhanced response by a photoreceptor result in a decrease in phototactic behavior? In Alkon's model, inhibitory synaptic interactions between two different types of photoreceptors were suggested as the mechanism by which the increased photoresponse of one photoreceptor ultimately resulted in decreased motor output. Crow (1985b) found, under the light-adapted conditions in which his behavioral experiments were performed, that conditioning produced a diminished photoreceptor response as a result of changes intrinisic to the photoreceptor itself, rather than to synaptic interactions. He concluded that suppression of phototactic behavior, following training, was due to this decreased

photoresponsiveness. Alkon et al (1985) have conceded that changes other than the decrease in potassium conductance reported by them may contribute to the conditioned response under conditions different to the ones they have used, but they reaffirm their model, particularly with respect to the early phase of the conditioned behavior (Lederhendler et al, 1986). It has not been established that changes in the number of active potassium channels are a sufficient condition for eliciting the behavioral changes normally seen following training.

In the two examples of learning cited above, covalent modification of preexisting proteins is the main mechanism by which neuronal responses are thought to be modified. Covalent modifications, which are catalysed by enzymes, can certainly explain the rapid changes in neuronal function which are required during learning and, in some models of memory, covalent modifications are also thought to account for permanent changes in function (Crick, 1984; Lisman, 1985). In both of the examples of learning in invertebrates, the changes are relatively short-term, for *Aplysia* less than an hour, and for *Hermissenda* less than four days. It has yet to be shown experimentally that covalent modifications are sufficient to explain long-term memory acquistion.

The alternative hypothesis, which is supported by the requirement for protein synthesis during the consolidation of long-term memory, is that at least some changes in gene expression are required for the formation of long-term memory. This hypothesis can take essentially two forms, either novel genes are expressed during learning or, alternatively, the level of expression of existing proteins is modified (Davis and Squire, 1984; Goelet et al, 1986). These different hypotheses are not necessarily mutually exclusive. It is possible that new genes are transiently expressed during learning as part of the mechanism of memory acquisition, and that these new gene products are required to induce changes in the level of constitutively produced proteins that are essential for normal neuronal function. The possible requirement for synthesis of novel proteins during learning has been discussed by Kandel and his colleagues and will not be pursued further here (Goelet et al, 1986; Montarolo et al, 1986).

In one sense it is trivial to suggest that the regulation of preexisting proteins is necessary for long-term memory, since it is self evident that the 'house-keeping' proteins of the cell must be expressed in adequate proportions or the neuron will simply die. It is presumably those proteins which are uniquely important to neuronal function which must be strictly regulated if the changes induced by training or learning are to be adequately encoded over a prolonged period of time.

In most models of memory, it is the function of the synapse which is thought to be the controlled variable during the establishment of long-term memory (Hebb, 1949; Marr, 1969), and a number of proteins, which are important for synaptic function, have been proposed as specific candidates for regulation during learning (Stent, 1973; Bailey and Chen, 1983; Black et al, 1984; Siekevitz, 1985). From an 'electrophysiocentric' point of view, the most important molecules contributing to synaptic function are the various voltage- and agonist-activated ion channels, and in a number of models of long-term memory, changes in

the level of expression of agonist-activated ion channels have been proposed (Stent, 1973; Changeux and Danchin, 1976; Lynch and Baudry, 1984).

Despite the emphasis to date on the role of changes in agonist-activated channel expression in long-term memory, it is important to remember that much of synaptic function is mediated by voltage-activated ion channels. The following synaptic events are all critically dependent upon voltage-gated channels:

i) The time course and amount of neurotransmitter release from the presynaptic cell (Llinas et al, 1981).

ii) The amplitude, time course and degree of propagation of synaptic inputs in the dendrites of the postsynaptic cell (Daut, 1973; Byrne, 1980; Cassell and McLachlan, 1986).

iii) The waveform of the response to excitatory synaptic input, and the propensity for bursting or repetitive firing as a result of synaptic input (Traub and Llinas, 1979).

For this reason, a relatively conservative hypothesis is the suggestion that changes in the level of expression of voltage-activated ion channels may contribute to the plasticity of neurons and to the establishment of long-term memory. In support of this hypothesis is the fact that the best understood molecular mechanisms of short-term memory involve relatively modest changes in the levels of active potassium channels. However, even if one tentatively accepts this hypothesis, it may prove exceedingly difficult to verify experimentally because of the background process of maintaining the existing levels of these proteins. It is, therefore, of some interest to find simple model systems in which the level of expression of voltage-gated ion channels is modulated by defined signals, and further to gain some understanding of the genetic and biochemical mechanisms involved in the regulation of channel expression.

Just as it has been necessary to use animals with relatively simple neuronal networks to study the mechanisms of learning at a cellular level, it may be necessary to find even further reduced sytems which are suitable for the study of ion channel expression at a molecular level. In general, the biological systems which can be manipulated most easily and exactly are those which can be studied in vitro and, for the AChR, in vitro approaches have already proven fruitful in increasing our understanding of the control of expression of this protein (Merlie and Smith, 1986). While in vitro systems can only indicate what can occur rather than what actually does occur in vivo, they can provide a window into the world of the whole animal and, in the case of cellular immunology, at least, they have provided the means to enormously accelerate the rate of progress in the understanding of in vivo phenomena.

CHAPTER 2

Changes in the Expression of Potassium Channels During Mouse T Cell Development

INTRODUCTION

Voltage-dependent potassium-selective ion channels have an important functional role in nerve cells, muscle cells and some hormone-releasing cells (Hille, 1984). In these cell types, a K^+ selective ion channel, known as the delayed rectifier K^+ channel, is opened, or activated, following depolarization of the cell membrane to potentials more positive than ≈-50 mV. Opening of the ion channel increases the permeability of the cell membrane to potassium ions which, in turn, acts to restore the cell membrane potential towards the equilibrium potential for potassium ions, typically, in the range -80 to -100 mV. A voltage-dependent K^+ conductance with similar characteristics to the delayed rectifier K^+ conductance of nerve axons (Hodgkin and Huxley, 1952) has recently been described in human peripheral blood T lymphocytes (DeCoursey et al, 1984; Matteson and Deutsch, 1984), human T cell clones (DeCoursey et al, 1985), mouse T cell clones (Fukushima et al, 1984), mouse peripheral lymph node T lymphocytes (DeCoursey et al, 1985) and mouse peritoneal macrophages (Ypey and Clapham, 1984). Using electrophysiological recording techniques it is possible to measure the number of functional K^+ channels in the plasma membrane and quantitate the differences in expression of this particular membrane protein between different T cell subpopulations.

While it has been recognized for many years that the thymus is the primary site for differentiation of T lymphocytes (Metcalf, 1966), attempts to elucidate the pathways of T cell maturation within the thymus have proved difficult and inconclusive. Using monoclonal antibodies (mAbs) to the cell surface determinants Lyt-2 and L3T4 and flow microfluorometry (FMF), four major subpopulations of thymocytes can be identified. A putative precursor population, the Lyt-2^-/L3T4^- cells, represents ≈3-5% of the total thymocyte population. This population of cells can be further subdivided, using a variety of markers, including the group of mAbs designated B2A2 (Scollay et al, 1984a), MI-69 (Springer et al, 1978), and J11d (Bruce et al, 1981). The other subpopulations are: the Lyt-2^+/L3T4^+ cells that make up the majority (≈80%) of all cells within the adult thymus, and the two 'mature' phenotype subpopulations, the Lyt-2^+/L3T4^- and Lyt-2^-/L3T4^+ cells representing 5 and 10% of the total thymocyte population, respectively. The lineage relationships between these subpopulations remains uncertain, although data obtained from thymic reconstitution experiments suggest that the Lyt-2^-/L3T4^- subpopulation contains cells that can give rise to all other thymocyte subsets.

The stages of differentiation and development of T cells are, however, relatively well understood (Rothenberg and Lugo, 1985), compared with our understanding of the cell lineage relationships within the mammalian nervous system. Also, there are a wide range of effective techniques for isolating and studying subsets of T cells at different stages during their maturation. The study of isolated mammalian neuronal cells, on the other hand, is still relatively difficult and there are few effective techniques available for the identification of distinct neuronal subsets. These two facts make T cells a very convenient system for

studying the developmental factors controlling ion channel expression. The purpose of this study is to describe the changes in the number of K^+ channels expressed in the cell surface membrane of T cells at various stages of maturation with the aim of establishing a model sytem suitable for the study of the genetic mechanisms responsible for the control of voltage-gated ion channel expression.

METHODS

Mice

Female C57BL/6 mice, 6-10 weeks old, were bred at the John Curtin School of Medical Research under specific pathogen-free conditions and maintained in a clean animal room for up to 1 week before use. Fetal mice were obtained from timed matings of C57BL/6 males and BALB/c female mice. Male and female mice were caged together overnight and the following morning plugged females isolated. The day of finding a vaginal plug was designated day 0 of embryonic development.

Cell Suspensions

Single cell suspensions were prepared in Dulbecco's Modified Eagle's medium (DMEM) containing 10% (vol/vol) fetal calf serum (FCS). For the preparation of adult thymocyte or lymphocyte suspensions, mice were killed by cervical dislocation. Thymuses were removed free of parathymic lymph nodes. Lymph node cells were obtained from pooled inguinal and axillary lymph nodes. Pregnant female mice were killed by ether anesthesia and embryos were dissected from the uterus. Fetal thymuses were removed using a dissecting microscope and fine forceps. Cortisone-resistant thymocytes (CRT) were obtained from adult mice 2 days after a single intraperitoneal injection of 4 mg hydrocortisone acetate (Merck, Sharp and Dohme (Australia) Pty. Ltd., Granville, N.S.W.).

Antibodies

All mAbs were obtained as culture supernatants from hybridomas grown in vitro. The following mAbs were used: hybridoma GK-1.5 (anti-L3T4, rat IgG2b) (Dialynas et al, 1983); hybridoma LICR.LAU.RL172.4 (RL172) (anti-L3T4, rat IgM) and hybridoma PC 61 (anti-IL-2 Receptor, rat IgG1) (Ceredig et al, 1985); hybridoma 53-6.7 (anti-Lyt-2, rat IgG2a) (Ledbetter and Herzenberg, 1979); hybridoma 31M (anti-Lyt-2, rat IgM) and hybridoma AT 83 (anti-Thy1.2, rat IgM) (Sarmiento et al, 1980); hybridoma J11d (recognising B cells, most thymocytes but not mature T cells, rat IgM) (Bruce et al, 1981). Fluorescein isothiocyanate (FITC)-coupled sheep anti-rat Ig (Silenus Laboratories, Melbourne) or rabbit anti-rat Ig (Nordic Immunological Laboratories, Tilburg, The Netherlands) sera were used as second stage reagents depending upon the class of the primary antibody. The source of complement (C) was agarose-absorbed rabbit complement.

Negative Selection Cytotoxic Procedures

Adult thymocytes, lymphocytes or CRT were incubated at cell concentrations less than 20×10^6 cells/ml with a 1:10 dilution of anti-Lyt-2 (31M) or anti-L3T4 (RL172) or with a 1:3 dilution of J11d hybridoma supernatants for 10 min at 37°C. Rabbit complement was then added at a 1:10 dilution and the cells incubated for a further 45 min at 37°C. Viable cells

were recovered following centrifugation over Ficoll-Hypaque (Pharmacia Fine Chemicals, Uppsala, Sweden). In some instances, and for the preparation of J11d$^-$/Lyt-2$^-$/L3T4$^-$ thymocytes, mAb and C treatment was carried out twice.

Fluorescence Staining and Fluorescence-activated Cell Sorter (FACS) Analysis

Indirect immunofluorescence was used in all instances and all incubations were carried out at 4°C. For analytical purposes, samples of 1 x 10^6 cells were incubated for 30 min in 0.1 ml primary antibody hybridoma supernatant. Samples were then centrifuged through FCS and the pellets were resuspended in a 1:10 dilution of the appropriate FITC-coupled anti-Ig sera for a further 30 min. The cells were centrifuged again through FCS and resuspended in 500 µl of DMEM. For sorting purposes, 5 x 10^6 cells were stained with the same final concentrations of primary and second-step reagents used above. Control samples were incubated with the FITC-coupled reagent only.

The fluorescence-activated cell sorter was a FACS IV (Becton Dickinson FACS Systems, Sunnyvale, CA). Viable cells were gated by narrow-angle forward light scatter (FLS). Laser excitation was with a Spectra-Physics laser (Spectra-Physics Inc., Mountain View, CA) with 800 mW output at 488 nm. FITC-fluorescence was measured using a 500-540 nm band pass filter. For each sample 10,000 gated events were accumulated. Results for fluorescence intensity, number of cells and FLS are expressed in arbitrary linear units (a.u.). The percentage of positive cells was calculated, for biphasic distributions, by counting cells in the range positive to the inflexion point and then subtracting the percentage of control cells in the same interval of fluorescence to yield a net value for percent positivity.

Analysis of Cellular DNA Content

Samples were processed for cellular DNA content according to the method of Taylor and Milthorpe (1980). After treatment with 80 kunitz units/ml RNase (Sigma, St Louis, MO), cells were stained with the DNA binding dye propidium iodide (PI) (50 µg/ml; Sigma) in the presence of 0.05% Nonidet P - 40. The samples were then analysed on the FACS.

FACS Sorting

Sorting was only attempted on cell populations with clearly biphasic fluorescence profiles. Gating parameters were set to include the majority of fluorescence positive cells. A percentage of cells around the inflexion point were always discarded. Cells were collected in glass tubes, whose inside surfaces had been coated with FCS. The flow rate of viable cells being sorted was in the range 0.6 to 1 x 10^3 gated events per second.

In vitro Cell Culture

To generate lymphoblasts, peripheral T cells were stimulated with 2 µg/ml of

Concanavalin A (Con-A, Pharmacia Fine Chemicals, Uppsala, Sweden) in the presence of 30-40 units/ml Interleukin-2 (IL-2). The source of IL-2 was the supernatent (S/N) of an EL-4 thymoma subline (Farrar et al, 1980) stimulated for 24 hr with 10 ng/ml phorbol myristate acetate (PMA, Sigma). This EL4 S/N contained 1,000 units/ml IL-2 as determined using the CTLL-2 cell proliferation assay (Gillis et al, 1978).

Electrophysiology

The whole-cell voltage-clamp recording procedure used was similar to that described by Sakmann and Neher (1983). Briefly, a glass micropipette was positioned above a cell using a 3-dimensional fluid-drive micromanipulator (Narashige, Tokyo, Japan). During the period while the pipette was maneuvered into position a positive pressure was maintained to stop debris from blocking the electrode tip. This pressure was released when the electrode tip was within close proximity to the cell surface and the tip was then slowly advanced until it touched the membrane surface. A small negative pressure was then applied to pull the membrane of the cell more tightly against the pipette. This pressure was then released and a high resistance seal would regularly form spontaneously over the next few minutes. Seal resistances were in the range 50-100 GΩ. Any stray capacitance associated with the electrode and electrode holder was compensated at this point. To break the membrane patch separating the inside of the pipette from the inside of the cell, brief pressure pulses were applied using an electrically controlled hydraulic switch (Clippard Instrument Laboratory, CI). Pulses of increasing pressure were used until a sudden increase in capacitive current was seen, indicating entry into the cell.

Ionic currents were recorded using an LS/EPC 7 patch clamp amplifier (List Electronics, Darmstadt, FRG) and current signals were low-pass filtered through a 4-pole Bessel filter set at a corner frequency of 500 Hz or 1 kHz, depending upon the sampling frequency. Series resistance compensation was used when voltage step errors were greater than ≈2 mV. The holding potential for all experiments was -80 mV and voltage steps were applied at a maximum frequency of one pulse per 30 seconds to avoid the effects of cumulative inactivation. A PDP 11/23 microcomputer (Digital Equipment Corporation, Marlboro, MA) was used to deliver voltage pulses and to record current responses. Analysis of currents was done off-line using a PDP 11/44 minicomputer (D.E.C.). All experiments were performed at room temperature (20-22°C).

The maximum peak potassium conductance was calculated by first plotting the peak potassium conductance for each voltage step (which was calculated from the peak current after leakage subtraction and assuming a linear I-V relationship) against membrane potential. The resulting data points were then fitted by the following equation using least squares minimization:

$$g_K(Vm) = g_{K,max} \Big/ \left(1 + e^{(Vm-Vn)/kn} \right)^4 \qquad (1)$$

where, $g_K(Vm)$ is the peak potassium conductance for a given membrane potential (Vm), $g_{K,max}$ is the maximum peak potassium conductance, V_n is the mid-point of the curve and k_n gives the steepness of the voltage dependence. For some cells, instead of fitting the above equation, the maximum peak conductance was calculated by taking the arithmetic mean of peak conductances measured from voltage steps to potentials greater than +10 mV. The cell membrane capacitance was measured by reading the dial settings of the LS/EPC 7 capacitive cancellation network following compensation of the capacitive current response to a 10 mV hyperpolarizing voltage step.

Patch pipettes were prepared from either micro-hematocrit tubes (Modulohm, Herlev, Denmark) or specialized electrode glass (Kovar 7052, Garner Glass Co., Claremont, CA). Electrodes were coated with Sylgard (Dow Corning, Midland, MI) and then fire-polished to give final resistances in the range 5-8 MΩ. The standard pipette solution contained 130 mM KF, 10 mM KCl, 11 mM K-EGTA and 5 mM K-HEPES. The standard bath solution contained 150 mM NaCl, 5 mM KCl, 2 mM $CaCl_2$, 1 mM $MgCl_2$ and 5 mM Na-HEPES. No correction was made for the junction potential between the pipette and bath solutions.

RESULTS

Characteristics of the delayed-rectifier potassium conductance in mouse thymocytes and T lymphocytes

Whole-cell voltage clamp current records from an adult Lyt-2$^-$/L3T4$^-$ mouse thymocyte are shown in Fig. 1a. The current response to a series of depolarizing voltage steps from a holding potential of -80 mV indicates the presence of a delayed-rectifier potassium conductance (G_K+) with similar kinetic and ion permeation properties to that described previously in T cells (Cahalan et al, 1985; DeCoursey et al, 1985; Fukushima et al, 1984).

The conductance activates at potentials positive to -50 mV with a sigmoidal time course and saturates in the voltage range +10 to +20 mV (Fig. 1b). The data points are well fitted by the equation:

$$g_K(Vm) = g_{K,max} \Big/ (1 + e^{(V_m - V_n)/k_n})^4 \qquad (1)$$

with average values for V_n and k_n of -39 ± 2 mV and -10.8 ± 0.8 mV, respectively (mean ± s.e.m.).

The time course of inactivation could be approximated by a single exponential function (Fig. 2a), the time constant of which was only slightly dependent upon membrane potential at potentials positive to -10 mV (Fig. 2b). The inactivation time constant showed a consistent dependence on membrane potential at voltages negative to -10 mV but this effect may reflect voltage-dependent changes in the rate of channel activation rather than a true voltage-dependence of the inactivation process (Aldrich, 1981; Aldrich et al, 1983). A series of eight voltage steps to +20 mV from a holding potential of -80 mV, when given at different rates, showed that when voltage steps were applied at rates greater than one pulse per 30 seconds, some inactivation of subsequent pulses could result (Fig. 3). For this reason, all voltage-clamp protocols used delays of at least 30 seconds between voltage steps and, for longer duration steps, such as those shown in Fig. 2, 60 seconds delay between pulses was used.

Steady state inactivation curves were well fitted by a Boltzman distribution (Fig. 4), with average values, Vh = -46 ± 1.0 mV and k = -5.4 ± 0.9 mV (mean ± s.e.m., n = 7). There was no significant steady-state inactivation of the conductance at the normal holding potential of -80 mV.

The instantaneous current-voltage relationship for all cells examined was close to linear over the voltage range -80 to +80 mV. A typical example is shown in Fig. 5. The reversal potential for this cell was -83 mV, which is close to the calculated Nernst potential for potassium ions of -87 mV, indicating that the ion channel is predominantly selective for potassium ions. In some cells, single channel openings could be resolved in whole-cell recording mode (Figs 14 and 21). Average single channel currents from seven cells were

used to construct the single channel I-V curve shown in Fig. 6. From these average values a single channel conductance of ≈15 pS was calculated. The I-V curve is approximately linear over the voltage range -40 to +30 mV.

Expression of G_K+ by subsets of mouse thymocytes defined by the antigens Lyt-2 and L3T4

When adult mouse thymocytes are stained by indirect immunofluorescence with mAbs to the antigens Lyt-2 and L3T4, four subpopulations of thymocytes can be observed (Fig. 7). In Fig. 7, each peak corresponds to a cell population with a different surface antigen phenotype. The proportion of cells expressing each of the four phenotypes are: Lyt-2^+/L3T4^+, 80%; Lyt-2^-/L3T4^-, 5%; Lyt-2^-/L3T4^+, 10%; and Lyt-2^+/L3T4^-, 5%. To dissect a homogeneous subset of thymocytes, with respect to surface phenotype, it is necessary to either negatively select cells using complement-mediated cell lysis or positively select such cells using a fluorescence-activated cell sorter (FACS).

Figure 8 shows that a homogeneous Lyt-2^-/L3T4^- cell population can be obtained using complement lysis. In the left-hand panel the staining pattern of a normal thymus is shown. The centre panel shows the pattern of staining obtained following depletion of Lyt-2 and L3T4 antigen-bearing cells. Negative depletion was carried out using a cocktail of IgM mAbs and the cells have been restained using mAbs of a different subclass to the same antigenic determinants. The level of staining observed is not significantly different from that of control cells stained with the second reagent alone, shown in the right-hand panel, indicating that the negatively selected population is at least 98% pure for Lyt-2^-/L3T4^- thymocytes.

The maximum peak potassium conductance, which is directly proportional to the number of functional potassium channels in the cell membrane, can be calculated for any given cell from electrophysiological experiments such as those shown in Fig. 1. The mean peak conductance of adult Lyt-2^-/L3T4^- thymocytes was 2.7 ± 0.5 nS and the cell membrane capacitance was 1.3 ± 0.1 pF (Table 1). Cell membrane capacitance is directly proportional to cell membrane area and, as such, is an indicator of cell size.

The adult Lyt-2^-/L3T4^- thymocyte population is thought to be largely comprised of cells at very early stages in the pathway committed to T lymphocyte development. Since the majority of these cells express K^+ channels at relatively high levels it was of some interest to observe at what stage during embryological development of the thymus that K^+ channels first appear. Thymocytes obtained from 14 day fetal thymuses are all Lyt-2^-/L3T4^- (Ceredig et al, 1983). Voltage clamp records of 14 day fetal thymocytes revealed a potassium conductance similar to that observed in adult Lyt-2^-/L3T4^- thymocytes, although the average mean peak conductance was somewhat lower (Table 1). This result indicates that embryologically, expression of K^+ channels is an early event in the differentiation pathway of T cells within the thymus.

Small Lyt-2^+/L3T4^+ cortical thymocytes, which make up ≈60% of cells in the normal

thymus, can only be isolated for electrophysiological experiments by positive selection using a fluorescence-activated cell sorter. Figure 9a shows a two-dimensional fluorescence profile of a total thymus suspension stained only for Lyt-2. Cells were sorted using a combination of fluorescence intensity and low angle forward light scatter to select for small Lyt-2^+ cells. An analysis of the resultant sorted population is shown in Fig. 9b. The efficacy of the sort, on the basis of fluorescence staining intensity, is clearly seen by comparing the two panels of Fig. 9. The initial cell population used for sorting was ≈80% Lyt-2^+, whereas the sorted cells were greater than 99% Lyt-2^+. The sorted population was, therefore, comprised primarily of Lyt-2^+/L3T4$^+$ thymocytes with a small contaminating population of Lyt-2^+/L3T4$^-$ thymocytes. The sorting procedure was less successful in separating cells on the basis of cell size, although the number of large blast cells was reduced. To ensure that only the small Lyt-2^+/L3T4$^+$ cortical thymocytes were used for recordings, it was also necessary to rely on visual indentification of the smallest cells during electrophysiological experiments.

The sorted cells were in good physical condition and binding of the primary antibody and the secondary fluoresceinated antibody did not appear to inhibit seal formation between the glass micropipette and the cell membrane. Voltage clamp records from Lyt-2^+/L3T4$^+$ thymocytes (Fig. 10) indicated the presence of a potassium conductance, similar to that observed in Lyt-2^-/L3T4$^-$ thymocytes, in all the cells examined, with an average peak conductance of 2.7 ± 0.6 nS (Table 1). The cell capacitance was 0.6 ± 0.03 pF, which confirms that only the smallest thymocytes were selected.

To study thymocytes with the 'mature' Lyt-2^+/L3T4$^-$ cell surface phenotype, normal thymocyte suspensions were first depleted of L3T4$^+$ cells by complement lysis. The staining profile of this depleted cell population is shown in Fig. 11a. Approximately 1.4 % of cells were L3T4$^+$. The remaining cells were either Lyt-2^+/L3T4$^-$ or Lyt-2^-/L3T4$^-$. These L3T4 depleted cells were then stained for Lyt-2 (first panel of Fig. 11b) and sorted for positive or negative fluorescence staining. Initially, 55% were Lyt-2^+ but, as shown in the third panel of Fig. 11b, a population ≈97% pure for Lyt-2^+/L3T4$^-$ cells could be obtained by sorting. Voltage clamp records from these cells (Fig. 12) revealed a potassium conductance with a relatively high average peak conductance of 4.8 ± 0.6 nS (Table 1).

Expression of G_{K+} in peripheral lymph node T lymphocytes

It was of some interest to obtain recordings from Lyt-2^+/L3T4$^-$ lymphocytes from peripheral lymphoid tissues to compare with 'mature' phenotype Lyt-2^+/L3T4$^-$ thymocytes. Since B lymphocytes have a considerable quantity of membrane bound Ig, there is a certain amount of non-specific anti-Ig staining of B cells by cross-reaction of the anti-rat FITC-conjugated antibody with membrane bound Ig. This non-specific reactivity reduces the apparent sensitivity of the specific anti-T cell staining, making cell sorting difficult. For this reason lymphocytes from inguinal and axillary nodes were first depleted of B cells using the monoclonal antibody J11d (Bruce et al, 1981). The resultant J11d depleted cell

population was 98% Thy-1^+ lymphocytes with ≈34% of cells Lyt-2^+/L3T4^-. These cells were sorted to give a population 98% pure for Lyt-2^+/L3T4^- lymphocytes (Fig. 13).

Voltage clamp records from Lyt-2^+/L3T4^- peripheral T cells were very different to those obtained from thymocytes with the same surface phenotype. Only a very few functional K^+ channels were present in the cell membrane and single channel openings could easily be observed in the current traces (Fig. 14). The mean peak conductance of the Lyt-2^+/L3T4^- lymphocytes was very low (0.12 ± 0.05 nS) compared with the Lyt-2^+/L3T4^- thymocytes. The cell capacitance, 0.8 ± 0.05 pF, was also reduced, which is consistent with the size differences reported previously using FACS analysis of forward light scatter (Scollay et al, 1984b).

It is possible that selection of J11d^- lymphocytes may have biased the resultant cell population against T lymphocytes strongly positive for K^+ channel expression since it is known that this can occur in the thymus (see later sections) and, in this respect, some early experiments in which unselected peripheral lymph node lymphocytes were used for electrophysiological experiments are relevant. In these preliminary experiments, only 1 cell out of 36 expressed a K^+ conductance greater than 0.5 nS. A value of 0.5 nS was chosen as an arbitrary cut-off point differentiating high from low expression levels of K^+ channels because this value clearly distinguished between resting peripheral T cells and in vitro activated T cells (Table 2). Although this untreated cell preparation was only ≈82-87% Thy-1^+, by FMF, it is clear that the majority of peripheral T lymphocytes do not express high levels of the K^+ channel.

Expression of G_{K^+} by peripheral T lymphocytes activated in vitro

Expression of K^+ channels in mouse peripheral lymphocytes can be up-regulated in vitro by stimulation with the mitogen Concanavalin A (Con A). Peripheral T lymphocytes of either Lyt-2^+/L3T4^- or Lyt-2^-/L3T4^+ surface phenotype were stimulated with Con A in the presence of IL2. Three days later their surface phenotype was analysed by FMF and any cells of the inappropriate phenotype were removed by negative selection using mAb and C. Voltage clamp studies of these cells showed that the number of K^+ channels per cell had increased considerably compared with resting cells of similar phenotype (Table 2). A typical voltage-clamp recording is shown in Fig. 15. As expected from their blast morphology, there was an increase in membrane capacitance (Table 2). Three day lymphoblasts were Thy-1^+, IL-2 receptor positive and rapidly proliferating, as assessed by propidium iodide staining (Fig. 16).

Lymphoblasts cultured for 7 days still expressed K^+ channels at moderate levels, although the cell membrane capacitance had fallen (Table 2). No effective protocol was found in which K^+ channel expression could be first induced and then seen to fall back to resting levels. Cells from mixed lymphocyte cultures left for up to 11 days still continued to express K^+ channels at high levels.

Expression of G_K+ by J11d-negative subsets of thymocytes

It has recently been shown that ≈87% of thymocytes with apparently 'mature' surface phenotypes (Lyt-2^+/L3T4^- or Lyt-2^-/L3T4^+), express high levels of the surface antigen recognized by the monoclonal antibody B2A2 (Scollay and Shortman, 1985). In contrast, apart from recent thymus migrants, peripheral lymph node T cells express very low levels of the antigen and are resistant to B2A2-directed complement lysis (Scollay and Shortman, 1985). Since differential expression of this antigen is one of the few indices, other than K^+ channel expression, which is capable of differentiating between 'mature' phenotype thymocytes and peripheral T lymphocytes, it was of some interest to examine the distribution of K^+ channels in B2A2^- thymocyte subpopulations.

It has been suggested that the monoclonal antibodies J11d and B2A2 recognize similar determinants (Scollay and Shortman, 1985). Since initial studies showed that, for the preparations of mAbs available, J11d was more effective than B2A2 at complement-mediated killing and fluorescence staining, J11d was used for all experiments.

Figure 17 shows the profile of normal, Lyt-2^-/L3T4^- and cortisone resistant thymocytes (CRT) labelled with J11d. The majority (86%) of normal thymocytes stained positively with J11d. Lyt-2^-/L3T4^- cells are clearly heterogeneous for J11d expression with 85% staining above the control. CRT stain very weakly with J11d, with only ≈5% of cells staining above control levels.

Clearly, ≈15% of the Lyt-2^-/L3T4^- thymocytes are also J11d^- (Fig. 17, right-hand panel). These J11d^-/Lyt-2^-/L3T4^- cells could be obtained by negative selection, using two rounds of mAb and C treatment. The FMF profile of such cells is shown in Fig. 18. Negative selection for a minor thymic subpopulation carries the danger of enriching for any non T cell lineage cells found within the thymus. This problem is reduced, though not entirely eliminated, with J11d depletion because this mAb recognizes a number of non T cell lineages including B cells and neutrophils (Bruce et al, 1981). As can be seen from the negative control in Fig. 18 there is less than 6% staining with anti-Ig reagents. Compared with this control, 70% of J11d^-/Lyt-2^-/L3T4^- cells were Thy-1^+ with no cells staining for Lyt-2, L3T4 or J11d. Interestingly, as determined by propidium iodide (PI) staining, most (≈ 95%) of such cells were in the G_0/G_1 phases of the cell cycle (Fig. 18). When examined electrophysiologically, four out of thirteen of the J11d^-/Lyt-2^-/L3T4^- cells tested had no K^+ channels at all (Fig. 19), and overall the mean conductance was low (0.5 ± 0.3 nS, Table 3).

A total population of J11d^- thymocytes, was also obtained by complement-mediated depletion and analysed by FMF. As shown in Fig. 20, the majority of cells (≈90%) were weakly Thy-1^+, with ≈27% Lyt-2^+ and 67% L3T4^+ and with both anti-Lyt-2 and anti-L3T4 mAb added simultaneously, only 5% of cells did not stain.

Typical voltage-clamp recordings from a J11d^- cell are shown in Fig. 21. The level of K^+ channel expression (0.4 ± 0.1 nS) is clearly much reduced compared with the majority of thymocytes (Table 1). The mean peak K^+ conductance is closer to the value found for peripheral T lymphocytes and only 2 out of 12 cells expressed a conductance greater than 0.5

nS (Table 3). It is clear that in most J11d$^-$ thymocytes K^+ channel expression is down-regulated.

As shown previously by Scollay and Shortman (1985), B2A2 (or J11d) expression among Lyt-2$^+$/L3T4$^-$ cells is heterogeneous. The results shown in Fig. 20 demonstrate the existence of J11d$^-$/Lyt-2$^+$/L3T4$^-$ cells. To examine whether K^+ channel expression among Lyt-2$^+$/L3T4$^-$ thymocytes was related to J11d expression, J11d$^-$/Lyt-2$^+$/L3T4$^-$ cells were obtained by positive selection of Lyt-2$^+$ cells from thymocyte suspensions first depleted of J11d$^+$ and L3T4$^+$ cells by mAb and C. These cells were found to have a mean peak conductance (1.1 ± 0.5 nS, Table 3) significantly (Student's t-test, $p < 0.001$) lower than that of the total subpopulation of Lyt-2$^+$/L3T4$^-$ thymocytes (4.8 ± 0.6 nS, Table 1).

Expression of G_{K^+} in cortisone-resistant thymocytes

A distinct subpopulation of thymocytes can be obtained two or three days after pretreatment of mice with an injection of corticosteroids. The surface phenotype of cortisone-resistant thymocytes (CRT) is shown in Fig. 22. The pattern of expression of Lyt-2 and L3T4 is very similar to that of J11d$^-$ thymocytes; with 33% Lyt-2$^+$/L3T4$^-$, 61% Lyt-2$^-$/L3T4$^+$ and only 6% Lyt-2$^-$/L3T4$^-$. Since only ≈3-5% of all thymocytes are cortisone resistant (Blomgren and Anderson, 1971), and ≈15% of the total number of thymocytes are 'mature' phenotype, this implies that cortisone pretreatment results in the recovery of only a subpopulation of the 'mature' phenotype thymocytes. As shown in Fig. 17, expression of J11d is very much reduced on CRTs compared with the normal thymus, suggesting that cortisone treatment specifically spares J11d$^-$ mature thymocytes. Voltage clamp studies on CRT show that such cells have reduced K^+ channel expression compared with the majority of both mature and immature thymocytes (Table 3).

DISCUSSION

Properties of the delayed rectifier K^+conductance in mouse thymocytes and T lymphocytes

The kinetic and ion permeation properties of the delayed rectifier potassium conductance observed in mouse thymocytes and T lymphocytes in this study are very similar to those described previously in human and mouse T lymphocytes and T cell clones (Cahalan et al, 1985; DeCoursey et al, 1985; Fukushima et al, 1984). One notable difference between the human and mouse studies is the relatively high expression of K^+ channels by resting human peripheral blood T lymphocytes compared with that of mouse lymph node T cells (DeCoursey et al, 1984; Deutsch et al, 1986). Since there is, at present, no electrophysiological study of either human lymph node lymphocytes or mouse peripheral blood T cells it is uncertain whether this discrepancy is due to differences between the general level of activation of T cells in the two tissues or to genuine species differences.

It has recently been observed that internal calcium ions can block K^+ channels in human T lymphocytes (Bregestovski et al, 1986). This calcium-dependent channel blockade was, however, observed at $[Ca]_i$ concentrations of the order of 0.1 μM, which are considerably higher than the $[Ca]_i$ of the pipette solutions used in this study. The peak K^+ conductance values calculated for any given cell in this study should, therefore, accurately reflect the number of K^+ channels available for activation in the cell membrane.

Cahalan et al (1985) found that there was significant steady state inactivation at a membrane potential of -80 mV in human peripheral blood lymphocytes. The average midpoint of Boltzman fits to their steady state inactivation data was -70 ± 6 mV compared with a value of -46 ± 1 mV observed for mouse T cells in this study. Measurement of maximum peak K^+ conductance values in this study should not be affected by any steady state inactivation.

Implications of K^+ channel distribution for T cell lineage relationships

In this study, an analysis has been made of the expression of voltage-activated K^+ channels in subpopulations of mouse thymocytes and T lymphocytes. The results suggest that the level of expression of K^+ channels by T cells is related to their stage of differentiation. As a consequence, analysis of K^+ channel expression provides additional information about the differentiation pathways of T cells.

Shown in Fig. 23 is a summary of the data on the expression of K^+ channels among subpopulations of thymocytes and peripheral T cells. The finding that K^+ channel expression in peripheral lymph node T lymphocytes is up-regulated after activation by mitogenic lectins suggests that T cells may, as a general response to mitogenic stimulation, increase their level of expression of K^+ channels (see also DeCoursey et al, 1985; Deutsch et al, 1986; Lee et al, 1986). It has been shown previously that K^+ channels are apparently necessary for mitogenesis, although their exact function remains uncertain (Chandy et al,

1984).

As for the thymus, the factors which control proliferation of cells therein are still unknown. It is clear, that the majority of Lyt-2$^-$/L3T4$^-$ cells are rapidly proliferating cells (Scollay et al, 1984a; Ceredig and MacDonald, 1985), and approximately half of these cells express an IL-2 receptor (Ceredig et al, 1985). The high level of K^+ channel expression by Lyt-2$^-$/L3T4$^-$ cells is consistent with the proposition that K^+ channel expression is high in cells recently stimulated to proliferate. This conclusion is also supported by results obtained from J11d$^-$/Lyt-2$^-$/L3T4$^-$ cells, which generally have a low level of K^+ channel expression and are largely non-cycling (Fig. 18) and IL-2 receptor negative (Lynch et al, 1987). In further confirmation of this general trend are the results obtained from day 14 fetal thymocytes, a high percentage of which are rapidly proliferating and express both the IL-2 receptor (Ceredig et al, 1985; Takacs et al, 1984) and the K^+ channel.

The relationship of J11d$^-$/Lyt-2$^-$/L3T4$^-$ cells to other subpopulations of thymocytes is, at present, uncertain. One possibility is that these cells are recent immigrants from the bone marrow which have not yet received an appropriate stimulus from the thymic microenvironment (Fig. 23). Consistent with this suggestion is the low rate of mitogenesis within this subpopulation and the lack of expression of the IL-2 receptor. The possibility cannot, however, be excluded that these cells are a quiescent population within the thymus unrelated to the major pathway of T cell maturation.

The very high K^+ channel expression, relative to membrane area, observed in the small cortical Lyt-2$^+$/L3T4$^+$ thymocytes is, in some ways, surprising since these cells have generally reduced rates of protein synthesis and are thought to die within the thymus (Rothenberg, 1982). These small thymocytes are presumeably derived from the rapidly cycling Lyt-2$^+$/L3T4$^+$ blast cells, and the K^+ channels that they express are, quite possibly, inherited from these precursor blast cells. This inheritance of K^+ channels may be analogous to the inheritance of the TL antigen by small cortical thymocytes (Rothenberg, 1982). There is, at present, no data available on the rate of turnover of the delayed rectifier K^+ channel in cell membranes. It is probable however, that the channel has a half-life in the cell membrane of the order of a few days at least; a proposition which is supported by the relatively slow decline of K^+ channel numbers in 7 day Con A blasts and mixed lymphocyte culture cells.

The Lyt-2$^+$/L3T4$^+$ blasts do not express the IL-2 receptor, and it therefore seems probable that the mechanisms controlling expression of the K^+ channel and the IL-2 receptor are independent, even though expression of these two membrane proteins appears to be linked in both immature (Lyt-2$^-$/L3T4$^-$) thymocytes and T lymphocytes. The significance of the failure of proliferating Lyt-2$^+$/L3T4$^+$ cells to express the IL-2 receptor is still not understood, and it is possible that a similar failure to express the IL-2 receptor by half of the Lyt-2$^-$/L3T4$^-$ cells indicates that these cells are already committed to becoming Lyt-2$^+$/L3T4$^+$ cells; although, the alternative possibility, that they are precursors of the IL-2 receptor positive cells cannot, at present, be excluded.

The high level of K^+ channel expression by Lyt-2$^+$/L3T4$^-$ thymocytes suggests that

these cells may be the direct products of a rapidly proliferating parent cell, of either Lyt-2$^-$/L3T4$^-$ or Lyt-2$^+$/L3T4$^+$ phenotype. The lower level of expression of K^+ channels by J11d$^-$/Lyt-2$^+$/L3T4$^-$ cells indicates that these cells represent a distinct stage of T cell maturation. There is evidence that peripheral T lymphocytes can recirculate back into the thymus (Fink et al, 1984). One possible interpretation of the data is that J11d$^-$/Lyt-2$^+$/L3T4$^-$ cells isolated from the thymus contain recirculating peripheral T cells, rather than cells solely in the intra-thymic cell lineage. Consistent with this suggestion is the observation that B2A2$^-$ thymocytes are enriched for antigen specific responsive cells after priming with Moloney murine sarcoma virus (Ceredig, 1986).

Cortisone-resistant thymocytes are a distinct subpopulation of mature phenotype thymocytes (Reichert et al, 1986). Phenotypically, CRT appear to be enriched for the J11d$^-$ subpopulations of Lyt-2$^+$/L3T4$^-$ and Lyt-2$^-$/L3T4$^+$ thymocytes (Fig. 17). The reduced expression of J11d among CRT appears to be in conflict with the data of Scollay et al (1984a) using B2A2 but is in agreement with Bruce et al (1981) where CRT were found to be expressing low levels of J11d, as determined by mAb and C cytotoxicity. Electrophysiologically, CRT appear to be very similar to the J11d$^-$ subpopulations.

For both the J11d$^-$ and CRT subpopulations, the Lyt-2$^+$/L3T4$^-$ cells expressed, on average, more K^+ channels than did the Lyt-2$^-$/L3T4$^+$ cells. This result is consistent with the reports of size differences between these cells (Ceredig et al, 1983; Scollay and Shortman, 1985), in which Lyt-2$^+$ cells were found to be, on average, larger than the L3T4$^+$ cells. The physiological significance of this difference between the two cell populations is uncertain.

In conclusion, it is clear that K^+ channel expression in T cells is developmentally regulated. Increased expression of the channel is apparently induced in response to mitogenic signals throughout the T cell lineage, and therefore, serves as a useful marker in defining the steps of T cell development. T cell differentiation provides an ideal model system for studying the genetic mechanisms controlling ion channel expression and further studies should provide additional information about ion channel expression; information which has, so far, proven difficult to obtain from other mammalian systems.

TABLE 1. Peak Potassium Conductance and Cell Membrane Capacitance of Subpopulations of Mouse Thymocytes Defined by the Antigens Lyt-2 and L3T4

Cell Type	Peak Potassium Conductance (nS)	Cell Membrane Capacitance (pF)	Fraction of Cells $G_{k^+} > 0.5$ nS
adult Lyt-2^-/L3T4^- thymocytes	2.7 ± 0.5 *	1.3 ± 0.1	13/15
14d fetal Lyt-2^-/L3T4^- thymocytes	1.4 ± 0.2	1.9 ± 0.1	17/18
adult Lyt-2^+/L3T4^+ thymocytes	2.7 ± 0.6	0.6 ± 0.03	7/7
adult Lyt-2^+/L3T4^- thymocytes	4.8 ± 0.6	1.2 ± 0.05	12/13

* mean ± s.e.m.

TABLE 2. Peak Potassium Conductance and Cell Membrane Capacitance of Subpopulations of Mouse Peripheral Resting and Con A Stimulated T Lymphocytes

Cell Type	Peak Potassium Conductance (nS)	Cell Membrane Capacitance (pF)	Fraction of Cells $G_{K^+} > 0.5$ nS
adult Lyt-2^+/L3T4$^-$ lymphocytes	0.12 ± 0.05 *	0.8 ± 0.05	0/9
3 day Con A Lyt-2^+/L3T4$^-$ blasts	3.5 ± 0.2	3.4 ± 0.5	7/7
3 day Con A Lyt-2^-/L3T4$^+$ blasts	3.9 ± 0.4	2.9 ± 0.2	10/10
7 day Con A blasts	2.0 ± 0.3	1.8 ± 0.2	12/12

* mean ± s.e.m.

TABLE 3. Peak Potassium Conductance and Cell Membrane Capacitance of J11d Negative and Cortisone-Resistant Subpopulations of Mouse Thymocytes

Cell Type	Peak Potassium Conductance (nS)	Cell Membrane Capacitance (pF)	Fraction of Cells $G_{k^+} > 0.5$ nS
J11d$^-$ thymocytes	0.4 ± 0.1 *	1.0 ± 0.04	2/12
J11d$^-$/Lyt-2$^-$/L3T4$^-$ thymocytes	0.5 ± 0.3	1.2 ± 0.2	2/13
J11d$^-$/Lyt-2$^+$/L3T4$^-$ thymocytes	1.1 ± 0.5	1.3 ± 0.2	4/8
Lyt-2$^+$/L3T4$^-$ CRT	1.2 ± 0.6	1.1± 0.1	3/8
Lyt-2$^-$/L3T4$^+$ CRT	0.4 ± 0.08	1.0 ± 0.2	1/8

* mean ± s.e.m.

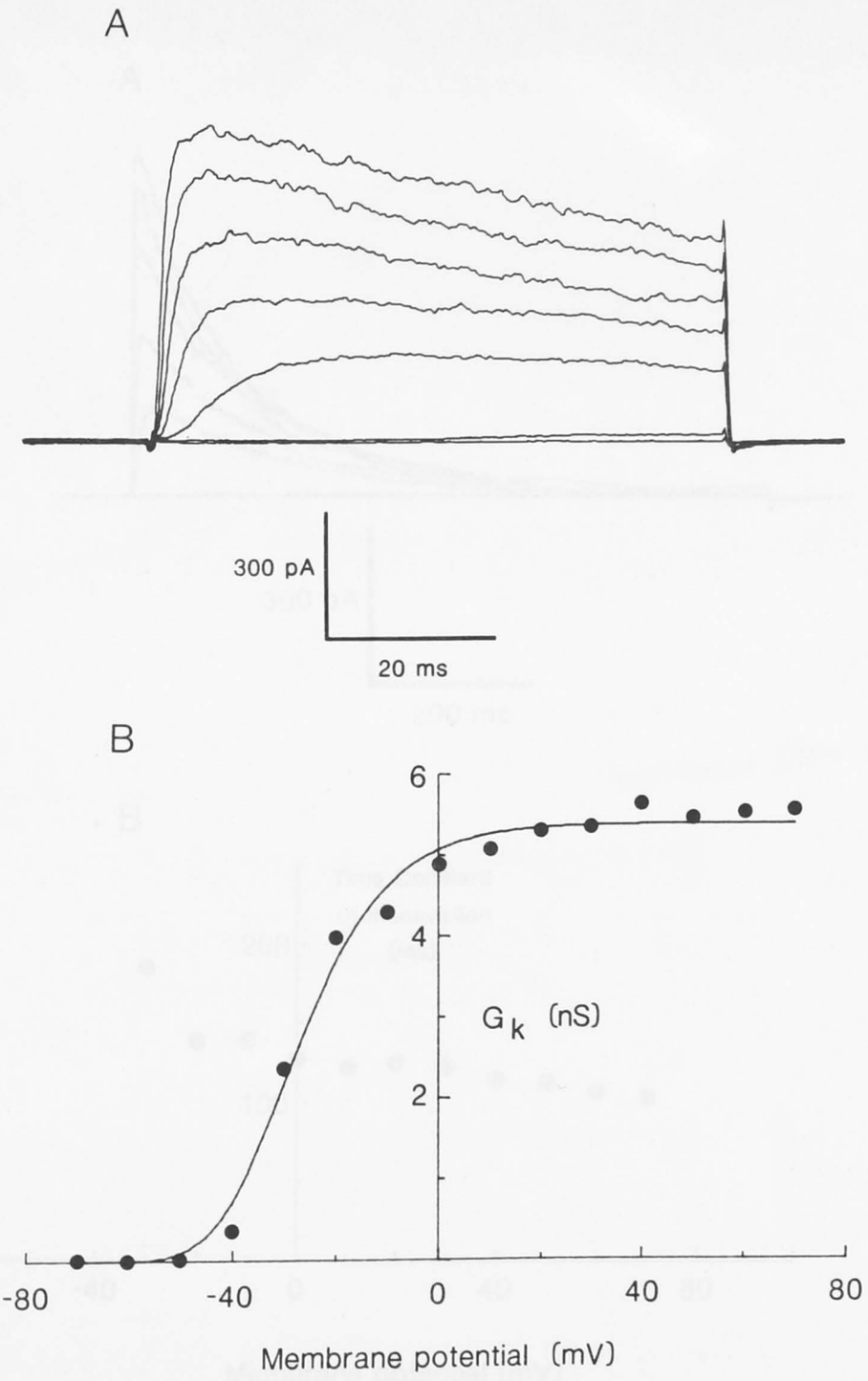

Figure 1. Activation of voltage-activated K^+ conductance in mouse thymocytes.

A) Whole-cell voltage-clamp current records from an adult Lyt-2^-/L3T4^- mouse thymocyte. Holding potential was -80 mV and voltage steps were applied at 30 second intervals. Voltage was stepped over the range -70 to +70 mV in 10 mV increments. (Only steps to -60, -40, -20, 0, 20, 40 and 60 mV are shown). Sampling interval 100 μs, filter 1 kHz.

B) Peak conductance-voltage relationship for the data shown in Fig. 1a. Data was fitted using equation (1) with V_n = -44.5 mV, k_n = -10.7 mV and $g_{K,max}$ = 5.4 nS.

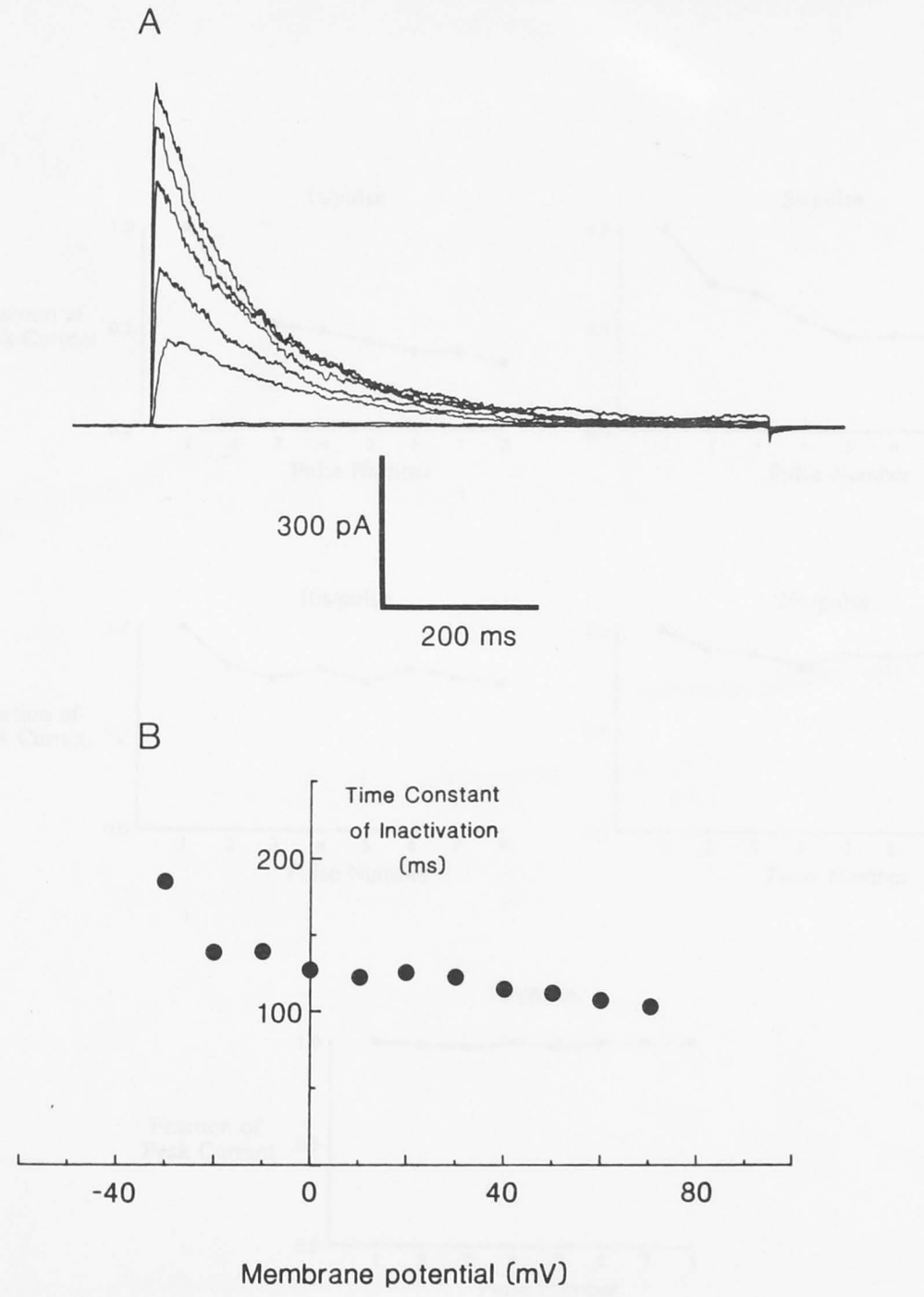

Figure 2. Inactivation of voltage-activated K^+ conductance in mouse thymocytes.

A) Whole-cell voltage-clamp current records from an adult Lyt-2^-/L3T4^- mouse thymocyte. Holding potential was -80 mV and voltage steps were of 800 ms duration and applied every 60 seconds. Voltage was stepped over the range -60 to +70 mV in 10 mV increments. (Only steps to -60, -40, -20, 0, 20, 40 and 60 mV are shown). Sampling interval 1 ms, filter 500 Hz.

B) Time constant of inactivation plotted against membrane potential. Values for the time constant are the average values obtained from three succesive runs.

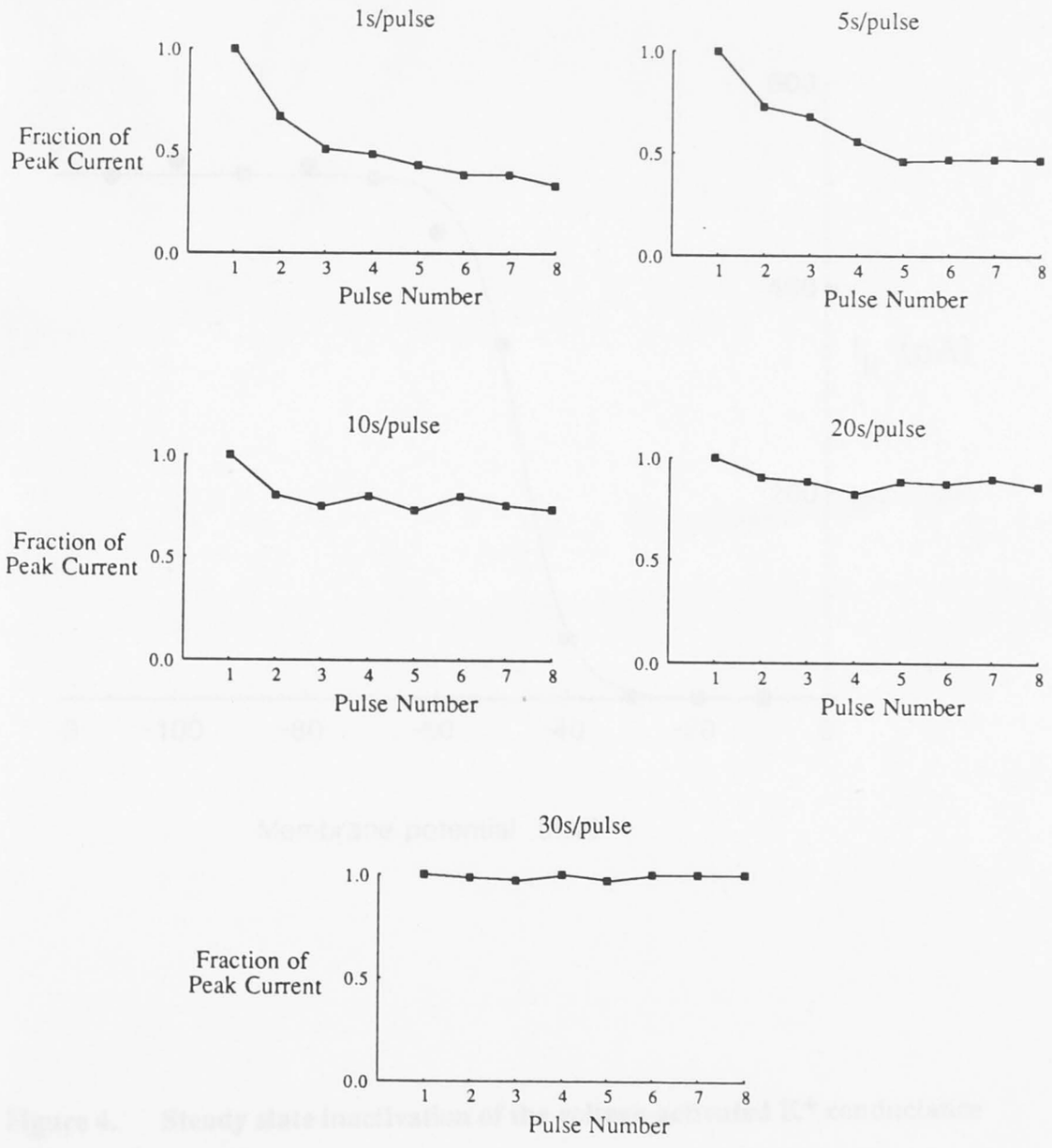

Figure 3. Inactivation of voltage-activated K^+ conductance during a series of voltage steps.

Whole-cell voltage-clamp currents were recorded during a series of eight 70 ms voltage steps from a holding potential of -80 mV to a test potential of +20 mV. Peak currents are expressed as a fraction of the peak current elicited by the first voltage step. Delays between pulses were, 1s, 5s, 10s, 20s and 30s.

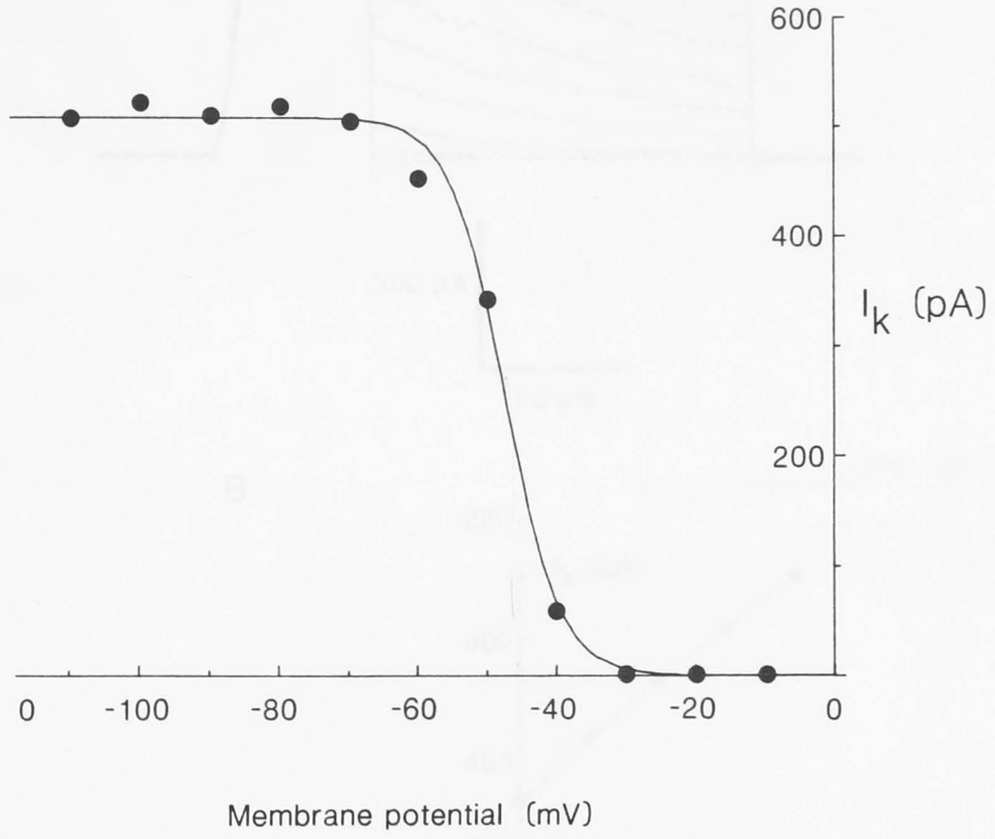

Figure 4. Steady state inactivation of the voltage-activated K^+ conductance in mouse thymocytes.

The peak current, from a single cell, following a 70 ms voltage step to +20 mV is plotted against holding potential, which is indicated on the x-axis. Holding potentials were stepped from -110 mV down to -10 mV in 10 mV increments and were maintained for 1 min before application of a single test pulse to +20 mV. The fitted curve represents a Boltzman distribution with V_h = -47.4 mV and k = -4.0 mV.

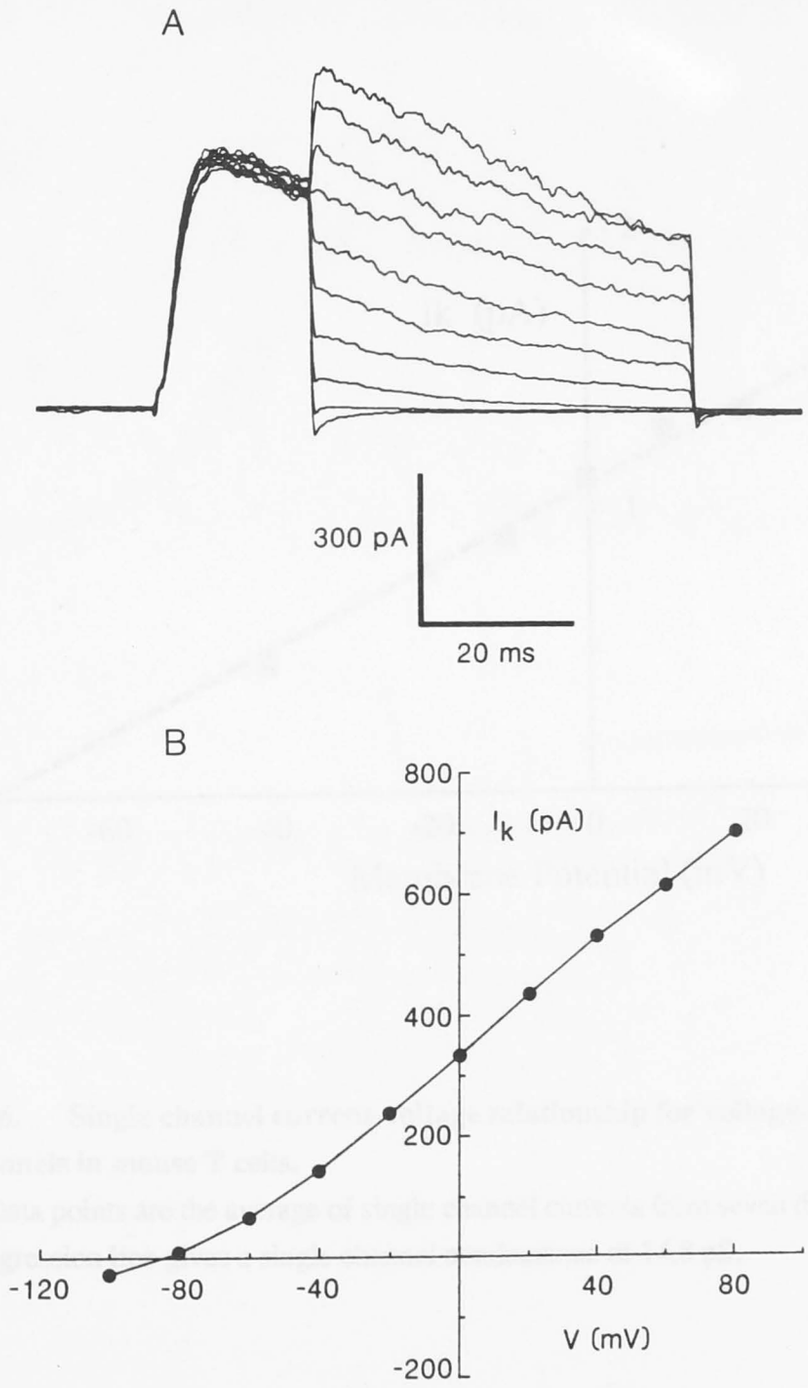

Figure 5. Instantaneous current-voltage relationship for the voltage-activated K^+ conductance in mouse thymocytes.

A) Two-pulse voltage clamp protocol. The K^+ conductance was maximally activated by a 15 ms step to +20 mV which was followed by a second step to membrane potentials in the range -100 to +80 mV. Successive voltage steps were delivered at 60 second intervals. Sampling interval 100 μs, filter 1 kHz.

B) Instantaneous current-voltage relationship calculated from the data shown in Fig. 5a. The reversal potential was -83 mV.

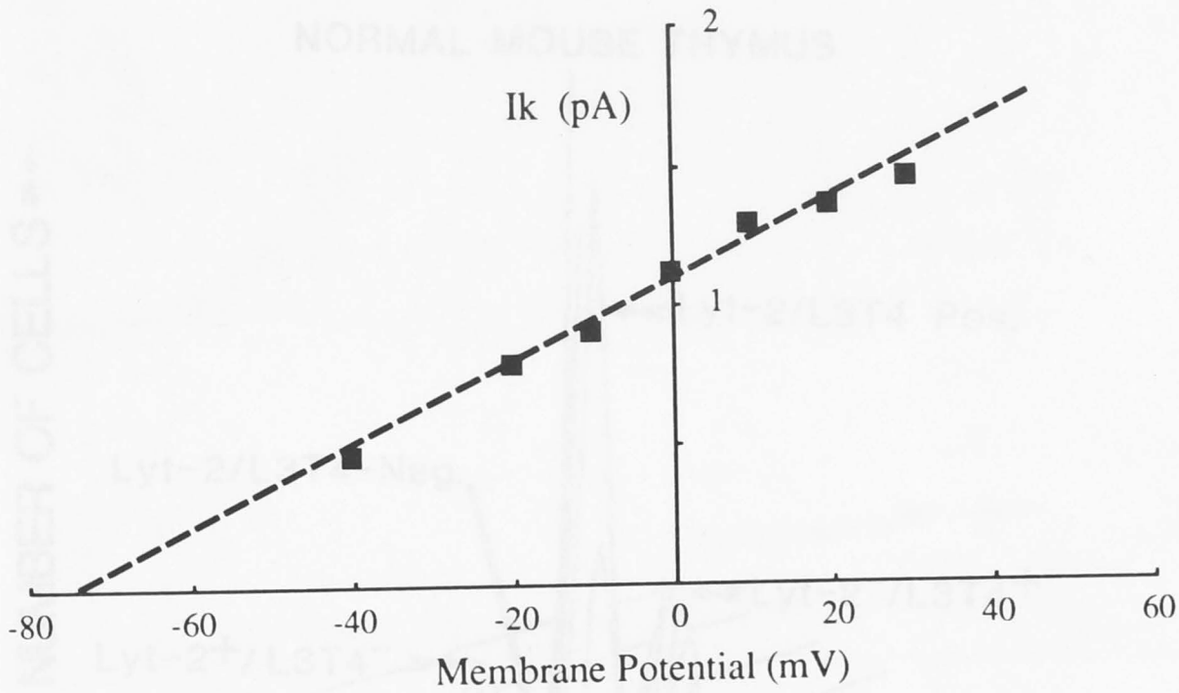

Figure 6. Single channel current-voltage relationship for voltage-activated K^+ channels in mouse T cells.

Data points are the average of single channel currents from seven different cells. The fitted regression line gives a single channel conductance of 14.8 pS.

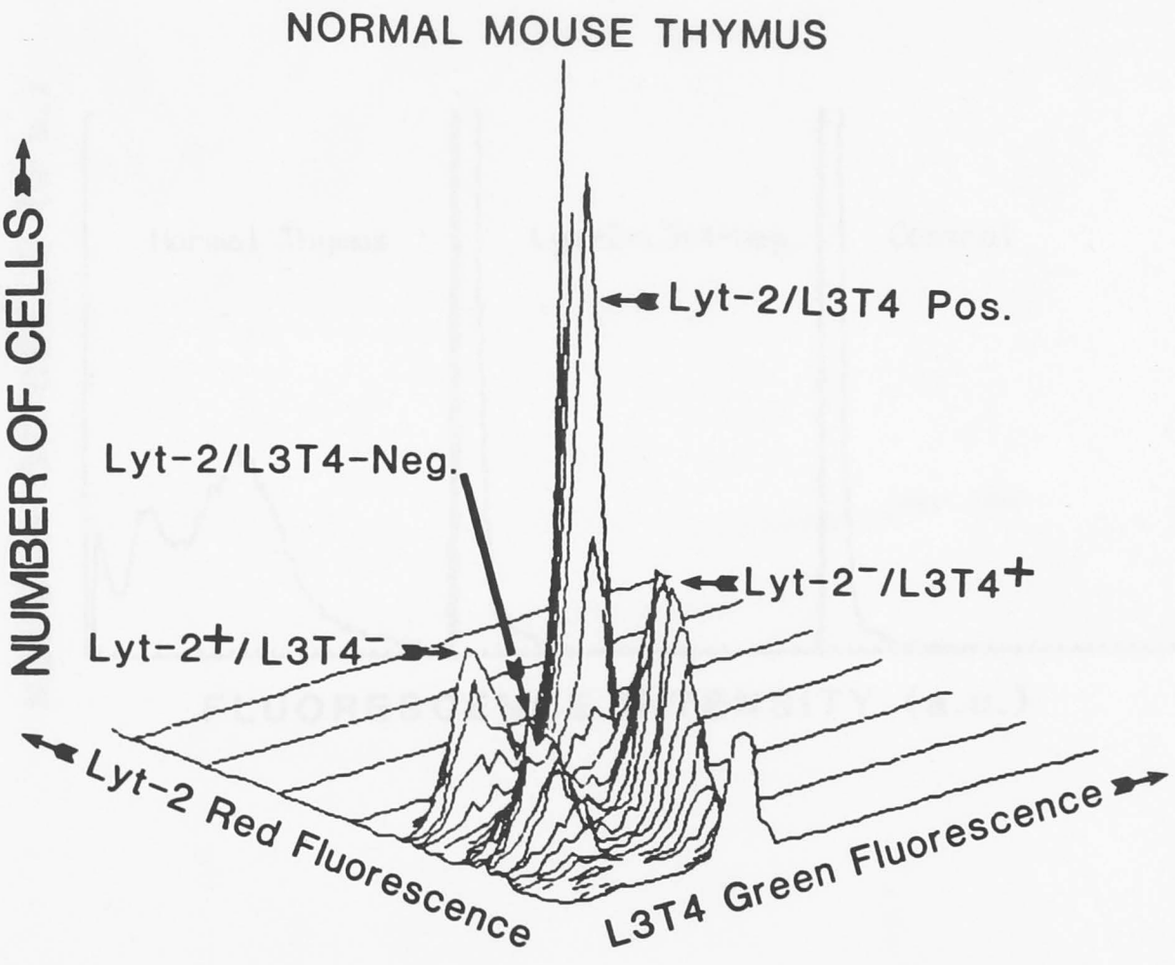

Figure 7. Two colour flow microfluorometric analysis of adult C57BL/6 mouse thymocytes.

Cells were labelled with anti-L3T4 and biotinylated anti-Lyt-2 mAbs which were revealed by FITC-labelled sheep-anti-rat Ig (L3T4) and streptavidin phycoerythrin (Lyt-2). A correlation of red (Lyt-2) and green (L3T4) fluorescence intensity for 30,000 analysed cells is shown. The vertical axis represents the number of cells. Most (80%) cells express both Lyt-2 and L3T4 antigens, some (5%) express neither antigen, 10% are Lyt-2^-/L3T4^+ and 5% are Lyt-2^+/L3T4^-.

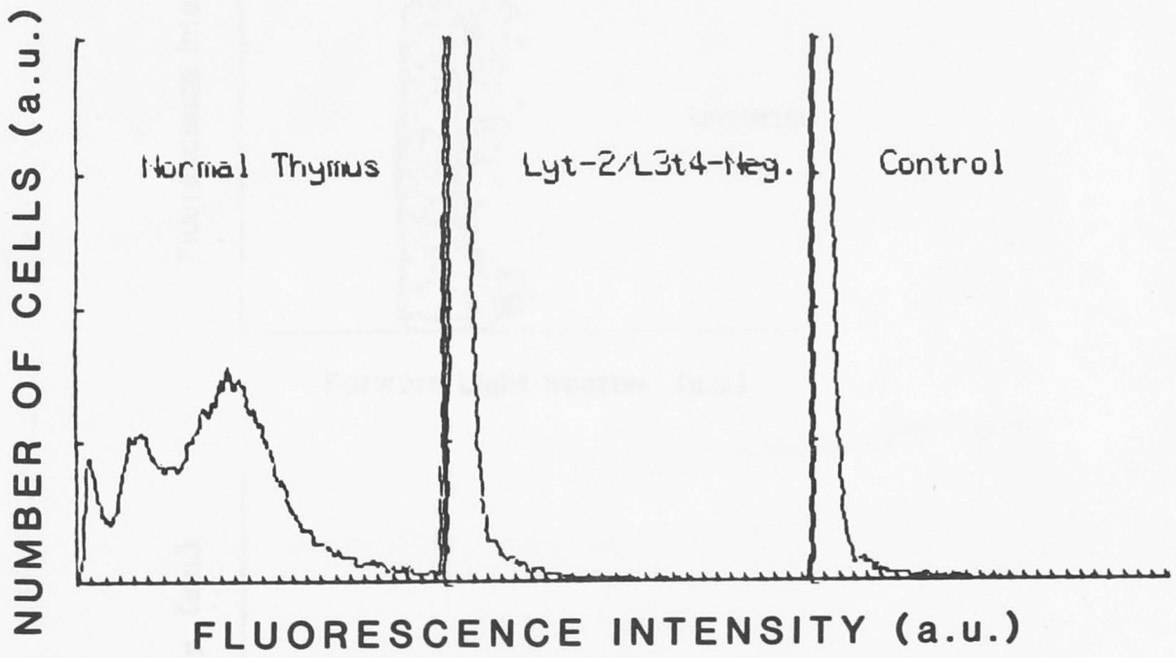

Figure 8. Negative selection of Lyt-2$^-$/L3T4$^-$ thymocytes.

The left hand panel shows the staining pattern of a normal thymus fluorescently labelled with both anti-Lyt-2 and anti-L3T4 mAbs. The centre panel shows the staining pattern obtained following complement lysis of cells bearing Lyt-2 and L3T4 determinants. This depleted population has less than 2% positive staining above the background fluorescence of the negative control shown in the right hand panel.

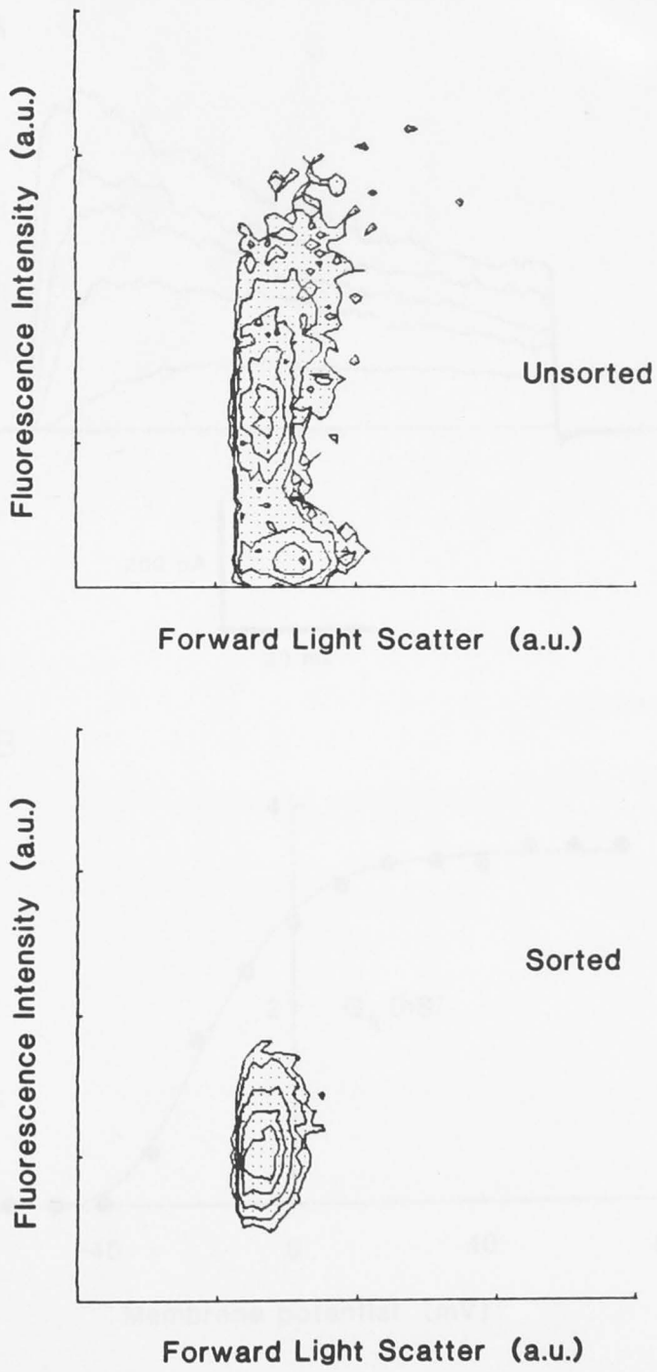

Figure 9. Positive selection of small Lyt-2$^+$/L3T4$^+$ thymocytes

A) Two-dimensional fluorescence profile of mouse thymcoytes fluorescently labelled with an anti-Lyt-2 mAb. Contours were 5%, 10%, 25%, 50% and 75% of the peak height.

B) Fluorescence profile of thymocytes positively selected for fluorescence-labelled cells.

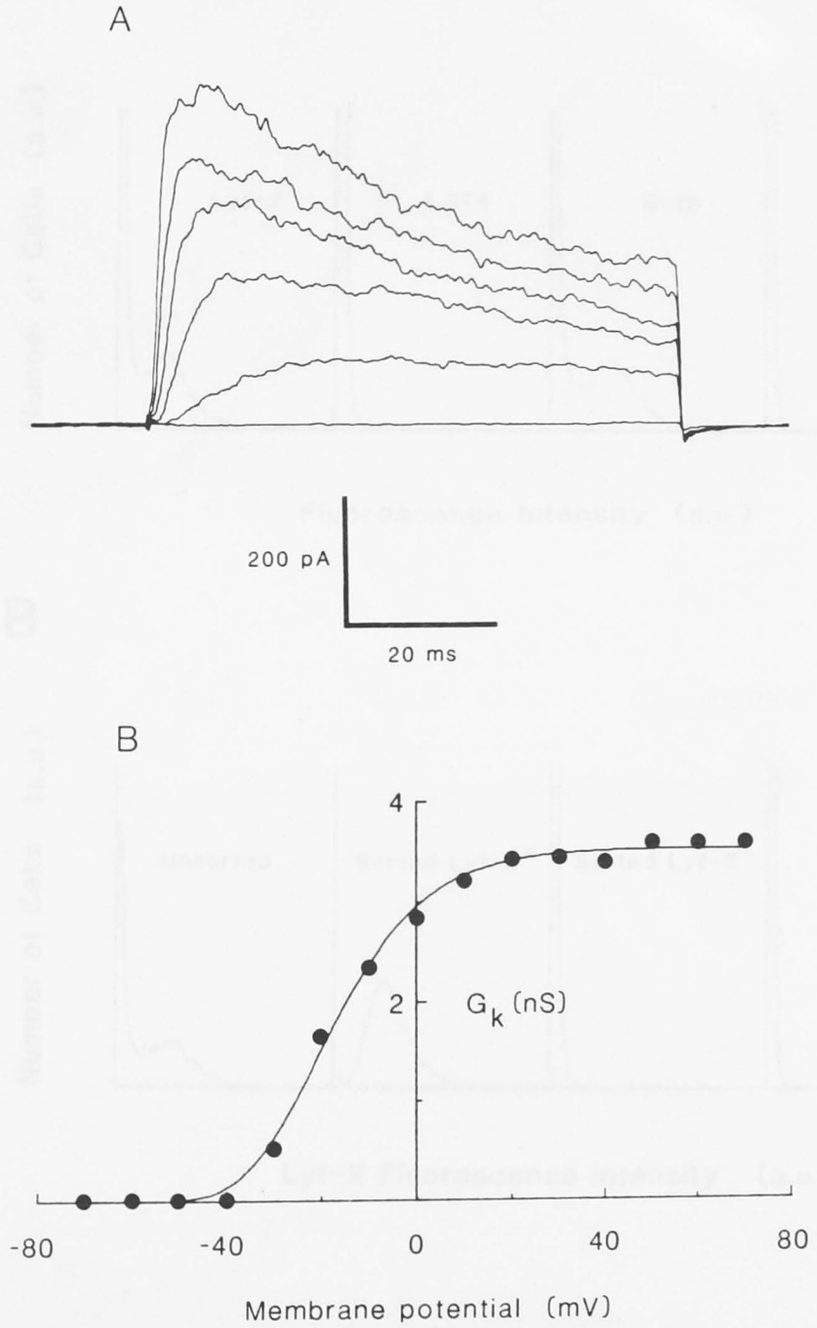

Figure 10. Voltage-activated K^+ channel expression by Lyt-2^+/L3T4^+ thymocytes.

A) Whole-cell voltage-clamp current records recorded from a Lyt-2^+/L3T4^+ thymocyte. Holding potential was -80 mV and voltage steps were applied at 30 second intervals. Voltage was stepped over the range -70 to +70 mV in 10 mV increments. (Only steps to -40, -20, 0, 20, 40 and 60 mV are shown). Sampling interval 100 µs, filter 1kHz.

B) Peak conductance-voltage relationship for the data shown in Fig. 10a. Data was fitted using equation (1) with V_n = -37.3 mV, k_n = -12.0 mV and $g_{K,max}$ = 3.54 nS.

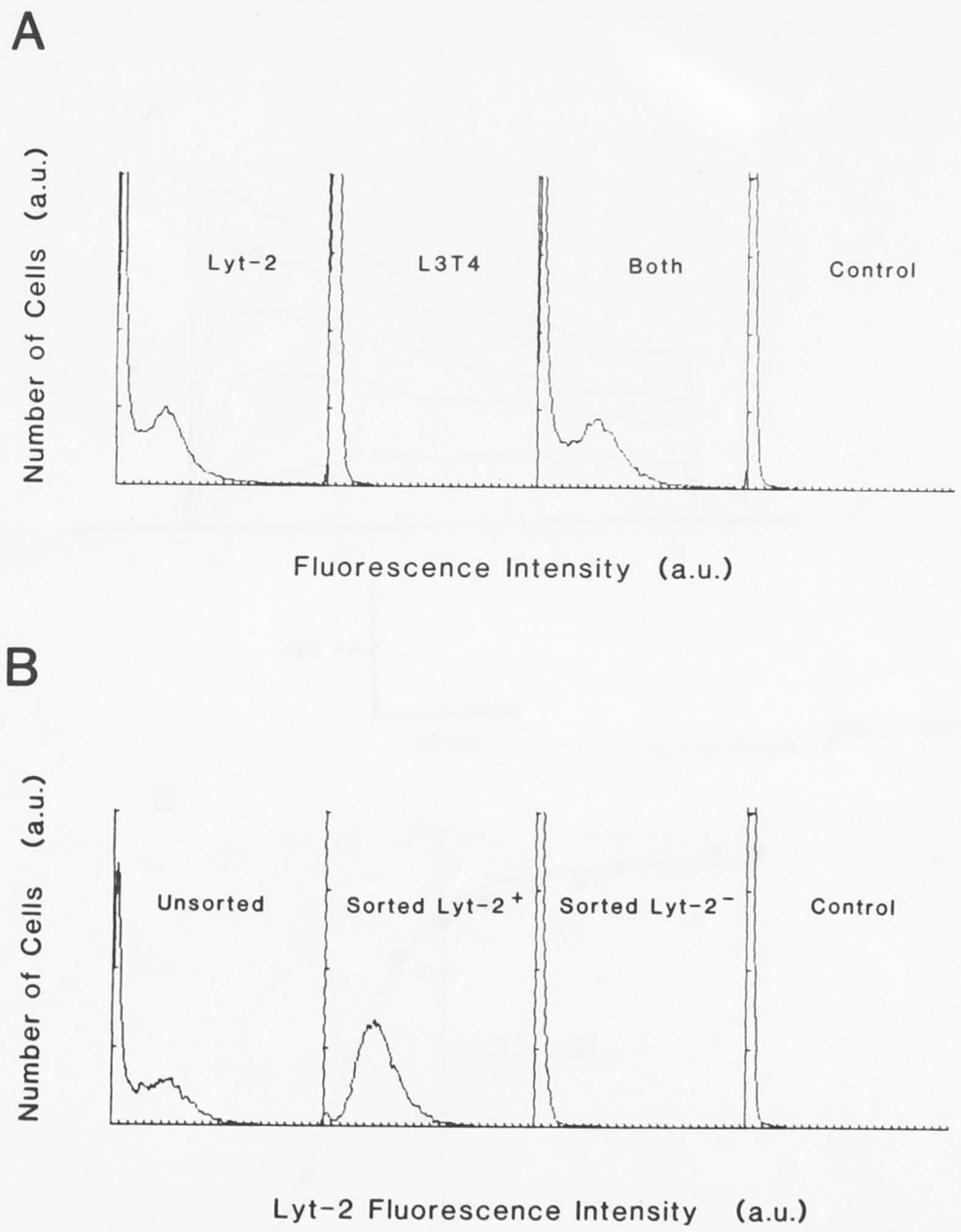

Figure 11. Positive and negative selection of Lyt-2$^+$/L3T4$^-$ thymocytes.
A) Fluorescence profile of thymocytes following depletion of L3T4$^+$ cells. The first three panels show cells labelled with either anti-Lyt-2 or anti-L3T4 mAbs or with both. This L3T4 depleted population was approximately 1.4 % L3T4$^+$ compared with the negative control shown in the right hand panel. **B)** Positive selection of Lyt-2$^+$/L3T4$^-$ thymocytes. The left-hand panel shows the fluorescence profile of L3T4$^-$ thymocytes stained with an anti-Lyt-2 mAb. Approximately 55% of cells were Lyt-2$^+$. The second and third panels show profiles of populations positively selected for fluorescent or non-fluorescent cells respectively. Following positive selection, cells were 97% Lyt-2$^+$ compared with the negative control shown in the right-hand panel.

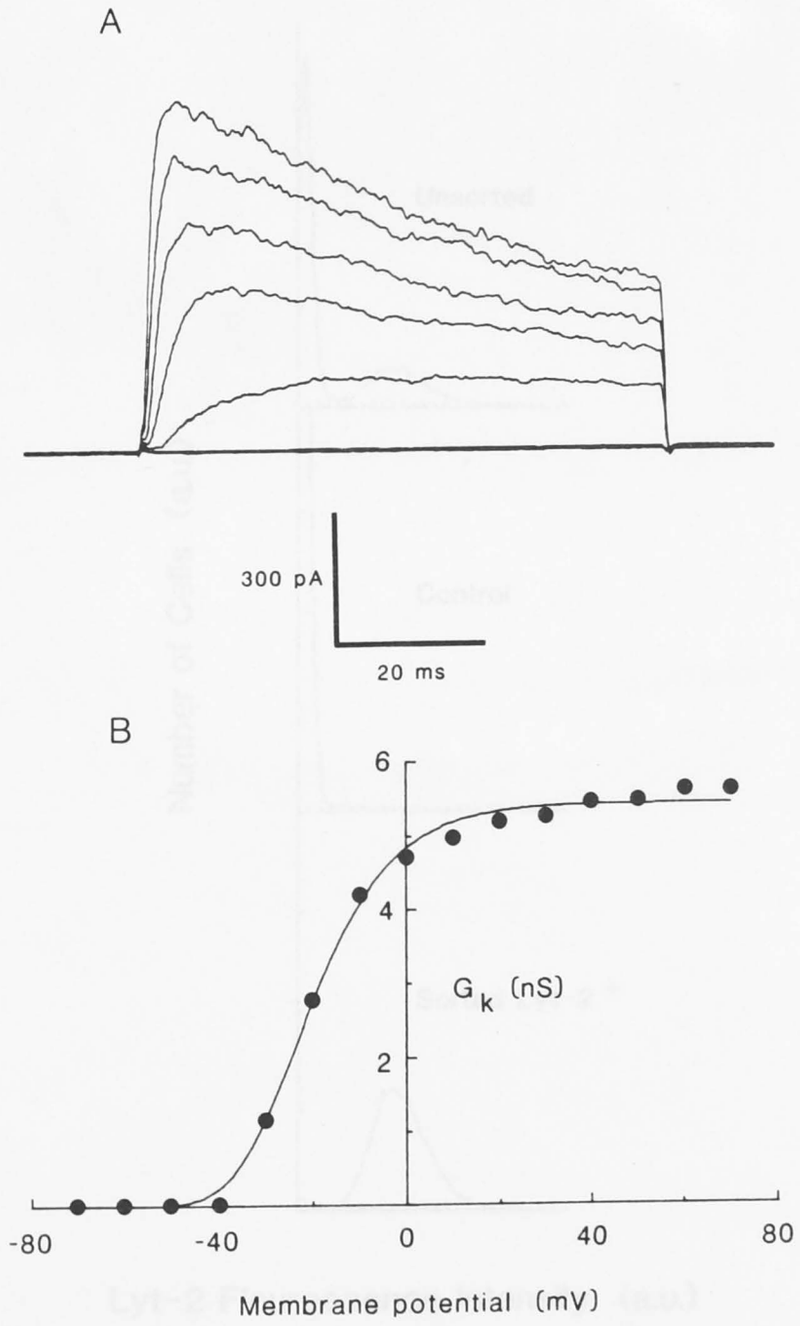

Figure 12. Voltage-activated K^+ channel expression by Lyt-2^+/L3T4$^-$ thymocytes.

A) Whole-cell voltage-clamp records from a Lyt2^+/L3T4$^-$ thymocyte. Voltage steps to -40, -20, 0, 20, 40 and 60 mV are shown. Sampling interval 100 µs, filter 1 kHz.

B) Peak conductance-voltage relationship for the data shown in Fig. 12a. Data were fitted using equation (1) with V_n = -38.1 mV, k_n = -10.8 mV and $g_{K,max}$ = 5.4 nS.

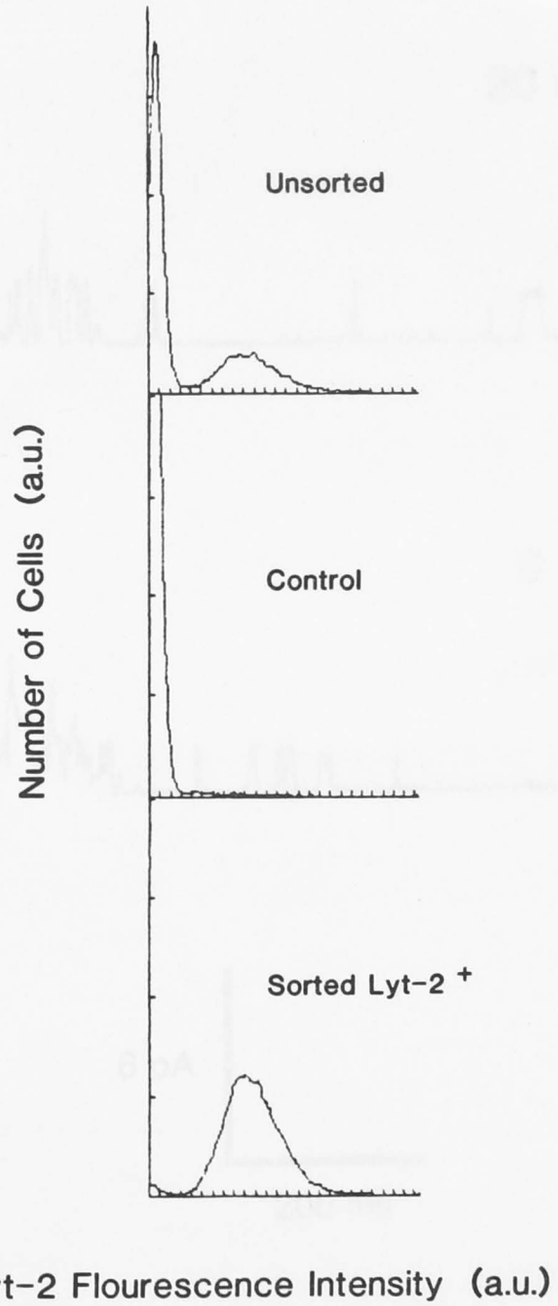

Figure 13. Positive selection of Lyt-2$^+$/L3T4$^-$ peripheral lymphocytes.

Fluorescence profile of J11d$^-$ pooled inguinal and axillary lymph node lymphocytes before and after sorting for Lyt-2$^+$/L3T4$^-$ lymphocytes. Top panel, cells labelled with anti-Lyt-2 mAb were 34% positive. Centre panel, negative control. Bottom panel, cells sorted for Lyt-2 fluorescence were 98% fluorescence positive.

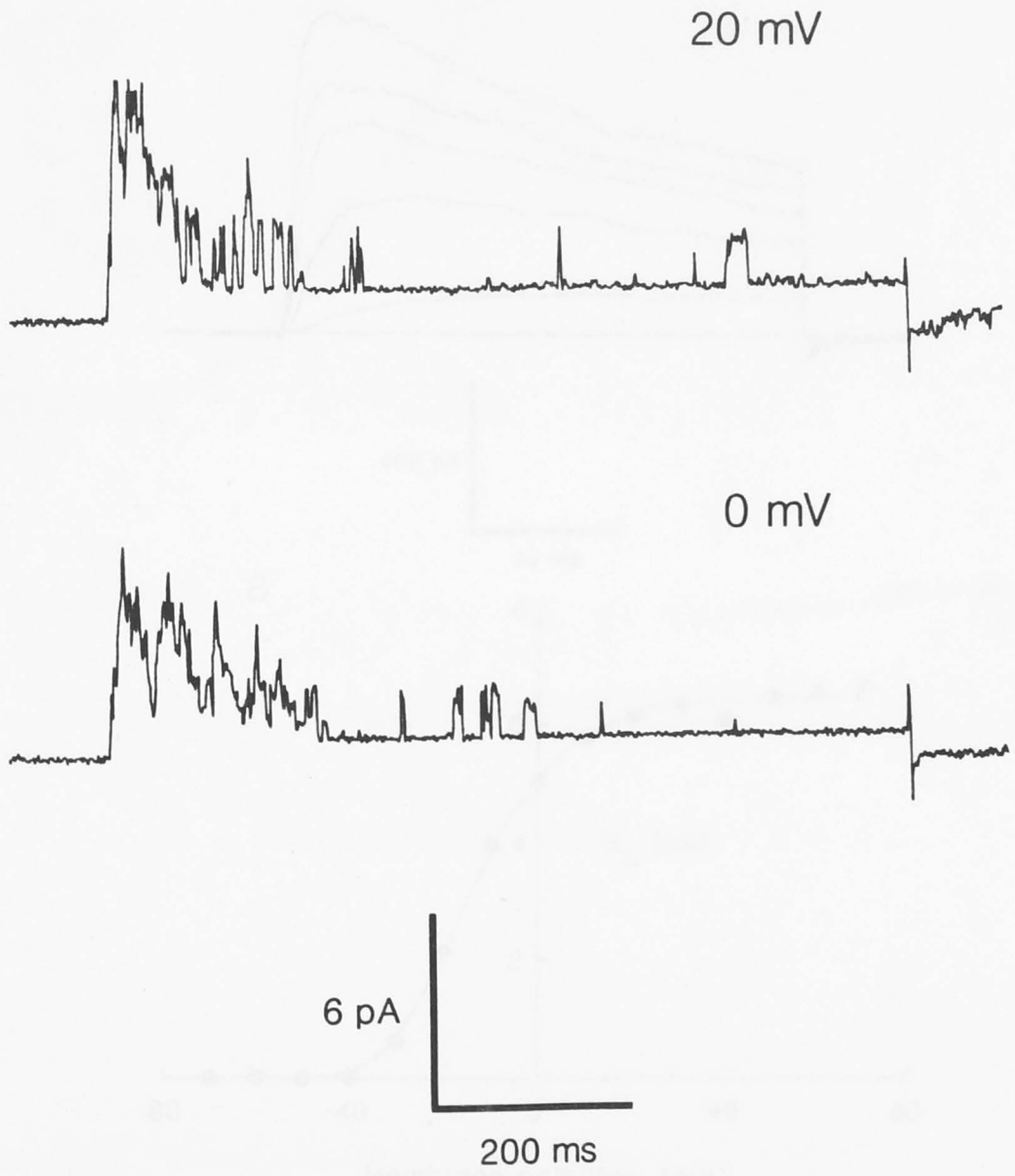

Figure 14. Voltage-activated K^+ channel expression by Lyt-2^+/L3T4$^-$ peripheral lymphocytes.

Whole-cell voltage clamp records from a Lyt-2^+/L3T4$^-$ peripheral lymphocyte. Holding potential -80 mV, 800 ms steps to 0 mV and +20 mV reveal single K^+ channels. Sampling interval 1 ms, filter 500 Hz.

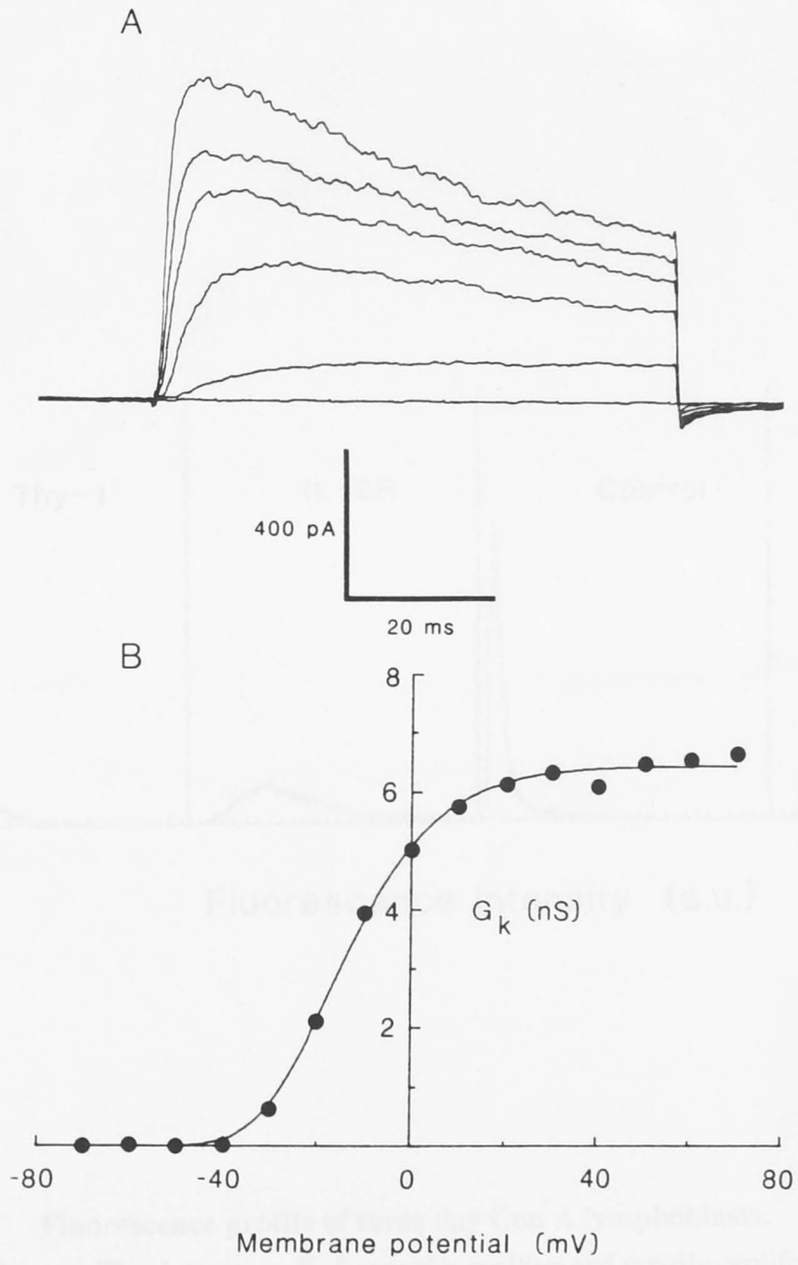

Figure 15. Voltage-activated K^+ channel expression by Lyt-2^+/L3T4$^-$ three day Con A lymphoblasts.

A) Whole-cell voltage clamp records from a Lyt-2^+/L3T4$^-$ three day Con A blast. Voltage steps to -60, -40, -20, 0, 20, 40 and 60 mV are shown. Sampling interval 100 µs, filter 1 kHz.

B) Peak conductance-voltage relationship. Data were fitted using equation (1) with V_n = -33.8 mV, k_n = -12.1 mV and $g_{K,max}$ = 6.5 nS.

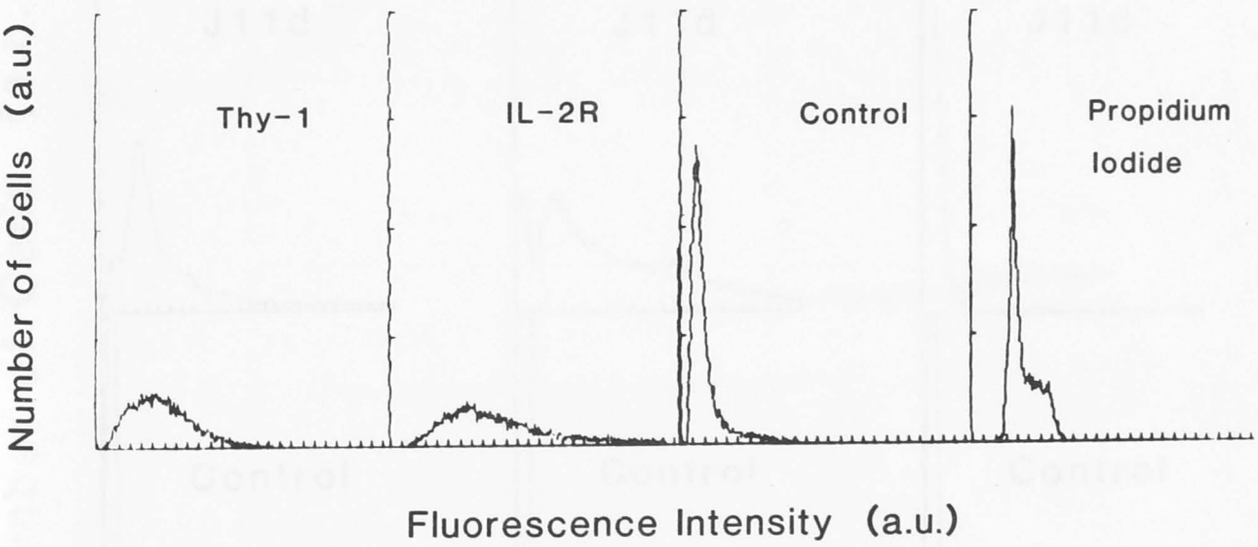

Figure16. Fluorescence profile of three day Con A lymphoblasts.

Cells were Thy-1 positive, IL-2 receptor positive and rapidly proliferating, as assessed by staining with the DNA binding dye propidium iodide.

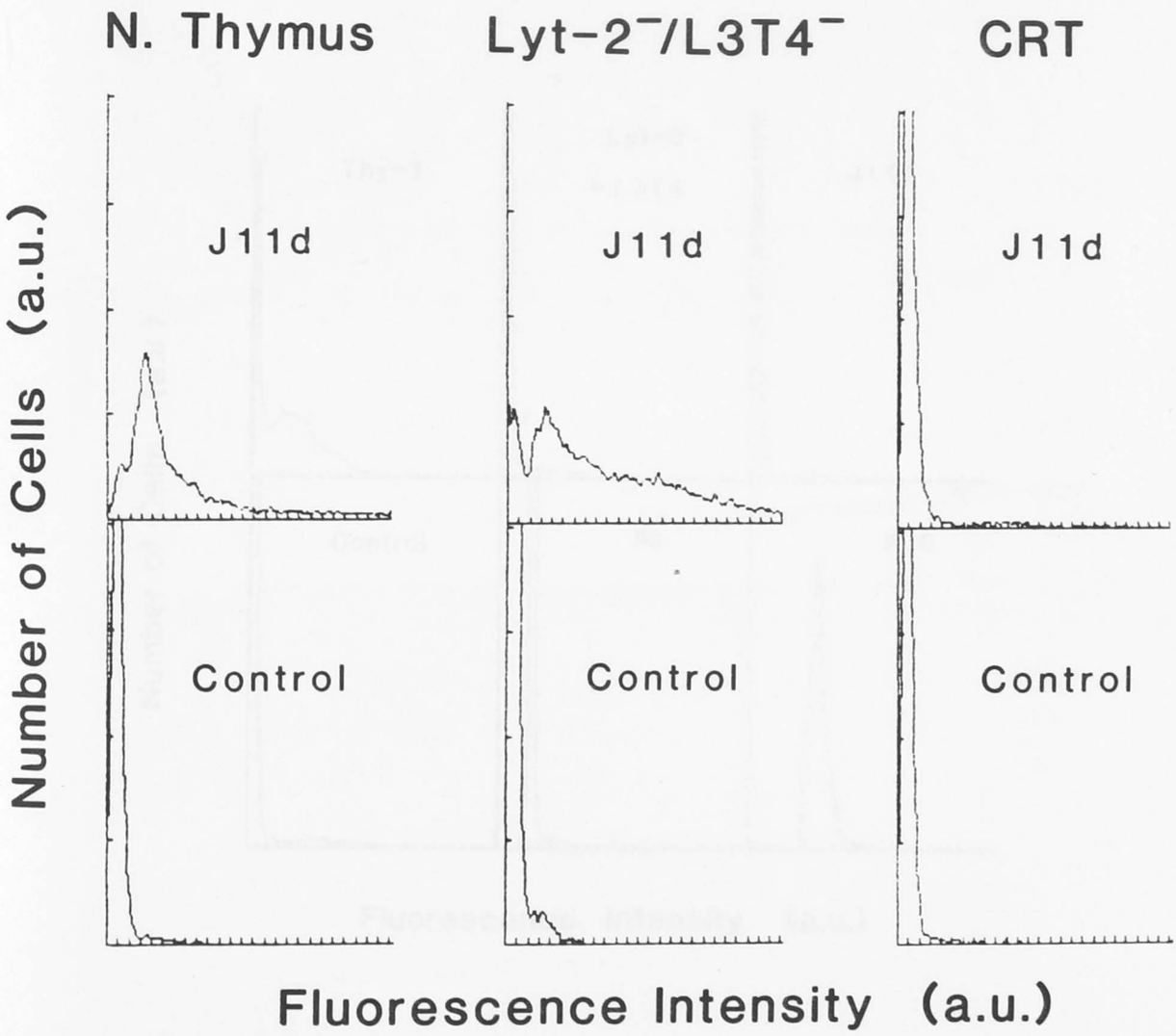

Figure 17. J11d staining profile of normal thymocytes, Lyt-2⁻/L3T4⁻ and CRT.

Normal thymocytes were 86% positive, Lyt-2⁻/L3T4⁻ thymocytes were 85% positive and CRT were ≈5% positive.

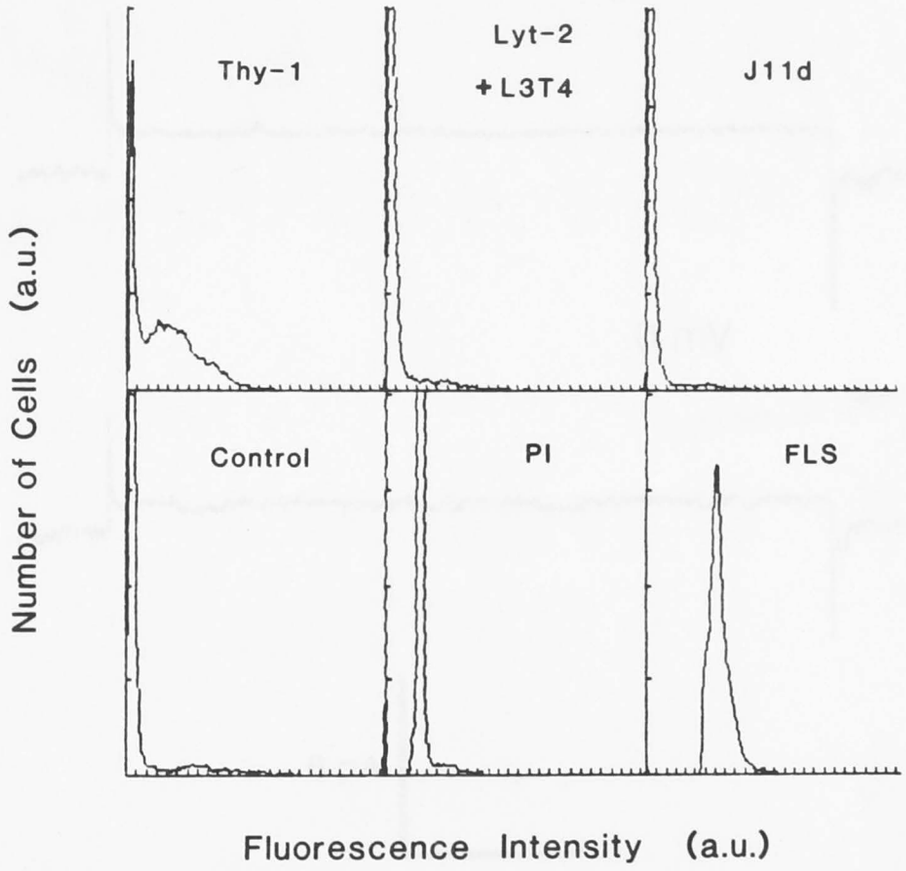

Figure 18. Fluorescence profile of J11d$^-$/Lyt-2$^-$/L3T4$^-$ thymocytes.

Cells were stained with mAbs to Thy-1, Lyt-2 plus L3T4 and J11d. Cells were stained for DNA content with the DNA binding dye propidium iodide. Also shown is the forward light scatter profile indicating a homogeneous population of cells with regard to cell size.

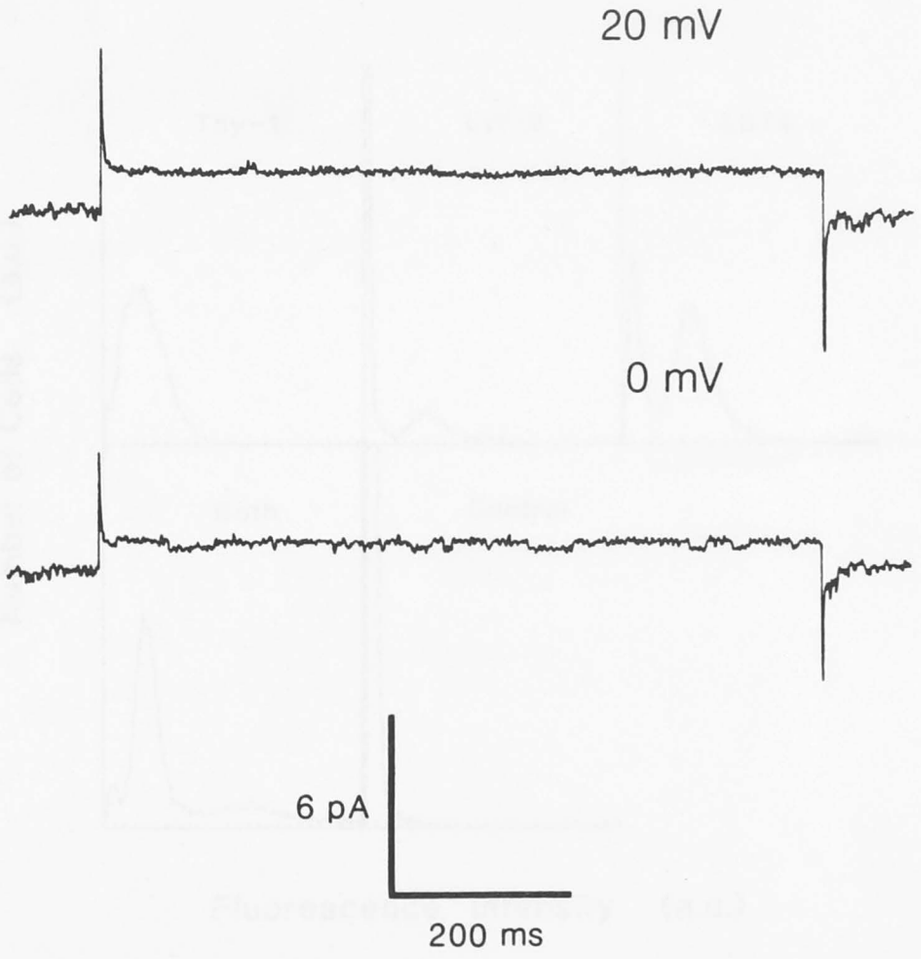

Figure 19. Whole-cell voltage-clamp records from a J11d$^-$/Lyt-2$^-$/L3T4$^-$ thymocyte.

Holding potential was -80 mV. Voltage steps to 0 mV and +20 mV are shown. No voltage-activated single channel currents were observed in this cell although a very small conductance channel was detected in some traces such as the the step to 0 mV. Sampling interval 1 ms, filter 500 Hz.

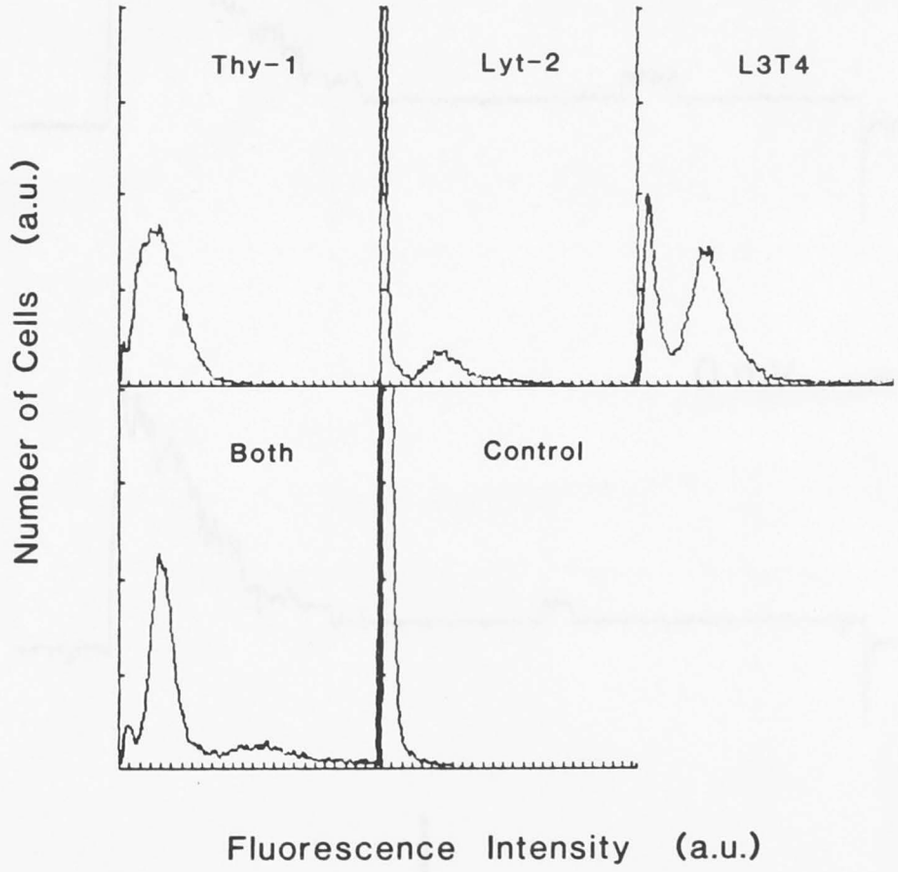

Figure 20. Surface phenotype of C57BL/6 adult J11d$^-$ thymocytes.

Negatively selected thymocytes were stained by indirect immunofluorescence with anti-Thy-1, anti-Lyt-2, anti-L3T4 and a mixture of both anti-Lyt-2 plus anti-L3T4 mAbs.

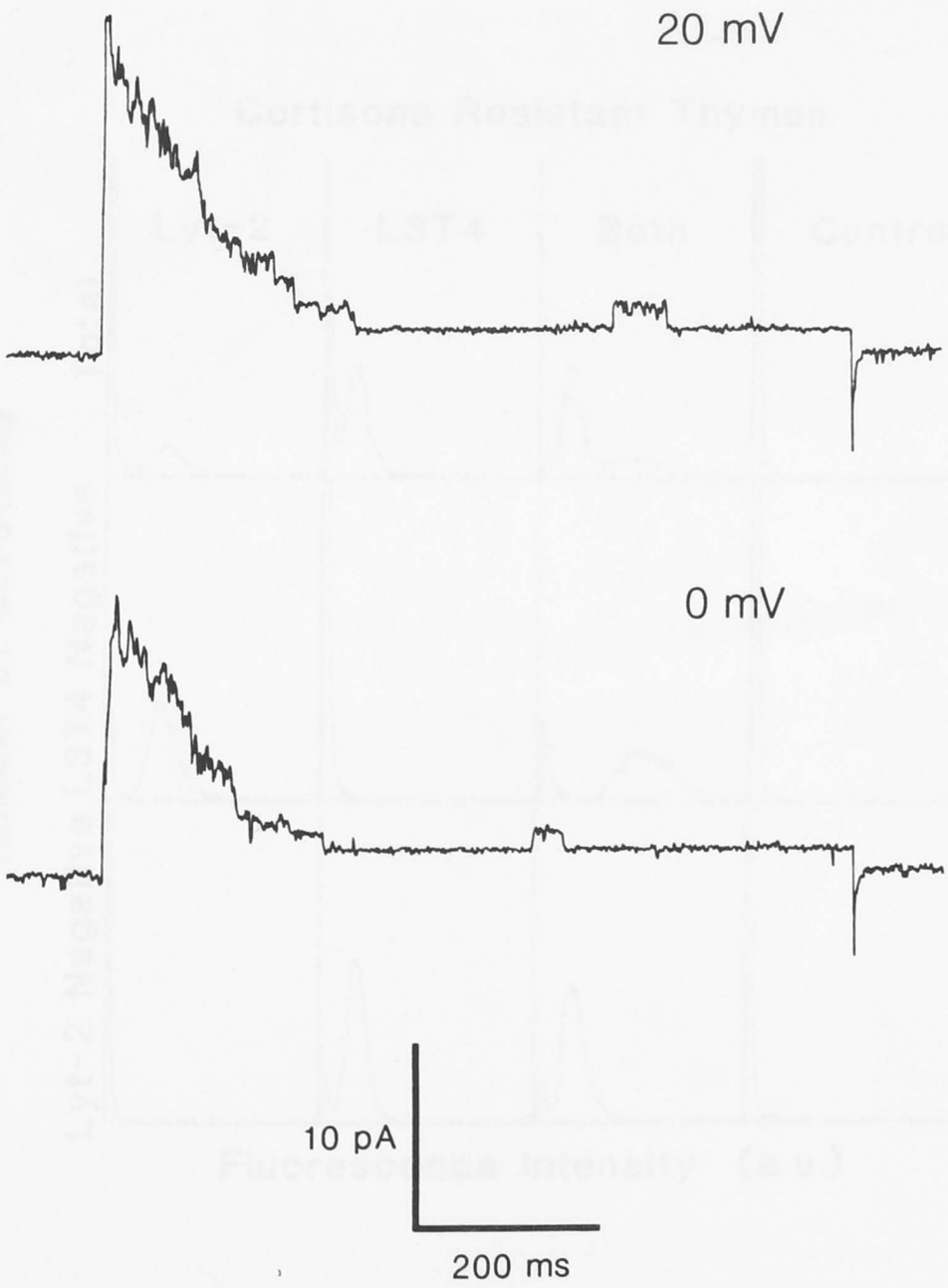

Figure 21. Voltage-activated K^+ channel expression by J11d$^-$ thymocytes.

Whole-cell voltage-clamp records from a J11d$^-$ thymocyte. J11d$^-$ thymocytes were obtained by negative selection using the mAb J11d plus complement. Holding potential -80 mV, 800 ms steps to 0 mV and +20 mV. Sampling interval 1 ms, filter 500 Hz.

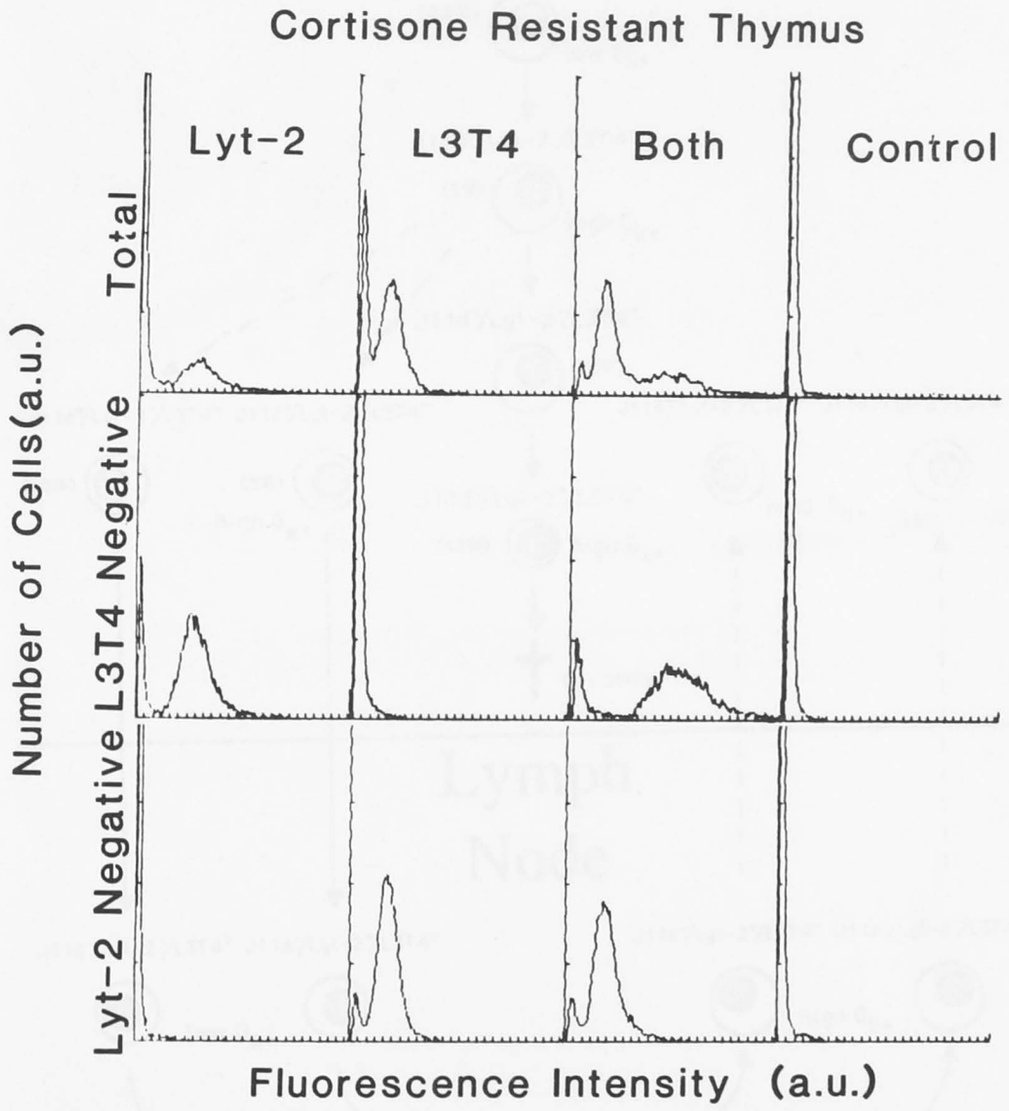

Figure 22. Surface phenotype of cortisone-resistant thymocytes.

CRT were separated into three groups: total, L3T4-depleted and Lyt-2-depleted. Cells were then stained by indirect immunofluorescence with anti-Lyt-2, anti-L3T4 or a mixture of the two mAbs (Lyt-2 + L3T4).

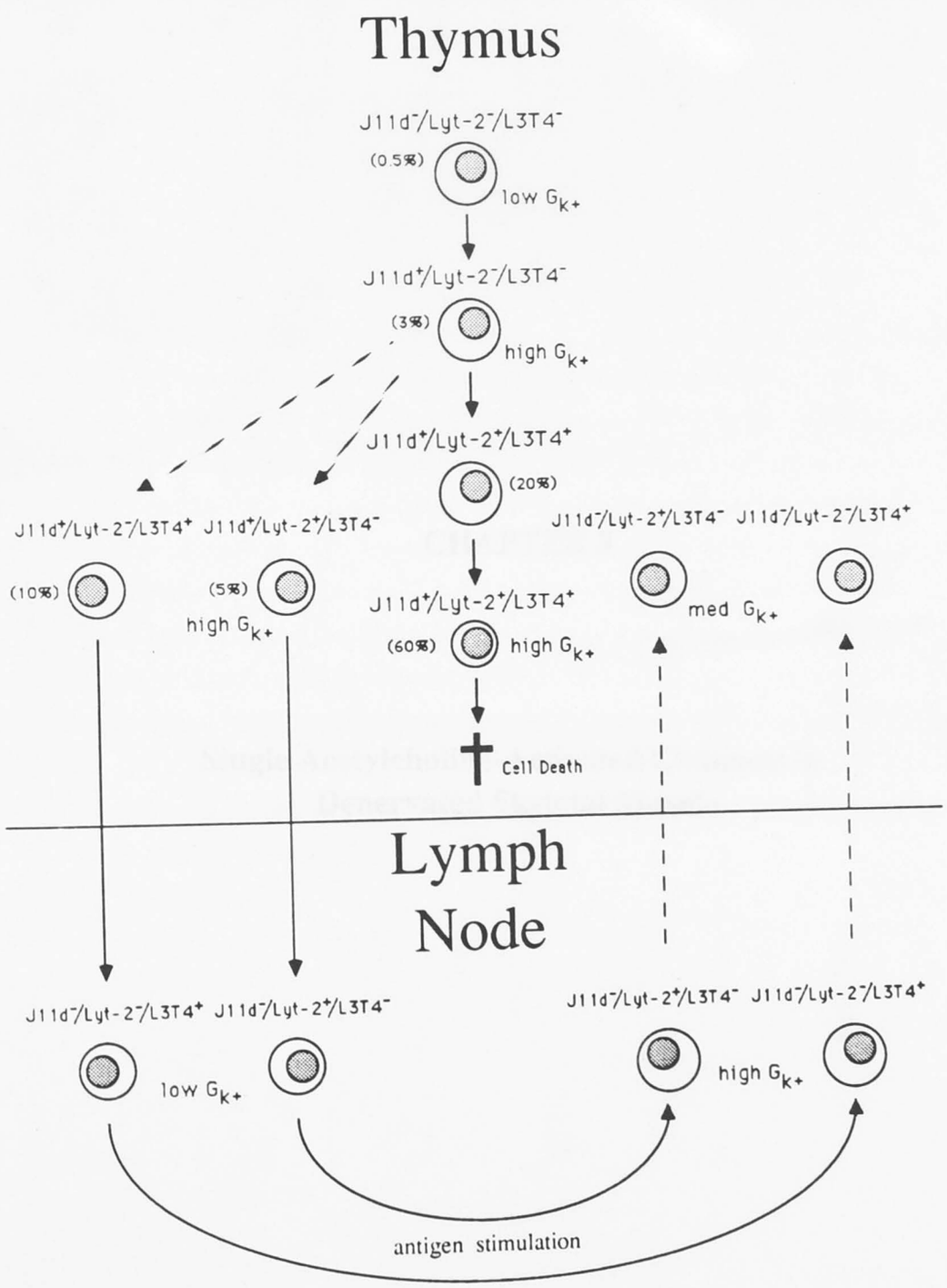

Figure 23. Summary of voltage-activated K^+ channel expression (G_K+) during T cell maturation.

Subpopulations of T cells are defined by the surface antigens Lyt-2, L3T4 and the antigen recognized by the mAb J11d. Lineage relationships, where they remain uncertain, are shown as dashed lines. The number of thymocytes within each subpopulation (if it has been determined), is shown in brackets as a percentage of the total number of thymocytes.

CHAPTER 3

Single Acetylcholine-Activated Channels in Denervated Skeletal Muscle

INTRODUCTION

If the nerve innervating an adult skeletal muscle is cut, the number of acetylcholine-activated channels expressed in the non-junctional region of the muscle's surface membrane greatly increases over a period of several days or weeks (Axelsson and Thesleff, 1959; Miledi, 1960). Extrajunctional AChRs have a number of physical and functional properties which are different to the AChRs at the neuromuscular junction (see Chapter 1 for details). In particular, noise analysis studies have shown that ACh channels in the extrajunctional regions of denervated rat muscle have a lower single channel conductance and longer average channel open time than do ACh channels at the end-plate (Sakmann, 1975). It has been assumed that the AChRs expressed in the extrajunctional region of the denervated muscle are a homogeneous population of receptors. In this chapter the single channel properties of AChRs in the extrajunctional regions of denervated rat muscles are described, and it is shown that there are two classes of receptors. The conductance and kinetic properties of these channels are very similar to those found in embryonic muscle.

METHODS

The Preparation Experiments were performed on denervated (12 to 16 days) extensor digitorum muscles of 300-400 g male Wistar rats. The collagenous matrix surrounding individual muscle fibres was removed by treatment with collagenase (0.3% Sigma type 1A) for 1.0-1.5 h at 35 °C. Following enzyme treatment, single muscle fibres were isolated with a small glass hook as described by Neher et al (1978).

Solutions The standard extracellular solution contained: 145 mM NaCl, 2.5 mM KCl, 2.5 mM $CaCl_2$, 1.0 mM $MgCl_2$, 30 nM tetrodotoxin, 2 mM Na-Hepes, pH adjusted to 7.3. The pipette solution also contained 200-400 nM acetylcholine.

Patch Pipettes Fabrication of patch pipettes is described in Chapter 5.

Electrophysiology Single channel currents were recorded using a List Electronics (L/M EPC-5) I-V converter headstage and amplifier. The membrane potential of isolated muscle fibres was measured with an independent intracellular electrode. The potential across the membrane patch was controlled by holding the potential inside the pipette at a voltage equal to the difference between the intracellular potential of the muscle fibre and the command potential. Current recordings were low-pass filtered (1.3 kHz -3dB point, 4 pole Bessel) and sampled at 10 kHz. Data were taken in blocks of 1s duration separated by 3 s intervals during which the data were stored on magnetic discs.

Data Analysis To analyse the data, a programme was used that automatically identified and subtracted the baseline current level from individual records. On a second pass of the corrected data, a mid-level threshold crossing routine was used to identify single channel events, and the duration of channel open and closed times within each record was stored in sequential order. The cumulative distribution of open and closed times could be calculated directly from the measured transition times. To calculate the burst length distribution, a critical closed time was calculated using a procedure similar to that of Magleby and Pallota (1983). Burst length was defined as the sum of open and closed times (within a single record) that were not separated by a closed time greater than the calculated critical closed time value. Typically, this value was 3 to 5 times greater than the time constant of the fast component of the closed time distribution. The cumulative lifetime distributions were fitted with single or double exponential functions using a non-linear, least squares procedure. The dead time for the midlevel threshold detection of events was 155 μs and, for this reason, curve fitting was restricted to events of duration greater than or equal to 200 μs.

RESULTS

Single Channel Conductance

Acetylcholine-activated single channel currents recorded from the extrajunctional region of denervated muscle are shown in Fig 1a. It can be seen that there are two main types of channel in denervated muscle, with different conductances and mean open times. The current-voltage relationships for both channels are linear over a wide range of potentials (Fig. 1b). The single channel conductances of the channels in the patch shown in Fig. 1 were 33 pS and 48 pS and the reversal potential for both channels was +3 mV. Average conductances of 32 ± 0.5 pS (mean ± s.e.m., n = 4) and 46 ± 0.5 pS were determined for the two types of channel at a temperature of 16°C.

It has been shown using noise analysis that ACh channels in the extrajunctional region of denervated rat muscle have a lower single channel conductance and longer channel lifetime than channels at the end-plate (Sakmann, 1975). It is likely, therefore, that the smaller conductance channel observed in the single channel records corresponds to the 'extrajunctional' channel identified using noise analysis, and that the large conductance channel corresponds to the 'junctional' channel found at the end-plate. The relative number of each channel type observed in different patches was variable. A small percentage of patches appeared to have only junctional channels, whereas others had only extrajunctional channels. Most commonly, however, a mixture of channels was observed, with extrajunctional channels being the most prevalent.

Channel Kinetics

Because of the relatively fast kinetics of the junctional channel and the difficulty in finding patches in which only the junctional channel was present, kinetic analysis was restricted to patches in which there was a predominance (greater than 95%) of extrajunctional channel openings. Channel kinetics were complex (Fig. 2), and were qualitatively similar to other studies on AChR activation in which brief duration closures interrupted channel openings to give 'bursts' of channel openings (Colquhoun and Sakmann, 1981; Sine and Steinbach, 1986). Cumulative distributions of the open times of extrajunctional channels had two components which could be fitted with a bi-exponential distribution (Fig. 3). Average values for the time constants of the fast and slow components of the distribution are shown in Table 1. The distribution of closed times and burst lengths were also composed of two separable components (Figs 4 and 5).

Assuming that there are two acetylcholine binding sites per receptor and that both sites must be occupied before the channel opens, then the following kinetic scheme is required to account for receptor activation (Colquhoun and Hawkes, 1981; Sine and Steinbach, 1986):

$$2A + R \underset{k_{-1}}{\overset{k_1}{\Longleftrightarrow}} AR \underset{k_{-2}}{\overset{k_2}{\Longleftrightarrow}} A_2R \underset{\alpha}{\overset{\beta}{\Longleftrightarrow}} A_2R^*$$

where, A is the agonist, R is the receptor, AR is a singly liganded receptor, A_2R is a doubly liganded receptor and A_2R^* is an activated receptor.

At low agonist concentrations the time constant for channel opening is α^{-1}, the time constant for short duration channel closures is $(\beta + k_{-2})^{-1}$ and the number of closures per burst is β / k_{-2}. Average values for these rate constants, calculated from the data in Table 1, are $\alpha = 54\ s^{-1}$, $\beta = 231\ s^{-1}$ and $k_{-2} = 857\ s^{-1}$. Sine and Steinbach (1986), in their kinetic study on the extrajunctional AChR in embryonic muscle, found three components in the closed time distribution. The rate constants calculated in this report, for the extrajunctional receptor in denervated muscle, are in reasonable agreement with those reported for embryonic muscle, if it is assumed that the fast component of the closed time distribution described here is comparable with the time constant of the intermediate duration closed times in embryonic muscle.

In an attempt to increase the effective frequency response, kinetic experiments were also performed at 13°C (Table 1). As expected, the burst length increased as the temperature decreased. The number of brief openings per burst also increased, indicating that a greater percentage of brief channel closures were being resolved. It was not possible, however, to resolve three components in the closed time distribution, and the fast component of the closed time distribution appeared to decrease with a decrease in temperature. This result can be accounted for by assuming that more of the fastest channel closures, which were inadequately resolved at 16°C, were contributing to the fast component of the closed time distribution at 13°C. The slight decrease in apparent channel open time is also due to better resolution of the fastest channel closures.

Subconductance States

It has been shown that some of the brief channel closures of ACh-activated channels in cultured embryonic muscle are not complete channel closures but rather, involve entry of the AChR into a subconductance state in which the channel conductance is some fraction of the normal open state conductance (Hamill and Sakmann, 1981). Similar phenomena were seen in denervated rat muscle. An example of one of these brief, partial closures is shown in Fig. 6. In this example, the channel appears to enter a state with a conductance of approximately 24% of the fully open conductance for a duration of 1.5 ms. Subconductance states were most easily resolved in records obtained at 13°C but they could also be seen at 16°C and an example is shown in the top trace of Fig 1a.

DISCUSSION

The extrajunctional AChR in denervated muscle is very similar to the AChR of cultured embryonic rat muscle with respect to conductance and kinetic properties (Sakmann et al, 1983; Siegelbaum et al, 1984; Sine and Steinbach, 1986). The frequency response of the experiments reported here was limited when compared with the detailed kinetic experiments of Sine and Steinbach (1986) which makes direct comparison difficult. Nevertheless, the fastest component of the closed time distribution of the extrajunctional AChR recorded in denervated muscle at 16°C corresponds well to the intermediate closed time component described in their report. Taking this into account, there is reasonable agreement between the values for the rate constants α, β and k_{-2} reported here and the values found in embryonic muscle. The single channel conductance values for the extrajunctional and junctional receptors are also similar to embryonic and adult rat muscle (Sakmann et al, 1983; Siegelbaum et al, 1984). Entry of the AChR channel into a subconductance state, which was first reported for the AChR of embryonic rat muscle (Hamill and Sakmann, 1981), was also observed in denervated muscle. Subconductance states always occurred within a burst of channel openings and were never seen to conclude a burst of channel openings, a result which is in contrast with observations in embryonic muscle (Hamill and Sakmann, 1981).

The structural difference between the extrajunctional and junctional forms of the AChR is apparently due to substitution of the ε subunit for the γ subunit during development (Mishina et al, 1986). The results reported here suggest that the ε subunit can be produced by nuclei in the extrajunctional regions of skeletal muscle following denervation, and that production and insertion of the mature, junctional form of the AChR can occur at sites other than the end-plate. In this respect, control of AChR biosynthesis and insertion into the extrajunctional membrane of denervated adult muscle is identical to that of embryonic muscle (Sakmann et al, 1983; Siegelbaum et al, 1984).

Table 1. Average Kinetic Parameters for Extrajunctional Acetylcholine-Activated Channels

Open Times		Closed Times	Burst Lengths		Gaps per Burst	Temperature	N
fast (μs)	*slow (ms)*	*fast (μs)*	*fast (μs)*	*slow (ms)*		℃	
634 ± 113*	18.6 ± 1.3	919 ± 207	655 ± 135	20.5 ± 1.8	0.27 ± 0.09	16	5
844 ± 189	16.8 ± 1.6	377 ± 49	998 ± 362	38.9 ± 1.9	1.1 ± 0.1	13	3

* mean ± s.d.

Figure 1. Acetylcholine-activated single channel currents in denervated rat muscle.

A) Currents recorded at membrane potentials of -140, -100 and -80 mV. Temperature 16°C, filter 1.3 kHz, -3 dB point.

B) Current-voltage relationship for the currents shown in Fig. 1a. Fitted lines are linear regressions with slopes of 33 and 48 pS and a reversal potential at +3 mV.

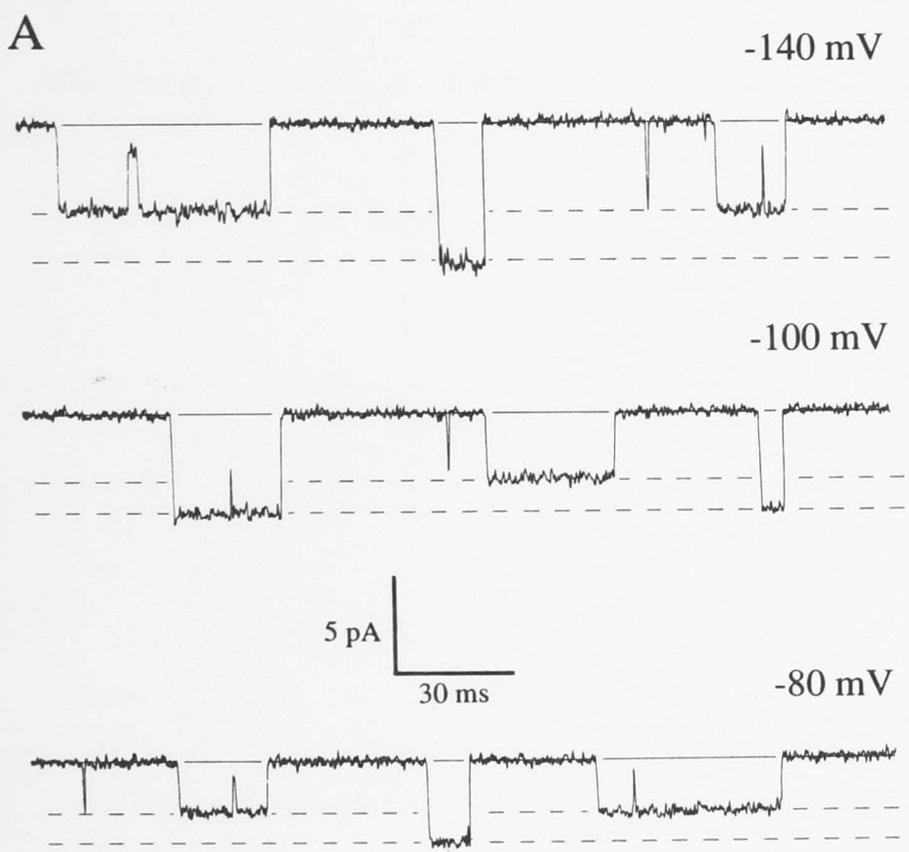
A
-140 mV
-100 mV
5 pA
30 ms
-80 mV

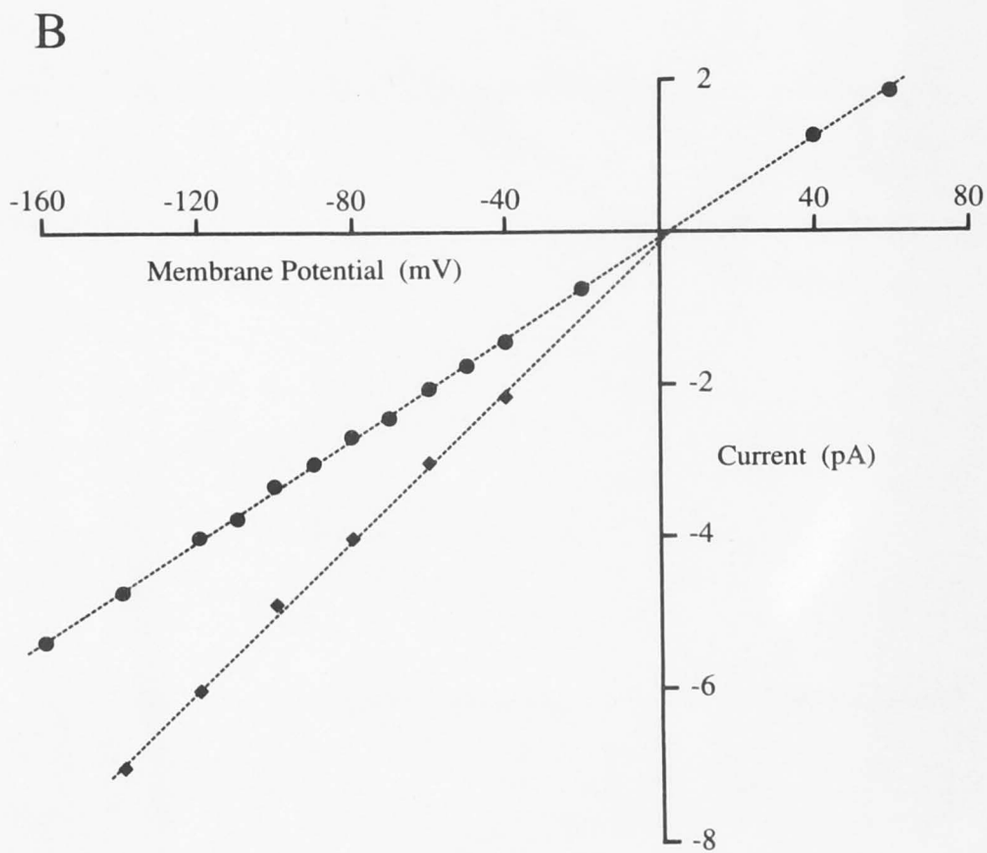
B
2
-160
-120
-80
-40
40
80
Membrane Potential (mV)
-2
Current (pA)
-4
-6
-8

Figure 2. Recordings of acetylcholine-activated single channel currents in denervated rat muscle showing complex kinetic behavior.

A) Membrane potential -100 mV, temperature 16°C. Filter 1.3 kHz, -3dB point.

B) Membrane potential -100 mV, temperature 13°C.

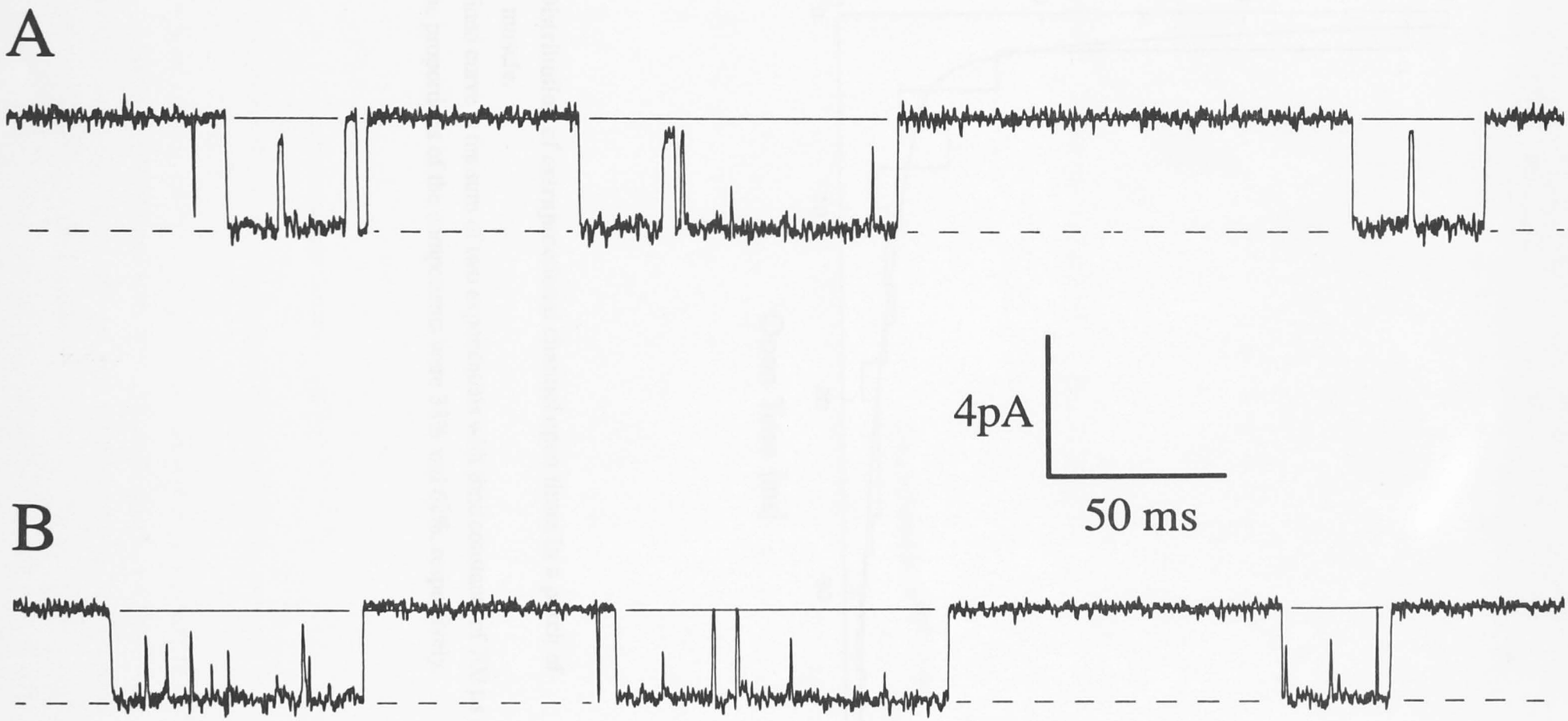
A
4pA
50 ms
B

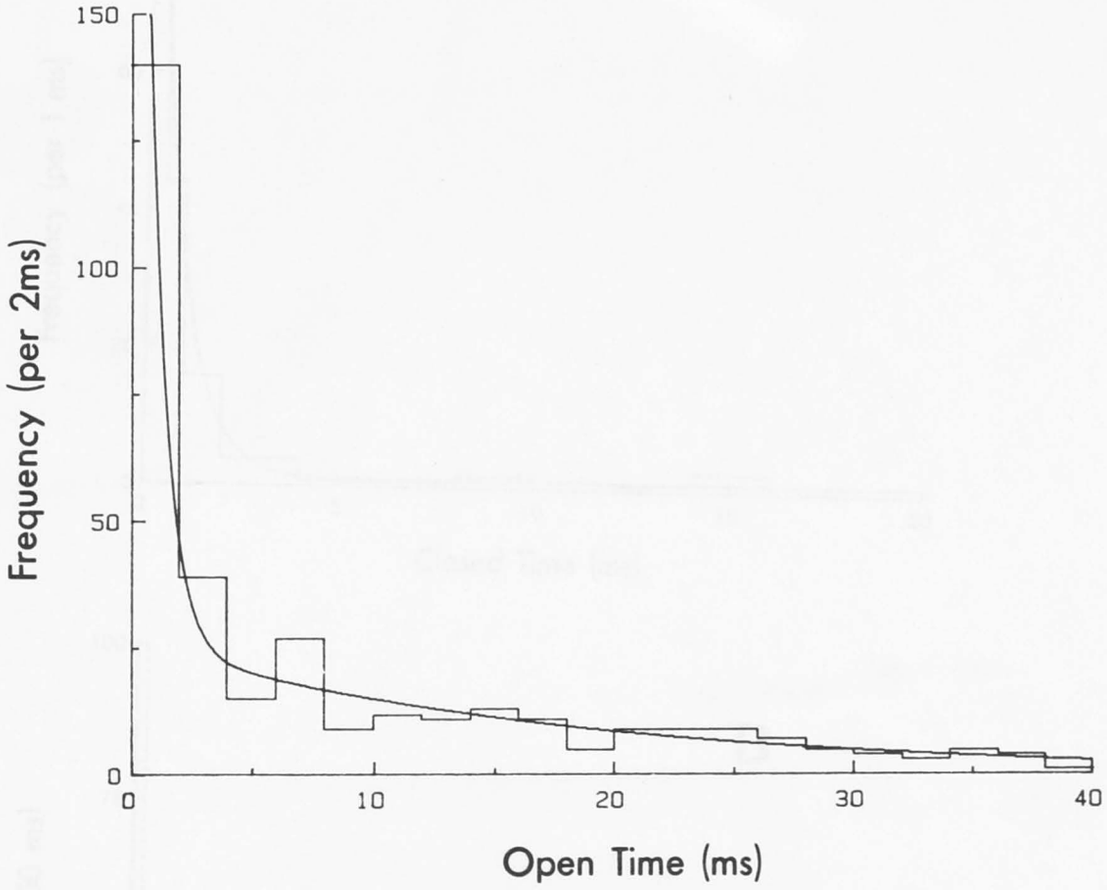

Figure 3. Distribution of extrajunctional channel open times in a patch of denervated muscle.

The fitted curve is the sum of two exponentials with time constants of 700 μs and 17.9 ms. The proportions of the components were 38% and 62%, respectively.

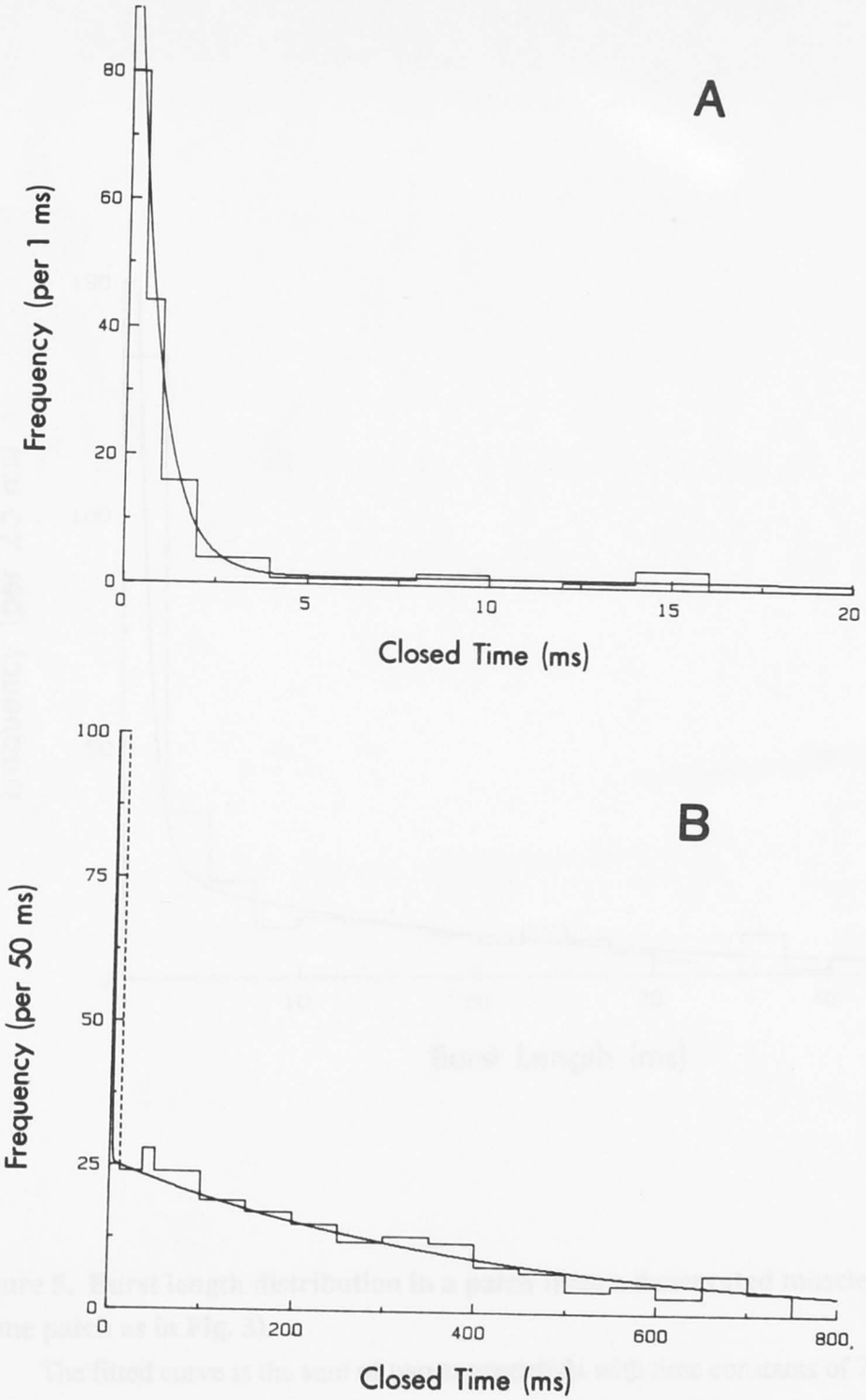

Figure 4. Distributions of channel closed times in a patch of denervated muscle (same patch as Fig. 3).

A) The fitted curve is the sum of two exponentials with time constants of 710 μs and 390 ms. The proportions of the components were 19% and 81% respectively.

B) The same data as in Fig. 4a replotted over the time interval 0 to 800 ms to illustrate the distribution of long closed times.

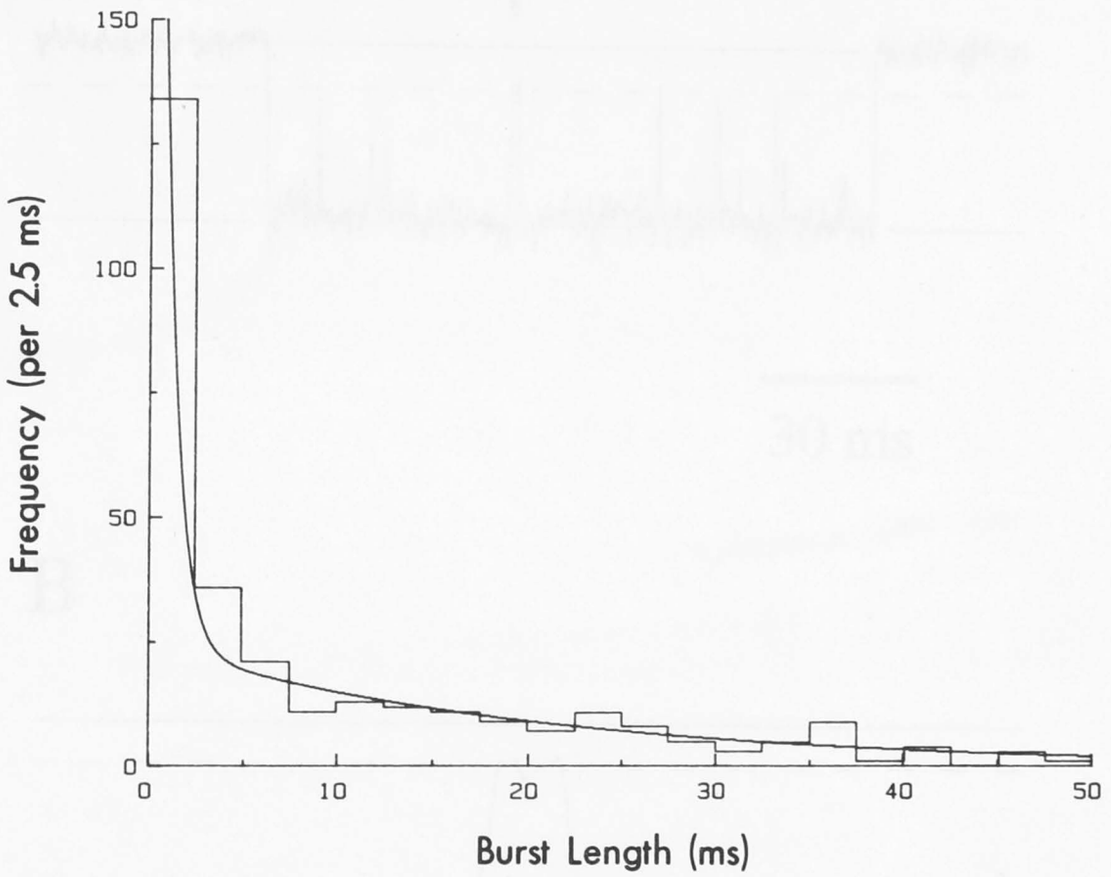

Figure 5. Burst length distribution in a patch from a denervated muscle fibre (same patch as in Fig. 3).

The fitted curve is the sum of two exponentials with time constants of 700 μs and 20.3 ms. The proportions of the components were 41% and 59%, respectively. The distribution of burst lengths was calculated using a gap of 2.6 ms calculated from the distrubution of closed intervals shown in Fig. 4.

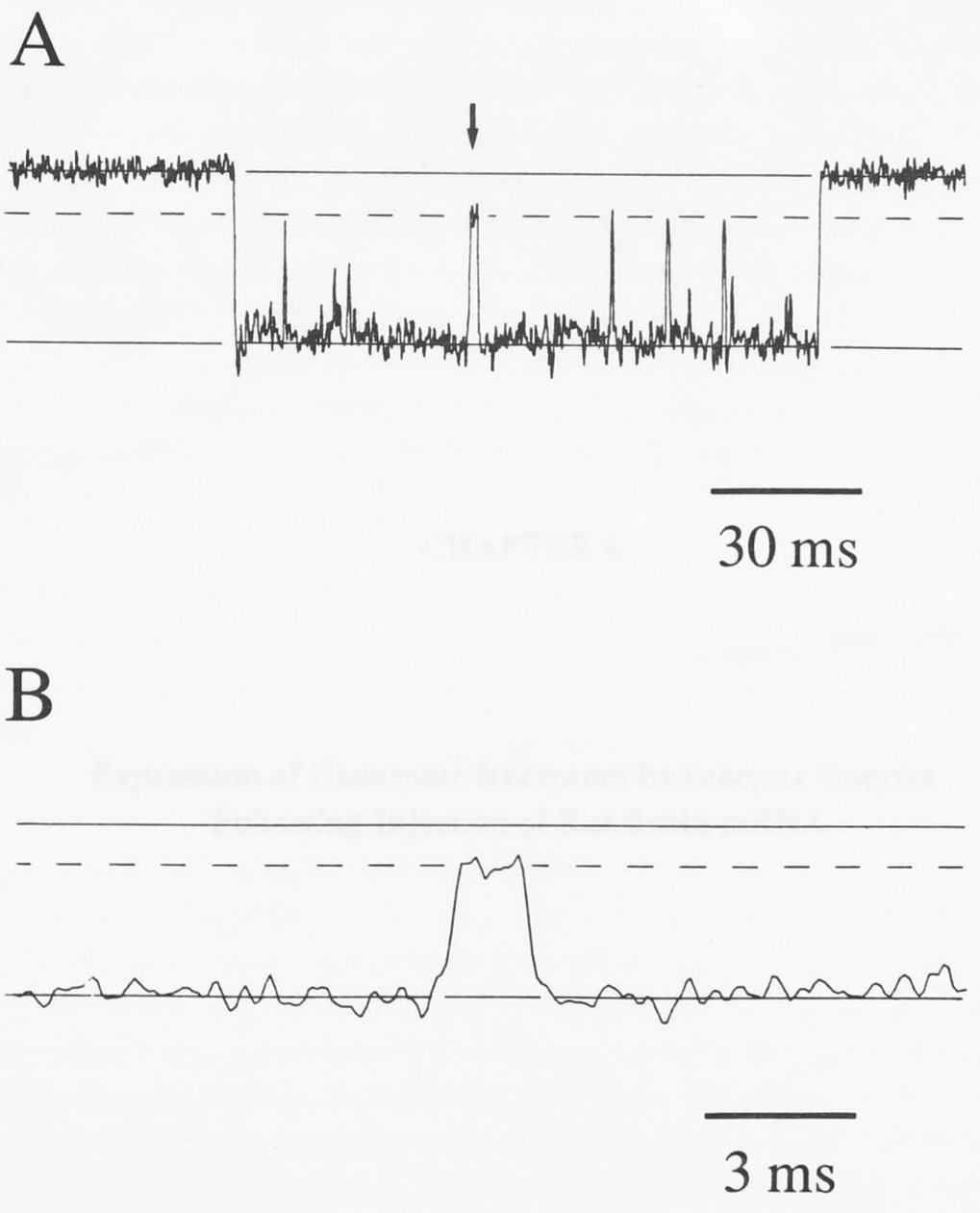

Figure 6. Subconductance state of an extrajunctional acetylcholine-activated channel.

A) Transition to subconductance state is marked by arrow. Solid lines mark closed and fully open conductance states, and dashed line marks 24% of the full open conductance. Temperature, 13°C.

B) Trace replotted on a faster time scale and expanded around the arrow in Fig. 6A.

CHAPTER 4

Expression of Histamine Receptors by *Xenopus* Oocytes Following Injection of Rat Brain mRNA

INTRODUCTION

The *Xenopus* oocyte expression system provides a sensitive assay for the presence of mRNA coding for a variety of distinct pharmacological receptors in various tissues including rat brain (Sumikawa et al, 1981; Barnard et al, 1982; Gunderson et al, 1983, 1984). In this chapter the oocyte expression system is used to show that mRNA isolated from 14-16 day rat brains codes for at least one, and possibly two, classes of functional histamine receptors.

Histamine is thought to function in the mammalian central nervous system as a neuromodulator and, possibly, as a neurotransmitter (Green, 1965; Snyder and Taylor, 1972; Schwartz, 1979; Prell and Green, 1986). Histaminergic neurons have been identified in immunohistochemical studies by means of antisera directed against either the histamine-synthesizing enzyme histidine decarboxylase (Tran and Snyder, 1981; Watanabe et al, 1983), or against histamine itself (Wilcox and Seybold, 1982; Panula et al, 1984). Histaminergic cell bodies appear to be restricted to the posterior hypothalamus, but histaminergic neuronal fibres project widely throughout the brain and into the spinal cord (Watanabe et al, 1984; Takeda et al, 1984; Panula et al, 1984; Wahlestedt et al, 1985). Histamine is released from brain slices in response to both electrical stimulation and high K^+ solutions and this stimulus-evoked release is Ca^{2+}-dependent (Taylor and Snyder, 1973; Biggs and Johnson, 1980; Mulder et al, 1983).

Electrophysiological experiments suggest that histamine may function as a neuromodulator. Histamine has been shown to reduce the after-hyperpolarization of hippocampal CA1 neurons by suppressing a calcium-activated potasssium conductance (Haas and Konnerth, 1983; Pellmar, 1986). Histamine can cause either a hyperpolarization or a depolarization of the resting membrane potential of hippocampal neurons depending upon the mode of drug application (Haas, 1981; Haas, 1984; Pellmar, 1986). Iontophoresis of histamine in vivo can produce either inhibitory or excitatory effects on the spontaneous acitivity of single neurons in the mammalian CNS (Geller et al, 1984).

Brain histamine receptors have been identified in binding studies. Specific binding of ^{3}H-mepyramine to H_1 histamine receptors has been demonstrated and this binding has been shown to be regionally localized within the brain (Tran et al, 1978; Hill et al, 1978; Palacios et al, 1981). Specific binding of the H_2 antagonist tiotidine has also been described (Gajtowski et al, 1983).

Histamine can act in the mammalian brain via at least two different intracellular messenger systems. Stimulation of the H_1 receptor in brain slices initiates the hydrolysis of inositol phospholipids (Daum et al, 1984; Brown et al, 1984), the breakdown products of which can act to release intracellular calcium and activate protein kinase C (Berridge, 1984; Downes and Michel, 1985). The H_2 receptor has been shown to be closely coupled to adenylate cylase activity (Schwartz, 1979).

METHODS

Isolation of mRNA

RNA was prepared by the guanidine thiocyanate-CsCl method (Chirgwin et al, 1979). Rats (14-16 d) were killed by cervical dislocation and the whole brain was rapidly removed and homogenized in 6 M guanidine thiocyanate. The homogenate was layered over 1.5 ml of 5.7 M CsCl and centrifuged for 18 hours at 28,000 rpm. The pellet was resuspended in TES, phenol extracted twice and ethanol precipitated (Maniatis et al, 1982). Poly $(A)^+$ RNA was selected by chromatography over an oligo(dT)-cellulose column (Aviv and Leder, 1972).

Animals, dissection and injection of oocytes

Adult female *Xenopus laevis* were purchased from the South African Snake Farm. Oocytes at stages V and VI (Dumont, 1972) were freed from the ovary by manual dissection, and were pressure injected with ≈50 ng of mRNA. Injected oocytes were then incubated at 19°C for 48 hrs in modified Barths' media (Barth and Barth, 1959).

Electrophysiology

Oocytes were held in a small experimental chamber by means of a ring of dissection pins and perfused continuously at a rate of ≈ 8 ml min^{-1}. The standard bath solution contained: NaCl 96 mM; KCl 2 mM; $CaCl_2$ 2 mM; $MgCl_2$ 1 mM; Na-HEPES 5 mM; pH 7.3.

Voltage clamp experiments were performed using a single micro-electrode switching voltage clamp (Axoclamp 2, Axon Instruments Inc., Burlingame, CA, U.S.A.). Typically, recordings were made with the voltage clamp switching frequency set in the range 10-25 kHz. The headstage of the clamp was continuously monitored to ensure that the voltage across the electrode settled to baseline before the membrane potential was sampled (Finkel and Redman, 1984). Currents were recorded on FM tape.

Electrodes were pulled from 1 mm o.d., fibre-filled glass (Clark Electromedical) and were filled with 3 M KCl to give final resistances in the range 0.7 to 1 MΩ. All experiments were performed at room temperature (20-22°C).

Materials

Histamine, glutamate, serotonin (5-hydroxytyptamine), promethazine and cimetidine were purchased from Sigma. Drug solutions were made up immediately before application.

RESULTS

Messenger RNA isolated from adult rat brains can, when injected into *Xenopus* oocytes, induce the de novo synthesis of a number of pharmacological receptors including receptors for serotonin and glutamate (Gunderson et al, 1983, 1984). Messenger RNA isolated from 14 to 16 day old rat brains could induce a responsiveness to serotonin which was essentially similar to that described previously by Gunderson et al (1983). Application of 10^{-4} M serotonin produced a large oscillatory inward current which washed out only very slowly (Fig. 1a). The reversal potential of this response was approximately -20 mV, similar to that reported previously (Gunderson et al, 1983). The response to a 1 minute application of 10^{-3} M glutamate is shown in the upper trace of Fig. 1b. An inward current with a smooth onset and washout was observed. No oscillatory response to glutamate was observed (n = 5), even during a prolonged 8 min application of the drug (lower trace, Fig. 1b), which is in contrast with the results reported by Gunderson et al (1984) using adult rat brain mRNA.

In addition to the responses to glutamate and serotonin, both an inward and an outward current response could be elicited in injected oocytes by bath applied histamine. As shown in Fig. 2a, the response to histamine was dose dependent. At concentrations of 10^{-5} and 10^{-4} M the primary response was a slowly activating outward current. The response to 10^{-3} M histamine, however, was more complex, with a rapidly activating inward current preceding the outward current. The net outward current increased during the initial phase of washout of the drug (Fig. 2a).

The response to 10^{-3} M histamine was found to be quite variable between oocytes from different donors. The responses of two other oocytes to 10^{-3} M histamine are shown in Fig. 2b. In both cases, in contrast to the results shown in Fig. 2a, there was a net inward current during application of the drug. However, in one cell a net outward currrent was seen during washout of the drug whereas in the other cell no outward current was observed. As has previously been reported (Kusano et al, 1977), it was found that histamine, at concentrations up to 10^{-3} M, had no effect on control non-injected oocytes.

These results suggest that there are two classes of response to histamine which can be induced in *Xenopus* oocytes following injection of rat brain mRNA; a slowly activating outward current elicited with micromolar concentrations of histamine and an inward current requiring a higher histamine concentration for activation. The level of expression of these two conductances was quite variable between different batches of oocytes, even when identical batches of messenger RNA were injected.

The magnitude of the outward current response was dependent upon membrane potential. For some cells, such as the one shown in Fig. 3a, the response to 10^{-4} M histamine was almost entirely due to the outward current. This current response was seen to decrease with more negative holding potentials, and did not reverse even when the holding potential was made as negative as -85 mV. This suggests that the primary current carrying

ion was K^+, since K^+ is the only ion with an equilibrium potential more negative than -85 mV (Kusano et al, 1982).

The pharmacological specificity of the outward current was tested using specific H_1 and H_2 antagonists. As shown in Fig. 3b, the response to 10^{-6} M histamine could be significantly attenuated by the H_2 blocker cimetidine (10^{-5} M). The H_1 blocker promethazine (10^{-5} M) did not significantly affect the response. Taken together, these results suggest that the outward current response to histamine is mediated by a H_2 receptor.

DISCUSSION

Xenopus oocytes, following injection of 14-16 day rat brain mRNA, were shown to be responsive to micromolar concentrations of histamine. Both an inward and an outward current response could be elicited by bath application of histamine. The outward current response was carried by K^+ ions and was mediated by a H_2 receptor. It has been shown previously that there is significant H_2 adenylate cyclase activity in rat brains (Schwartz, 1979). It has also been shown that increases in intracellular cAMP levels induce an outward K^+ current in *Xenopus* oocytes (Van Renterghem et al, 1985; Lotan et al, 1985). It is probable therefore that the outward current observed in injected oocytes was due to a H_2 mediated increase in cAMP. This hypothesis is consistent with the slow onset of the current, suggesting activation by a second messenger system rather than direct activation of a receptor-channel complex.

The pharmacological specificity of the inward current response could not be determined, because of the high drug concentration required to elicit the response. The rate of activation of the inward current appeared to be limited only by the rate of application of the drug, suggesting that histamine might be acting directly to open an ion channel. Without demonstrating the pharmacological specificity of the response to histamine, however, it is impossible to exclude the possibility that histamine may be activating some other receptor in the oocyte membrane in a non-specific manner.

Why only one class of histamine response could be recorded in oocytes from different donors remains uncertain. The variability in responsiveness between different batches of oocytes may be due to differences in the efficiency with which oocytes from different donors can translate exogenous mRNA (Asselbergs et al, 1979). Alternatively, the response to histamine may be dependent upon some cellular component which is not found in a constant amount in oocytes from different donors. An agonist response dependent upon a second messenger system would be particulary susceptible to variation between oocytes if there were significant variations in the amount of the endogenous proteins in the second messenger system in different cells. In this context, it is of interest to note that the response to acetylcholine, which is mediated by an endogenous muscarinic receptor and is thought to be dependent upon a second messenger system, has been shown to vary greatly between oocytes from different donors (Kusano et al, 1977; Dascal and Landau, 1980).

One notable feature of the response to high concentrations of histamine was that the outward current often increased during washout of the drug (Fig. 2). In general, the inward current response washed out more rapidly than did the outward current. As a consequence, the increase in outward current during washout might be due, in part at least, to a more rapid decrease of the inward current response compared with the outward current during the initial stages of drug washout. This explanation does not account for the increased outward current which was seen during washout of 10^{-4} M histamine (Figs 2a and 3a), since an increase in outward current was observed when there was very little competing inward current. The

histamine induced increase in cAMP concentrations in brain slices can be inhibited at histamine concentrations greater than 5×10^{-4} M (Palmer et al, 1972). If this is also true in the oocyte system, a falling concentration of histamine during drug washout might be more effective in maximally activating H_2 adenylate cyclase activity than a maintained dose of 10^{-3} or 10^{-4} M.

In conclusion, 14 to 16 day rat brains contain mRNA coding for histamine receptors which can be detected functionally in the oocyte expression system. The cellular origin of the mRNA coding for the histamine receptor cannot be directly determined from whole brain preparations of mRNA, but the fact that ionic currents in single neurons can can be modulated by histamine (Haas and Konnerth, 1983) suggests that at least some fraction of the histamine message is neuronal in origin.

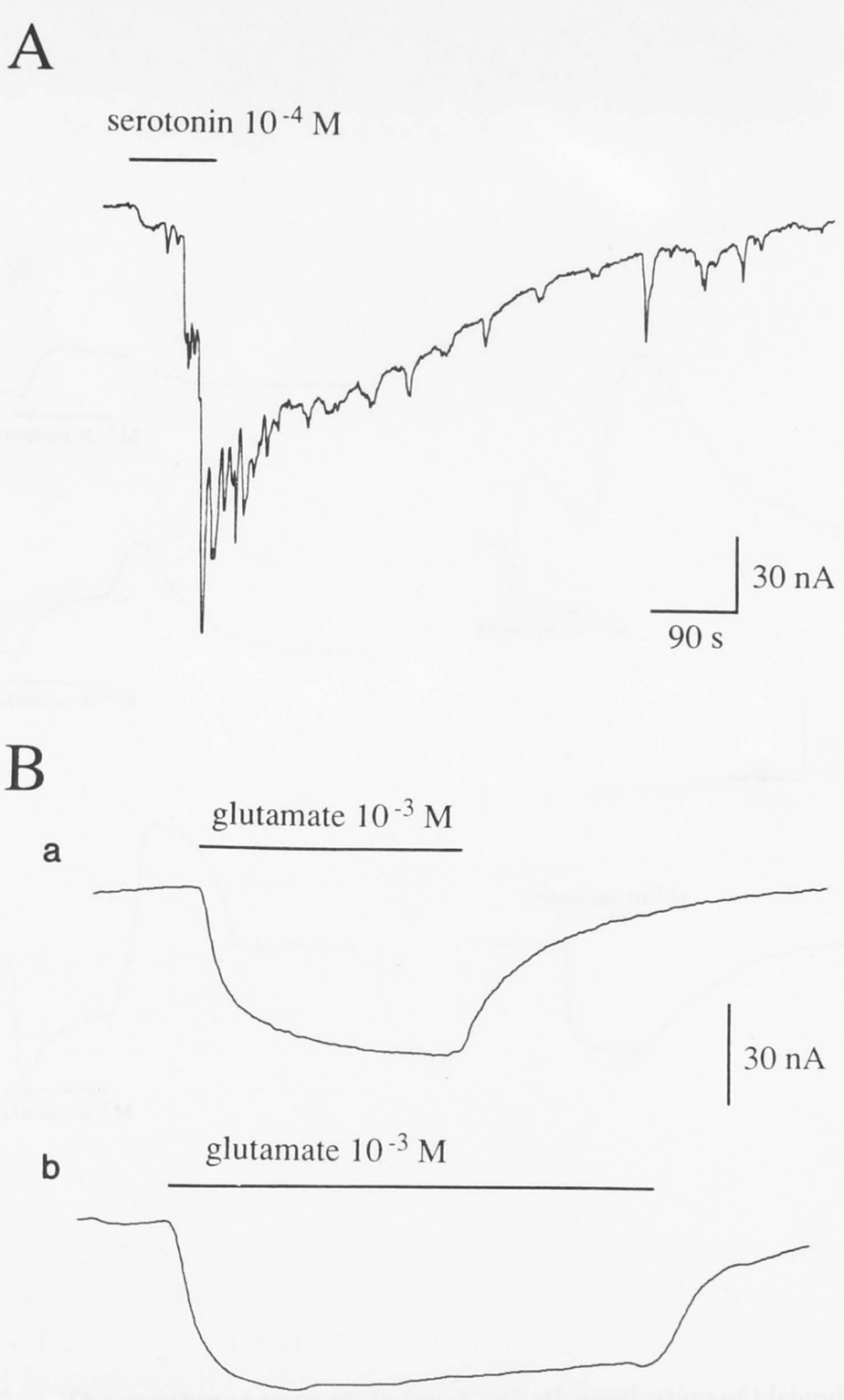

Figure 1. Response of an oocyte injected with rat brain mRNA to bath applied serotonin and glutamate.

A) Serotonin (10^{-4}) was perfused for 90s.

B) Glutamate (10^{-3}) was applied for either a) 1 minute or b) 8 minutes. The membrane potential was clamped at -60 mV. The horizontal bars denote duration of drug application.

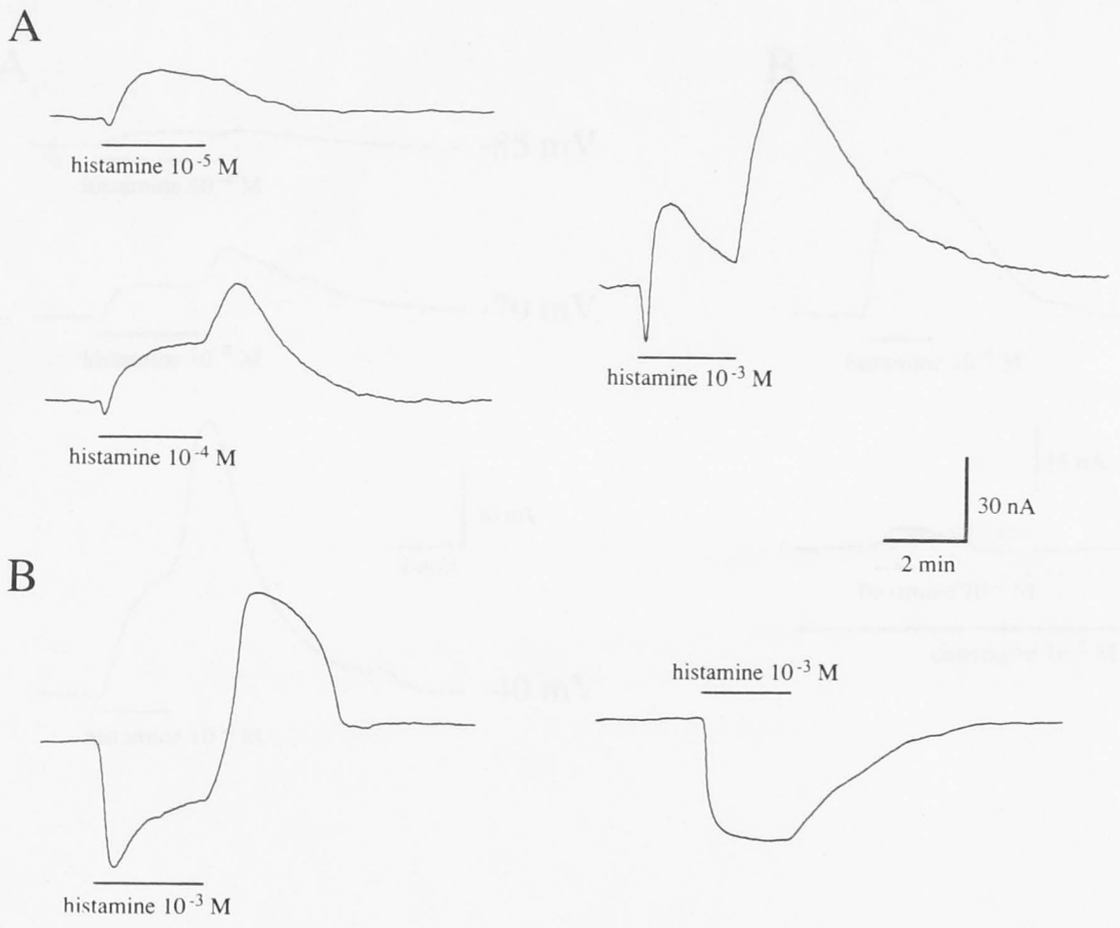

Figure 2. The membrane currents induced by bath application of histamine to oocytes injected with rat brain mRNA.

A) The current response of a single oocyte to different concentrations of histamine.

B) The response of two other oocytes from different donors to 10^{-3} M histamine. For all cells the membrane potential was clamped at -60 mV. The horizontal bars denote duration of drug application.

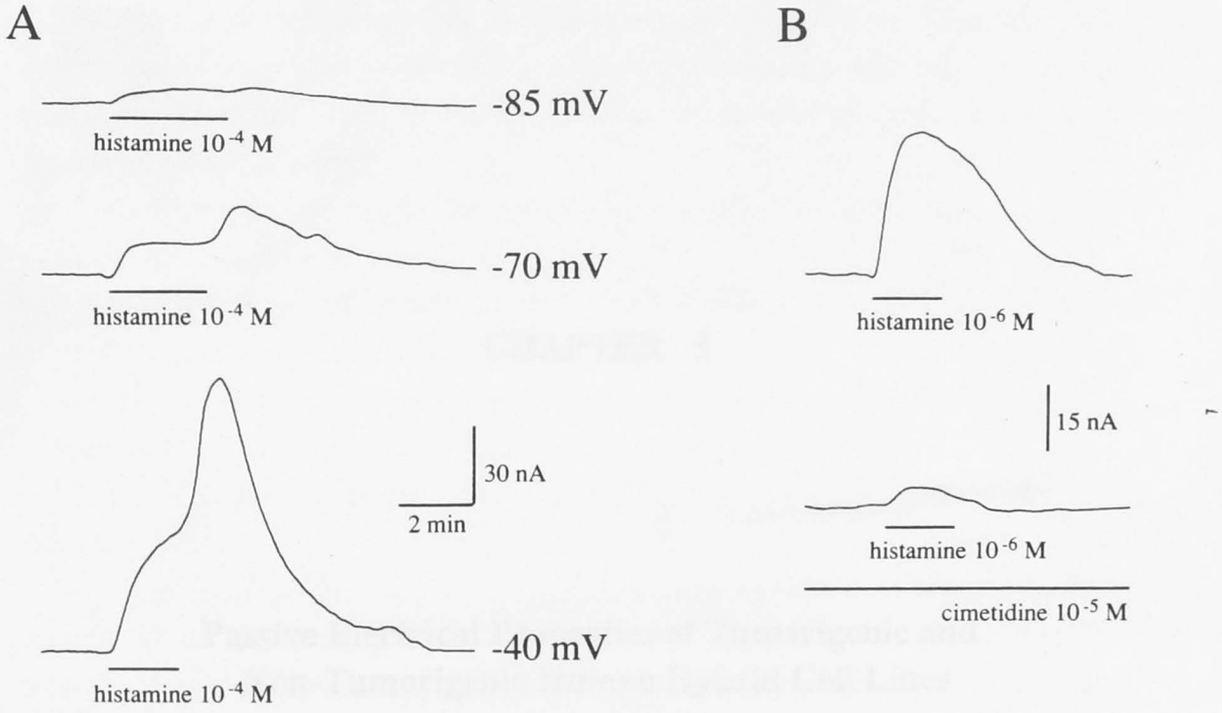

Figure 3. Reversal potential and pharmacological specificity of the outward current response to histamine.

A) The outward current response to 10^{-4} M histamine when the oocyte membrane potential was clamped to the different holding potentials indicated.

B) Antagonism of the response to 10^{-6} M histamine by the H_2 blocker cimetidine (10^{-5} M). Membrane potential was clamped to -20 mV. The horizontal bars denote duration of drug application. Cimetidine had been washed in for 20 minutes before perfusion with histamine.

CHAPTER 5

Passive Electrical Properties of Tumorigenic and Non-Tumorigenic Human Hybrid Cell Lines

INTRODUCTION

The defining characteristic of cancer cells is the loss or disruption of the normal cellular in vivo growth control mechanisms. Neoplastic cells divide in a relatively uncontrolled manner and are apparently unresponsive to the conditions or factors that regulate the division of normal cells. Some of the best studied model systems of neoplastic transformation are cell culture systems in which transformation is induced by tumor viruses. A susceptible cell line, when infected by a tumor virus, shows a number of abnormal growth properties, which include:

(i) Immortality of the transformed cells in vitro. The transformed cell line can be passaged indefinitely.

(ii) Decreased density-dependent inhibition of growth. Transformed cells grow to higher cell densities in culture than do normal cells.

(iii) A reduced requirement for growth factors in serum compared with primary cultured cells, or non-transformed cell lines.

(iv) The ability to produce tumors when injected into immuno-suppressed animals (Ruddon, 1981).

Following viral transformation, significant changes occur in the composition and function of cell membrane components (Nicolson, 1976). One membrane function altered by viral transformation is the rate of passive ion fluxes. Large changes in passive potassium fluxes have been observed in mouse 3T3 fibroblasts following transformation by infection with SV40 virus (Spaggiare et al, 1976; Adam et al, 1979). Killion (1984) has also observed that 3T3 cells transformed with polyoma virus have an increased cell input resistance and a more negative membrane potential compared with uninfected cells, and these changes have been attributed to a decrease in the permeability of the cell membrane to sodium ions.

It has been proposed that changes in ion fluxes across the cell membrane may play a role in the control of cell proliferation (Leffert, 1980; Boynton et al, 1982; Sparks et al, 1982). The relative importance of this role, however, remains contentious. To test whether changes in membrane permeablity properties are associated with the abnormal in vivo growth patterns of tumorigenic cells, the passive electrical properties of a non-tumorigenic and a tumorigenic human hybrid cell line were compared.

Intraspecific human cell hybrids were chosen for study because they display very stable karyotypes and phenotypes compared with other hybrid cell systems (Stanbridge, 1976). The cell lines used in this study were originally derived by fusing cervical carcinoma cells (HeLa) with normal human diploid fibroblasts (Stanbridge et al, 1982). The hybrid cells initially had a chromosome complement close to that expected if chromosomes from both parental cells were retained. These hybrid cells did not form tumors when injected into immuno-incompetent mice. Extended passaging of individual clones of the non-tumorigenic

hybrid cells occasionally resulted in the appearance of a tumorigenic segregant which was as tumorigenic as the HeLa parent. This change was associated with the loss of a small number of chromosomes (Stanbridge et al, 1982). Of the two cell lines examined in this study, the 5E cell line is the original non-tumorigenic hybrid and the 5L cell line is its tumorigenic segregant.

METHODS

Cells and Tissue Culture

Cell lines were cultured in DMEM (Dulbeco's Modified Eagle's Medium) from Gibco. This was supplemented with 5% fetal calf serum, 5% newborn calf serum, 2 mM pyruvate and antibiotics (50 units/ml penicillin G, 50 units/ml streptomycin sulphate and 180 units/ml neomycin sulphate). Incubation was at 37°C in a 5% CO_2 humidified atmosphere.

For patch clamp experiments, cells were plated at low densities (10^4 cells/cm^2) and used after two or three days in culture. For intracellular recordings, cells were plated at higher densities (2 to 8 x 10^4 cells/cm^2) and recordings were obtained from cultures approaching confluency.

All cell lines were routinely tested for tumorigenicity by the injection of 5 x 10^6 cells subcutaneously into nude mice. A cell line was classified as tumorigenic if it produced a tumor within 2 to 3 weeks of inoculation. Cells were also regularly tested for contamination by mycoplasma using the method of Chen (1977).

Solutions

The standard external solution contained 150 mM NaCl, 3.5 mM KCl, 2.5 mM $CaCl_2$, 1 mM $MgCl_2$ and 5 mM Na-HEPES, pH 7.3. The standard internal solution contained 120 mM K aspartate, 20 mM NaCl, 1 mM $CaCl_2$, 2 mM $MgCl_2$, 11 mM Na_2EGTA and 5 mM Na-HEPES, pH 7.3. The internal K^+ and Na^+ concentrations were chosen to give a Na:K ratio close to 0.27 which is the value observed in HeLa cells (Cook et al, 1975). The internal chloride concentration was chosen to give a Nernst potential for chloride close to the resting membrane potential (E_{Cl} = -46 mV, E_K = -89 mV, E_{Na} = 38 mV), because chloride ions are probably passively distributed across HeLa cell membranes (Okada et al, 1973). The osmolarity of the bath solution was in the range 295 to 300 milliosmoles and the internal solution was maintained at 5 to 10 milliosmoles hyperosmotic compared with the external solution in an attempt to reduce the possibility of intracellular organelles plugging the tip of the patch electrode. All solutions were filtered through a 0.2 μm Millipore filter.

Patch Electrodes

Patch pipettes were prepared from micro-hematocrit tubes (Clay Adams 1021) according to the procedure of Hamill et al (1981). Pipettes were given a hydrophobic coating by dipping them into a 2% solution of liquid silicone (Dow Corning, DC 200 fluid) and then drying for at least 24 hours. The tip of each pipette was fire polished on a microforge to give a final resistance in the range 1 to 3 MΩ.

Recording and Data Processing

Whole-cell recordings were made only from flattened, fully adherent cells; mitotic or detached cells were not used. The experimental chamber was mounted on a fixed stage

detached cells were not used. The experimental chamber was mounted on a fixed stage microscope modified for Hoffman modulation contrast optics and the cells were viewed at a magnification of x600. Initial seal resistances were of the order of 60 to 100 GΩ. The whole-cell recording procedure was similar to that described by Neher and colleagues for isolated cells (Hamill et al, 1981; Marty and Neher, 1983). An extension to the technique was to record from colonies or clusters of cells in which a number of neighbouring cells were electrically coupled to the cell under whole-cell clamp. Ionic currents were recorded using an LS/EPC 7 patch-clamp amplifier (List Electronics) and current signals were low-pass filtered through a 4-pole anti-aliasing Bessel filter. The holding potential used for voltage clamp experiments was -42 mV. Series resistance compensation, where necessary, was typically in the range 65% to 90%. A PDP 11/23 microcomputer was used to deliver voltage pulses and record current responses. Analysis of currents was done off-line using a PDP 11/44 microcomputer. All experiments were performed at room temperature (20-22°C).

Resting membrane potentials were measured from the zero current point on the current-voltage (I-V) curve. Input resistances were measured in the linear region of the I-V curve, around the resting membrane potential. Cell membrane capacitance was calculated from the integral of the current transient produced by a 10 mV voltage step.

Measurement and Correction of Liquid-Junction Potentials

Junction potentials were measured by comparing the zero-current voltage with intracellular solutions in both the bath and pipette, with the zero-current voltage after replacement of the bath solution with the standard extracellular solution. The reference electrode was a 3 M KCl-agar bridge. All data presented have been corrected for the liquid-junction potential between the pipette and bath solutions which, for the standard aspartate internal solution, was -12.0 ± 0.2 mV (mean ± s.e.m.). This experimental value is close to the theoretical value of -11 mV calculated using the Henderson equation (Henderson, 1907).

Intracellular Recording

Intracellular electrodes were fabricated on a Brown-Flaming puller and, when filled with 3 M KCl, had resistances in the range 40 to 80 MΩ. Membrane potentials were recorded using a high impedance voltage follower. Impalements were judged successful if the membrane potential did not vary by more than ± 5 mV over a 5 minute period.

Thin Section Electron Microscopy

Cells were fixed for 2 hrs in 2% gluteraldehyde in 0.1 M cacodylate buffer, pH 7.4. They were then post-fixed in 1% OsO_4 in 0.1 M cacodylate buffer, pH 7.4 for, 1.5 hrs. Samples were then stained with 1% aqueous uranyl acetate for 1.5 hrs, dehydrated and embedded in 'Spurrs' resin. Sections were cut on a Reichert ultramicrotome and stained with 'Reynolds' lead citrate. Micrographs were taken on a Philips 301 electron microscope.

Scanning Electron Microscopy

Cells were fixed for 2 hrs in 3% gluteraldehyde in 0.1 M cacodylate buffer, pH 7.4. They were then post-fixed in 1% OsO_4 in 0.1 M cacodylate buffer pH 7.4 for 1.5 hrs and subsequently dehydrated and critical point dried for scanning electron microscopy. Micrographs were taken on a JOEL 35 CX scanning electron microscope.

Equivalent Circuit Analysis

The electrical circuit simulation program SPICE was used for passive network analysis as described by Segev et al (1985). A cell colony was modelled as a hexagonal array of 37 cells, current injection was at the central cell and this cell was surrounded by concentric rings of 6, 12 and 18 cells (Fig. 13a). Each cell was represented as a simple RC circuit with a resistance of 6 GΩ and a capacitance of 30 pS. Connecting the 37 nodes were a total of 90 resistive elements representing the intercellular resistances. The resistance of these elements was varied until the difference between the steady-state voltage of an outermost cell and the central cell, following a current step, was less than 5%. To represent smaller colonies fewer concentric rings of RC circuits were used for transient analysis.

RESULTS

Cell Morphology

Cells of the non-tumorigenic 5E cell line have a morphology intermediate between the epithelial HeLa cell and the normal fibroblastic parents (Der and Stanbridge, 1980). Scanning electron micrographs show that the cells are well spread and flattened, and are strongly attached to the glass cover-slip by numerous thin cytoplasmic processes (Fig. 1).

Scanning electron micrographs of the tumorigenic 5L cell line are shown in Fig. 2. These cells are more rounded than the 5E cells and have a morphology similar to that of the HeLa parent. The 5L cells are smaller than the 5E cells and generally do not possess cytoplasmic processes extending from the body of the cell to the glass surface. The cell surface of the 5L cells is extensively covered by microvilli of variable length and density. The density of microvilli on the membrane surface of the 5L cells, is greatly increased compared with the 5E cell line.

The occurence of isolated cells, unconnected to any other cell, was relatively rare after two or more days in culture and cells were usually found grouped into small clusters or colonies.

Passive Electrical Properties of Single Cells

Currents generated by voltage steps in a single 5E cell under whole-cell voltage clamp conditions are shown in Fig. 3a. Voltage steps were applied every 1 second, and the voltage was stepped from a holding potential of -42 mV, in 20 mV increments, over the range -142 mV to +58 mV. The currents show no obvious time dependent components in response to either hyperpolarizing or depolarizing voltage steps.

The current-voltage (I-V) curve for the same cell is shown in Fig. 3b. There is rectification in both the depolarizing and hyperpolarizing directions, which gives the I-V curve a characteristic sigmoidal shape. A sigmoidal relationship was a consistent feature of all the single cell I-V curves.

Current clamp data from the same cell is shown in Fig. 3c. The voltage response of the cell following injection of 5 pA of current was well fitted by a single exponential function with a time constant of 247 ms. This result indicates that, despite the irregular geometry and long cytoplasmic processes of the 5E cell, there is no significant distributed capacitance.

The average values for the measured membrane properties of single 5E cells are shown in Table 1. The mean input resistance was 4.0 ± 0.4 GΩ (mean $\pm$ s.e.m.) and the mean cell capacitance was 42 ± 3 pF. Assuming a value of 1 μF cm^{-2} for the specific membrane capacitance, the specific resistance was 1.7×10^5 Ω cm^2.

Passive electrical Properties of Cell Colonies

For both of the cell lines studied, the normal state in culture is for the majority of cells to be both electrically and metabolically coupled to neighboring cells. For this reason, it was

considered important to examine the electrical properties of cell colonies. The current response of a thirty two cell colony of 5L cells to a 10 mV voltage step is shown in Fig. 4a. The decay of the capacitive current is clearly monophasic, as illustrated in Fig. 4b in which the logarithm of the capacitive current, normalised to the peak current, is plotted against time. Integration of the area under the current transient and division by the voltage step gave a value of 918 pF for the membrane capacitance of all of the cells in the colony. The time constant for decay of the capacitive transient was 6.8 ms which shows that the access resistance across the electrode tip could have been no greater than approximately 7 MΩ.

The voltage response of the same colony to a 50 pA current step is shown in Fig. 5a. The potential change following the current step was well described by a single exponential with a time constant of 259 ms. The plot of $\log_{10} V / V_0$ versus time, shown in Fig. 5b, has a monophasic decay.

These results show that cell colonies up to at least thirty two cells in size can be adequately space clamped, indicating that there is a relatively low resistance connection between the cells of a colony compared with the input resistance of single cells. The membrane capacitance and resistance of each of the cells in a colony appears, electrically, to be lumped together to give a transient response similar to that of a single resistor and capacitor in parallel. The interior of all the cells of a small colony will therefore remain isopotential following a voltage or current step. Similar results to those shown in Figs 4 and 5, were observed in the majority of colonies that were successfully voltage clamped. An example from a 26 cell colony is shown in Fig. 6.

For those colonies that showed deviations from a simple exponential response, to either voltage or current steps, the most likely explanation is that they were connected to other colonies by cytoplasmic bridges that were too fine to resolve under the light microscope, resulting in a more complex equivalent circuit with capacitance in series with a significant resistance. Colonies larger than approximately 36 cells had transient responses which generally showed systematic deviations from simple exponential decays. Colonies which were not space clamped by the above criteria were not included for analysis.

Figure 7a shows the current response of a thirty two cell colony of 5L cells when the voltage was stepped from -100 mV to +100 mV, relative to the holding potential of -42 mV. The current response is very similar to that of the single cell response shown in Fig. 3a. The I-V curve shown in Fig. 7b has a sigmoidal shape similar to the single cell I-V curves (Fig. 3b).

Following establishment of whole-cell recording conditions the intracellular contents of single cells normally would be expected to equilibrate rapidly with the electrode solution (Fenwick et al, 1982). Equilibration of intracellular solutions will not occur as rapidly in cell colonies because of the larger effective cell volume and the greater resistance to diffusion between cells. It is probable that throughout the period of recording from cell colonies (10 to 40 minutes), the intracellular contents were slowly changing in composition. However, no large or consistent changes in either the value of the cell input resistance or cell capacitance

were observed under these conditions.

The relationship between the number of cells in a colony and the total membrane capacitance for both 5E and 5L cells was linear (Fig. 8), with a relatively small spread of the data points around the regression line. Figure 9 shows the relationship between colony membrane conductance and colony size. This relationship also appears to be linear but there is a greater relative spread of the data points around the regression line than was seen for the membrane capacitance data.

Comparison Between the Membrane Properties of Single Cells and Colony Cells

Table 1 gives a comparison between the membrane properties of single 5E cells and colony 5E cells. The mean cell capacitance and resistance for colony cells was calculated by dividing the lumped capacitance or conductance of the colony by the number of individual cells counted in that colony. There is no significant difference between any of the parameters measured. This suggests that little or no change occurs in permeability of the membrane to the major permeant ions following establishment of electrical and metabolic contact with neighboring cells. This is in contrast to the results reported by Cone and Tongier (1973) for 3T3 and Chinese hamster ovary cells.

Comparison Between the Membrane Properties of 5E and 5L Cells

Average values of the measured membrane properties for 5E and 5L cells are given in Table II. Two parameters show statistically significant differences; mean single cell capacitance (Student's t-test, $p < 0.001$) and mean single cell resistance ($p < 0.001$). The distributions of single cell capacitance values are shown in Figs 10a and 10b. The different distributions obtained from the two cell lines can be explained by differences in cell surface area. The 5E cells had, on average, a larger membrane surface area than did the 5L cells. The distributions of the mean single cell input resistances are shown in Figs 10c and 10d, and these results are also consistent with a difference in size between the two cell populations.

Statistical comparison of either the cell membrane potential ($p > 0.2$) or the specific membrane resistance ($p > 0.1$) showed no significant difference between the two cell lines. Figure 11 shows the distributions of the values for these two parameters, indicating that there is complete overlap of their respective ranges. This result suggests that the specific membrane properties of the two cell lines are very similar.

It is clear from the scanning electron micrographs of the two cell lines (Figs 1 and 2), that microvilli must contribute a much greater percentage of the total membrane surface area for the 5L cells than for the 5E cells. It is difficult to give an exact estimate of the contribution of the microvilli to total membrane area because the geometry and size of cells from both cell lines was quite variable and any simplified geometric representation of the cell dimensions can only give very approximate answers. Nevertheless, if the 5L cells are

assumed, on average, to be approximated by spheres 16 μm in diameter, then an estimate for the contribution of the microvilli to total surface area is of the order of 73%, which is comparable with results on other cells with extensive surface microvilli (Wiebel et al, 1969; Siegenbeek van Heukelom, 1972).

Intracellular Recording

Intracellular recording was attempted only in confluent sheets of 5L cells. This precaution was taken to reduce the possibility of recording an artificially low resting membrane potential because of the leakage resistance produced by an intracellular electrode in parallel with the cell input resistance (Lassen and Rasmussen, 1977; Ince et al, 1984). The average membrane potential recorded in 5L colonies was -46 ± 1.3 mV (mean ± s.e.m., N = 30), which is not significantly different from the value of -50 ± 3 mV obtained with the whole-cell clamp technique. This result suggests that the correction for the liquid-junction potential, which was needed for the whole-cell clamp data, does not unduly bias the membrane potential values obtained with this technique.

Equivalent Circuit Analysis

Using thin section electron microscopy it was possible to discern regions of close membrane apposition which were assumed to be gap junctions (Fig. 12), but it was difficult to find a clear example with the characteristic regular 80 Å spacing of intermembranous particles. Intercellular commmunication in some tumorigenic cell lines, including some HeLa cell clones, is impaired but not abolished (Pitts, 1972; Corsaro and Migeon, 1977, Loewenstein, 1979), and correspondingly, cells with impaired intercellular communication either have relatively small and scarce gap junctions or have junctions with disrupted structure (Loewenstein, 1979; Atkinson et al, 1986). It is even possible that effective electrical communication between cells can occur in the absence of readily identifiable gap junction structures, if isolated channels are scattered throughout a region of plasma membrane apposition (Williams and DeHann, 1981). The high input resistance of the cells used in this study means that relatively few junctional channels were necessary to explain the space clamp conditions seen in the electrical recordings from cell colonies. To obtain a lower limit for the number of intercellular channels connecting cells in cell colonies, circuit analysis of an equivalent circuit was undertaken.

A reasonable approximation of the geometric arrangement of cells in a subconfluent monolayer is a hexagonal array of cells (Siegenbeek van Heukelom et al, 1972), shown in Fig. 13a. For the purposes of simplicity, an equivalent circuit of the cell colony was constructed assuming that each cell had an identical cell input resistance and membrane capacitance, and that all the intercellular resistances were equal. Values of 6 GΩ and 30 pS were chosen for the single cell resistance and capacitance respectively, to give a time constant similar to the experimental values obtained from the 5L cells. Space clamp was taken to mean that the steady-state voltage differed by no more than 5% across all the cells in a colony

following a current step.

A single channel conductance of approximately 120 pS has been calculated for the gap junction channel of rat lacrimal gland cells (Neyton and Trautmann, 1985). To obtain space clamp conditions in a 37 cell colony, equivalent circuit analysis suggests that each cell needs to be coupled to each of its neighbours by a single gap junction containing 220 channels, assuming a value for the conductance of the intercellular channel of 120 pS. The simulated voltage response of a network of 37 cells, with intercellular resistances of 38 MΩ (equivalent to 220 channels), is shown in Fig. 13b. Obviously, for smaller colonies, smaller coupling resistances and fewer intercellular channels are required to obtain space clamp conditions: for a 19 cell colony 100 channels per gap junction are required and for a 7 cell colony only 27 channels are necessary.

Large Conductance Chloride Channel

A large conductance anion-selective channel was observed in approximately 50% of membrane patches following detachment of the membrane patch from the surface of either 5E or 5L cells. The channel was usually not observed immediately following isolation of the patch but was consistently seen following a variable waiting period. This channel was not seen in cell attached patches. The channel had similar properties to previously described large conductance chloride channels (Blatz and Magleby, 1983; Gray et al, 1984; Nelson et al, 1984; Schneider et al, 1985). Single channel currents recorded with 150 mM CsCl in the patch pipette and 150 mM NaCl in the bath are shown in Fig. 14a. The voltage across the patch was stepped over the range -100 to +100 mV from a holding potential of 0 mV. The channel kinetics were quite complex, although, the channel consistently entered an inactivated state following a sustained voltage jump. As shown in Fig. 14b, the I-V relationship was approximately linear with a slope conductance, for this patch, of 374 pS. The reversal potential was close to 0 mV, the predicted reversal potential for chloride ions.

This large conductance anion channel was not observed during recordings in whole-cell clamp mode, even though it could quite easily have been resolved, since the whole-cell membrane conductance was of the order of 160 to 250 pS. This result suggests that this channel does not normally affect the membrane permeability properties of these cells, and that activation of the channel requires isolation of the channel from some unidentified intracellular component. Alternatively, the presence of some factor not normally present in the experimental media may be necessary for activation of the channel.

DISCUSSION

Comparison of Results to other Electrophysiological Studies on HeLa Cells

In patch clamp studies on HeLa cells, two different potassium channels have been found, an inward rectifying potassium channel of 40 pS conductance (Sauve et al, 1983) and a 10 pS potassium channel, which has a probability of opening dependent on the internal calcium concentration (Sauve et al, 1984). The presence of an inward rectifying potassium channel in the cell membrane will result in a membrane conductance which is higher when the membrane potential is negative to the potassium equilibrium potential than when it is positive (Katz, 1949; Adrian et al, 1970). This rectifying behavior was in fact observed in the whole-cell voltage clamp records from both 5E and 5L cells (Figs 3 and 7), suggesting the presence in the hybrid cells of an inward rectifying potassium channel similar to that observed in HeLa cells. The outward rectification observed in the I-V relationships recorded from both cell lines resembles classical Goldman-Hodgkin-Katz rectification which is due to the unequal distribution of permeant ions across the cell membrane (Goldman, 1943; Hodgkin and Katz, 1949).

Electrophysiological studies on HeLa cells which used intracellular electrodes have produced variable results. Membrane potentials reported in two early studies were -46 mV (Hulser, 1971) and -48 mV (Okada et al, 1973). In a more recent study by Roy and Sauve (1982), a phasic membrane potential response occurred following electrode impalement. An initial peak potential of approximately -53 mV decayed over a period of a few minutes to an average stable value of -38 mV. The average membrane potential for 5L cells recorded using intracellular electrodes was -46 mV, which is in agreement with the earlier electrophysiological studies on HeLa cells (Hulser, 1971; Okada et al, 1973). No transient hyperpolarization was observed following electrode impalement. The membrane potential either decayed rapidly to a baseline level or remained at a relatively stable potential close to the initial potential observed following impalement. The reason for the discrepancy with the results of Roy and Sauve (1982) is not clear. It is possible that the level of expression of Ca^{2+}-activated K^+ channels, which are the channels thought to be responsible for the initial hyperpolarization, is higher in the HeLa clone used by those investigators than it is in the 5L cells used in this study.

Aiton and Pitman (1975) studied two different strains of HeLa cells and found that they had different average membrane potentials, -37 mV or -18 mV. This result could reflect a real difference in membrane ion permeabilities, or it could be due to the technical difficulties associated with the leakage resistance produced by impalement of a cell with an intracellular electrode. Some, but not all, HeLa cell strains are connected by gap junctions (Cox et al, 1972 Corsaro and Migeon, 1977), and in those strains lacking electrical coupling, lower membrane potentials could result if the leakage resistance is significant compared with the cell input resistance. Given the very high input resistances observed for single cells in this study, intracellular recording of membrane potentials from cells not electrically coupled to

other cells would almost certainly result in an artificially low estimate of the resting membrane potential. Measurement of electrical coupling using two microelectrodes may also give artifactual results if the electrode induced leakage resistance is comparable to the intercellular resistance.

Comparison with other Whole-Cell Clamp Studies on Mammalian Cells

The whole-cell clamp results in this study gave the relatively high values for cell input resistance of 4.2 GΩ and 6.3 GΩ for the 5E and 5L cells respectively (Table 2). Input resistances in the gigaohm range have also been found, using the whole-cell clamp technique, in bovine chromaffin cells (Fenwick et al, 1982), rat pituitary tumor cells (Dubinsky and Oxford, 1984; Matteson and Armstrong, 1984) and pancreatic acinar cells (Maruyama and Peterson, 1984). The specific membrane resistance of the hybrid cells used in this study was 1 to 2 x 10^5 Ω cm^2 which may be typical for a nonexcitable cell membrane. A description of the membrane properties of mouse fibroblasts using the whole-cell clamp technique (Hosoi and Slayman, 1985) gives a range for the specific cell membrane resistance of 0.7 to 2 x 10^5 Ω cm^2 which is very similar to the values obtained from human hybrid cells in this study.

The Role of Gap Junctions in Growth Control

Loewenstein and his associates have used the somatic cell hybridization technique in a number of studies to argue that intercellular communication via gap junctions plays an important role in normal growth control (reviewed in Loewenstein, 1979). Their basic approach was to hybridize non-communicating tumorigenic cells with communicating normal cells, and their main finding was that in the hybrid progeny non-communication was well correlated with tumorigenicity (Azarnia and Loewenstein, 1977). These results are not strictly comparable to the present study, because the tumorigenic HeLa cell derivative D98/AH-2, used as a parent cell in this study, is capable of metabolic communication in vitro (Corsaro and Migeon, 1977), a phenomen which is generally thought to be dependent upon the presence of gap junctions (Gilula, 1974). It is not surprising therefore that both the tumorigenic and non-tumorigenic hybrid cells have gap junctions and are electrically coupled.

Comparison with Earlier Studies on Transformed Cells

In a number of studies (Stanbridge and Wilkinson, 1978; Stanbridge et al, 1982), it has been shown that many characteristics of the transformed phenotype such as anchorage independent growth, lowered serum requirement and the loss of density-dependent inhibition of growth are dissociable from the tumorigenic phenotype. The technique of somatic cell hybridization has proven very successful in isolating those in vitro phenotypic characteristics which are not correlated with in vivo tumorigenicity. There is a considerable body of circumstantial evidence suggesting a role for passive monovalent ion fluxes in the control of cell proliferation (for reviews see, Leffert, 1980; Boynton et al, 1982; Sparks et al, 1982).

There is also some evidence that the passive permeability properties of the cell membrane may be altered in the transformed phenotype (Spaggiare et al, 1976; Adam et al, 1979; Killion, 1984). However, in this study, no difference was found in the passive membrane properties of a non-tumorigenic cell line when compared with a tumorigenic cell line sharing a similar genetic background. This suggests that altered passive monovalent ion fluxes are not an essential requirement for the loss of in vivo growth control.

The SV40 or polyoma viruses used in the viral studies (Spaggiare et al, 1976; Adam et al, 1979; Killion, 1984) are genetically similar, and share the ability to alter a wide range of cellular functions (Tooze, 1980). It is unlikely, however, that all or even a majority of the phenotypic changes observed following viral transformation are important in conferring the release from in vivo growth control which characterizes the fully transformed cell (Stanbridge et al, 1982). The results reported in this study suggest that altered ionic permeabitities of the plasma membrane are not necessarily associated with the tumorigenic phenotype. The permeability changes observed following viral transformation may, therefore, be secondary to alterations in the organization of the cytoskeleton or, alternatively, may be associated with the increased growth rates of transformed cells.

Table 1. Comparison of the Membrane Properties of Single 5E Cells and 5E Colony Cells

Cell Type	Membrane Potential (mV)	Mean Cell Capacitance (pF)	Mean Cell Resistance (GΩ)	Specific Resistance ($x10^5$ Ω cm^2)	N
Single 5E Cells	-47 ± 2 *	42 ± 3	4.0 ± 0.4	1.7 ± 0.2	10
Colony 5E Cells	-47 ± 2	39 ± 1	4.3 ± 0.3	1.7 ± 0.1	22

* mean ± s.e.m.

Table 2. Comparison of the Membrane Properties of 5E Cells and 5L Cells

Cell Type	Membrane Potential (mV)	Mean Cell Capacitance (pF)	Mean Cell Resistance (GΩ)	Specific Resistance ($x10^5$ Ω cm^2)	N
5E Cells	-47 ± 2 *	40 ± 1	4.2 ± 0.3	1.7 ± 0.1	32
5L Cells	-50 ± 3	30 ± 1	6.3 ± 0.4	1.9 ± 0.1	25

* mean ± s.e.m.

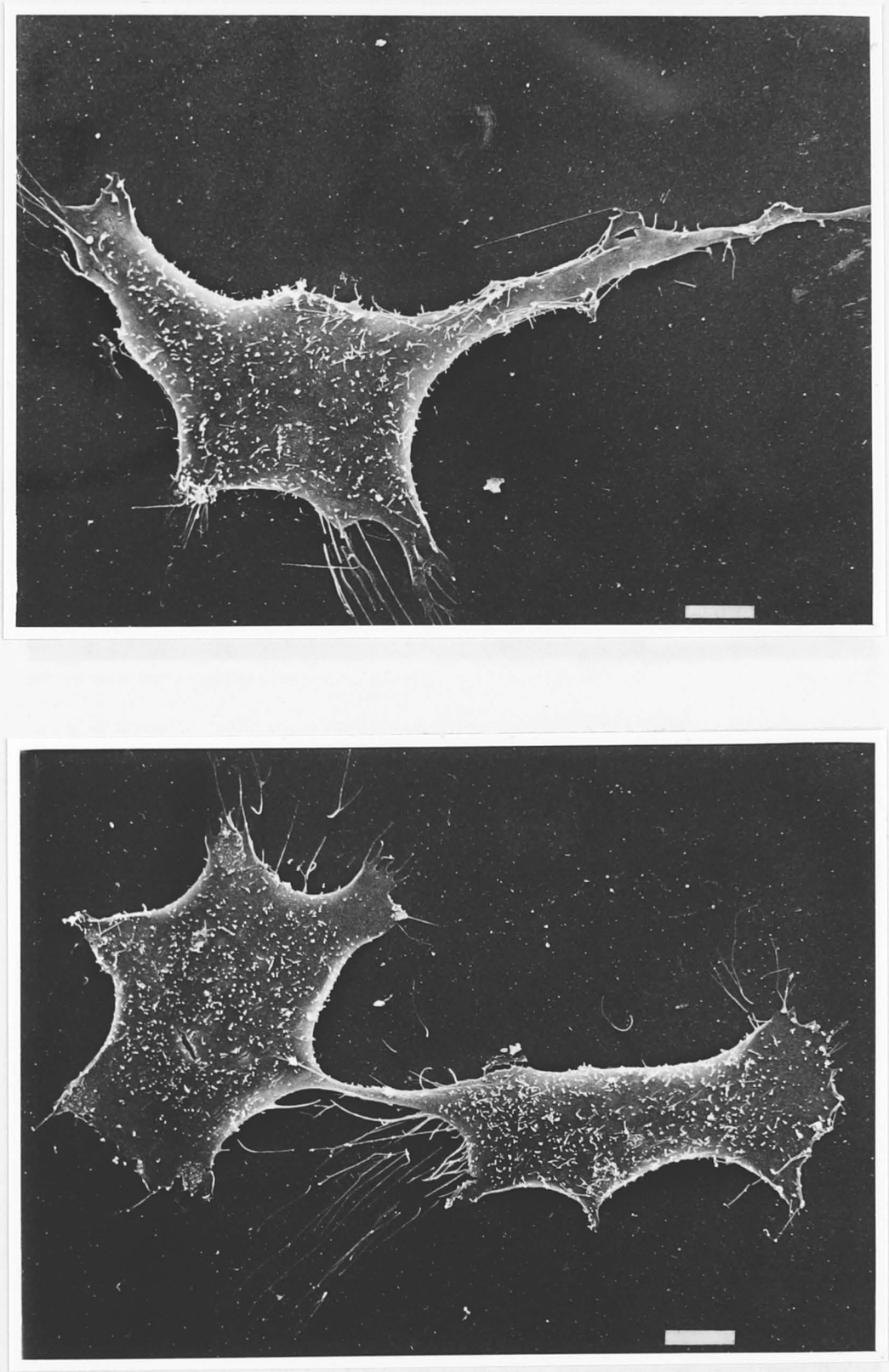

Figure 1. Scanning electron micrographs of cells from the non-tumorigenic 5E cell line. Scale bar corresponds to a length of 10 μm.

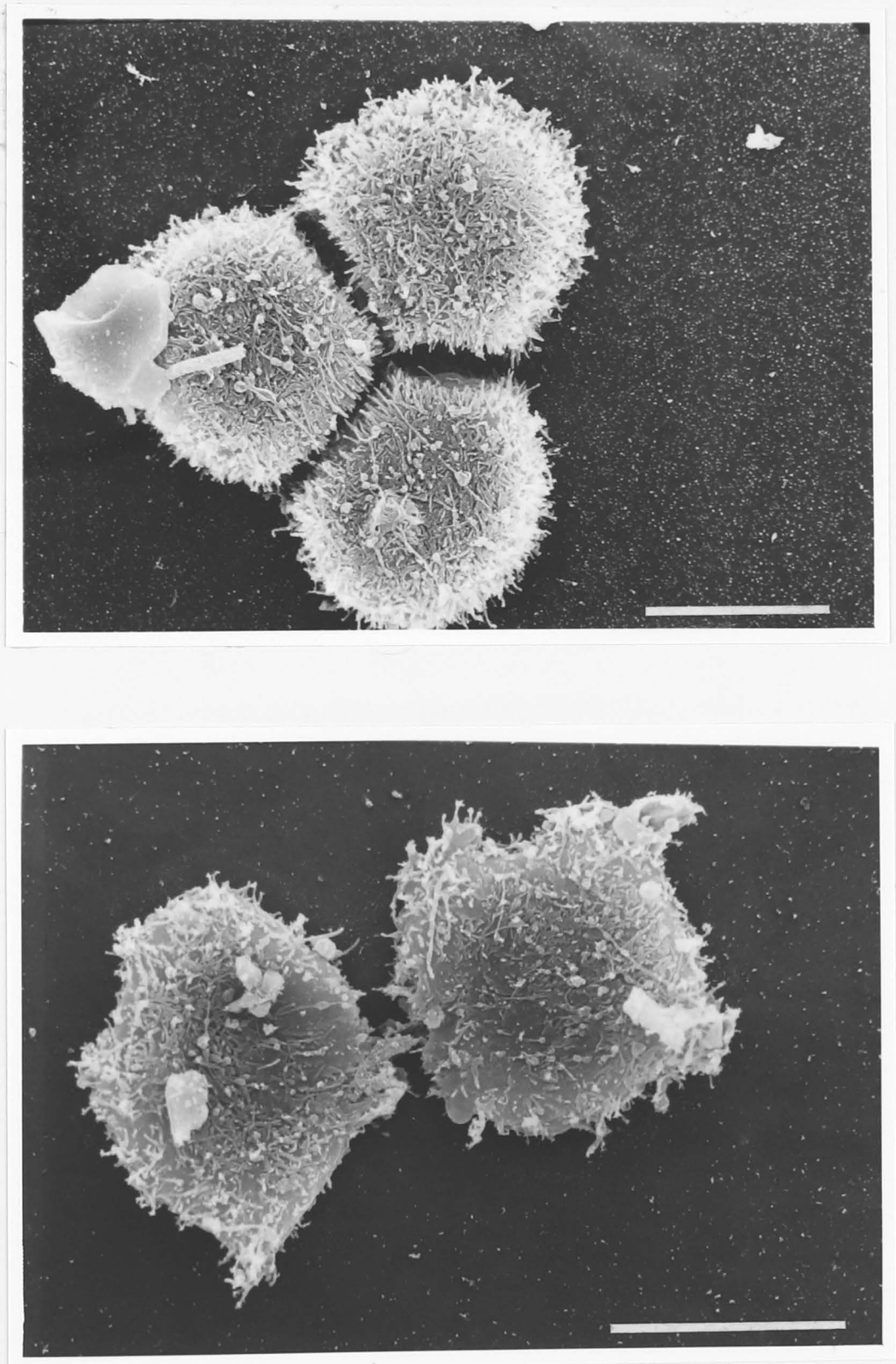

Figure 2. Scanning electron micrographs of cells from the tumorigenic 5L cell line. Scale bar corresponds to a length of 10 μm.

Figure 3. Whole-cell voltage and current clamp of a single 5E cell.

A) Current responses to voltage steps lasting 500 ms. Holding potential was -42 mV and voltage steps were applied at 1 second intervals. Voltage was stepped over the range -142 to +58 mV in 20 mV increments.

B) Current-voltage relationship for the data shown in Figure 3a.

C) Whole-cell current clamp of a single 5E cell. The voltage record is the average of four records following successive 1200 ms, 5 pA current steps. A single exponential function with a time constant of 257 ms is superimposed on the voltage trace as a dashed line.

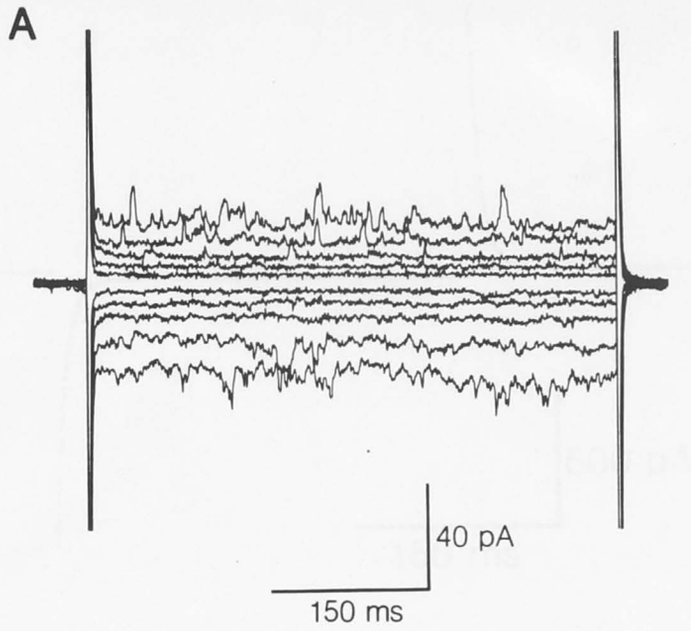
A
40 pA
150 ms

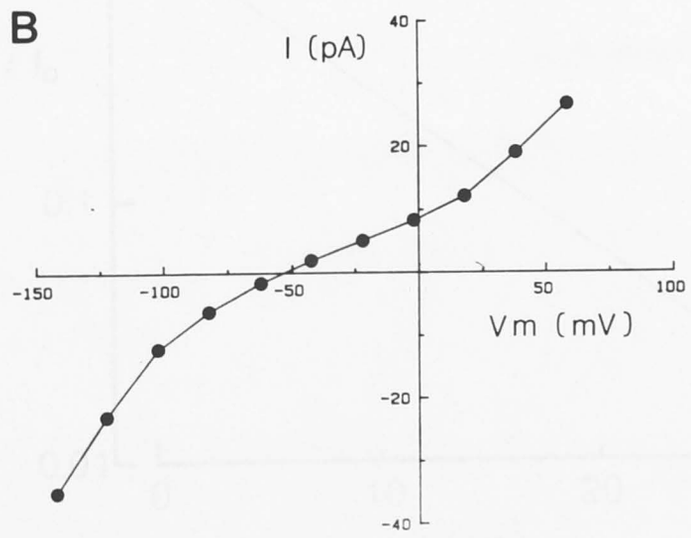
B
I (pA)
40
20
-20
-40
-150
-100
-50
50
100
Vm (mV)

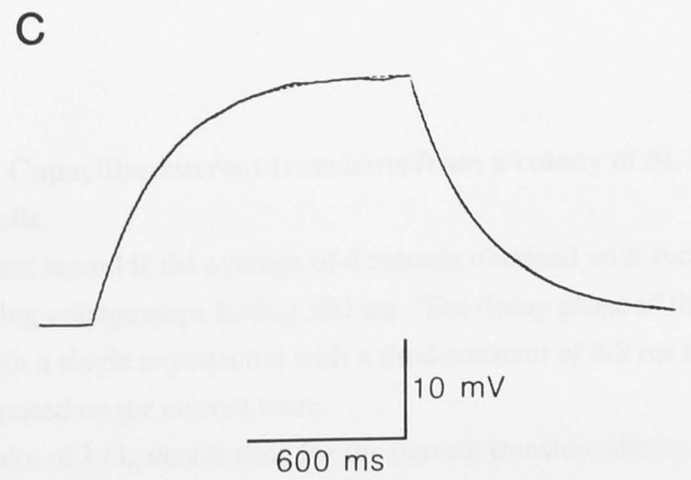
C
10 mV
600 ms

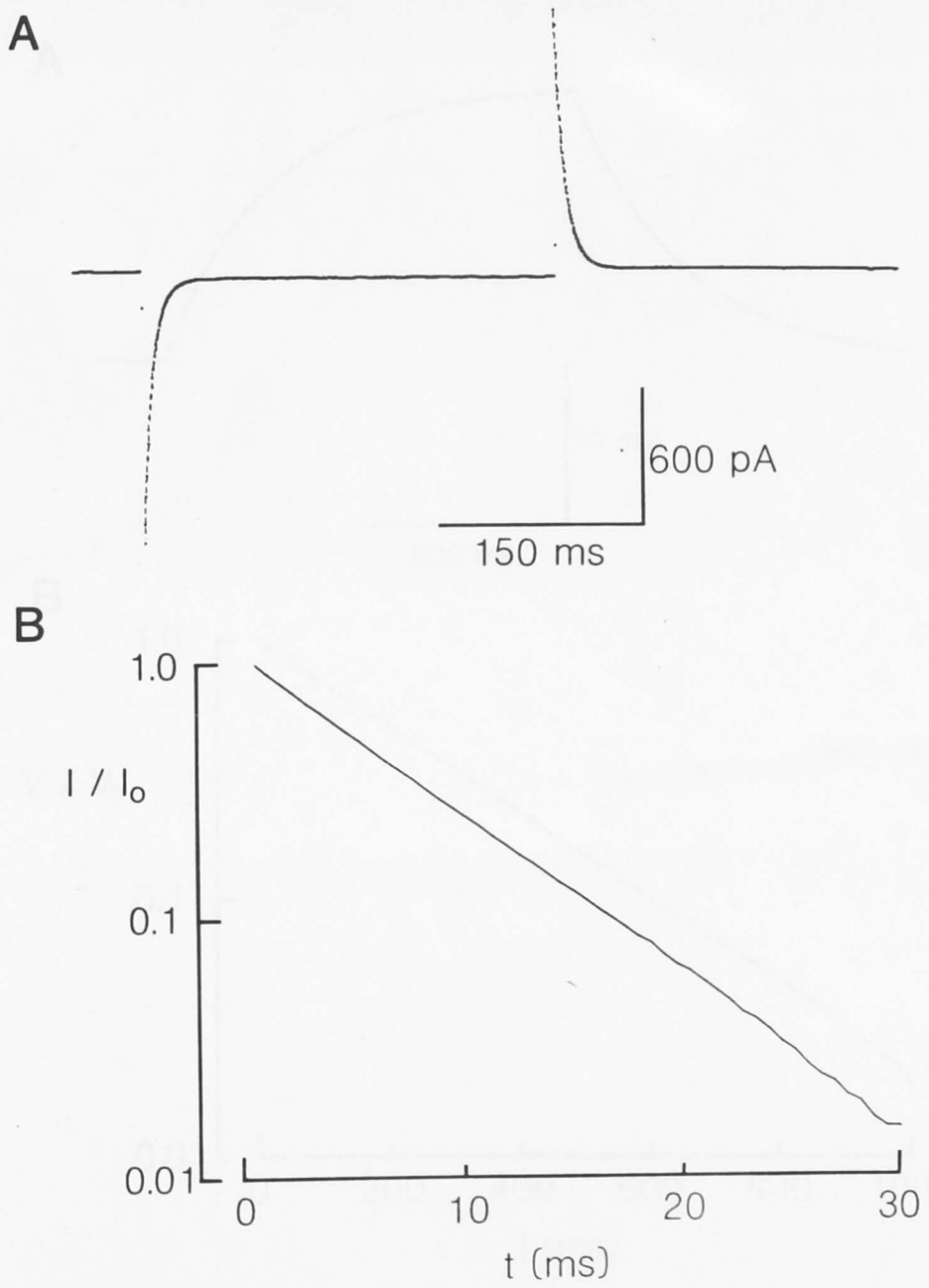

Figure 4. Capacitive current transients from a colony of 5L cells containing thirty two cells.

A) The current record is the average of 4 records obtained with successive 10 mV hyperpolarizing voltage steps lasting 300 ms. The decay phase of the capacitive transient was fitted with a single exponential with a time constant of 6.8 ms and is shown as a dashed line superimposed on the current trace.

B) Inverse plot of I / I_0 versus time for the current transient shown in Figure 4a. I_0 was taken as the peak current following the 10 mV voltage step.

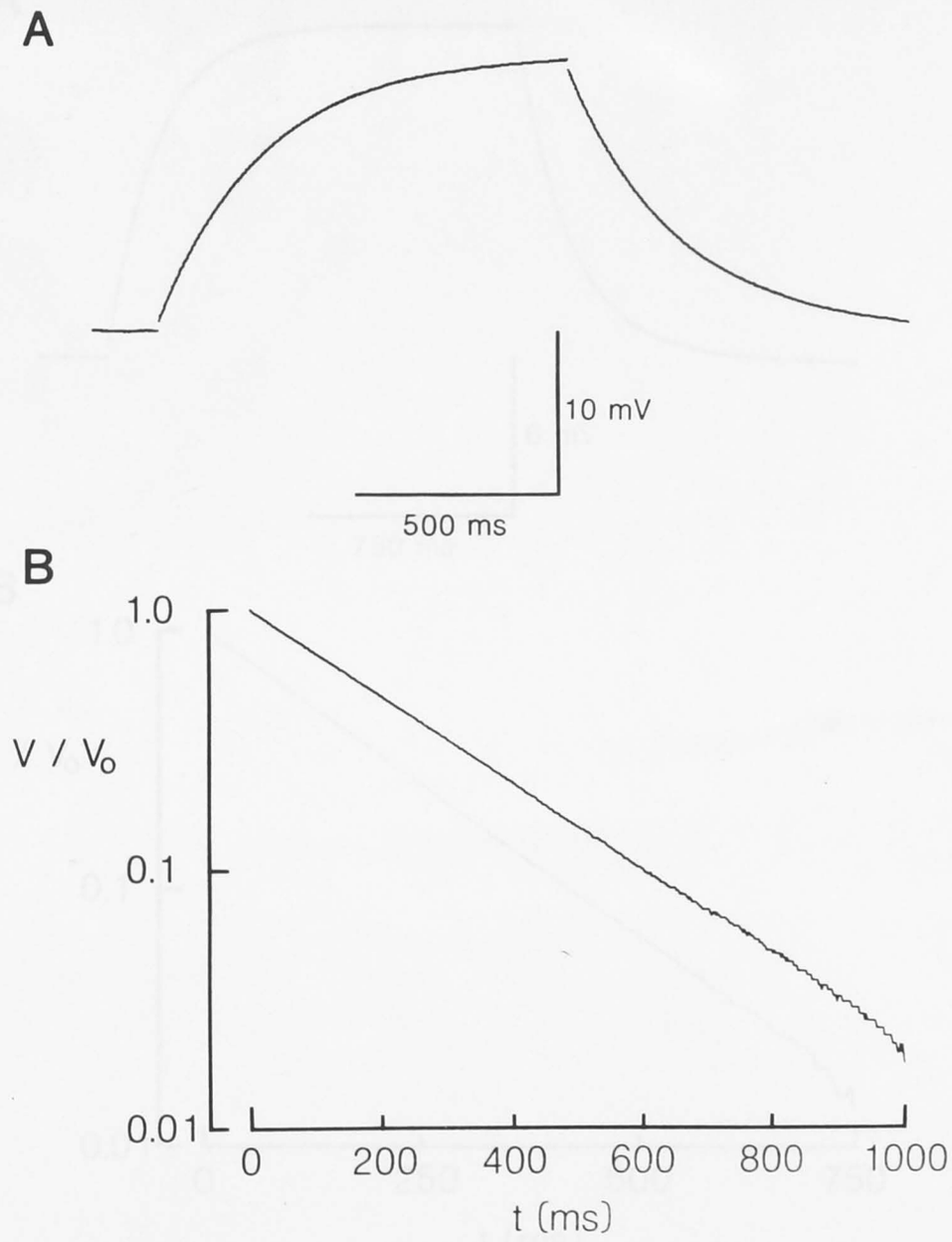

Figure 5. Voltage transient from a thirty two cell colony of 5L cells.

A) The voltage record is the average of 4 records following successive 50 pA current steps lasting 1000 ms. The rising phase has been fitted with a single exponential function with a time constant of 259 ms and is shown as a dashed line superimposed on the voltage trace.

B) Inverse plot of V / V_0 versus time for the voltage transient shown in Figure 5a. V_0 is the first voltage value recorded following the 50 pA current step.

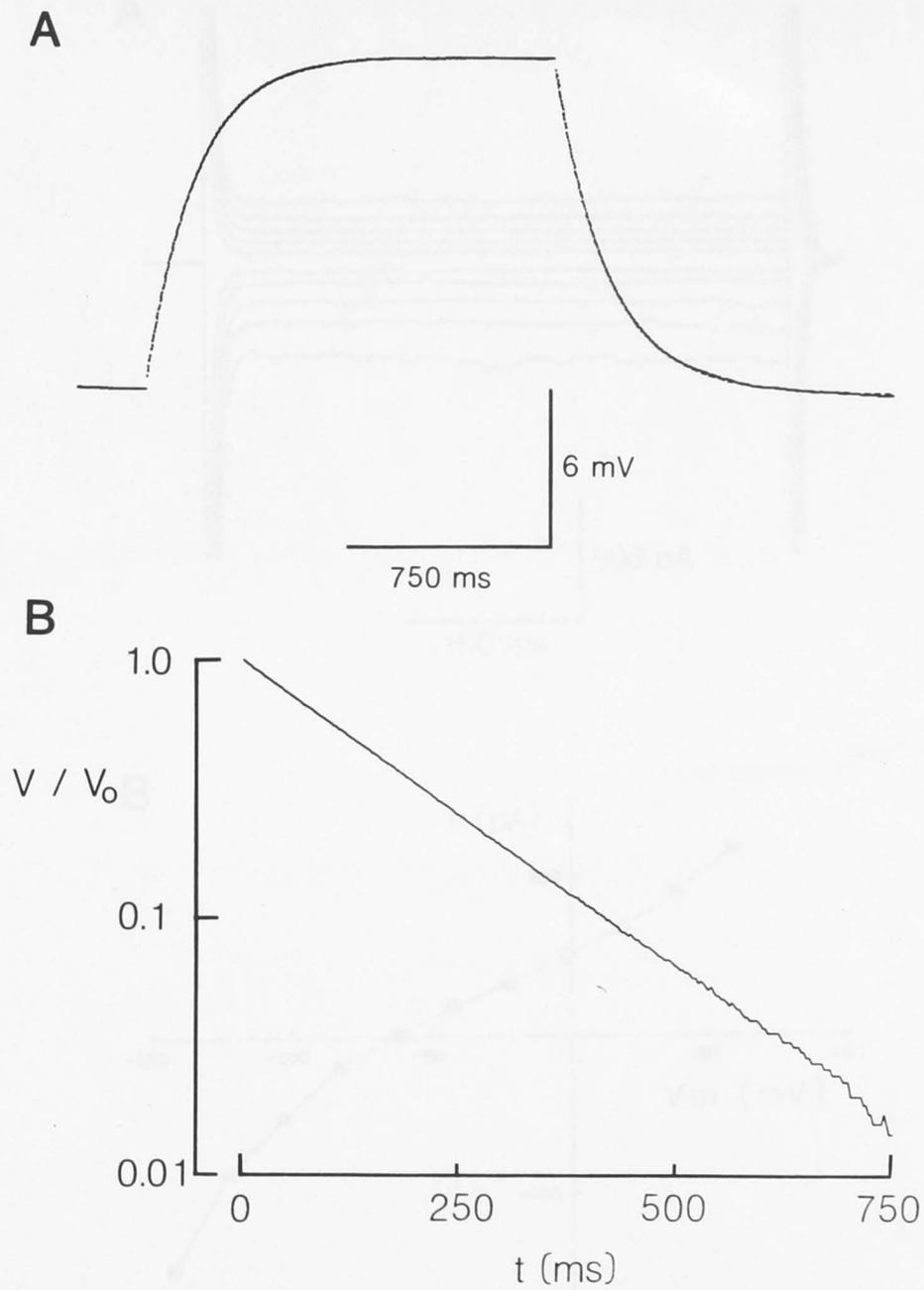

Figure 6. Voltage transient from a twenty six cell colony of 5L cells.

A) The voltage record is the average of 4 records following successive 50 pA current steps lasting 1500 ms. The rising phase has been fitted with a single exponential function with a time constant of 188 ms and is shown as a dashed line superimposed on the voltage trace. **B)** Plot of V / V_0 versus time for the voltage transient shown in Figure 6a. V_0 is the first voltage value recorded following the 50 pA current step.

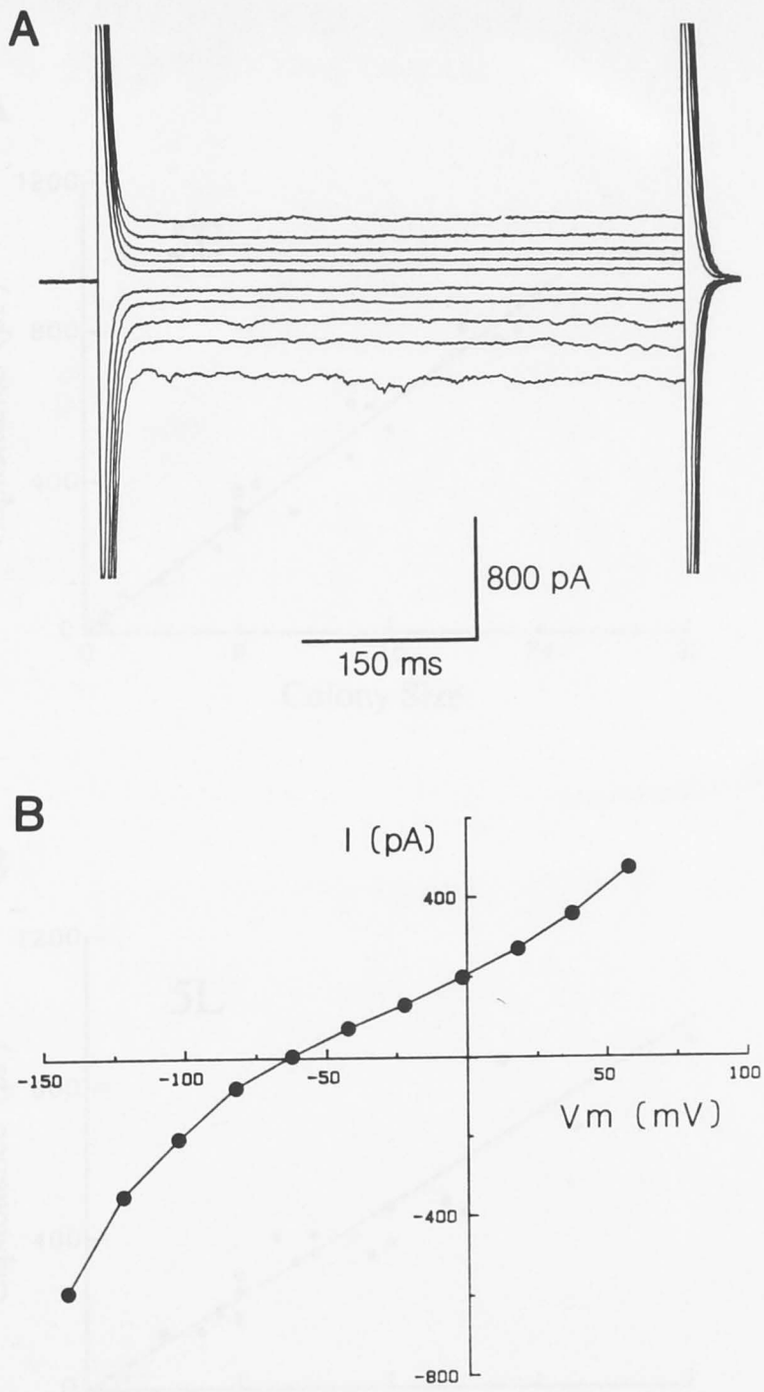

Figure 7. Whole-cell voltage clamp of a thirty two cell 5L colony.

A) Current responses to voltage steps lasting 500 ms. Holding potential was -42 mV and voltage steps were applied at 1 second intervals. Voltage was stepped over the range -142 to + 58 mV in 20 mV increments.

B) Current-voltage relationship for the data shown in Figure 7a.

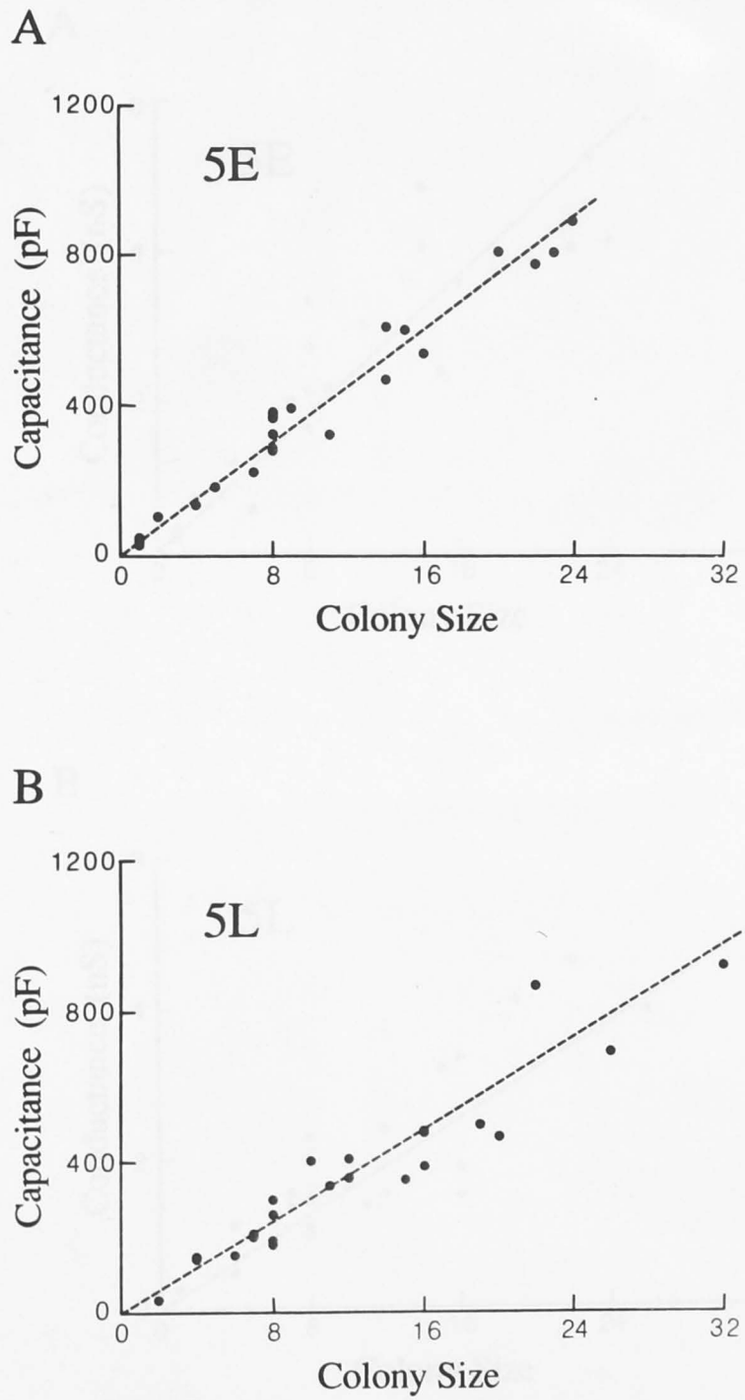

Figure 8. Membrane capacitance is correlated with colony size.

A) Plot of cell membrane capacitance versus colony size for the non-tumorigenic 5E cells. The dashed line corresponds to a mean single cell capacitance of 40 pF.

B) Plot of cell membrane capacitance versus colony size for the tumorigenic 5L cells. The dashed line corresponds to a mean single cell capacitance of 30 pF.

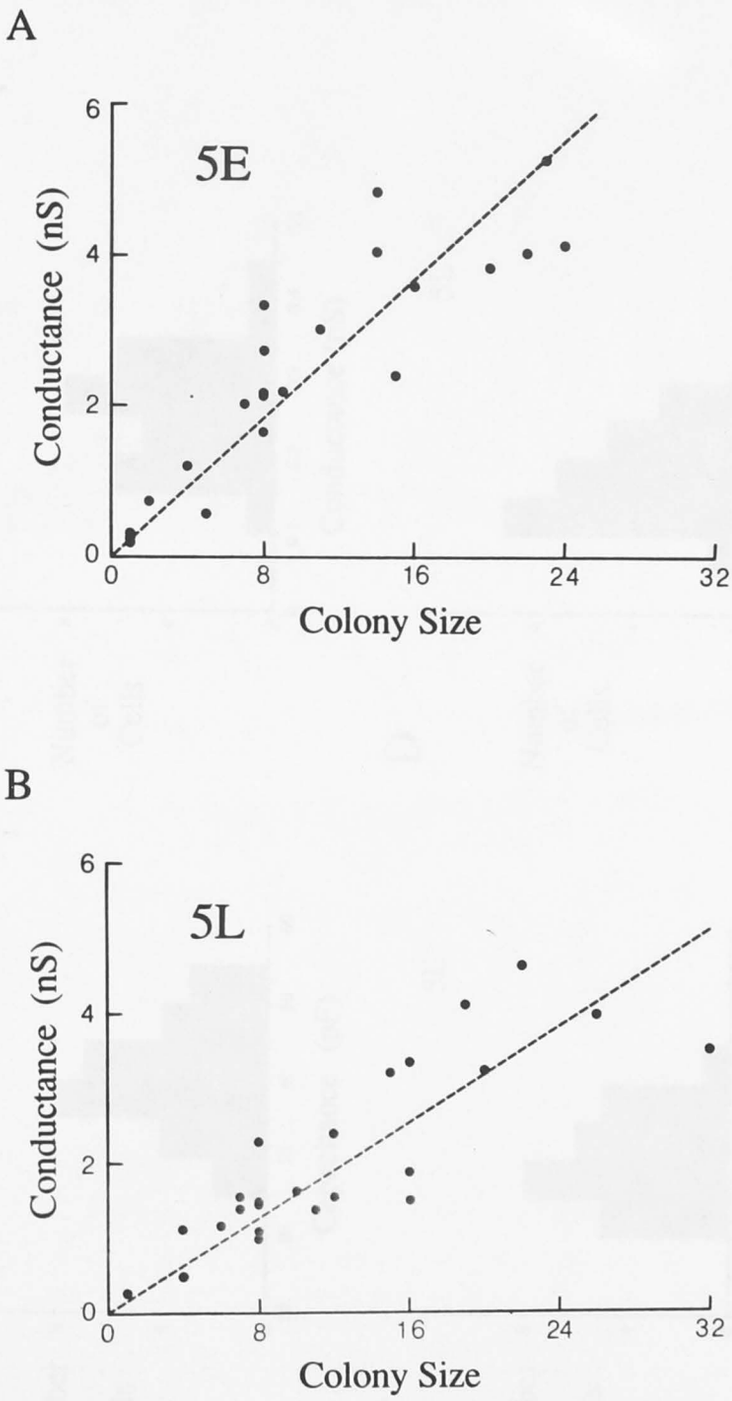

Figure 9. Membrane conductance is correlated with colony size.

A) Plot of cell membrane conductance versus colony size for the non-tumorigenic 5E cells. The dashed line corresponds to a mean single cell conductance of 0.236 nS.

B) Plot of cell membrane conductance versus colony size for the tumorigenic 5L cells. The dashed line corresponds to a mean single cell conductance of 0.159 nS.

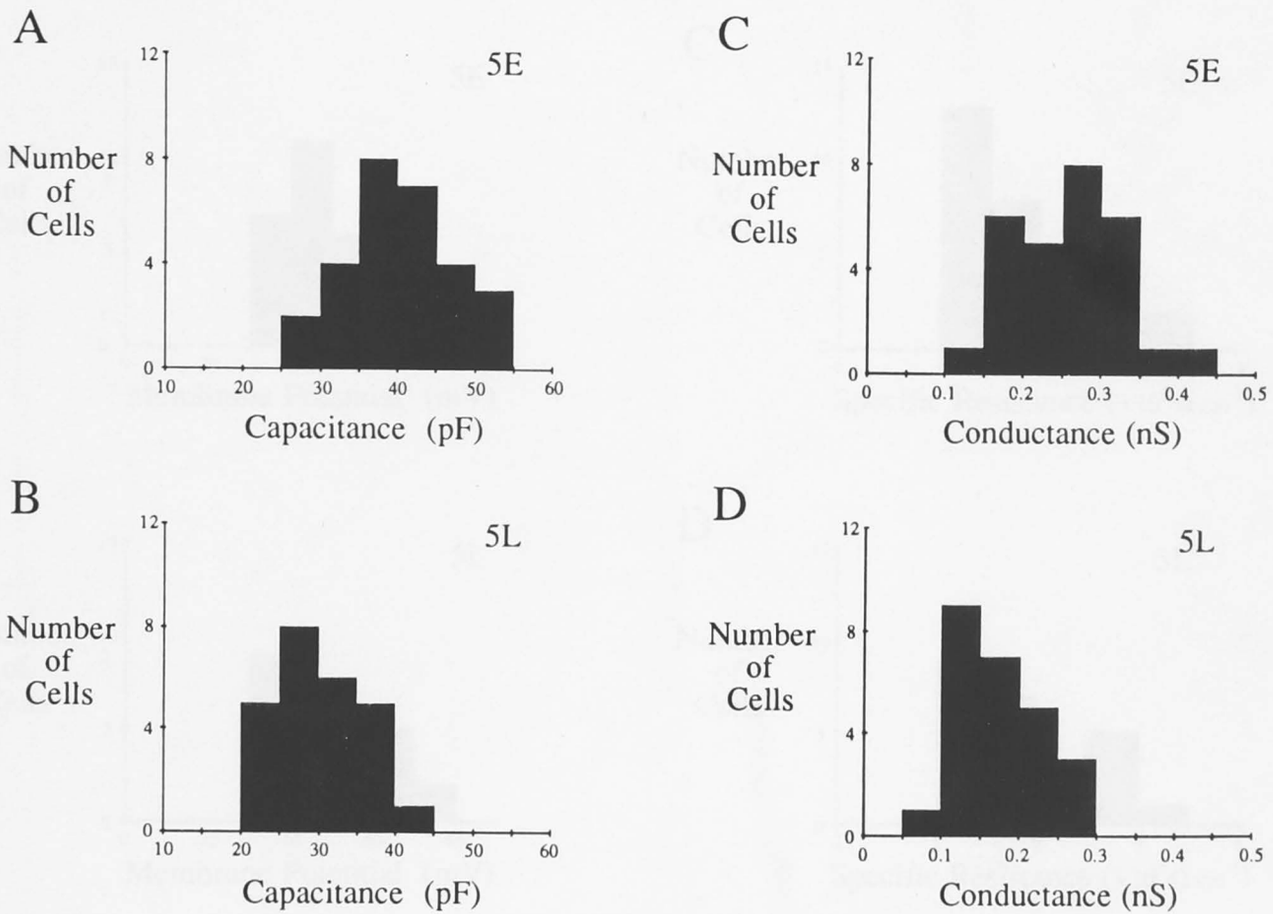

Figure 10. Comparison of the distributions of membrane capacitance and membrane conductance values for 5E and 5L cells.

A) Distribution of 5E cell membrane capacitance values. **B)** Distribution of 5L cell membrane capacitance values. **C)** Distribution of 5E cell membrane conductance values. **D)** Distribution of 5L cell membrane conductance values.

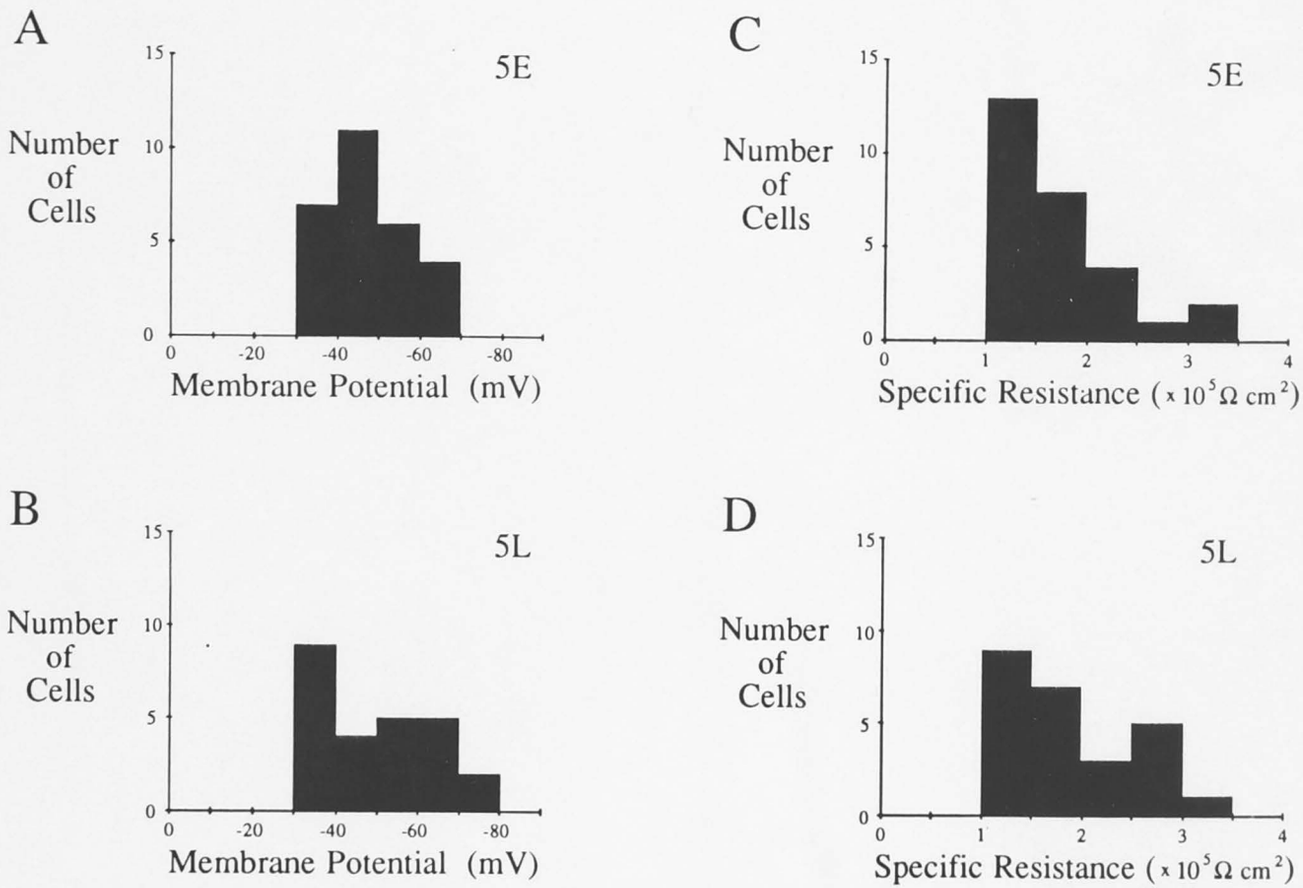

Figure 11. Comparison of the distributions of membrane potential and specific resistance values for 5E and 5L cells.

A) Distribution of 5E cell membrane potential values. **B)** Distribution of 5L cell membrane potential values.

C) Distribution of 5E cell specific resistance values. **D)** Distribution of 5L cell specific resistance values.

Figure 12.

Thin section electron micrographs of gap junction-like structures from both a 5E cell (upper micrograph) and a 5L cell (lower micrograph).

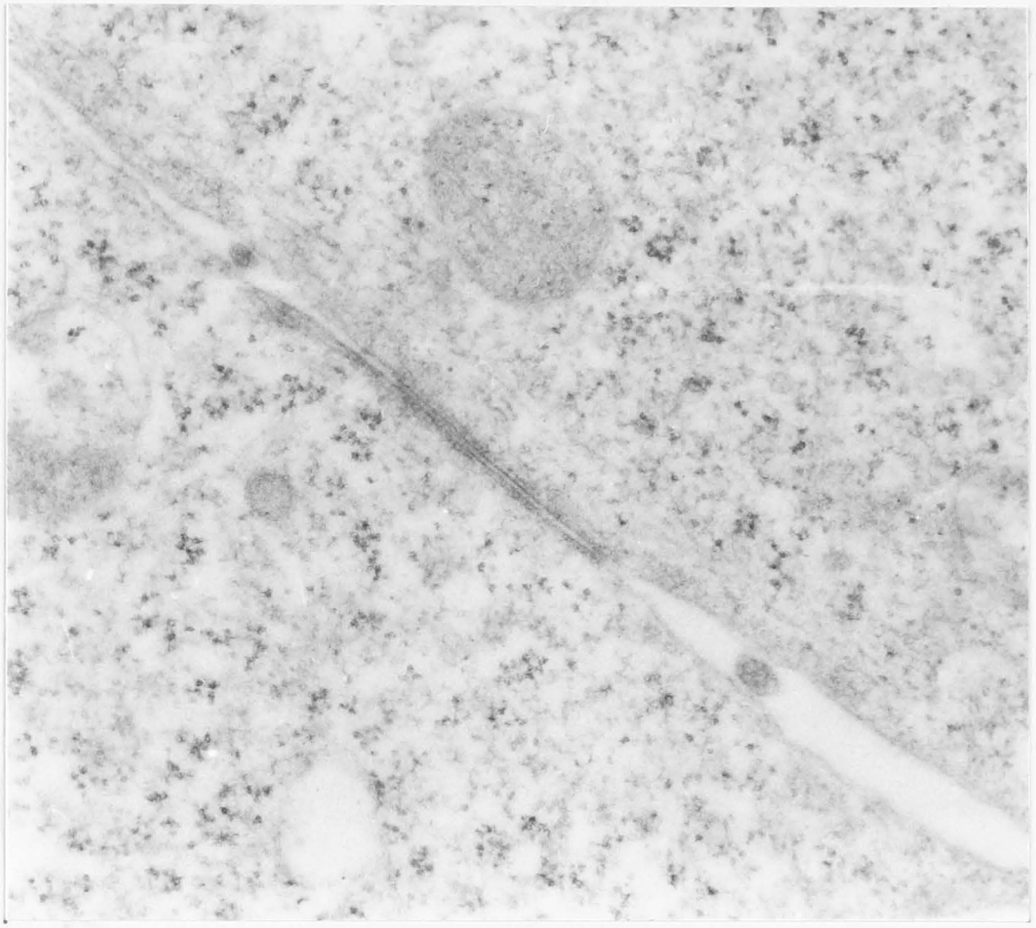

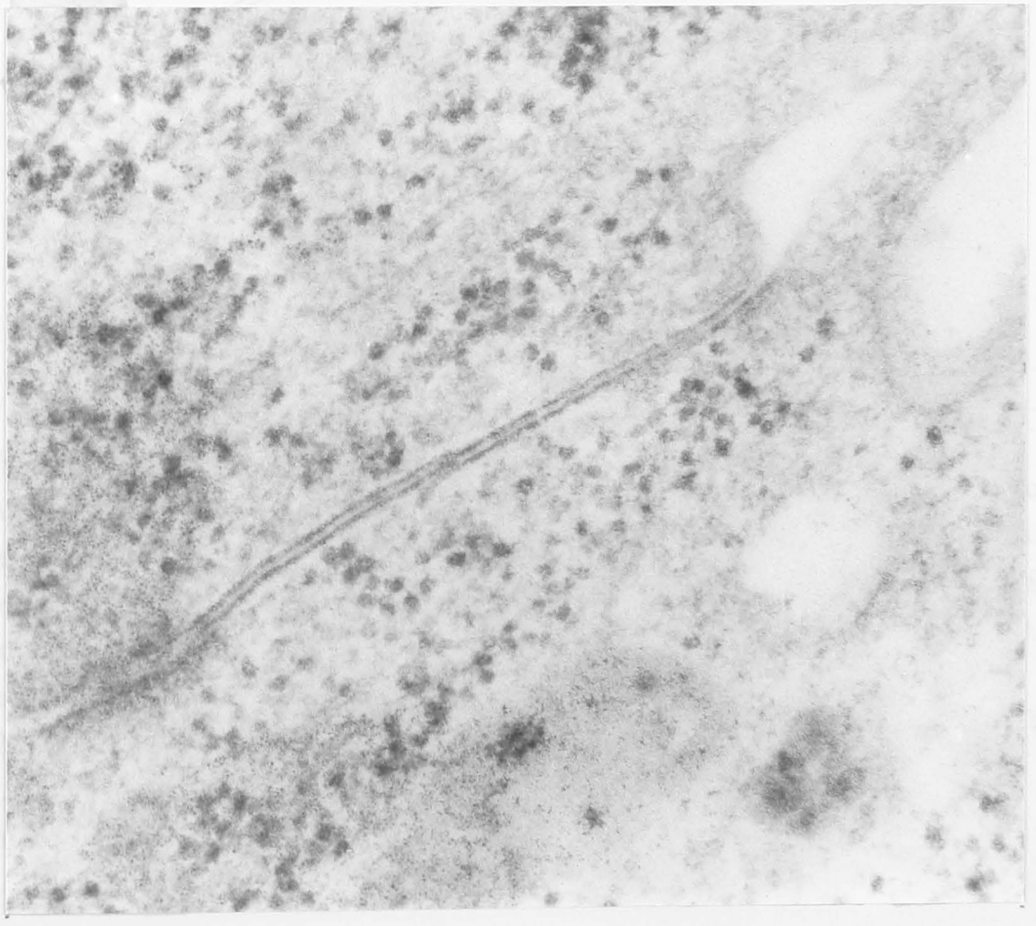

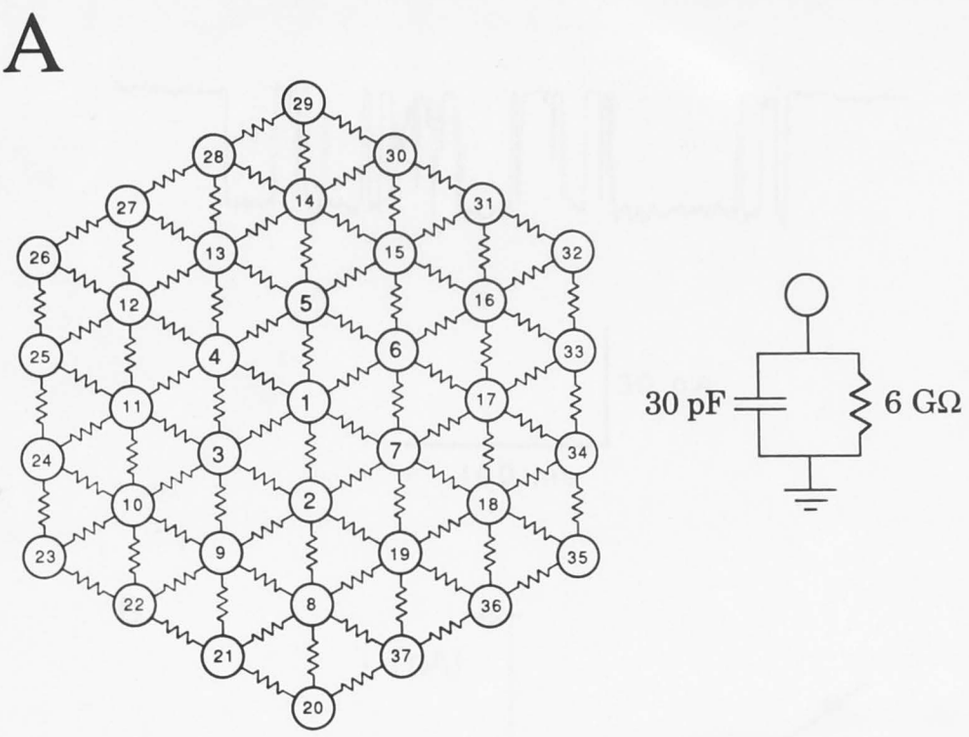

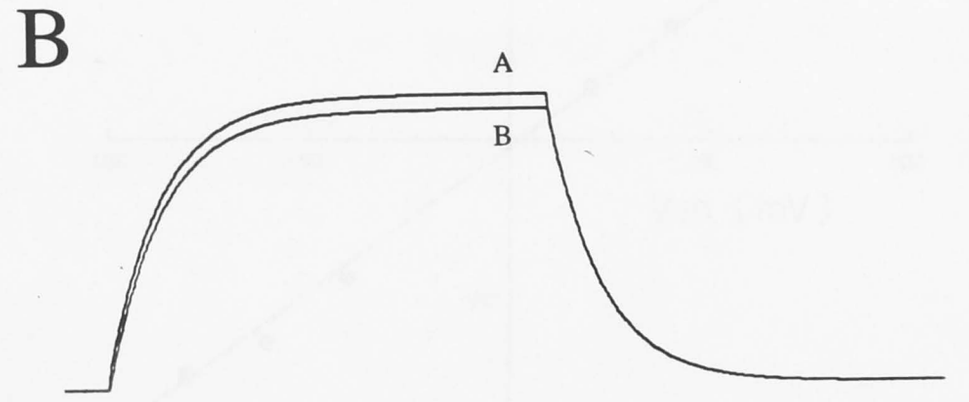

Figure 13. Equivalent circuit analysis of a cell network.

A) Equivalent circuit for a colony of thirty seven cells in a hexagonal array. Each node represents one cell in the colony and every cell is connected to each of its neighbours by a resistor whose value could be varied. At every node a simple RC circuit (shown at right) with a capacitance of 30 pF and a resistance of 6 GΩ was connected to ground. The point of current injection was the central cell of the colony (cell 1).

B) Simulated transient voltage response to a 50 pA current step lasting 1500 ms. Transient (A) is the voltage response of the central cell (cell 1), and transient (B) is the voltage response of a cell in the outermost ring of cells (cell 20).

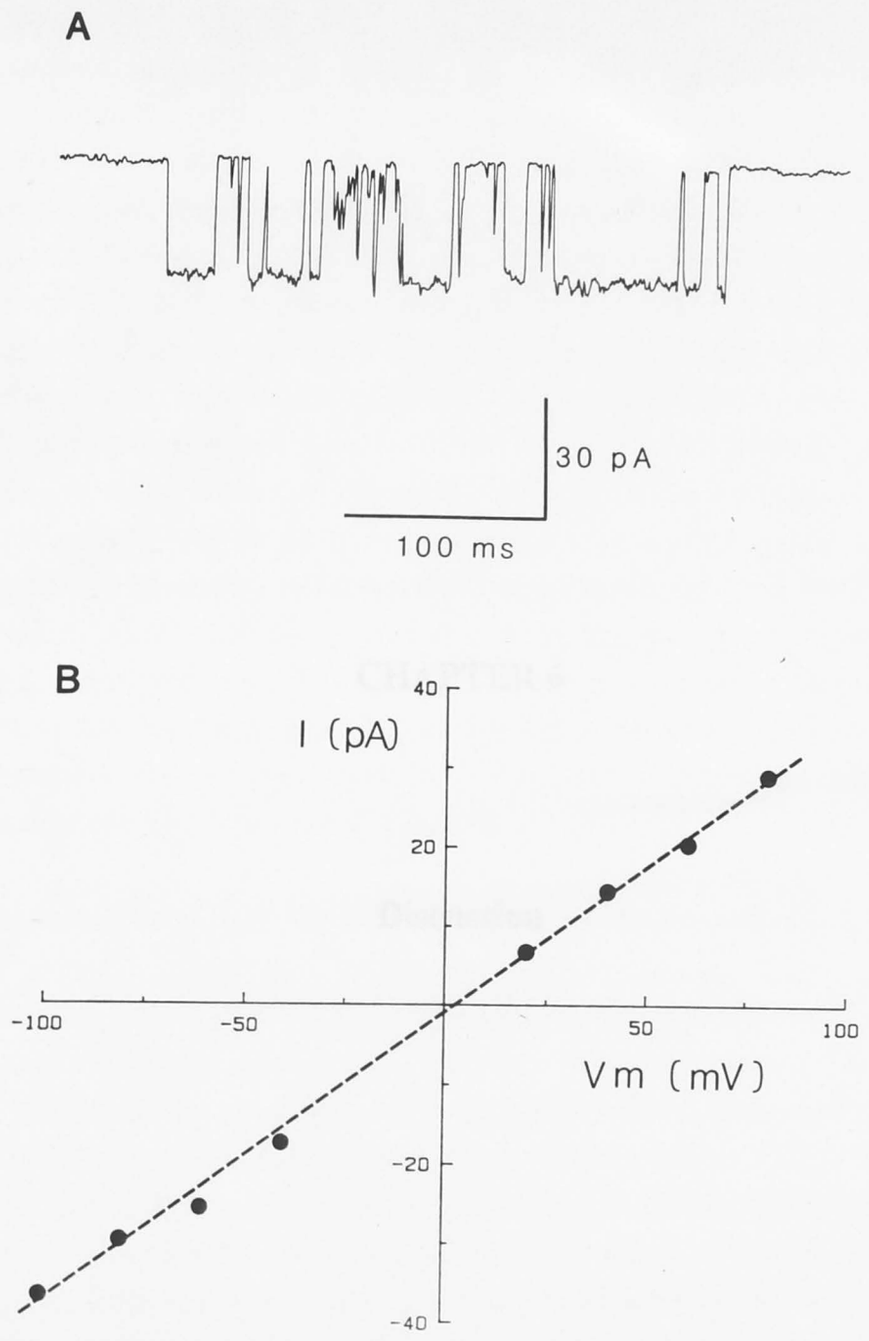

Figure 14. Conductance of the large chloride channel.

A) Single channel currents from an isolated patch of membrane. Transmembrane potential was -80 mV. Pipette solution contained 150 mM CsCl and the bath solution contained 150 mM NaCl.

B) Current-voltage relationship for the large chloride channel. Regression line corresponds to a single channel conductance of 374 pS.

CHAPTER 6

Discussion

In this thesis modulation of ion channel expression was examined in a number of defined cell systems with the aim of finding a convenient and easily manipulated culture system for the study of ion channel expression. In many respects, the upregulation of potassium channel expression which occurs following mitogenic activation of resting T cells, is such a system (Chapter 2). In addition to its advantages as a biological system, a considerable body of information about the specific requirements for T cell activation and the sequence of gene expression during activation already exists, and this should facilitate further study (MacDonald and Nabholz, 1986; Weiss et al, 1986). The T cell fails as a complete system in two important respects: there is neither a cDNA clone for the potassium channel, nor are there specific antibodies for the channel. These omissions preclude any detailed biochemical analysis of transcriptional and/or translational control of channel expression. Before further significant progress can be made in understanding the regulation of this protein, it will be necessary to develop a strategy for cloning the potassium channel. For this reason, the first section of this discussion considers the options available for cloning a cDNA coding for a voltage-gated potassium channel. Strategies for studying the expression of ion channels in neuronal cells are also considered, and the physiological signals which might regulate channel expression in vivo are discussed.

6.1 Strategies for Isolating a cDNA Clone Coding for the Potassium Channel

Identifying and isolating a cDNA clone coding for a voltage-activated potassium channel has proven to be an elusive goal. The protein sequencing approach used to isolate the AChR and sodium channel genes is not yet applicable because of the technical difficulties associated with isolating potassium channel proteins. Dendrotoxin, a toxin isolated from the venom of the Green Mamba snake, can irreversibly block some potassium channels, suggesting that it may bind with very high affinity to a subset of potassium channels (Halliwell et al, 1986; Penner et al, 1986). This toxin may provide a tool with which to affinity purify a potassium channel protein, although such an approach would still be a considerable technical challenge because of the small contribution to total cellular protein made by the potassium channel. Unfortunately, this toxin has no detectable effect on the potassium currents in T cells (data not shown, dendrotoxin was a gift from Dr F. Dreyer). Since the protein isolation approach has yet to yield results it is worthwhile considering alternative strategies for isolating a cDNA clone. As noted by Hille (1984), there are quite a number of similarities between all of the voltage-gated potassium channels with respect to pharmacological and ion permeation properties. It is probable, therefore, that isolation of one potassium channel gene from any species or tissue will lead quickly to isolation of all other voltage-gated potassium channels.

Genetic analysis of the *Shaker* locus of *Drosophila* may provide one opportunity to isolate the gene for the I_A potassium channel via a technique known as 'chromosome

walking' (Jan et al, 1983; Salkoff and Tanouye, 1986). However, this approach has been slow to bear fruit, despite considerable expenditure of effort. An alternative approach, to screen a cDNA library using the *Xenopus* oocyte expression system (Chapter 4), has proven very successful in cloning cDNAs encoding a number of soluble lymphokines (Fung et al, 1984; Noma et al, 1986; Sharma et al, 1987). However, this strategy is only feasible when a relatively purified source of mRNA coding for the protein of interest is available and when a reliable and rapid assay system can be used. Neither requirement seems to be satisfied for any potassium channel at the moment, although at least one group is attempting to use this technique to isolate clones for the I_A channel (Dr S. Siegelbaum, personal communication). In particular, the assay system, using voltage-clamped oocytes, is relatively slow and somewhat unpredictable (Chapter 4). These limitations would make screening a large library of cDNAs very difficult.

Another approach to cloning the T cell potassium channel is to construct a cDNA subtraction library. Using this technique, a cDNA library could be made from mRNA which is present in stimulated T cells but not in resting cells (Davis et al, 1984). The problem with this technique may be one of sensitivity. Only ≈ 250 channels are present in an activated T cell (Chapter 2), and production of these channels could possibly be accounted for by the presence of a single mRNA molecule. Thus, it might be necessary to isolate a mRNA present at a frequency of ≈ 0.001% or less, which is very close to the resolution limits of this technique (Davis et al, 1984). A second problem is that the failure of resting T cells to express potassium channels might be due to post-transcriptional rather than transcriptional control, and mRNA coding for the channel may already be present in the resting cell. To circumvent this problem, a T cell line which does not express the potassium channel, such as CTLL-2 (DeCoursey et al, 1985), could be used for subtraction.

A cDNA clone which codes for a channel-like protein has recently been isolated from a T cell subtraction library (Alonso and Weissman, 1987). This protein is only 17 kD in size but shares a number of structural features with other known channel proteins. It remains to be seen exactly what function this channel performs, but it is unlikely to be associated with the potassium channel since its expression appears to be restricted to mature T cells (Alonso and Weissman, 1987).

One approach which could greatly enhance the chance of isolating a cDNA clone for the potassium channel would be to develop a cell line which overproduced the potassium channel. To do this, it might be possible to take advantage of the fact that potassium channel blockers can block mitogenesis of T cells (Chandy et al, 1984). It is possible that growing a T cell line in media containing relatively high concentrations of a potassium channel blocking drug could select for a mutant cell line which overproduced the channel. Such a procedure has been used to develop cell lines which overproduce the enzyme dihydrofolate reductase (Chang and Littlefield, 1976). Unfortunately, this selection procedure does not always produce a mutant with increased gene expression. It is possible, for example, that a mutation in the gene product on which the selective agent is acting could cause a reduction in the

binding affinity between the selective agent and the protein. This mutation would be equally effective in conferring drug-resistance on the mutant cell line (Lewin, 1980).

6.2 In Vitro Systems for the Study of Ion Channel Expression in Cells from the Mammalian CNS

The fluorescence-activated cell sorter can be used to isolate cells from the mammalian embryonic central nervous system which will survive in culture for up to several weeks (Campbell et al, 1977; St John et al, 1986). Cells isolated from the mammalian CNS using the FACS should be good starting material for studies on the developmental control of ion channel expression in vitro. Although analysis of the cell surface phenotype of CNS cells is at a relatively primitive stage compared with the T cell lineage, use of the FACS will be helpful in screening for mAbs to useful cell surface markers.

To gain a full understanding of ion channel expression it will be important to combine electrophysiological and biochemical experiments on the same biological material. Electrophysiological studies can be conducted on just a few cells, but the choice of tissue for biochemical studies is much more limited, since relatively large amounts of homogeneous tissue are normally required. Neural tissue is, of course, extremely heterogeneous and is unsuitable for many biochemical investigations. Procedures which can select for a homogeneous CNS cell population cannot normally provide sufficient material for many biochemical procedures. Therefore, to combine electrophysiological and biochemical studies it may be necessary to use established cell lines.

In the past, neuronal cell lines have been established from either naturally occurring tumors or from chemically or virally induced tumors (Nelson, 1975; Schubert et al, 1974; De Vitry et al, 1974). This approach is necessarily limited, since the cell population giving rise to the tumor cannot be well defined. The origin of a cell line can, in theory, be defined on the basis of its phenotype in culture, but this approach will not necessarily give the correct answer. For example, the finding that glial cells in primary culture are electrically excitable suggests that an electrically excitable cell line may not be neuronal in origin (Chiu et al, 1984; Bevan et al, 1985; Nowak et al, 1987). For this reason, the best strategy is to produce cell lines from well defined cell populations. In this respect, use of the FACS to isolate neuronal subpopulations may prove to be of considerable benefit for the development of neuronal cell lines.

Strategies similar to those used to study the differentiation of hemopoietic cell lineages may prove useful for studying neuronal cells and for establishing cell lines from a defined starting population of cells. In hemopoietic lineages, precursor cells are relatively rare and normally comprise a tiny fraction of the total number of cells in a given lineage. These cells are, however, the most interesting cells in the lineage, because it is at this early stage of development that commitment to a particular differentiation pathway will occur. A number of techniques have been used to establish cell lines which have similar phenotypic characteristics to cells in the early phase of differentiation.

One succesful technique for B-lymphocyte lineage cells has been to immortalize precursor cells with Abelson murine leukemia virus (Baltimore et al, 1979). It has been possible to obtain B-cell tumors at a number of different developmental stages, and this has allowed dissection of the stages of gene rearrangement and expression associated with immunoglobulin production (Hanley-Hyde and Lynch, 1986). To be of use, a viral agent is required which is both very efficient at transformation and which does not greatly distort the normal pattern of gene expression. One possibility for neuronal cells in the temperature-sensitive mutants of Rous sarcoma virus, which may be able to transform neuronal precursors (Giotta et al, 1980). Temperature-sensitive mutants could be of particular value because it is important to have some means of inactivating the viral oncogene product, which can modify channel function and expression (van der Valk et al, 1987; Schneider et al, 1987).

A second approach, somatic cell hybridization, has also proven successful for studying B cell differentiation. Cell fusion has been used to produce neuronal cell lines (Greene et al, 1975; Platika et al, 1985). This approach has a number of disadvantages, however, and typically results in karyotypically unstable cell lines. The combination of genetic material from both parent cells cannot be controlled, and the resultant phenotype of the hybrids is unpredictable (Platika et al, 1985). For these reasons, cell fusion does not appear to be a technique of choice.

A third technique, which has been used to produce T-lymphocyte clones, is to maintain T-cell growth in vitro by supplying the correct growth factors and antigenic stimulation (Fathman and Frelinger, 1983). Neuronal cells do not grow readily in vitro so it is not possible, at present, to produce neuronal cell lines without some transforming agent. There is no reason, in principle, why cell lines cannot be grown directly from early neuronal cells if the correct growth conditions, which inhibit terminal differentiation and maintain mitogenesis, could be found. However, neuronal mitogenic factors, in contrast to differentiation factors such as NGF, have yet to be well characterised.

A fourth technique, which is the least disruptive of normal cell function, is to transfect a factor dependent cell line or cell population with a gene for the factor on which the cell is dependent, thereby producing an autocrine system. This approach has been applied with success to hemopoietic cell development (Lang et al, 1985), but cannot be used for neuronal cells until factors which can stimulate or maintain neuronal mitogenesis have been isolated.

Finally, it has been found that a number of neuroblastoma cell lines overproduce the cellular oncogenes known as N-*myc* and N-*ras* (Land et al, 1983; Schwab et al, 1983). It might be possible to transfect a defined starting population of neuronal cells with these oncogenes, possibly in tandem with an inducible promoter such as the metallothionein promoter (Mayo et al, 1982), to produce neuronal cell lines of defined parentage. These cell lines could then be converted back to something approaching the starting cell population by removal of the induction factor.

6.3 Contribution of Developmental and Experiential Factors to Ion Channel Expression in Adult Neurons

For a given subpopulation of neurons, there appears to be a stereotyped pattern of ion channel expression which occurs during development. The best evidence for this assertion is the observation that neurons will gain mature electrical excitability in vitro in the absence of the normal factors which might modulate channel expression in vivo (see Chapter 1). In addition to this stereotyped expression of channels, neurons can probably respond to their environment by modulating their expression of ion channels. Environment, in this context, should be interpreted as meaning both the micro-environment of an individual neuron - the neurotransmitters and differentiation factors present in its immediate surrounds, and the macro-environment - the environment of the entire organism which is modulated into biochemical signals by the organism's sense organs.

Positive identification of the physiological signals which modulate ion channel expression in vivo has yet to be achieved. There is some evidence that the classical neurotransmitters such as acetylcholine can modulate gene expression. Activation of nicotinic AChRs induces expression of the Met-enkephalin gene in cultured adrenal chromaffin cells (Eiden et al, 1984). An increase in the amount of mRNA coding for Met-enkephalin can be seen within 2 hrs following exposure to 10 μM nicotine. Induction of the gene may depend upon calcium influx via voltage-activated calcium channels, following membrane depolarization. The effect of nicotine can be blocked with the calcium channel antagonist D600 and is mimicked by high potassium solutions and the ionophore A23187 (Eiden et al, 1984; Siegel et al, 1985; Kley et al, 1987). Activation of expression of the proto-oncogene c-*fos* in PC12 cells following stimulation with 100 μM nicotine has also been reported (Greenberg et al, 1986). Induction of c-*fos* expression was also dependent on calcium influx. Thus, the rate and type of synaptic input into a neuron may be one factor modulating gene expression in that neuron.

A number of neurotransmitters and neuromodulators (e.g. acetylcholine, glutamate, noradrenaline and neuropeptides such as substance P) can stimulate the breakdown of inositide phospholipids into the second messengers inositol trisphosphate and diacylglycerol (Downes and Michel, 1985; Sugiyama et al, 1987). Stimulation of the T cell receptor with the mitogenic lectin Con A, which initiates phosphoinositide breakdown (Michell, 1982; Imboden et al, 1987), up-regulates expression of the delayed rectifier potassium channel (Chapter 2). It is possible that a similar mechanism could work in neurons, although the effect might not be as dramatic, because neurons normally maintain a high basal level of voltage-gated ion channel expression. A recent report that PMA, an activator of protein kinase C, can up-regulate expression of calcium channels in chick muscle cells, as measured by dihydropyridine binding, suggests that such a mechanism may indeed exist in some excitable cells (Navarro, 1987).

6.4 Conclusion

In recent years there have been considerable technical advances in both the electrophysiology and the molecular biology of ion channels. There has not been, however, a concomitant increase in our understanding of ion channel expression. With the exception of a number of structural studies, there have been few successful attempts to weld these technologies together. Progress has been limited, in part, by the relative weakness in understanding and technical control of neuronal cell biology. This weakness is particularly apparent when comparison is made with the technical and conceptual advances made in the cell biology of the immune system. To gain a better understanding of the processes controlling ion channel expression in neurons it will be necessary to combine molecular biology, cell biology and electrophysiology to study a common problem in a well defined cell system.

APPENDIX

A Model of T Cell-Target Cell Interaction Leading to Lymphokine Release

Introduction

The following characteristics of antigen triggered lymphokine release from activated T lymphocytes have been established. The antigen bearing target cell need not be metabolically active (Andrus and Lafferty, 1981; Shimonkevitz et al., 1983). Cytotoxic T lymphocytes, defined either functionally or by their Lyt-2^+ phenotype, can secrete lymphokines following antigen exposure (Andrus et al., 1984; Dennert et al., 1981; Kelso and MacDonald, 1982; Guerne et al., 1984; Prystowsky et al., 1982). The range and amount of each lymphokine produced varies considerably between T cells but for an individual clone it is relatively invariant following each antigen stimulation (Kelso and Glasebrook, 1984; Sanderson et al., 1985). There appears to be a common controlling mechanism by which antigen stimulation activates release of all the lymphokines produced by a given T cell (Sanderson et al., 1985).

It follows from these observations that a sensitive method for detecting activated T cells reactive to a given antigen is to assay lymphokine production under conditions where the antigen signal is the only stimulus. This can be achieved using metabolically inactive target cells, which are incapable of triggering lymphokine production from resting T cells (Andrus et al., 1980). It is also necessary to use short assay times, to avoid the secondary effects due to production of lymphokines such as interleukin 2 which may enhance the rate of lymphokine release (Kelso et al., 1984).

When using lymphokine release to detect T cell activation it is important to understand the behaviour of the assay when using different concentrations of antigenic cells and T cells. In this paper we examine the relationship between cell number and lymphokine titre using the H-2^d tumour cell line P815 to trigger interleukin 3 (IL3) release from activated C57BL/6 anti-BALB/c T cells. Analysis of the amount of lymphokine released at different T cell and antigenic cell concentrations revealed quite complex cellular interactions. We show that this behaviour is consistent with a steady state binding model of T cell-target cell interaction if it is assumed that triggering is an all or none event which requires the binding of at least two target cells to the allo-reactive T cell.

Materials and Methods

Animals and cell lines

The inbred mouse strains C57BL/6J and BALB/c were maintained and bred at the John Curtin School of Medical Research, Canberra. The DBA/2 mastocytoma, P815, was maintained by serial passage in Eagle's Minimal Essential Medium (EMEM) supplemented with 10% heat-inactivated foetal calf serum (HIFCS) and antibiotics (streptomycin 100 µg/ml; penicillin 100 U/ml; neomycin 100 µg/ml).

Mixed lymphocyte culture (MLC)

The method of mixed lymphocyte culture has been described previously (Woolnough and Lafferty, 1979). Briefly, cultures containing 2×10^6 C57BL/6J lymph node cells and 3.16×10^6 gamma-irradiated (800 rads) BALB/c spleen cells in a total of 2 ml EMEM supplemented with 10% HIFCS and 10^{-4} M 2-mercaptoethanol (2-ME) were prepared in wells of a 24 well tissue culture tray (LINBRO, 76-035-05). Cultures were incubated at 37° C for 4 days in a humidified atmosphere of 10% CO_2, 83% N_2 and 7% O_2.

Preparation of activated T lymphocytes

Homogeneous populations of activated T lymphocytes were prepared from 4 day old MLC using the method of Woolnough and Lafferty (1979). Cells from MLC were washed and resuspended at 10^5/ml in fresh medium containing 3% v/v Concanavalin A stimulated spleen cell supernatant (prepared as previously described (Woolnough and Lafferty, 1979)). These cultures were gassed with 7% O_2, 10% CO_2 and 83% N_2 and incubated a further 3 days at 37^0. Following this period, cells reach approximately 10^6 cells/ml and are >99% Thy 1^+ as determined by flow microfluorometry (data not shown). Cells prepared in this manner are referred to as activated T cells.

Stimulation of lymphokine release

The required number of activated T cells were mixed with UV-irradiated (960 $\mu W/cm^2$) P815 tumour cells in a fixed volume of 200 µl EMEM containing 10^{-4} M 2-ME in individual wells of a 96 well microtitre tray (NUNC 1-67008). These cultures were incubated 5-6 hours in a humidified atmosphere of 10% CO_2 in air. Supernatants were then removed and stored at 20° C. Each data point of an assay was prepared in 4 replicates.

IL3 assay

The ability of IL3 to maintain the growth of the cell line FDC-P1 (Dexter et al., 1980) was used to detect IL3. Twelve serial twofold dilutions of the test supernatant were prepared in 96 well microtitre trays using RPMI plus 5% HIFCS as diluent and yielding a final volume per well of 50 µl. Each well then received 2×10^4 FDC-P1 cells in 50 µl RPMI containing 5% HIFCS. These cultures were incubated at 37° C in a humidified atmosphere of 10% CO_2 in air for 48 hours before the level of the lysosomal enzyme hexosaminidase was measured to indicate cell proliferation using the colorimetric method developed by Landegren (1984). Plots of $\log_{10}$ optical density (O.D.) versus $\log_{10}$ supernatant dilution yielded a sigmoidal curve, the central section of which approximated a straight line. The intersection between a line drawn through the linear portion of the curve and the background O.D., defined as the mean plus three standard deviations of 24 control wells containing medium and cells only, was taken as the endpoint titre. The $\log_{10}$ endpoint titre was measured for each of four replicates. The mean value of four replicates has an associated

95% confidence interval of ± 0.14 $\log_{10}$ endpoint units as measured by analysis of variance.

Results

The basic relationships between lymphokine release and antigenic cell or T cell number are shown in Fig. 1. The relationship between the logarithm of IL3 titre and the logarithm of allo-antigenic P815 cell number, for a constant number of T cells, is shown in Fig. 1a. This relationship is linear, with an approximate slope of two in the region of T cell excess, reaching a plateau in the region where T cell and antigenic cell numbers are comparable. The amount of IL3 produced by different numbers of T cells when the antigenic cell number is kept constant is shown in Fig. 1b. The slope of lymphokine titre versus T cell number is close to one throughout the region of antigenic cell excess. Fig. 1c shows the dose response curve obtained when the total number of cells, containing an equal concentration of both T cells and target cells, was varied. The slope of the relationship lies between two and three over the main region of the graph showing a very gradual roll-off at the highest total cell number.

These simple relationships between cell number and lymphokine titre define the essential characteristics of any model of the interaction between T cells and antigenic cells which leads to lymphokine release. The fact that the relationship between target cell number and lymphokine titre has a slope greater than one (Fig. 1a) indicates that the order of the reaction between T cells and antigenic cells must be greater that one, i.e. more than one antigenic cell must bind to the T cell before lymphokine release can be triggered. That the slope is approximately equal to two suggests that a minimum requirement for triggering of a single T cell is the binding of at least two antigenic cells. The fact that the slope of lymphokine titre versus T cell number is approximately equal to one (Fig. 1b) indicates that there is no effective interaction between T cells which can influence the rate of lymphokine release, under the specific conditions of these experiments.

It is clear that a gradual increase in antigenic cell number produces, for the same total number of T cells, a gradual increase in lymphokine titre (Fig. 1a). The form of this empirical relationship between antigenic cell number and lymphokine titre, a linear region at low antigenic cell number asymptoting to a fixed value in the region of antigen excess, is similar to the dose response curves of classical pharmacology (Hill, 1909; Stephenson, 1956). By this analogy, lymphokine titre is the measured response and the dose, or controlled variable, is the change in antigenic or T cell numbers. This suggests that T cell-antigenic cell interactions may be treated as simple steady state binding reactions.

A basic model relating T cell and antigenic cell number to lymphokine release can now be derived with the use of two assumptions. The first assumption is that the rate limiting step of lymphokine expression is the intra-cellular process of lymphokine production and

release, and not the initial inter-cellular triggering events. That is to say, the processes of T cell-antigenic cell recognition, binding and triggering are considered to be fast compared to the time necessary for a triggered T cell to manufacture and release sufficient lymphokine to be detected in our biological assays. The second assumption is that the amount of lymphokine released is directly proportional to the number of T cells bound to at least two antigenic cells. Thus, triggering is seen as an all or none process and the amount of lymphokine produced can be expressed by the following equation:

$$[LK] = a\,[TA_2]$$

where, [LK] is the concentration of lymphokine in the supernatant, $[TA_2]$ is the total number of T cells bound to two antigenic cells and a is a proportionality constant.

Using the two preceding assumptions, the simplest binding model which is consistent with the results shown in Fig. 1 is:

$$T + A \underset{}{\overset{K}{\rightleftharpoons}} TA + A \overset{K}{\rightleftharpoons} TA_2 \xrightarrow{\alpha} [LK]$$

where, T is a T cell unbound to any antigenic cells, TA is a T cell bound to a single antigenic cell, TA_2 is a T cell bound to two antigenic cells and α is the proportion of T cells which are triggered to produce lymphokine by binding to two antigenic cells. This model predicts that the amount of lymphokine released by a given number of T cells and target cells can be described by the following equation:

$$[LK] = a\,[TA_2] = (a \times Tn) \,/\, \left(1 + \frac{2K}{[A]} + \frac{(K)^2}{([A])^2}\right)$$

where, Tn is the total number of T cells per well and [A] is the number of antigenic cells unbound to any T cell. Derivation of this equation is given in the Appendix.

A family of curves, predicted by the steady state binding model, relating antigenic cell number to lymphokine release for different values of total T cell number are shown in Fig. 2a. The main predictions of the model are that the linear region of the dose response relationship will have a slope of two and that this linear region will merge in assays in which there are high T cell concentrations. The merging of the lymphokine titre curves when T cells are in relative excess is due to competition between T cells for target cells. Target cells will tend to become 'coated' with T cells and the possibility of a T cell binding to two targets is reduced. The model also predicts that the difference between asymptote values of lymphokine titre should remain directly proportional to the total number of T cells per well.

Experimental target cell dose response curves for different T cell numbers are shown

in Figs 2b and 2c. The data points were fitted with curves derived from the steady state binding model described above. There is clearly a good agreement between the predictions of the model and the experimental results.

T cell dose response curves are shown in Figs 1b and 3. In these experiments, the number of T cells was varied and the antigenic cell number was kept constant. The data points were again fitted using the steady state binding model. The model predicts an intitial linear region with a slope approximately equal to unity followed by a short plateau region. The experimental results are well fitted by the model.

When T cell and antigenic cell numbers are increased simultaneously, the steady state binding model predicts an initial region with a slope of three, then a transitional region with slope gradually changing from three to one and then a final region with a slope equal to one. The practical experimental range is restricted to the transition region of the curve and in this region, as predicted, the slope of lymphokine titre versus total cell number is less than three and greater than one (Fig. 1c).

We have found that the model does not hold over the extreme range of cell numbers. At the very highest T cell or P815 cell concentrations the amount of lymphokine produced was lower than that predicted by the model. This may be a result of some relatively non-specific metabolic effect due to cell crowding, or to non-specific binding between like cells. However, over a wide range of cell concentrations there is a reasonable agreement between theory and experiment.

Discussion

We have shown that there is agreement between the predictions of the steady state binding model of T cell-target cell interactions and the experimental results obtained under a number of different conditions: when antigenic cell number is varied and T cell number is kept constant (Figs 1a and 2), when T cell number is varied and antigenic cell number is kept constant (Figs 1b and 3) and when both T cell and antigenic cell numbers are varied simultaneously (Fig. 1c). Even though the relationships between cell number and lymphokine titre initially look quite complex, lymphokine titre can be predicted by making only two assumptions. First, we assume that the processes of cell recognition and binding achieve equilibrium rapidly compared with the time required for the production and release of lymphokine. The second assumption is that T cell triggering is an all or none process. In terms of the steady state binding model this means that T cells which have bound only one antigenic cell do not receive a sufficient stimulus to trigger lymphokine release, whereas T cells which have bound two or more antigenic cells do receive the threshold stimulus necessary to trigger lymphokine production. Different T cells will not necessarily produce the same amount or kinds of lymphokine, but once triggered, it is assumed that the binding

of more antigenic cells to the T cell will not result in an increase in lymphokine production over that produced by the threshold amount of stimulation.

Some of the consequences of assuming that binding of two or more antigenic cells is necessary for triggering can best be seen by considering a simple numerical example. The prediction of the steady state binding model when some proportion of T cells are triggered by binding to only one antigenic cell is shown in Fig. 4. In curve (a), all T cells bound to a single antigenic cell as well as those bound to two antigenic cells were triggered. The slope of the linear region of the curve is now equal to one. For curve (b) only 15% of T cells bound to a single antigenic cell were triggered and curve (c) represents the case where there is no triggering of T cells bound to only a single antigenic cell. It is clear that there is significant deviation from a slope of two even when only a relatively small fraction of T cells bound to a single antigenic cell can trigger. The lymphokine assay system potentially seems to be sensitive to variations in the threshold for triggering and, while it is obvious that a T cell can bind to more than two antigenic cells, this condition appears to be a minimum requirement for triggering under the specific conditions of the experiments reported here.

It has been shown previously that antigenic cell dose response curves can have slopes close to one, when the target cells are infected with virus (Sinickas et al., 1985). It is clear, therefore, that there is no absolute requirement for a T cell to bind two or more antigenic cells before lymphokine release is triggered. The question that remains unanswered therefore, is what factors control the trigger threshold? There are at least four possibilities: 1) the density of receptors on the T cell, 2) the density of antigen on the target cell, 3) the affinity between receptor and antigen, and 4) the efficacy with which a particular antigen can stimulate the receptor (efficacy can be thought of as a measure of the efficiency with which a given antigen can stimulate the T cell receptor, and is independent of the affinity with which it binds). Since it is unlikely that the T cell receptor number will vary with antigen specificity, some combination of the other three possibilities presumably determines the triggering threshold.

The technique of measuring lymphokine release is widely used to detect the presence of activated T cells. The development of sensitive and accurate proliferation assays for IL3 and IL2, and the availability of simple methods for processing large numbers of plates, makes it possible to determine very accurately the relationship between target cell number and lymphokine titre. This experimental accuracy means that it is possible to interpret cell dose response curves in terms of theoretical models of cellular interactions. This approach has already been successfully applied to the analysis of T cell recognition of processed soluble antigens (Ashwell et al.,1986). According to the model we have developed, accurate target cell dose response curves can be used to give quantitative information about the number of reactive T cells, the average affinity between T cells and target cells and the efficiency of stimulation by a given target cell.

The assumptions upon which the model described in this paper are based are not the

only ones which could be used to explain the data. It is true for almost any binding or kinetic study that a number of different models will give predictions which are indistinguishable within experimental error. It is to be hoped, however, that quantification of the relationships controlling lymphokine release at a cellular level will ultimately result in a more accurate description of these processes.

Mathematical Appendix

For the following binding reaction,

$$T + A \underset{k_{-1}}{\overset{k_1}{\rightleftharpoons}} TA + A \underset{k_{-1}}{\overset{k_1}{\rightleftharpoons}} TA_2$$

assuming that binding between cells is in equilibrium, then,

$$\frac{d[T]}{dt} = 0 = k_{-1}[TA] - 2k_1[A][T] \qquad (1)$$

$$\frac{d[TA_2]}{dt} = 0 = k_1[A][TA] - 2k_{-1}[TA_2] \qquad (2)$$

Rearranging equation (2) gives,

$$[TA] = \frac{2K}{[A]}[TA_2] \qquad (3)$$

where, $K = k_{-1}/k_1$.

Rearranging (1) and substituting into equation (3) gives,

$$[T] = \left(\frac{K}{[A]}\right)^2 [TA_2] \qquad (4)$$

Since it is expected that the total number of T cells and antigenic cells will remain constant during the initial binding and triggering period, the following relationships will also hold true.

$$[T] + [TA] + [TA_2] = Tn \qquad (5)$$

$$[A] + [TA] + 2[TA_2] = An \qquad (6)$$

where, Tn is the total number of T cells per well and An is the total number of antigenic cells per well.

Substituting equations (3) and (4) into (5) gives,

$$[TA_2] = Tn \Big/ \left(1 + \frac{2K}{[A]} + \left(\frac{K}{[A]}\right)^2\right) \qquad (7)$$

If we write $x = 1 + (K / [A])$, equation (7) can be rewritten as,

$$Tn = [TA_2]\ x^2 \qquad (7a)$$

Substituting equations (3) and (4) into (6) gives,

$$An = [TA_2] \left(2 + \frac{2K}{[A]} \right) + [A]$$

$$= 2\,[TA_2]\,x + [A] \qquad (8)$$

It can be checked, using equations (7a) and (8) that,

$$(2[TA_2] + An)\,x = 2[TA_2] + \frac{2K}{[A]}\,[TA_2] + 2[TA_2]\,x^2 + [A]\,x$$

$$= An - [A] + 2Tn + [A]\,x$$

$$= An + 2Tn + [A]\,(x-1)$$

$$= An + 2Tn + K$$

It follows that,

$$(An + 2Tn + K)^2\,[TA_2] = (2\,[TA_2] + An)^2\,x^2\,[TA_2]$$

$$= (2[TA_2] + An)^2\,Tn \qquad (\text{by (7a)})$$

Expanding this gives equation (9),

$$4Tn\,[TA_2]^2 - (K^2 + 4Tn^2 + 4KTn + 2KAn + An^2)\,[TA_2] + An^2Tn = 0 \qquad (9)$$

To evaluate $[TA_2]$ it is necessary to solve the quadratic equation (9).

To fit the data points, it was necessary to take account of the fact that not all of the T cells were primed against the P815 antigenic cell. This was acheived by scaling the number of T cells per well by a constant factor 'tf' which was taken to be the proportion of T cells primed against the antigenic cell P815. The effective number of T cells per well is then given by,

$$Tn_{(effective)} = tf \times Tn \qquad (10)$$

The other free parameters for fitting were K, the apparent dissociation constant and a, the scale factor for the average amount of lymphokine released per triggered T cell during the time of the assay.

Bibliography

Andrus, L. and K. J. Lafferty. 1981. Interleukin 2 production by alloantigen (H-2) activated T cells. *Aust. J. Exp. Biol. Med. Sci.* **59:** 413.

Andrus, L., A. Granelli-Piperno and E. Reich. 1984. Cytotoxic T cells both produce and respond to interleukin 2. *J. Exp. Med.* **159:** 647.

Andrus, L., S. J. Prowse and K. J. Lafferty. 1980. Interleukin 2 production by T cells: triggering of T cell activation and lymphokine release. *Behring. Inst. Mitt.* **67:** 61.

Ashwell, J. D., B. S. Fox and R. H. Schwartz. 1986. Functional analysis of the interaction of the antigen-specific T cell receptor with its ligands. *J. Immunol.* **136:** 757.

Dennert, G., S. Weiss and J. F. Warner. 1981. T cells may express multiple activities: Specific allohelp, cytolysis and delayed-type hypersensitivity are expressed by a cloned T-cell line. *Proc. Natl. Acad. Sci. U.S.A.* **78:** 4540.

Dexter, T. M., J. M. Garland, D. Scott, E. Scolnick and D. Metcalf. 1980. Growth of factor-dependent hemopoietic precursor cell lines. *J. Exp. Med.* **152:** 1036.

Guerne, P. A., P. F. Piguet and P. Vasalli. 1984. Production of interleukin 2, interleukin 3, and interferon by mouse T lymphocyte clones of lyt-2^+ and lyt-2^- phenotype. *J. Immunol.* **132:** 1869.

Hill, A. V. 1909. The mode of action of nicotine and curari determined by the form of the contraction curve and the method of temperature coefficients. *J. Physiol.* **39:** 361.

Kelso, A. and A. L. Glasebrook. 1984. Secretion of interleukin 2, macrophage-activating factor, interferon, and colony-stimulating factor by alloreactive T lymphocyte clones. *J. Immunol.* **132:** 2924.

Kelso, A. and H. R. MacDonald. 1982. Precursor frequency analysis of lymphokine-secreting alloreactive T lymphocytes. Dissociation of subsets producing interleukin 2, macrophage-activating factor, and granulocyte-macrophage colony-stimulating factor on the basis of lyt-2 phenotype. *J. Exp. Med.* **156:** 1366.

Kelso, A., H. R. MacDonald, K. A. Smith, J. C. Cerottini and K. T. Brunner. 1984. Interleukin 2 enhancement of lymphokine secretion by T lymphocytes: analysis of estimated clones and primary limiting dilution microcultures. *J. Immunol.* **132:** 2932.

Landegren, U. 1984. Measurement of cell numbers by means of the endogenous enzyme hexosaminidase. Application to detection of lymphokines and cell surface antigens. *J. Immunol. Meth.* **67:** 379.

Prystowsky, M. B., J. M. Ely, D. I. Beller, L. Eisenberg, J. Goldman, M. Goldman, E. Goldwasser, J. Ihle, J. Quintans, H. Remold, S. N. Vogel and F. W. Fitch. 1982. Alloreactive T cell lines. VI. Multiple lymphokine activities secreted by helper and cytolytic cloned T lymphocytes. *J. Immunol.* **129:** 2337.

Sanderson, C. J., M. Strath, D.J. Warren, A. O'Garra and T. B. L. Kirkwood. 1985. The production of lymphokines by primary alloreactive T-cell clones: a co-ordinate analysis of 233 clones in seven lymphokine assays. *Immunology.* **56:** 575.

Shimonkevitz, R., J. Kappler, P. Marrack, and H. Grey. 1983. Antigen recognition by H-2-restricted T cells. I. Cell-free antigen processing. *J. Exp. Med.* **158:** 303.

Sinickas, V. G., R. B. Ashman, P. D. Hodgkin and R. V. Blanden. 1985. The cytotoxic response to murine cytomegalovirus. III. Lymphokine release and cytotoxicity are dependent upon phenotypically similar immune cell populations. *J. Gen. Virol.* **66:** 2551.

Stephenson, R. P. 1956. A modification of receptor theory. *Br. J. Pharmacol.* **11:** 379.

Woolnough, J. A. and K. J. Lafferty. 1979. Generation of homogenous population of alloreactive T cells in vitro. *Aust. J. Exp. Biol. Med. Sci.* **57:** 127.

FIGURE 1.

A) Antigenic cell dose response curve. Varying numbers of UV-irradiated P815 were incubated with 2×10^5 C57BL/6 anti-BALB/c seven day-activated T cells for 5 hours in a final volume of 200µl EMEM containing 10^{-4} M 2-ME. Four replicate supernatants for each data point were assayed for IL3 activity. The data points were fitted using equation (9) with $K = 5 \times 10^4$ and tf = 0.6.

B) T cell dose response curve. Varying numbers of C57BL/6 anti-BALB/c seven day-activated T cells were incubated with 10^6 UV-irradiated P815 for 5 hours in a final volume of 200µl. Each data point is the mean IL3 titre of four replicates. Fitted parameters were $K = 1 \times 10^5$ and tf = 0.5.

C) Combined T cell and P815 cell dose response curve. Equal numbers of UV-irradiated P815 and C57BL/6 anti-BALB/c seven day-activated T cells were incubated at different total cell numbers in 200µl medium for 5 hours. Fitted parameters were $K = 1 \times 10^5$ and tf = 0.4.

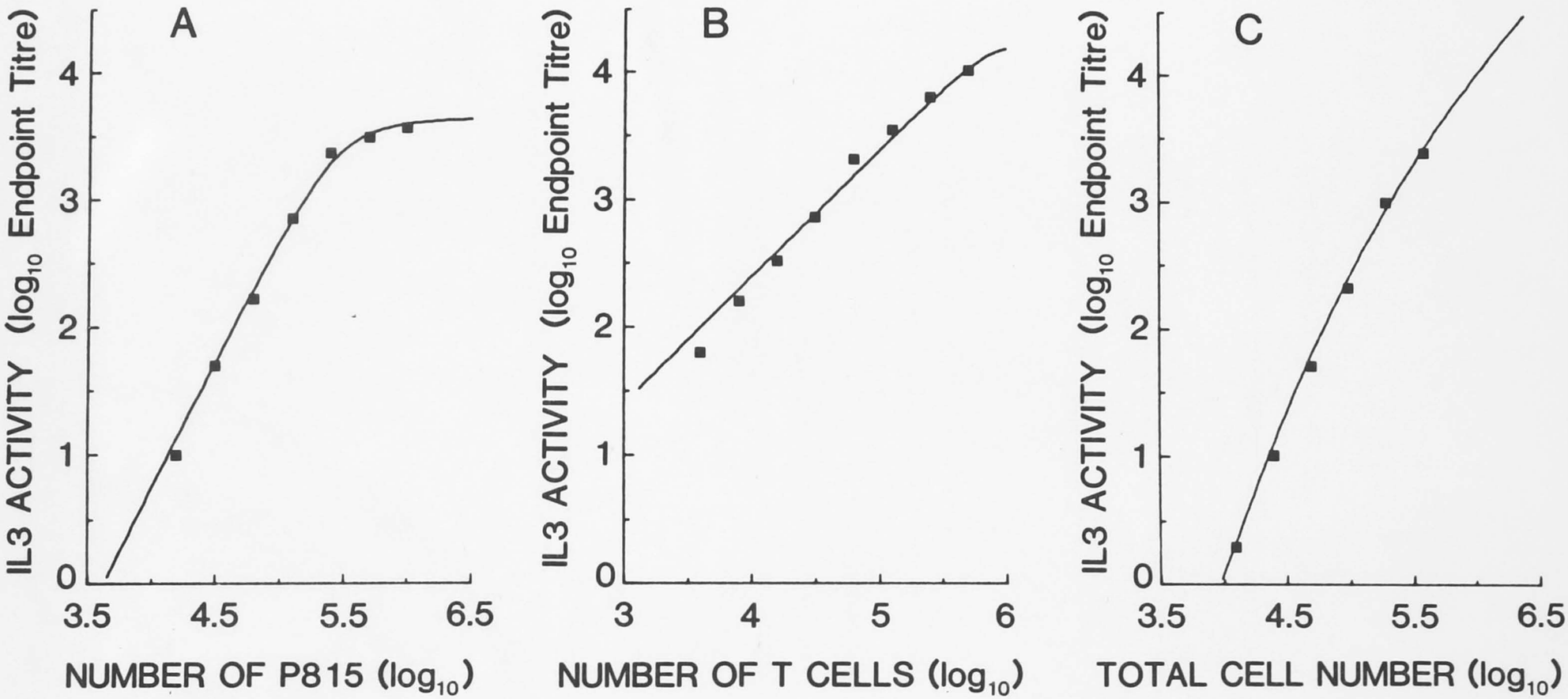
A
B
C
IL3 ACTIVITY (log10 Endpoint Titre)
0
1
2
3
4
3.5
4.5
5.5
6.5
3
4
5
6
NUMBER OF P815 (log10)
NUMBER OF T CELLS (log10)
TOTAL CELL NUMBER (log10)

FIGURE 2.

A) Simulated family of antigenic cell dose response curves with T cell number equal to 10^5, $10^{4.5}$, 10^4 and $10^{3.5}$, using equation (9) with K = 8 x 10^4 and tf = 0.5.

B) Family of experimental P815 dose response curves. Varying numbers of UV-irradiated P815 were incubated with (from top to bottom) 10^5, $10^{4.5}$, 10^4 and $10^{3.5}$, C57BL/6 anti-BALB/c activated T cells in a fixed volume of 200µl. Fitted parameters were K = 5 x 10^4 and tf = 0.25.

C) Family of experimental P815 dose response curves. Same as (b) using T cell numbers (top to bottom) $10^{4.7}$, $10^{4.2}$ and $10^{3.7}$. The data points were fitted using equation (9) with K = 9 x 10^4 and tf = 0.75.

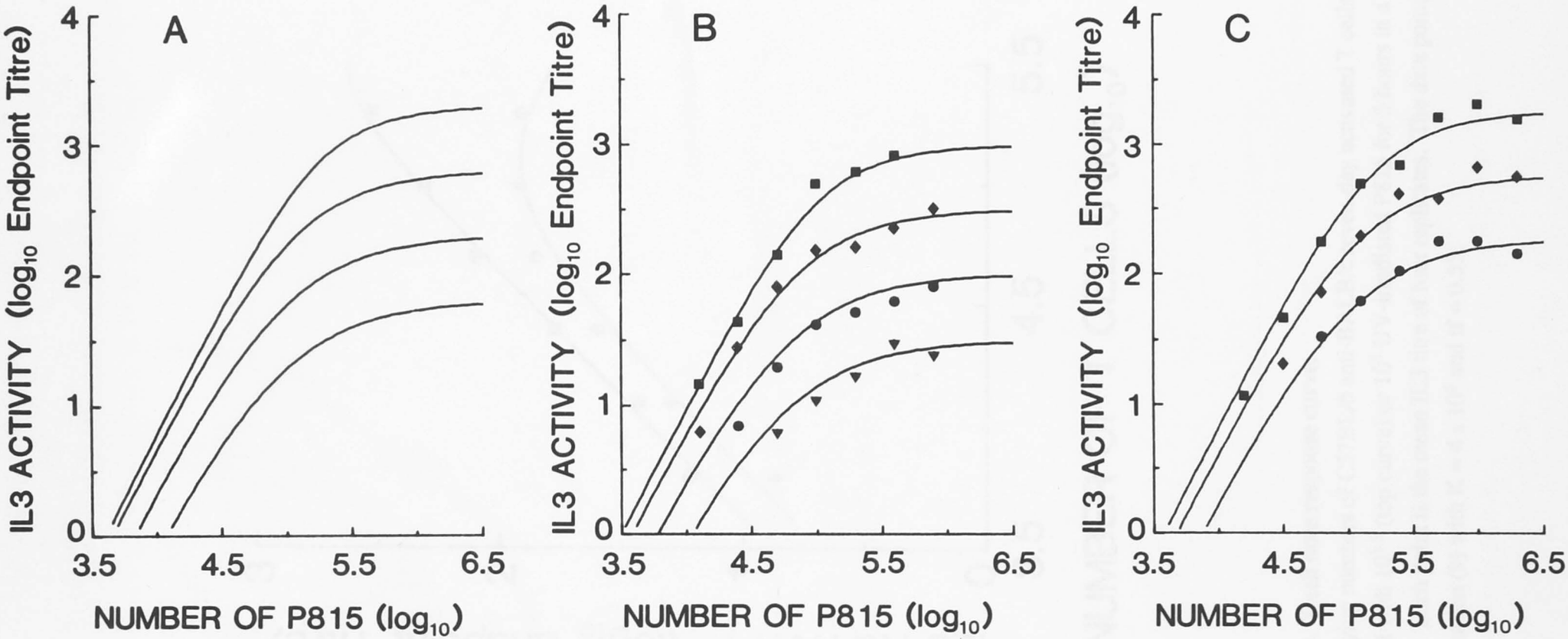
A
B
C
IL3 ACTIVITY (log10 Endpoint Titre)
NUMBER OF P815 (log10)
0
1
2
3
4
3.5
4.5
5.5
6.5

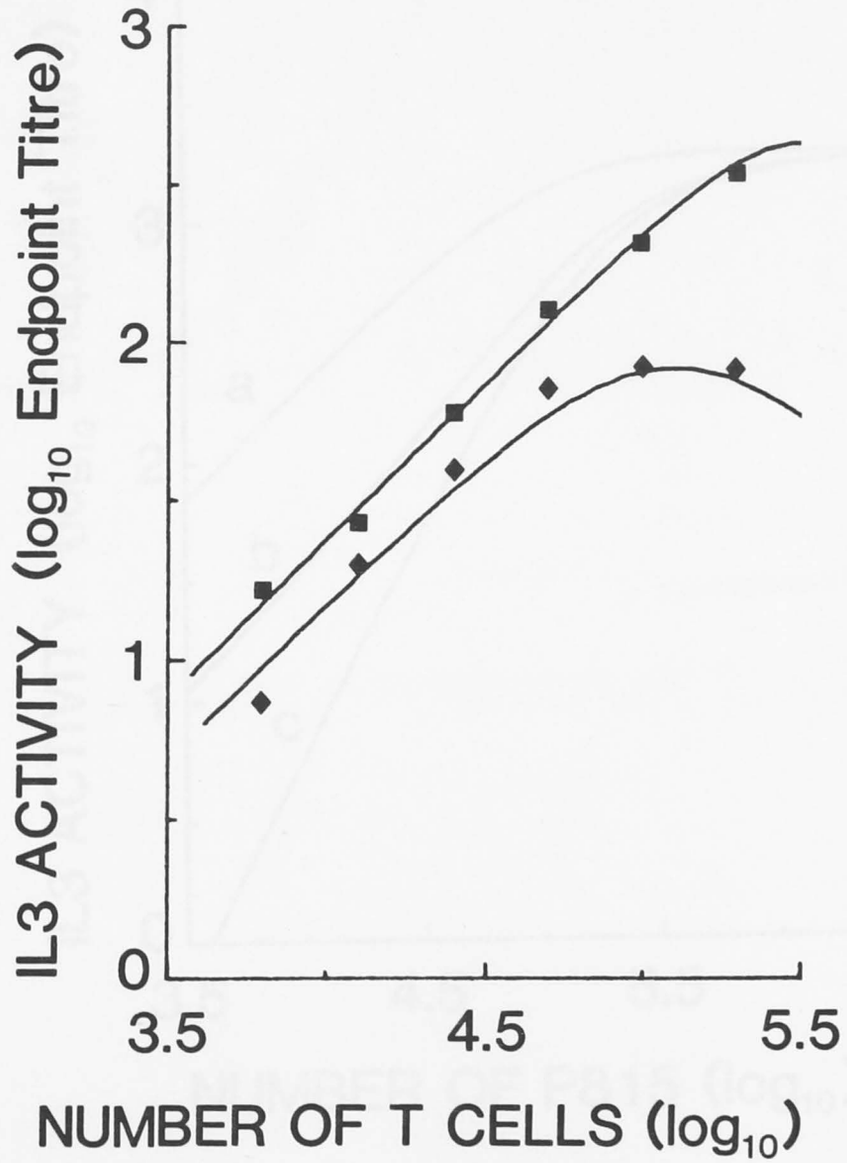

FIGURE 3. T cell dose response curve.

Varying numbers of C57BL/6 anti-BALB/c seven-day activated T cells were incubated with $10^{5.5}$ (top curve) or 10^5 UV-irradiated P815 for 5 hours in a final volume of 200µl. Each point is the mean IL3 titre of four replicates. The data points were fitted using equation (9) with $K = 4 \times 10^4$ and tf = 0.55.

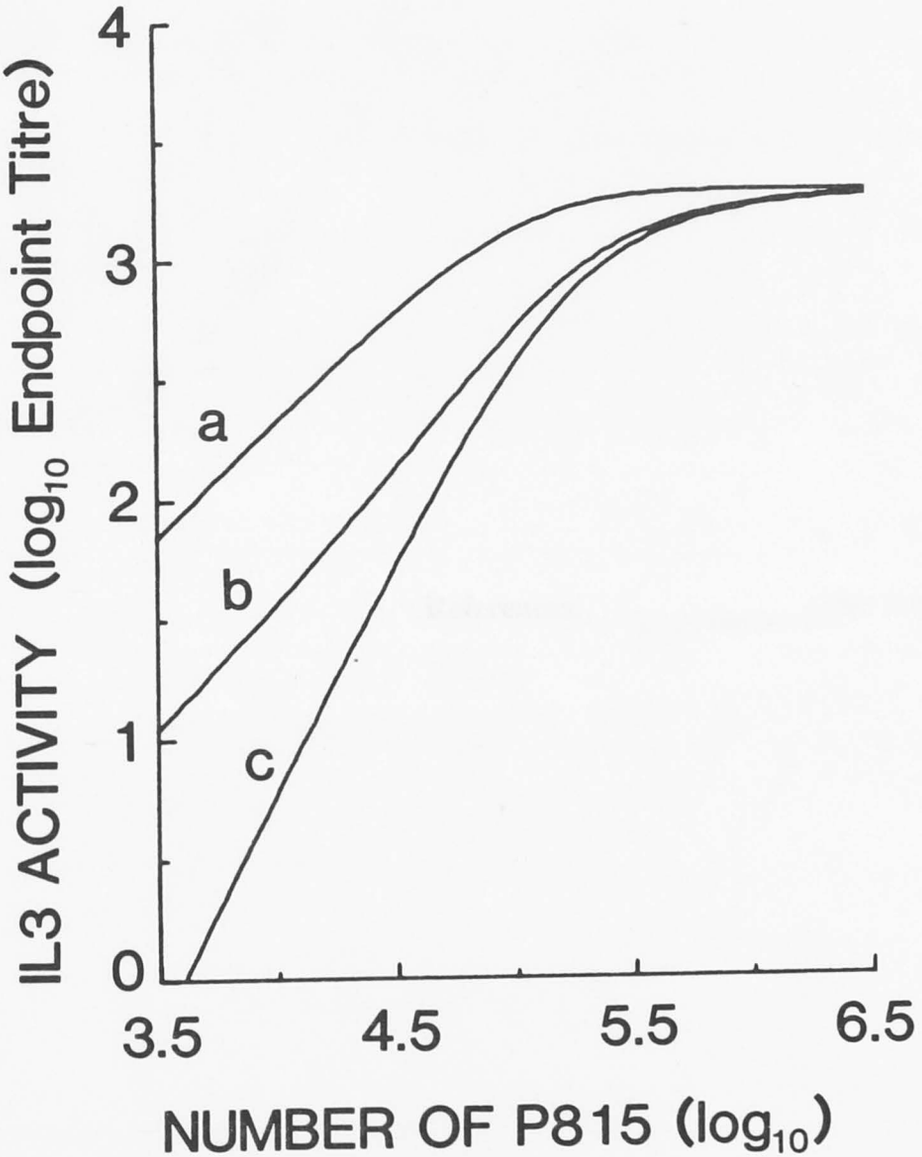

FIGURE 4. Simulated antigenic cell dose response curve with T cell number equal to 10^5, $K = 8 \times 10^4$ and tf = 0.5.

Curve (a) represents the response when T cells release IL3 following binding to 1 or 2 target cells. Curve (b) is obtained if 15% of reactive T cells are capable of triggering following binding to only 1 target cell and the other 85% of cells are triggered only after binding to two target cells. Curve (c) is generated if all T cells must bind at least 2 target cells before triggering IL3 release.

References.

Adam, A., Ernst, M. and Seher, J.-P. (1979). Regulation of passive membrane permeability for potassium ions by cell density of 3T3 and SV40-3T3 cells. Exp. Cell Res., 120, 127-139.

Adrian, R. H. (1975). Conduction velocity and gating current in the squid giant axon. Proc. R. Soc. Lond. B., 189, 81-86.

Adrian, R. H., Chandler, W. K. and Hodgkin, A. L. (1970). Slow changes in potassium permeability in skeletal muscles. J. Physiol., 208, 645-668.

Aiton, J.F. and Pitman, R.M. (1975). Measurement of membrane potential in HeLa cells. J. Physiol. 251, 9P-10P.

Aldrich, R. W. (1981) Inactivation of voltage-gated delayed potassium current in molluscan neurons. Biophys. J., 36, 519-532.

Aldrich, R. W., Corey, D. P. and Stevens, C. F. (1983) A reinterpretation of mammalian sodium channel gating based on single channel recording. Nature, 306, 436-441.

Alkon, D. L. (1984). Calcium-mediated reduction of ionic currents: a biophysical memory trace. Science, 226,1037-1045.

Alkon, D. L., Lederhendler, I. and Shoukimas, J. J. (1982). Primary changes of membrane currents during retention of associative learning. Science, 215, 693-695.

Alkon, D. L., Sakahibara, M., Forman, R., Harrigan, J., Lederhendler, I. and Farley, J. (1985). Reduction of two voltage-dependent K^+ currents mediates retention of a learned association. Behav. Neural Biol., 44, 278-300.

Alonso, M. A. and Weissman, S. M. (1987). cDNA cloning and sequence of MAL, a hydrophobic protein associated with human T-cell differentiation. Proc. Natl. Acad. Sci., 84, 1997-2001.

Almers, W. and Stirling, C. (1984). Distribution of transport proteins over animal cell membranes. J. Mem. Biol., 77, 169-186.

Anderson, D. J. and Blobel, G. (1983). Molecular events in the synthesis and assembly of a nicotinic acetylcholine receptor. Cold Spring Harbor Symp. Quant. Biol., 48, 125-134.

Asselbergs, F. A. M., Van Venrooij, W. J. and Bloemendal, H. (1979). Messenger RNA competition in living *Xenopus* oocytes. Eur. J. Biochem., 94, 249-254.

Atkinson, M. M., Anderson, S. K. and Sheridan, J. D. (1986). Modification of gap junctions in cells transformed by a temperature-sensitive mutant of Rous sarcoma virus. J. Mem. Biol., 91, 53-64.

Aviv, H. and Leder, P. (1972). Purification of biologically active globin messenger RNA by chromatography on oligothymidylic acid-cellulose. Proc. Natl. Acad. Sci., 69, 1408-1412.

Axelsson, J. and Thesleff, S. (1959). A study of supersensitivity in denervated mammalian muscle. J. Physiol., 147, 178-193.

Azarnia, R. and Loewenstein, W.R. (1977). Intercellular communication and tissue growth: VIII. A genetic analysis of junctional communication and cancerous growth. J. Mem. Biol., 34, 1-28.

Baccaglini, P. I. and Spitzer, N. C. (1977). Developmental changes in the inward current

of the action potential of Rohon-Beard neurones. J. Physiol., 271, 93-117.

Bader, C. R., Bertrand, D., Dupin, E. and Kato, A. C. (1983). Development of electrical properties in cultured avian neural crest. Nature, 305, 808-810.

Bader, C. R., Bertrand, D. and Dupin, E. (1985a). Voltage-dependent potassium currents in developing neurones from quail mesencephalic neural crest. J. Physiol., 366, 129-151.

Bader, C. R., Bernheim, L., Bertrand, D. and Dupin, E. (1985b). Study of neuronal potassium current in different culture conditions. J. Physiol. (Paris), 80, 262-267.

Bailey, C. H. and Chen, M. (1983). Morphological basis of long-term habituation and sensitization in *Aplysia*. Science, 220, 89-91.

Baltimore, D., Rosenberg, N. and Witte, O. N. (1979). Transformation of immature lymphoid cells by Abelson murine leukemia virus. Immunol. Rev., 48, 3-21.

Barish, M. E. (1985). A model of inward and outward membrane currents in cultured embryonic amphibian spinal neurons and reconstruction of the action potential. J. Physiol. (Paris), 80, 298-306.

Barish, M. E. (1986). Differentiation of voltage-gated potassium current and modulation of excitability in cultured amphibian spinal neurones. J. Physiol., 375, 229-250.

Barnard, E. A., Miledi, R. and Sumikawa, K. (1982). Translation of exogenous messenger RNA coding for nicotinic acetylcholine receptors produces functional receptors in *Xenopus* oocytes. Proc. Natl. Acad. Sci., 215, 241-246.

Bar-Sagi, D. and Prives, J. (1983). Tunicamycin inhibits the expression of surface Na^+ channels in cultured muscle cells. J. Cell. Physiol., 114, 77-81.

Barth, L. G. and Barth, L. J. (1959). Differentiation of cells of the *Rana pipiens* gastrula in unconditioned medium. J. Embryol. exp. Morph., 7, 210-222.

Beam, K. G., Knudson, C. M. and Powell, J. A. (1986). A lethal mutation in mice eliminates the slow calcium current in skeletal muscle cells. Nature, 320, 168-170.

Belardetti, F., Schacher, S., Kandel, E. R. and Siegelbaum, S. A. (1986). The growth cones of *Apysia* sensory neurons: Modulation by serotonin of action potential duration and single potassium channel currents. Proc. Natl. Acad. Sci., 83, 7094-7098.

Berridge, M. J. (1984). Inositol trisphosphate and diacylglycerol as second messengers. Biochem. J., 220, 345-360.

Bevan, S., Chiu, S. Y., Gray, P. T. A. and Ritchie, J. M. (1985). The presence of voltage-gated sodium, potassium and chloride channels in rat cultured astrocytes. Proc. R. Soc. Lond. B, 225, 299-313.

Biggs, M. J. and Johnson, E. S. (1980). Electrically-evoked release of [^{3}H]-histamine from the guinea-pig hypothalamus. Br. J. Pharmacol.. 70, 555-560.

Birnbaum, M., Reis, M. A. and Shainberg, A. (1980). Role of calcium in the regulation of acetylcholine receptor synthesis in cultured muscle cells. Pflugers Arch., 385, 37-43.

Black, I. B., Adler, J. E., Dreyfus, C. F., Jonakait, G. M., Katz, D. M., LaGamma, E. F. and Markey, K. M. (1984). Neurotransmitter plasticity at the molecular level. Science, 225, 1266-1270.

Blair, L. A. C. (1983). The timing of protein synthesis required for the development of the sodium action potential in embryonic spinal neurons. J. Neurosci., 3, 1430-1436.

Blair, L. A. C. and Dionne, V. E. (1985). Developmental acquisition of Ca^{2+}-sensitivity by K^+ channels in spinal neurones. Nature, 315, 329-331.

Blatz., A. L. and Magleby, K. L. (1983). Single voltage-dependent chloride-selective channels of large conductance in cultured rat muscle. Biophys. J., 43, 237-241.

Blomgren, H. and Andersson, B. (1971) Characteristics of the immunocompetent cells in the mouse thymus: cell population changes during cortisone-induced atrophy and subsequent regeneration. Cell. Immunol., 1, 545-560.

Boulter, J., Luyten, W., Evans, K., Mason, P., Ballivet, M., Goldman, D., Stengelin, S., Martin, G., Heinemann, S. and Patrick, J. (1985). Isolation of a clone coding for the α-subunit of a mouse acetylcholine receptor. J. Neurosci., 5, 2545-2552.

Boulter, J., Evans, K., Goldman, D., Martin, G., Treco, D., Heinemann, S. and Patrick, J. (1986). Isolation of a cDNA clone coding for a possible neural nicotinic acetylcholine receptor α-subunit. Nature, 319, 368-374.

Bower, G. H. and Hilgard, E. R. (1981). Theories of learning. Prentice-Hall Inc., New Jersey.

Boynton, A. L., McKeehan, W. L., and Whitfield, J. F. (1982). (eds.) Ions, Cell Proliferation and Cancer. Academic Press, N. Y.

Breer, H., Kleene, R. and Hinz, G. (1985). Molecular forms and subunit structure of the acetylcholine receptor in the central nervous system of insects. J. Neurosci., 5, 3386-3392.

Bregestovski, P., Redkozubov, A. and Alexeev, A. (1986) Elevation of intracellular calcium reduces voltage-dependent potassium conductance in human T cells. Nature, 319, 776-778.

Brenner, H. R. and Sakmann, B. (1983). Neurotrophic control of channel properties at neuromuscular synapses of rat muscle. J. Physiol., 337, 159-171.

Brenner, H. R., Meier, Th. and Widmer, B. (1983). Early action of nerve determines motor endplate differentiation in rat muscle. Nature, 305, 536-537.

Brisson, A. and Unwin, P. N. T. (1985). Quaternary structure of the acetylcholine receptor. Nature, 315, 474-477.

Brown, E., Kendall, D. A. and Nahorski, S. R. (1984). Inositol phopholipid hydrolysis in rat cerebral cortical slices: I. Receptor characterisation. J. Neurochem., 42, 1379-1387.

Bruce, J., Symington, F. W., McKearn, T. J. and Sprent, J. (1981) A monoclonal antibody discriminating between subsets of T and B cells. J. Immunol., 127, 2496-2501.

Brockes, J. P. and Hall, Z. W. (1975). Acetylcholine receptors in normal and denervated rate diaphragm muscle. II. Comparison of junctional and extrajunctional receptors. Biochemistry, 14, 2100-2106.

Bursztajn, S. and Fischbach, G. D. (1984). Evidence that coated vesicles transport acetylcholine receptors to the surface membrane of chick myotubes. J. Cell Biol., 98, 498-506.

Byrne, J. H. (1980). Quantitative aspects of ionic conductance mechanisms contributing to firing pattern of motor cells mediating inking behavior in *Aplysia californica*. J. Neurophysiol., 43, 651-668.

Cahalan, M. D., Chandy, K. G., Decoursey, T. E. and Gupta, S. (1985) A voltage-gated potassium channel in human T lymphocytes. J. Physiol., 358, 197-237.

Campbell, G. LeM., Schachner, M. and Sharrow, S. O. (1977). Isolation of glial cell-enriched and -depleted populations from mouse cerebellum by density gradient centrifugation and electronic cell sorting. Brain Res., 127, 69-86.

Cassell, J. F. and McLachlan, E. M. (1986). The effect of a transient outward current (I_A) on synaptic potentials in sympathetic ganglion cells of the guinea-pig. J. Physiol., 374, 273-288.

Catterall, W. A. (1984). The molecular basis of neuronal excitability. Science, 223, 653-661.

Ceredig, R. (1986) Major histocompatibility-restricted cytolytic T-lymphocyte precursors from the thymus of in vivo primed mice; increased frequency and resistance to anti-Lyt-2 antibody inhibition. Curr. Top. Micro. Immunol., 126, 27-33.

Ceredig, R., Dialynas, D. P., Fitch, F. W. and MacDonald, H. R. (1983) Precursors of T cell growth factor producing cells in the thymus. J. Exp. Med., 158, 1654-1671.

Ceredig, R., Lowenthal, J. W., Nabholz, M. and MacDonald, H. R. (1985) Expression of interleukin-2 receptors as a differentiation marker on intrathymic stem cells. Nature, 314, 98-100.

Ceredig, R. and MacDonald, H. R. (1985) Intrathymic differentiation: some unanswered questions. Surv. Immunol. Res., 4, 87-95.

Chandy, K. G., DeCoursey, T. E., Cahalan, M. D., McLaughlin, C. and Gupta, S. (1984) Voltage-gated potassium channels are required for human T lymphocyte activation. J. Exp. Med., 169, 369-385.

Chang, S. E. and Littlefield, J. W. (1976). Elevated dihydrofolate reductase mRNA levels in methotrexate-resistant BHK cells. Cell, 7, 391-396.

Changeux, J.-P. and Danchin, A. (1976). Selective stabilisation of developing synapses as a mechanism for the specification of neuronal networks. Nature, 264, 705-712.

Changeux, J.-P., Devillers-Thiery, A. and Chemouilli, P. (1984). Acetylcholine receptor: an allosteric protein. Science, 225, 1335-1345.

Chen, T. R. (1977). In situ detection of mycoplasma contamination in cell cultures by fluorescent Hoeschst 33258 stain. Expl. Cell Res., 104, 255-268.

Chirgwin, J. M., Pryzbyla, A. E., MacDonald, R. J. and Rutter, W. J. (1979). Isolation of biologically active ribonucleic acid from sources enriched in ribonuclease. Biochemistry, 18, 5294-5299.

Chiu, S. Y., Schrager, P. and Ritchie, J. M. (1984). Neuronal-type Na^+ and K^+ channels in rabbit cultured Schwann cells. Nature, 311, 156-157.

Clarke, P. B. S., Schwartz, R. D., Paul, S. M., Pert, C. B. and Pert, A. (1985). Nicotinic binding in rat brain: Autoradiographic comparison of [^{3}H]acetylcholine, [^{3}H] nicotine and [^{125}I]-α-bungarotoxin. J. Neurosci., 5, 1307-1315.

Claudio, T., Ballivet, M., Patrick, J. and Heineman, S. (1983) Nucleotide and deduced amino acid sequences of *Torpedo californica* acetylcholine receptor γ subunit. Proc. Natl. Acad. Sci., 80,1111-1115.

Cohen, S. A. and Fischbach, G. D. (1973). Regulation of muscle acetylcholine sensitivity by muscle activity in cell culture. Science, 181, 76-78.

Colquhoun, D. and Hawkes, A. G. (1981). On the stochastic properties of single ion channels. Proc. R. Soc. B, 211, 205-235.

Colquhoun, D. and Sakmann, B. (1981). Fluctuations in the microsecond time range of the current through single acetylcholine receptor ion channels. Nature, 294, 464-466.

Cone, C. D. and Tongier, M. (1973). Contact inhibition of division: involvement of the electrical transmembrane potential. J. Cell. Physiol., 82, 373-386.

Connor, J. A. and Stevens, C. F. (1971). Voltage clamp studies of a transient outward membrane current in gastropod neural somata. J. Physiol., 213, 21-30.

Conti-Tronconi, B. M., Gotti, C. M., Hunkapiller, M. W. and Raftery, M. A. (1982). Mammalian muscle acetylcholine receptor: a supramolecular structure formed by four related proteins. Science, 218, 1227-1229.

Cook, J. S., Vaughan, G. L., Proctor, W. R. and Brake, E. T. (1975). Interaction of two mechanisms regulating alkali cations in HeLa cells. J. Cell. Physiol., 86, 59-70.

Corsaro, C. M. and Migeon, B. R. (1977). Comparison of contact-mediated communication in normal and transformed human cells in culture. Proc. Natl. Acad. Sci., 74, 4476-4480.

Cox, R. P., Krauss, M. R., Balis, M. E. and Dancis, J. (1972). Communication between normal and enzyme deficient cells in tissue culture. Exp. Cell Res., 74, 251-268

Craik, F. I. M. and Lockhart, R. S. (1972). Levels of processing: A framework for memory research. J. verb. Learn. verb. Behav., 11, 671-684.

Crick, F. (1984). Memory and molecular turnover. Nature, 312, 101.

Crow, T. (1985a). Conditioned modification of phototactic behavior in *Hermissenda*. I. Analysis of light intensity. J. Neurosci., 5, 209-214.

Crow, T. (1985b). Conditioned modification of phototactic behavior in *Hermissenda*. II. Differential adaptation of B-photoreceptors. J. Neurosci., 5, 215-223.

Crow, T. J. and Alkon, D. L. (1980). Associative behavioral modification in *Hermissenda*: Cellular correlates. Science, 209, 412-414.

Curtis, B. M. and Catterall, W. A. (1986). Reconstitution of the voltage-sensitive calcium channel purified from skeletal muscle transverse tubules. Biochemistry, 25, 3077-3083.

Dascal, N. and Landau, E. M. (1980). Types of muscarinic response in *Xenopus* oocytes. Life Sci., 27, 1423-1428.

Daum, P. R., Downes, C. P. and Young, J. M. (1984). Histamine stimulation of inositol 1-phosphate accumulation in lithium-treated slices from regions of guinea pig brain. J. Neurochem., 43, 25-32.

Daut, J. (1973). Modulation of the excitatory synaptic response by fast transient K^+ current in snail neurones. Nature, 246, 193-196.

Davis, H. P. and Squire, L. R. (1984). Protein synthesis and memory: a review. Psychol. Bull., 96, 518-559.

Davis, M. M., Chien, Y.-H., Gascoigne, N. R. J. and Hedrick, S. M. (1984). A murine T cell receptor gene complex: isolation, structure and rearrangement. Immunol. Rev., 81, 235-258.

DeCoursey, T. E., Chandy, K. G., Gupta, S. and Cahalan, M. D. (1984) Voltage-gated K^+ channels in human T lymphocytes: a role in mitogenesis? Nature, 307, 465-468.

DeCoursey, T. E., Chandy, K. G., Gupta, S. and Cahalan, M. D. (1985) Voltage-dependent ion channels in T-lymphocytes. J. Neuroimmunol., 10, 71-95.

Der, C. J. and Stanbridge, E. J. (1980). Alterations in the extracellular matrix organization associated with the reexpression of tumorigenicity in human cell hybrids. Int. J. Cancer, 26, 451-459.

Deutsch, C., Krause, D. and Lee, S. C. (1986) Voltage-gated potassium conductance in human T lymphocytes stimulated with phorbol ester. J. Physiol., 372, 405-423.

De Vitry, F. Camier, M., Czernichow, P., Benda, Ph., Cohen, P. and Tixier-Vidal, A. (1974). Establishment of a clone of mouse hypothalamic neurosecretory cells synthesizing neurophysin and vasopressin. Proc. Natl. Acad. Sci., 71, 3575-3579.

Dialynas, D. P., Quan, Z. S., Wall, K. A., Pierres, A., Quintas, J., Loken, M. R., Pierres, M. and Fitch, F. W. (1983) Characterization of the murine T cell surface molecule, designated L3T4, identified by monoclonal antibody GK1.5: similarity of L3T4 to the human Leu-3/T4 molecule. J. Immunol., 131, 2445-2451.

Downes, C. P. and Michell, R. H. (1985). Inositol phospholipid breakdown as a receptor-controlled generator of second messengers. In, Molecular Mechanisms of Transmembrane Signalling, ed. P. Cohen and M. D. Houslay, pp. 3-56., Amsterdam, Elsevier Science Publishers.

Drachman, D. B. and Witzke, F. (1972). Trophic regulation of acetylcholine sensitivity of muscle: effect of electrical stimulation. Science, 176, 514-516.

Dubinsky, J. M. and Oxford, G. S. (1984). Ionic currents in two strains of rat anterior pituitary tumor cells. J. Gen. Physiol., 83, 309-339.

Duggan, A. W., Hall, J. G. and Lee, C Y. (1976). Alpha-bungarotoxin, cobra neurotoxin and excitation of Renshaw cells by acetylcholine. Brain Res., 107, 166-170.

Dumont, J. N. (1972). Oogenesis in *Xenopus laevis* (Daudin). I. Stages of oocyte development in laboratory maintained animals. J. Morph., 136, 153-180.

Edwards, C. (1979). The effects of innervation on the properties of acetylcholine receptors in muscle. Neuroscience, 4, 565-584.

Eiden, L. E., Giraud, P., Dave, J. R., Hotchkiss, A. J. and Affolter, H.-U. (1984). Nicotinic receptor stimulation activates enkephalin release and biosynthesis in adrenal chromaffin cells. Nature, 312, 661-663.

Fathman, C. G. and Frelinger, J. G. (1983). T-lymphocyte clones. Ann. Rev. Immunol., 1, 633-655.

Fambrough, D. M. (1970). Acetylcholine sensitivity of muscle fiber membranes: mechansim of regulation by motoneurons. Science, 168, 372-373.

Fambrough, D. M. (1974). Revised estimates of extrajunctional receptor densitiy in denervated rat diaphragm. J. Gen. Physiol., 64, 468-472.

Fambrough, D. M. (1979). Control of acetylcholine receptors in skeletal muscle. Physiol. Rev., 59, 165-227.

Fambrough, D. M. and Hartzell, H. C. (1972). Acetylcholine recpetors: number and distribution at neuromuscular junctions in rat diaphragm. Science, 176, 189-191.

Farley, J. and Alkon, D. L. (1985). Cellular mechanisms of learning, memory, and information storage. Ann. Rev. Psychol., 36, 419-494.

Farrar, J. J., Fuller-Farrar, J., Simon, P. L., Hilfiker, M. L., Stadler, B. M. and Farrar, W. L. (1980) Thymoma production of T cell growth factor (Interleukin 2). J. Immunol., 125, 2555-2558.

Fenwick, E. M., Marty, A. and Neher, E. (1982). A patch-clamp study of bovine chromaffin cells and of their sensitivity to acetylcholine. J. Physiol., 331, 577-597.

Fertuck, H. C. and Salpeter, M. P. (1974). Localization of acetylcholine receptor by ^{125}I-labelled α-bungarotoxin binding at mouse motor endplates. Proc. Natl. Acad. Sci., 71, 1376-1378.

Finer-Moore, J. and Stroud, R. M. (1984). Amphipathic analysis and possible formation of the ion channel in an acetylcholine receptor. Proc. Natl. Acad. Sci., 81, 155-159.

Fink, P. J., Bevan, M. J. and Weissman, I. L. (1984) Thymic cytotoxic T lymphocytes are primed in vivo to minor histocompatibility antigens. J. Exp. Med., 159, 436-451.

Finkel, A. S. and Redman, S. (1984). Theory and operation of a single microelectrode voltage clamp. J. Neurosci. Meth., 11, 101-127.

Fischbach, G. D. and Schuetze, S. M. (1980). A post-natal decrease in acetylcholine channel open time at rat end-plates. J. Physiol., 303, 125-137.

Forrest, J. W., Mills, R. G., Bray, J. J. and Hubbard, J. I. (1981). Calcium-dependent regulation of the membrane potential and extrajunctional receptors of rat skeletal muscle. Neuroscience, 6, 741-749.

Frank, E., Gautvik, K. and Sommerschild, H. (1975). Cholinergic receptors at denervated mammalian motor end-plates. Acta Physiol. Scand., 95, 66-76.

Fukushima, Y., Hagiwara, S. and Henkart, M. (1984) Potassium current in clonal cytotoxic T lymphocytes from the mouse. J. Physiol., 351, 645-656.

Fung, M. C., Hapel, A. J., Ymer, S., Cohen, D. R., Johnson, R. M., Campbell, H. D. and Young, I. G. (1984). Molecular cloning of cDNA for murine interleukin-3. Nature, 307, 233-237.

Gage, P. W. and McKinnon, D. (1985). Effects of pentobarbitone on acetylcholine-activated channels in mammalian muscle. Br. J. Pharmac., 85, 229-235.

Gajtkowski, G. A., Norris, D. B., Rising, T. J. and Wood, T. P. (1983). Specific binding of ^{3}H-tiotidine to histamine H_2 receptors in guinea pig cerbral cortex. Nature, 304, 65-67.

Geller, H. M., Springfield, S. A. and Tiberio, A. R. (1984). Electrophysiological actions of histamine. Can. J. Physiol. Pharmacol., 62, 715-719.

Gillis, S., Ferm, M. M., Ou, W. and Smith, K. A. (1978) T cell growth factor: parameters of production and a quantitative microassay for activity. J. Immunol., 120, 2027-2032.

Gilula, N. B. (1974). Junctions between cells. In, Cell Communication, (ed.) Cox, R. P. John Wiley and Sons Inc., N. Y., pp. 1-29.

Giotta, G. J., Heitzmann, J. and Cohn, M. (1980). Properties of two temperature-sensitive Rous sarcoma virus transformed cerebellar cell lines. Brain Res., 202, 445-458.

Goelet, P., Castellucci, V. F., Schacher, S. and Kandel, E. R. (1986). The long and the short of long-term memory- a molecular framework. Nature, 322, 419-422.

Goldman, D. E. (1943). Potential, impedance and rectification in membranes. J. Gen. Physiol. 27, 37-60.

Goldman, D., Boulter, J., Heinemann, S. and Patrick, J. (1985). Muscle denervation increases the levels of two mRNAs coding for the acetylcholine receptor α-subunit. J. Neurosci., 5, 2553-2558.

Goldman, D., Deneris, E., Kochar, A., Patrick, J. and Heinemann, S. (in press). Members of a nicotinic acetylcholine receptor gene family are expressed in different regions of the mammalian central nervous system.

Goodman, C. S. and Spitzer, N. C. (1981). The development of electrical properties of identified neurones in grasshopper embryos. J. Physiol., 313, 385-403.

Gray, P. T. A., Bevan, S. and Ritchie, J. M. (1984). High conductance anion-selective channels in rat cultured Schwann cells. Proc. R. Soc. Lond. B., 221, 395-409.

Green, J. P. (1964). Histamine and the nervous system. Fed. Proc., 23, 1095-1102.

Greene, L. A., Shain, W., Chalazonitis, A., Breakfield, X., Minna, J., Coon, H. G. and Nirenberg, M. (1975). Neuronal properties of hybrid neuroblastoma X sympathetic ganglion cells. Proc. Natl. Acad. Sci., 72, 4923-4927.

Greenberg, M. E., Ziff, E. B. and Greene, L. A. (1986). Stimulation of neuronal acetylcholine receptors induces rapid gene transcription. Science, 234, 80-83.

Gunderson, C. B., Miledi, R. and Parker, I. (1983). Serotonin receptors induced by exogenous messenger RNA in *Xenopus* oocytes. Proc. R. Soc. Lond. B., 219, 103-109.

Gunderson, C. B., Miledi, R. and Parker, I. (1984). Glutamate and kainate receptors induced by rat brain messenger RNA in *Xenopus* oocytes. Proc. R. Soc. Lond. B., 221, 127-143.

Guy, H. R. (1984). A structural model of the acetylcholine receptor channel based on partition energy and helix packing calculations. Biophys. J., 45, 249-261.

Haas, H. L. (1981). Histamine hyperpolarizes hippocampal neurones in vitro. Neurosci. Lett., 22, 75-81.

Haas, H. L. (1984). Histamine potentiates neuronal excitation by blocking a calcium-dependent potassium conductance. Agents Actions, 14, 534-537.

Haas, H. L. and Konnerth, A. (1983). Histamine and noradrenaline decrease calcium-activated potassium conductance in hippocampal pyramidal cells. Nature, 302, 432-434.

Haga, N., Forte, M., Ramanathan, R., Hennessey, T., Takahashi, M. and Kung, C. (1984). Characterization and purification of a soluble protein controlling Ca-channel activity in *Paramecium*. Cell, 39, 71-78.

Hagiwara, S. (1983). Membrane Potential-Dependent Ion Channels in Cell Membrane. Raven Press, New York.

Hagiwara, S., Kusano, K. and Saito, N. (1961). Membrane changes of *Onchidium* nerve cell in potassium-rich media. J. Physiol., 219, 217-232.

Halliwell, J. V., Othman, I. B., Pelchen-Matthews, A. and Dolly, J. O. (1986). Central action of dendrotoxin: Selective reduction of a transient K conductance in hippocampus and binding to localized acceptors. Proc. Natl. Acad. Sci., 83, 493-497.

Hamill, O. P., Marty, A., Neher, E., Sakman, B. and Sigworth, F. J. (1981). Improved patch-clamp technique for high-resolution current recording from cells and cell-free membrane patches. Pflugers Arch, 391, 85-100.

Hamill, O. P. and Sakmann, B. (1981). Multiple conductance states of single acetylcholine receptor channels in embryonic muscle cells. Nature, 294, 462-464.

Hanke, W. and Breer, H. (1986). Channel properties of an insect neuronal acetylcholine receptor protein reconstituted in planar lipid bilayers. Nature, 321, 171-174.

Hanley-Hyde, J. M. and Lynch R. G. (1986). The physiology of B cells as studied with tumor models. Ann. Rev. Immunol., 4, 621-649.

Harris, J. B. and Marshall, M. W. (1973). Tetrodotoxin-resistant action potentials in newborn rat muscle. Nature, 243, 191-192.

Hebb, D. O. (1949). The Organization of Behavior. John Wiley and Sons Inc., New York.

Henderson, P. (1907). Zur Thermodynamik der Flussigkeitsketten. Z. Phys. Chem., 59, 118-127.

Hill, S. J., Emson, P. C. and Young, J. M. (1978). The binding of [^{3}H]mepyramine to histamine H_1 receptors in guinea-pig brain. J. Neurochem., 31, 997-1004.

Hille, B. (1984) Ionic channels of excitable membranes. Sinauer Assoc. Inc., Sunderland, MA, USA.

Hodgkin, A. (1975). The optimum density of sodium channels in an unmyelinated nerve. Phil. Trans. R. Soc. Lond. B., 270, 297-300.

Hodgkin, A. L. and Huxley, A. F. (1952) A quantitative description of membrane current and its application to conduction and excitation in nerve. J. Physiol., 117, 500-544.

Hodgkin, A. L. and Katz, B. (1949). The effect of sodium ions on the electrical activity of the giant axon of the squid. J. Physiol., 108, 37-77.

Hosoi, S. and Slayman, C. L. (1985). Membrane voltage, resistance and channel switching in isolated mouse fibroblasts (L cells): a patch-electrode analysis. J. Physiol., 367, 267-290.

Hulser, D. F. (1971). Electrophysiologische untersuchungen an saugerzellkulturen: Der einfluss von bicarbonat und pH auf das membranpotential. Pflugers Arch., 325,

174-187.

Imboden, J., Weyand, C. and Goronzy, J. (1987). Antigen recognition by a human T cell clone leads to increases in inositol trisphosphate. J. Immunol., 138, 1322-1324.

Ince, C., Leijh, P. C. J., Meijer, J., Van Bavel, E. and Ypey, D. L. (1984). Oscillatory hyperpolarizations and resting membrane potentials of mouse fibroblast and macrophage cell lines. J. Physiol., 352, 625-635.

Jan, L. Y., Barbel, S., Timpel, L., Laffer, C., Salkoff, L., O'Farrell, P. and Jan, Y. N. (1983). Mutating a gene for a potassium channel by hybrid dysgenesis: An approach to the cloning of the *Shaker* locus in *Drosophila*. Cold Spring Harbor Symp. Quant. Biol., 48, 233-245.

Jan, Y. N., Jan, L. Y. and Dennis, M. J. (1977). Two mutations of synaptic transmission in *Drosophila*. Proc. R. Soc. Lond. B., 198, 87-108.

Jessell, T. M., Siegel, R. E. and Fischbach, G. D. (1979). Induction of acetylcholine receptors on cultured skeletal muscle by a factor extracted from brain and spinal cord. Proc. Natl. Acad. Sci., 76, 5397-5401.

Kandel, E. R. (1976). Cellular Basis of Behavior. W. H. Freeman and Co., San Francisco.

Kandel, E. R., Klein, M., Castellucci, V. F., Schacher, S. and Goelet, P. (1986). Some principles emerging from the study of short- and long-term memory. Neurosci. Res., 3, 498-520.

Katz, B. (1949). Les constantes electriques de la membrane du muscle. Arch. Sci. Physiol., 2, 285-299.

Killion, J. J. (1984). Electrical properties of normal and transformed mammalian cells. Biophys. J., 45, 523-528.

Kistler, J., Stroud, R. M., Klymkowsky, M. W., Lalancette, R. A. and Fairclough, R. H. (1982). Structure and function of an acetylcholine receptor. Biophys. J., 37, 371-383.

Klarsfeld, A. and Changeux, J. P. (1985). Activity regulates the levels of acetylcholine receptor α-subunit mRNA in cultured chicken myotubes. Proc. Natl. Acad. Sci., 82, 4558-4562.

Kley, N., Loeffler, J.-P., Pittius, C. W. and Hollt, V. (1987). Involvement of ion channels in the induction of proenkephaline A gene expression by nicotine and cAMP in bovine chromaffin cells. J. Biol. Chem., 262, 4083-4089.

Kubo, T., Noda, M., Takai, T., Tanabe, T., Kayano, T., Shimizu, S., Tanaka, K., Takahashi, H., Hirose, T., Inayama, S., Kikuno, R., Miyata, T. and Numa, S. (1985). Primary structure of δ subunit precursor of calf muscle acetylcholine receptor deduced from cDNA sequence. Eur. J. Biochem., 149, 5-13.

Kung, C. (1979). Neurobiology and neurogenetics of *Parmecium* behavior. In, Neurogenetics: Genetic Approaches to the Nervous System, (ed.) X. O. Breakefield, Elsevier, New York.

Kusano, K., Miledi, R. and Stinnakre, J. (1977). Acetylcholine receptors in the oocyte membrane. Nature, 270, 739-741.

Kusano, K., Miledi, R. and Stinnakre, J. (1982). Cholinergic and catecholaminergic receptors in the *Xenopus* oocyte membrane. J. Physiol., 328, 143-170.

Land, H., Parada, L. F. and Weinberg, R. A. (1983). Cellular oncogenes and multistep carcinogenesis. Science, 222, 771-778.

Lang, R. A., Metcalf, D., Gough, N. M., Dunn, A. R. and Gonda, T. J. (1985). Expression of a hemopoietic growth factor cDNA in a factor-dependent cell line results in autonomous growth and tumorigenicity. Cell, 43, 531-542.

LaPolla, R. J., Mayne, K. M. and Davidson, N. (1984). Isolation and characterization of a cDNA clone for the complete protein coding region of the δ subunit of the mouse acetylcholine receptor. Proc. Natl. Acad. Sci., 81, 7970-7974.

Lassen, U. V. and Rasmussen, B. E. (1977). Use of microelectrodes for measurement of membrane potentials. In, Transport across Biological Membranes. (eds.) G. Giebisch, D. C. Tosteson and H. H. Ussing., pp. 169-203., Springer Verlag, Heidelberg.

Ledbetter, J. A. and Herzenberg, L. A. (1979) Xenogeneic monoclonal antibodies to mouse lymphoid differentiation antigens. Immunol. Rev., 47, 63-90.

Lederhendler, I. I., Gart, S. and Alkon, D. L. (1986). Classical conditioning of *Hermissenda*: origin of a new response. J. Neurosci., 6, 1325-1331.

Lee, S. C., Sabath, D. E., Deutsch, C. and Prystowski, M. B. (1986) Increased voltage-gated potassium conductance during interleukin 2 stimulated proliferation of a mouse helper T lymphocyte clone. J. Cell Biol., 102, 1200-1208.

Leffert, H. L. (ed.) (1980). Growth Regulation by Ion Fluxes. Ann. N. Y. Acad. Sci., 339.

Lewin, B. Gene Expression: Eucaryotic Chromosomes. vol. 2., John Wiley and Sons, New York. pp. 152.

Linden, D. C. and Fambrough, D. M. (1979). Biosynthesis and degradation of acetylcholine receptors in rat skeletal muscles. Effects of electrical stimulation. Neuroscience, 4, 527-538.

Lisman, J. E. (1985). A mechanism for memory storage insensitive to molecular turnover: a bistable autophosphorylating kinase. Proc. Natl. Acad. Sci., 82, 3055-3057.

Llinas, R. and Sujimori, M. (1979). Calcium conductances in Purkinje cell dendrites: their role in development and integration. Prog. Brain Res., 51, 323-334.

Llinas, R., Steinberg, I. Z. and Walton, K. (1981). Relationship between presynaptic calcium current and postsynaptic potential in squid giant synapse. Biophys. J., 33, 323-352.

Loewenstein, W. R. (1979). Junctional intercellular communication and the control of growth. Biochim. Biophys. Acta, 560, 1-65.

Lomo, T. and Rosenthal, J. (1972). Control of ACh sensitivity by muscle activity in the rat. J. Physiol., 221, 493-513.

Lomo, T. and Slater, C. R. (1980). Control of junctional acetylcholinesterase by neural and muscular influences in the rat. J. Physiol., 303, 191-202.

Lomo, T. and Westgaard, R. H. (1975). Further studies on the control of ACh sensitivity by muscle activity in the rat. J. Physiol., 252, 603-626.

Lomo, T. and Westgaard, R. H. (1976). Control of ACh sensitivity in rat muscle fibres.

Cold Spring Harbor Symp. Quant. Biol., 40, 263-274.

Lotan, I., Dascal, N., Oron, Y., Cohen, S. and Lass, Y. (1985). Adenosine-induced K^+ current in *Xenopus* oocyte and the role of adenosine 3',5'-monophosphate. Mol. Pharmacol., 28, 170-177.

Lynch, F., Chaudhri, G., Allan, J. E., Doherty, P. C. and Ceredig, R. (1987). Expression of Pgp-1 (or Ly24) by subpopulations of mouse thymocytes and activated peripheral T lymphocytes. Eur. J. Immunol., 17, 137-140.

Lynch, G. and Baudry, M. (1984). The biochemistry of memory: a new and specific hypothesis. Science, 224,1057-1063.

MacDonald, H. R. and Nabhoz, M. (1986). T-cell activation. Ann. Rev. Cell Biol., 2, 231-253.

McGaugh, J. L. (1966). Time-dependent processes in memory storage. Science, 153, 1351-1358.

McGaugh, J. L. (1969). Facilitation of memory storage processes. In, The Future of the Brain Sciences. Plenum Press, New York.

McManaman, J. L., Blosser, J. C. and Appel, S. H. (1982). Inhibitors of membrane depolarization regulate acetylcholine receptor synthesis by a calcium-dependent, cyclic nucleotide-independent mechansim. Biochim. Biophys. Acta, 720, 28-35.

Magleby, K. L. and Pallotta, B. S. (1983). Burst kinetics of single calcium-activated potassium channels in cultured rat muscle. J. Physiol., 339, 663-678.

Maniatis, T., Fritsch, E. F. and Sambrook, J. (1982). Molecular Cloning: A Laboratory Manual. Cold Spring Harbor Laboratory, Cold Spring Harbor, New York.

Marr, D. (1969). A theory of cerebellar cortex. J. Physiol., 202, 437-470.

Marshall, L. M. (1985). Presynaptic control of synaptic channel kinetics in sympathetic neurones. Nature, 317, 621-623.

Marshall, L. M. (1986). Different synaptic channel kinetics in sympathetic B and C neurons of the bullfrog. J. Neurosci., 6, 590-593.

Marty, A. and Neher, E. (1983). Tight-seal whole cell recording. In, Single-Channel Recording, (eds.) Sakmann, B. and Neher, E., pp. 107-121. Plenum Press, N. Y.

Maruyama, Y. and Peterson, O. H. (1984). Control of K^+ conductance by cholecystokinin and Ca^{2+} in single pancreatic acinar cells studied by the patch-clamp technique. J. Mem. Biol., 79, 293-300.

Matteson, D. R. and Armstrong, C. M. (1984). Na and Ca channels in a transformed line of anterior pituitary cells. J. Gen. Physiol., 83, 371-394.

Matteson, D. R and Deutsch, C. (1984) K channels in T lymphocytes: a patch clamp study using monoclonal antibody adhesion. Nature, 307, 468-471.

Mayo, K. E., Warren, R. and Palmiter, R. D. (1982). The mouse metallothionein-I gene is transcriptionally regulated by cadmium following transfection into human or mouse cells. Cell, 29, 99-105.

Merlie, J. P. and Lindstrom, J. (1983). Assembly in vivo of mouse muscle acetylcholine receptor: indentification of an α subunit species that may be an assembly intermediate.

Cell, 34, 747-757.

Merlie, J. P. and Sanes, J. R. (1985). Concentration of acetylcholine receptor mRNA in synaptic regions of adult muscle fibres. Nature, 317, 66-68.

Merlie, J. P. and Smith, M. M. (1986). Synthesis and assembly of acetylcholine receptor, a multisubunit membrane glycoprotein. J. Membrane Biol., 91, 1-10.

Merlie, J. P., Sebbane, R., Gardner, S., Olsen, E. and Lindstrom, J. (1983). The regulation of acetylcholine receptor expression in mammalian muscle. Cold Spring Harbor Symp. Quant. Biol., 48, 135-146.

Merlie, J. P., Isenberg, K. E., Russell, S. D. and Sanes, J. R. (1984). Denervation supersensitivity in skeletal muscle: analysis with a cloned cDNA probe. J. Cell Biol., 99, 332-335.

Messner, D. J. and Catterall, W. A. (1986). The sodium channel from rat brain. Role of the β1 and β2 subunits in saxitoxin binding. J. Biol. Chem., 261, 211-215.

Metcalf, D. (1966). The Thymus. Recent Results Cancer Res., 5, 43-52.

Michell, R. H. (1982). Inositol lipid metabolism in dividing and differentiating cells. Cell Calcium, 3, 429-440.

Miledi, R. (1960). The acetylcholine sensitivity of frog muscle fibres after complete or partial denervation. J. Physiol., 151, 1-23.

Miledi, R. and Zelena, J. (1966). Sensitivity to acetylcholine in rat slow muscle. Nature, 210, 855-856.

Mishina, M., Kurosaki, T., Tobimatsu, T., Morimoto, Y., Noda, M., Yamamoto, T., Terao, M., Lindstrom, J., Takahashi, T., Kuno, M. and Numa, S. (1984). Expression of functional acetylcholine receptor from cloned cDNAs. Nature, 307, 604-608.

Mishina, M., Takai, T., Imoto, K., Noda, M., Takahashi, T., Numa, S., Methfessel, C. and Sakmann, B. (1986). Molecular distinction between fetal and adult forms of muscle acetylcholine receptor., Nature, 321, 406-411.

Montarolo, P. G., Goelet, P., Castellucci, V. F., Morgan, J., Kandel, E. R. and Schacher, S. (1986). A critical period for macromolecular synthesis in long-term heterosynaptic facilitation in *Aplysia*. Science, 234, 1249-1254.

Mulder, A. H., van Amsterdam, R. G. M., Wilbrink, M. and Schoffelmeer, A. N. M. (1983). Depolarization-induced release of[^{3}H]histamine by high potassium concentrations, electrical stimulation and veratrine from rat brain slices after incubation with the radiolabelled amine. Neurochem. Int., 5, 291-297.

Navarro, J. (1987). Modulation of [^{3}H] dihydropyridine receptors by activation of protein kinase C in chick muscle cells. Biophys. J., 51, 33a.

Neary, J. T. (1984). Biochemical correlates of associative learning: protein phosphorylation in *Hermissenda crassicornis*, a nudibranch mollusk. In, Primary neural substrates of learning and behavioral change. Cambridge Univ. Press, Cambridge.

Nef, P., Mauron, A., Stadler, R., Alliod, C. and Ballivet, M. (1984). Structure, linkage and sequence of the two genes encoding the δ and γ subunits of the nicotinic acetylcholine receptor. Proc. Natl. Acad. Sci., 81, 7975-7979.

Neher, E. (1971). Two fast transient current components during voltage clamp on snail neurons. J. Gen. Physiol., 58, 36-53.

Neher, E., Sakmann, B. and Steinbach, J. H. (1978). The extracellular patch clamp: a method for resolving currents through individual open channels in biological membranes. Pflugers Arch., 375, 219-228.

Nelson, P. G. (1975). Nerve and muscle cells in culture. Physiol. Rev., 55, 1-61.

Nelson, D. J., Tang, J. M. and Palmer, L. G. (1984). Single-channel recordings of apical membrane chloride conductance in A6 epithelial cells. J. Mem. Biol., 80, 81-89.

Neyton, J. and Trautmann, A. (1985). Single-channel currents of an intercellular junction. Nature, 317, 331-335.

Nicolson, G. L. (1976). Trans-membrane control of the receptors on normal and tumour cells. II. Surface change associated with transformation and malignancy. Biochim. Biophys. Acta, 458, 1-72.

Noda, M., Takahashi, H., Tanabe, T., Toyosato, M., Furutani, Y., Hirose, T., Asai, M., Inayama, S., Miyata, T. and Numa, S. (1982). Primary structure of *Torpedo californica* acetylcholine receptor deduced from cDNA sequence. Nature, 299, 793-797.

Noda, M., Furutani, Y., Takahashi, H., Toyosato, M., Tanabe, T., Shimizu, S., Kikyotani, S., Kayano, T., Hirose, T., Inayama, S. and Numa, S. (1983a) Cloning and sequence analysis of calf cDNA and human genomic DNA encoding α-subunit precursor of muscle acetylcholine receptor. Nature, 305, 818-823.

Noda, M., Takahashi, H., Tanabe, T., Toyosato, M., Kikyotani, S., Hirose, T., Asai, M., Takashima, H., Inayama, S., Miyata, T. and Numa, S. (1983b). Primary structures of β- and δ-subunit precursors of *Torpedo californica* acetylcholine receptor deduced from cDNA sequences. Nature, 301, 251-255.

Noda, M., Takahashi, H., Tanabe, T., Toyosato, M., Kikyotani, S., Furutani, Y., Hirose, T., Takashima, H., Inayama, S., Miyata, T. and Numa, S. (1983c). Structural homology of *Torpedo californica* acetylcholine subunits. Nature, 302, 528-532.

Noda, M., Shimizu, S., Tanabe, T., Takai, T., Kayano, T., Ikeda, T., Takahashi, H., Nakayama, H., Kanaoka, Y., Minamino, N., Kangawa, K., Matsuo, H., Raftery, M. A., Hirose, T., Inayama, S., Hayashida, H., Miyata, T. and Numa, S. (1984). Primary structure of *Electrophorus electricus* sodium channel deduced from cDNA sequence. Nature, 312, 121-127.

Noda, M., Ikeda, T., Kayano, T., Suzuki, H., Takeshima, H., Kurasaki, M., Takahashi, H. and Numa, S. (1986a). Existence of distinct sodium channel messenger RNAs in rat brain. Nature, 320, 188-192.

Noda, M., Ikeda, T., Suzuki, H., Takeshima, H., Takahashi, T., Kuno, M. and Numa, S. (1986b). Expression of functional sodium channels from cloned cDNA. Nature, 322, 826-828.

Noma, Y., Sideras, P., Naito, T., Bergstedt-Lindquist, S., Azuma, C., Severinson, E., Tanabe, T., Kinashi, T., Matsuda, F., Yaoita, Y. and Honjo, T. (1986). Cloning of cDNA encoding the murine IgG1 induction factor by a novel strategy using SP6 promoter. Nature, 319, 640-646.

Nowak, L., Ascher, P. and Berwald-Netter, Y. (1987). Ionic channels in mouse astrocytes in culture. J. Neurosci., 7, 101-109.

O'Dowd, D. K. (1983). RNA synthesis dependence of action potential development in spinal cord neurones. Nature, 303, 619-621.

Ogden, D. C., Gray, P. T. A., Colquhoun, D. and Rang, H. P. (1984). Kinetics of acetylcholine activated ion channels in chick ciliary ganglion neurones grown in tissue culture. Pflugers Arch., 400, 44-50.

Okada, Y., Ogawa, M., Aoki, N. and Izutsu, K. (1973). The effect of K^+ on the membrane potential in HeLa cells. Biochim. Biophys. Acta, 291, 116-126.

Olsen, E. N., Glaser, L., Merlie, J. P., Sebanne, R. and Lindstrom, J. (1983). Regulation of surface expression of acetylcholine receptors in response to serum and cell growth in the BC_3H1 muscle cell line. J. Biol. Chem., 258, 13946-13953.

Olsen, E. N., Glaser, L., Merlie, J. P. and Lindstrom, J. (1984). Expression of acetylcholine α-subunit mRNA during differentiation of the BC_3H1 muscle cell line. J. Biol. Chem., 259, 3330-3335.

Pappone, P. A. (1980). Voltage-clamp experiments in normal and denervated mammalian skeletal muscle fibres. J. Physiol., 306, 377-410.

Palacios, J. M., Wamsley, J. K. and Kuhar, M. J. (1981). The distribution of histamine H_1-receptors in the rat brain: An autoradiographic study. Neuroscience, 6, 15-37.

Palmer, G. C., Schmidt, M. J. and Robison G. A. (1972). Development and characteristics of the histamine-induced accumulation of cyclic AMP in the rabbit cerebral cortex. J. Neurochem., 19, 2251-2256.

Panula, P., Yang, H.-Y. T. and Costa, E. (1984). Histamine-containing neurons in the rat hypothalamus. Proc. Natl. Acad. Sci., 81, 2572-2576.

Paton, W. D. M. and Zaimis, E. J. (1951). Paralysis of autonomic ganglia by methonium salts. Br. J. Pharmacol., 6, 155-168.

Patrick J. and Stallcup, B. (1977a). α-Bungarotoxin binding and cholinergic receptor function on a rat sympathetic nerve line. J. Biol. Chem., 252, 8629-8633.

Patrick, J. and Stallcup, B. (1977b). Immunological distinction between acetylcholine receptor and the α-bungarotoxin-binding component on sympathetic neurons. Proc. Natl. Acad. Sci., 74, 4689-4692.

Pellmar, T. C. (1986). Histamine decreases calcium-mediated potassium current in guinea pig hippocampal CA1 pyramidal cells. J. Neurophysiol., 55, 727-738.

Penner, R., Petersen, M., Pierau, Fr.-K. and Dreyer, F. (1986). Dendrotoxin: a selective blocker of a non-inactivating potassium current in guinea-pig dorsal root ganglion neurones. Pflugers Arch, 407, 365-369.

Petersen, M., Penner, R., Pierau, Fr.-K. and Dreyer, F. (1986). β-Bungarotoxin inhibits a non-inactivating potassium current in guinea pig dorsal root ganglion neurones. Neursci. Lett., 68, 141-145.

Peterson, L. R. and Peterson, M. J. (1959). Short-term retention of individual verbal items. J. Exp. Psychol., 58,193-198.

Pitts, J. D. (1972). Direct interaction between animal cells. In, Cell Interactions. (3rd Lepetit Colloquium), (ed.) L. G. Silvestri, North Holland Publishing Co., Amsterdam, pp. 277-285.

Platika, D., Boulos, M. H., Baizer, L. and Fishman, M. C. (1985). Neuronal traits of clonal cell lines derived by fusion of dorsal root ganglia neurons with neuroblastoma cells. Proc. Natl. Acad. Sci., 82, 3499-3503.

Prell G. D. and Green, J. P. (1986). Histamine as a neuroregulator. Ann. Rev. Neurosci., 9, 209-254.

Purves, D. and Sakmann, B. (1974). The effect of contractile activity on fibrillation and extrajunctional acetylcholine-sensitivity in rat muscle maintained in organ culture. J. Physiol., 237, 157-182.

Raftery, M. A., Hunkapiller, M. W., Strader, C. D. and Hood, L. E. (1980). Acetylcholine receptor: complex of homologous subunits. Science, 208,1454-1457.

Rayport, S. G. and Schacher, S. (1986). Synaptic plasticity in vitro: Cell culture of identified *Aplysia* neurons mediating short term habituation and sensitization. J. Neurosci., 6, 759-763.

Redfern, P., Lundh, H. and Thesleff, S. (1970). Tetrodotoxin resistant action potentials in denervated rat skeletal muscle. Eur. J. Pharmacol., 11, 263-265.

Reichert, R. A., Weissman, I. L. and Butcher, E. C. (1986) Dual immunofluorescence studies of cortisone-induced thymic involution: evidence for a major cortical component to cortisone-resistant thymocytes. J. Immunol., 136, 3529-3534.

Reiness, C. G. and Hall, Z. W. (1977). Electrical stimulation of denervated muscles reduces incorporation of methionine into the ACh receptor. Nature, 268, 655-657.

Rios, E., Brum, G. and Stefani, E. (1986). E-C coupling effects of interventions that reduce slow Ca current suggest a role of t-tubule Ca channels in skeletal muscle function. Biophys. J., 49, 13a.

Role, L. W., Matossian, V. R., O'Brian, R. J. and Fischbach, G. D. (1985). On the mechanism of acetylcholine receptor accumulation at newly formed synapses on chick myotubes. J. Neurosci., 5, 2197-2204.

Rothenberg, E. (1982) A specific biosynthetic marker for immature thymic lymphoblasts. Active synthesis of thymus-leukemia antigen restricted to proliferating cells. J. Exp. Med., 155, 140-154.

Rothenberg, E. and Lugo, J. P. (1985) Differentiation and cell division in the mammalian thymus. Dev. Biol., 112, 1-17.

Roy, G. and Sauve, R. (1982). Stable membrane potentials and mechanical K^+ responses activated by internal Ca^{2+} in HeLa cells. Can. J. Physiol. Pharm., 61, 144-148.

Rubin, L. L. (1985). Increases in muscle Ca^{2+} mediate changes in acetylcholinesterase and acetylcholine receptors caused by muscle contraction. Proc. Acad. Sci., 82, 7121-7125.

Ruddon, R. W. (1981). Cancer Biology. Oxford University Press, Oxford.

Sakmann, B. (1975). Noise analysis of acetylcholine induced currents in normal and denervated muscle fibres. Pflugers Arch., 359, R89.

Sakmann, B. and Brenner, H. R. (1978). Change in synaptic channel gating during neuromuscular development. Nature, 276, 401-402.

Sakmann, B. and Neher, E. (eds.) (1983) Single-Channel Recording. Plenum Press, New York.

Sakmann, B., Bormann, J. and Hamill, O. P. (1983). Ion transport by single receptor channels. Cold Spring Harbour Symposia on Quantitative Biology, 48, 247-257.

Sakmann, B., Methfessel, C., Mishina, M., Takahashi, T., Takai, T., Kurasaki, M., Fukuda, K. and Numa, S. (1985). Role of acetylcholine receptor subunits in gating of the channel. Nature, 318, 538-543.

Salvalterra, P. M. and Moore, W. J. (1973). Binding of ^{125}I-α-bungarotoxin to particulate fractions of rat and guinea-pig brain. Biochem. Biophys Res. Commun., 55, 1311-1319.

Salkoff, L. (1983). Genetic and voltage-clamp analysis of a *Drosophila* potassium channel. Cold Spring Harbor Symp. Quant. Biol., 48, 221-231.

Salkoff, L. (1985). Development of ion channels in the flight muscles of *Drosophila*. J. Physiol. (Paris), 80, 275-282.

Salkoff, L. B. and Tanouye, M. A. (1986). Genetics of ion channels. Physiol. Rev., 66, 301-329.

Salkoff, L. and Wyman, R. (1981). Genetic modification of potassium channels in *Drosophila Shaker* mutants. Nature, 293, 228-230.

Salkoff, L. and Wyman, R. J. (1983). Ion currents in *Drosophila* flight muscles. J. Physiol., 337, 687-709.

Sarmiento, M., Glasebrook, A. L. and Fitch, F. W. (1980) IgG or IgM monoclonal antibodies reactive with different determinants on the molecular complex bearing Lyt-2 antigen block T cell-mediated cytolysis in the absence of complement. J. Immunol., 125, 2665-2672.

Sauve, R., Bedfer, G. and Roy, G. (1984). Single Ca^{++} dependent K^+ currents in HeLa cancer cells. Biophys. J., 45, 66-68.

Sauve, R., Roy, G. and Payet, D. (1983). Single channel K^+ currents from HeLa cells. J. Mem. Biol., 74, 41-49.

Schein, S. J., Bennett, M. V. L. and Katz, G. M. (1976). Altered calcium conductance in pawns, behavioural mutants of *Paramecium aurelia*. J. Exp. Biol., 65, 699-724.

Schmidt, J. W. and Catterall, W. A. (1986). Biosynthesis and processing of the α subunit of the voltage-sensitive sodium channel in rat brain neurons. Cell, 46, 437-445.

Schneider, G. T., Cook, D. K., Gage, P. W. and Young, J. A. (1985). Voltage-sensitive high-conductance chloride channels in the luminal membrane of cultured pulmonary alveolar (type II) cells. Pflugers Arch., (1985), 404, 354-357.

Schneider, M. D., Caffrey, J. M. and Brown, A. M. (1987). Transfected oncogenes can block expression of specfic voltage-gated ion channels. Biophys. J., 51, 32a.

Schubert, D., Heinemann, S., Carlsisle, W., Tarikas, H., Kimes, B., Patrick, J., Steinbach, J. H., Culp, W. and Brandt, B. L. (1974). Clonal cell lines from the rat central nervous system. Nature, 249, 224-227.

Schwab, M., Alitalo, K., Klempnauer, K.-H., Varmus, H. E., Bishop, J. M., Gilbert, F., Brodeur, G., Goldstein, M. and Trent, J. (1983). Amplified DNA with limited

homology to *myc* cellular oncogene is shared by human neuroblastoma cell lines and a neuroblastoma tumor. Nature, 305, 245-248.

Schwartz, J.-C. (1979). Histamine receptors in brain. Life Sci., 25, 895-912.

Scollay, R., Bartlett, P. and Shortman, K. (1984a) T cell development in the adult murine thymus: changes in the expression ot the surface antigens Ly2, L3T4 and B2A2 during development from early precursor cells to emigrants. Immunol. Rev., 82, 79-103.

Scollay, R., Wilson, A. and Shortman, K. (1984b) Thymus cell migration: analysis of thymus emigrants with markers that distinguish medullary thymocytes from peripheral T cells. J. Immunol., 132, 1089-1094.

Scollay, R. and Shortman, K. (1985) Identification of early stages of T lymphocyte development in the thymus cortex and medulla. J. Immunol., 134, 3632-3642.

Segev, I., Fleshman, J. W., Miller, J. P. and Bunow, B. (1985). Modeling the electrical behavior of anatomically complex neurons using a network analysis program: passive membranes. Biol. Cybern., 53, 27-40.

Sharma, S., Mehta, S. Morgan, J. and Maizel, A. (1987). Molecular cloning and expression of a human B-cell growth factor gene in *Eschericia coli*. Science, 235, 1489-1492.

Sherman, S. J. and Catterall, W. A. (1982). Biphasic regulation of development of the high-affinity saxitoxin receptor by innervation in rat skeletal muscle. J. Gen. Physiol., 80, 753-768.

Sherman, S. J. and Catterall, W. A. (1984). Electrical activity and cytosolic calcium regulate levels of tetrodotoxin-sensitive sodium channels in cultured rat muscle cells. Proc. Natl. Acad. Sci., 81, 262-266.

Sherman, S. J., Lawrence, J. C., Messner, D. J., Jacoby, K. and Catterall, W. A. (1983). Tetrodotoxin-sensitive sodium channels in rat muscle cells developing *in Vitro*. J. Biol. Chem., 258, 2488-2495.

Shibahara, S., Kubo, T., Perski, H. J., Furutani, Y., Takahashi, H., Noda, M. and Numa, S. (1985). Cloning and sequence analysis of human genomic DNA encoding γ subunit precursor of muscle acetylcholine receptor. Eur. J. Biochem., 146, 15-22.

Siegel, R. E., Eiden, L. E. and Affolter, H.-U. (1985). Elevated potassium stimulates enkephalin biosynthesis in bovine chromaffin cells. Neuropeptides, 6, 543-552.

Siegelbaum, S. A., Trautmann, A. and Koenig, J. (1984). Single acetylcholine-activated channel currents in developing muscle cells. Dev. Biol., 104, 366- 379.

Siegenbeek van Heukelom, J., Denier van der Gon, J. J. and Prop, F. J. A. (1972). Model approaches for evaluation of cell coupling in monolayers. J. Mem. Biol., 7, 88-110.

Siekevitz, P. (1985). The postsynaptic density: A possible role in long-lasting effects in the central nervous system. Proc. Natl. Acad. Sci., 82, 3494-3498.

Siman, R., Baudry, M. and Lynch, G. (1985). Regulation of glutamate receptor binding by the cytoskeletal protein fodrin. Nature, 313, 225-228.

Sine, S. M. and Steinbach, J. H. (1986). Activation of acetylcholine receptors on clonal mammalian BC3H-1 cells by low concentrations of agonist. J. Physiol., 373, 129-162.

Snyder, S. H. and Taylor, K. M. (1972). Histamine in the brain: A neurotransmitter? In, Perspectives in Neuropharmacology-A Tribute to Julius Axelrod, ed. S. H. Snyder, pp. 43-73., New York, Oxford Univ. Press.

Sorensen, R. G. and Blaustein, M. P. (1986). m-Azido-phencyclidine covalently labels the rat brain PCP receptor, putative K channel. J. Neurosci., 6, 3676-3681.

Spaggiare, S., Wallach, M. J. and Tupper, J. T. (1976). Potassium transport in normal and transformed mouse 3T3 cells. J. Cell. Physiol. 89, 403-416.

Sparks, R. L., Pool, T. B., Smith, N. K. R. and Cameron, I. L. (1982). The role of ions, ion fluxes and Na^+, K^+- ATPase activity in the control of proliferation, differentiation and transformation. In, Genetic Expression in the Cell Cycle. (eds.) G. M. Padilla and K. S. McCarty, pp.363-392. Academic Press, N.Y.

Spitzer, N. C. (1979). Ion channels in development. Ann. Rev. Neursci., 2, 363-397.

Spitzer, N. C. (1985). The control of development of neuronal excitability. In, Molecular Bases of Neural Development, (ed.) G. M. Edelman, W. E. Gall and W. M. Cowan., pp. 67-88. Neurosciences Research Foundation Inc., New York.

Spitzer, N. C. and Baccaglini, P. I. (1976). Development of the action potential in embryo amphibian neurons in vivo. Brain Res., 107, 610-616.

Spitzer, N. C. and Lamborghini, J. E. (1976). The development of the action potential mechanism of amphibian neurons isolated in culture. Proc. Natl. Acad. Sci., 73, 1641-1645.

Springer, T., Galfre, G., Secher, D. S. and Milstein, C. (1978). Monoclonal xenogeneic antibodies to murine cell surface antigens: identification of novel leukocyte differentiation antigens. Eur. J. Immunol., 8, 539-544.

Squire, L. R. (1986). Mechanisms of memory. Science, 232,1612-1619.

Squire, L. R., Slater, P. C. and Chace, P. M. (1975). Retrograde amnesia: Temporal gradient in very long term memory following electroconvulsive therapy. Science, 187, 77-79.

Stanbridge, E. J. (1976). Suppression of malignancy in human cells. Nature, 260, 17-20.

Stanbridge, E. J., Der, C. J., Doersen, C.-J., Nishimi, R. Y., Peehl, D. M., Weisman, B. E. and Wilkinson, J. E. (1982). Human cell hybrids: Analysis of transformation and tumorigenicity. Science, 215, 252-259.

Stanbridge, E. J. and Wilkinson, J. (1978). Analysis of malignancy in human cells: Malignant and transformed phenotype are under separate genetic control. Proc. Natl. Acad. Sci., 75, 1466-1469.

Stent, G. S. (1973). A physiological mechanism for Hebb's postulate of learning. Proc. Natl. Acad. Sci., 70, 997-1001.

Sterz, R., Pagala, M. and Peper, K. (1983). Postjunctional characteristics of endplates in mammalian fast and slow muscles. Pflugers Arch., 398, 48-54.

St. John, P. A., Kell, W. M., Mazzetta, J. S., Lange, G. D. and Barker, J. L. (1986). Analysis and isolation of embryonic mammalian neurons by fluorescence-activated cell sorting. J. Neurosci., 6, 1492-1512.

Stroud, R. and Finer-Moore, J. (1985). Acetylcholine receptor structure, function, and

evolution. Annu. Rev. Cell Biol., 1, 317-351.

Sugiyama, H., Ito, I. and Hirono, C. (1987). A new type of glutamate receptor linked to inositol phopholipid metabolism. Nature, 325, 531-533.

Sumikawa, K., Houghton, M., Emtage, J. S., Richards, B. M. and Barnard, E. A. (1981). Active multi-subunit ACh receptor assembled by translation of heterologous mRNA in *Xenopus* oocytes. Nature, 292, 862-864.

Sumikawa, K., Parker, I. and Miledi, R. (1984). Partial purification and functional expression of brain mRNAs coding for neurotransmitter receptors and voltage-operated channels. Proc. Natl. Acad. Sci., 81, 7994-7998.

Takacs, L., Osawa, H. and Diamanstein, T. (1984) Detection and localization by the monoclonal anti-interleukin 2 receptor antibody AMT-13 of IL2 receptor-bearing cells in the developing thymus of the mouse embryo and in the thymus of cortisone-treated mice. Eur. J. Immunol., 14, 1152-1156.

Takai, T., Noda, M., Furutani, Y., Takahashi, H., Notake, M., Shimizu, S., Kayano, T., Tanabe, T., Tanaka, K., Hirose, T., Inayama, S. and Numa, S. (1984). Primary sequence of γ subunit precursor of calf-muscle acetylcholine receptor deduced from the cDNA sequence. Eur. J. Biochem., 143, 109-115.

Takai, T., Noda, M., Mishina, M., Shimizu, S., Furutani, Y., Kayano, T., Ikeda, T., Kubo, T., Takahashi, H., Takahashi, T., Kuno, M. and Numa, S. (1985). Cloning, sequencing and expression of cDNA for a novel subunit of acetylcholine receptor from calf muscle. Nature, 315, 761-764.

Takeda, N., Inagaki, S., Taguchi, Y., Tohyama, M., Watanabe, T. and Wada, H. (1984). Origins of histamine-containing fibers in the cerebral cortex of rats studied by immunohistochemistry with histidine decarboxylase as a marker and transection. Brain Res., 323, 55-63.

Tanabe, T., Noda, M., Furutani, Y., Takai, T., Takahashi, H., Tanaka, K., Hirose, T., Inayama, S. and Numa, S. (1984). Primary sequence of β subunit precursor of calf muscle acetylcholine receptor deduced from cDNA sequence. Eur. J. Biochem., 144, 11-17.

Tanouye, M. A., Ferrus, A. and Fujita, S. C. (1981). Abnormal action potentials associated with the *Shaker* complex locus of *Drosophila*. Proc. Natl. Acad. Sci., 78, 6548-6552.

Tanouye, M. A., Kamb, C. A., Iverson, L. E. and Salkoff, L. (1986). Genetics and molecular biology of ionic channels in *Drosophila*. Ann. Rev. Neurosci., 9, 255-76.

Taylor, I. W. and Milthorpe, B. K. (1980) An evaluation of DNA fluorochrome staining techniques and analysis for flow cytometry. 1. Unperturbed cell populations. J. Histochem. Cytochem., 28, 1224-1228.

Taylor, K. M. and Snyder, S. H. (1973). The release of histamine from tissue slices of rat hypothalamus. J. Neurochem., 21, 1215-1223.

Tooze, J., (ed.) (1980). Molecular Biology of Tumor Viruses 2nd edition: DNA Tumor Viruses. Cold Spring Harbour Laboratory, Cold Spring Harbour, N. Y.

Tran, V. T. and Snyder, S. H. (1981). Histidine decarboxylase: Purification from fetal rat liver, immunologic properties and histochemical localization in brain and stomach. J. Biol. Chem., 256, 680-686.

Tran, V. T., Chang, R. S. L. and Snyder, S. H. (1978). Histamine H_1 receptors identified in mammalian brain membranes with [^{3}H]mepyramine. Proc. Nati. Acad. Sci., 75, 6290-6294.

Traub, R. D. and Llinas, R. (1979). Hippocampal pyramidal cells: significance of dendritic ionic conductances for neuronal function and epileptogenesis. J. Neurophysiol., 42, 476-496.

Usdin, T. B. and Fischbach, G. D. (1986). Purification and characterization of a polypeptide from chick brain that promotes the accumulation of acetylcholine receptors in chick myotubes. J. Cell Biol., 103, 493-507.

van der Valk, J., Verlaan, I., de Laat, S. and Moolenaar, W. H. (1987). Expression of $pp60^{v\text{-}src}$ alters the ionic permeability of the plasma membrane in rat cells. J. Biol. Chem., 262, 2431-2434.

Van Renterghem, C., Penit-Soria, J. and Stinnakre, J. (1985). β-Adrenergic induced K^+ current in *Xenopus* oocytes: role of cAMP, inhibition by muscarinic agents. Proc. R. Soc. Lond. B., 223, 389-402.

Waechter, C. J., Schmidt, J. W. and Catterall, W. A. (1983). Glycosylation is required for maintenance of functional sodium channels in neuroblastoma cells. J. Biol. Chem., 258, 5117-5123.

Wahlestedt, C., Skagerberg, G., Hakanson, R., Sundler, F., Wada, H. and Watanabe, T. (1985). Spinal projections of hypothalamic histidine decarboxylase-immunoreactive neurones. Agents Actions, 16, 231-233.

Watanabe, T., Taguchi, Y., Hayashi, H., Tanaka, J., Shiosaka, S., Tohyama, M. Kubota, H., Terano, Y. and Wada, H. (1983). Evidence for the presence of a histaminergic neuron system in the rat brain: An immunohistochemical analysis. Neurosci. Lett., 39, 249-254.

Watanabe, T., Taguchi, Y., Shiosaka, S., Tanaka, J., Kubota, H., Terano, Y., Tohyama, M. and Wada, H. (1984). Distribution of the histaminergic neuron system in the central nervous system of rats: A fluorescent immunohistochemical analysis with histidine decarboxylase as a marker. Brain Res., 295, 13-25.

Waxman, S. G. and Ritchie, J. M. (1985). Organization of ion channels in the myelinated nerve fiber. Science, 228, 1502-1507.

Weibel, E. R., Staubli, W., Gnagi, H. R. and Hess, F. A. (1969). Correlated morphometric and biochemical studies on the liver cell. J. Cell. Biol., 42, 68-91.

Weiss, A., Imboden, J., Hardy, K., Manger, B., Terhorst, C. and Stobo, J. (1986). The role of the T3/antigen receptor complex in T-cell activation. Ann. Rev. Immunol., 4, 593-619.

White, M. M., Mayne, K. M., Lester, H. A. and Davidson, N. (1985). Mouse-*Torpedo* hybrid acetylcholine receptors: Functional homology does not equal sequence homology., 82, 4852-4856.

Wilcox, B. J. and Seybold, V. S. (1982). Localization of neuronal histamine in rat brain. Neurosci. Lett., 29, 105-110.

Willard, A. L. (1980). Electrical excitability of outgrowing neurites of embryonic neurones in cultures of dissociated neural plate of *Xenopus laevis*. J. Physiol., 301, 115-128.

Williams, E. H. and DeHann, R. L. (1981). Electrical coupling among heart cells in the

absence of ultrastructurally defined gap junctions. J. Mem. Biol., 60, 237-248.

Ypey, D. L. and Clapham, D. E. (1984) Development of a delayed outward-rectifying K^+ conductance in cultured mouse peritoneal macrophages. Proc. Natl. Acad. Sci., 81, 3083-3087.

Ziskind-Conhaim, L., Geffen, I. and Hall, Z. W. (1984). Redistribution of acetylcholine receptors on developing rat myotubes. J. Neurosci., 4, 2346-2349.